Developing an impact-based combined drought index for monitoring crop yield anomalies in the Upper Blue Nile Basin, Ethiopia

Bayissa, Yared

Publication date
2018

Document Version
Final published version

Citation (APA)
Bayissa, Y. (2018). *Developing an impact-based combined drought index for monitoring crop yield anomalies in the Upper Blue Nile Basin, Ethiopia*. [Dissertation (TU Delft), Delft University of Technology]. CRC Press / Balkema - Taylor & Francis Group.

DEVELOPING AN IMPACT-BASED COMBINED DROUGHT INDEX FOR MONITORING CROP YIELD ANOMALIES IN THE UPPER BLUE NILE BASIN, ETHIOPIA

Yared Ashenafi BAYISSA

DEVELOPING AN IMPACT-BASED COMBINED DROUGHT INDEX FOR MONITORING CROP YIELD ANOMALIES IN THE UPPER BLUE NILE BASIN, ETHIOPIA

DISSERTATION

Submitted in fulfillment of the requirements of
the Board for Doctorates of Delft University of Technology
and
of the academic Board of IHE Delft
Institute for Water Education
for
the degree of DOCTOR
to be defended in public
on September 11, 2018 at 12:30pm
in Delft, The Netherlands

by

Yared Ashenafi BAYISSA

Masters of Science in Hydraulic Engineering, Addis Ababa University, Ethiopia
born in Ambo, Ethiopia

This dissertation has been approved by the
Promotor: Prof. dr. D.P. Solomatine
Copromotor: Dr. S.J. van Andel

Composition of Doctoral Awarding Committee:

Rector Magnifcus	Chairman
Rector IHE Delft	Vice-chairman
Prof. dr. D.P. Solomatine	IHE Delft / TU Delft, promotor
Dr. S.J. van Andel	IHE Delft, copromotor

Independent members:

Dr. D.H. Asfaw	School of Civil and Environmental Ing, AAU, Ethiopia
Prof. dr. M. Hayes	University of Nebraska, Lincoln, USA
Prof. dr. W.G.M Bastiaanssen	IHE Delft / TU Delft
Prof. dr. ir. N.C. van de Giesen	TU Delft
Prof. dr. M.E. McClain	IHE Delft / TU Delft, reserve member

The research reported in this dissertation has been funded by the Netherlands Fellowship Programmes (NFP). This research was conducted under the auspices of the Graduate School for Socio-Economic and Natural Sciences of the Environment (SENSE)

CRC Press/Balkema is an imprint of the Taylor & Francis Group, an informa business

Published by:
CRC Press/Balkema
Schipholweg 107C, 2316 XC, Leiden, the Netherlands
Pub.NL@taylorandfrancis.com
www.crcpress.com – www.taylorandfrancis.com
ISBN: 978-0-367-02451-2.

Acknowledgements

First and foremost, I would like to Praise the Omnipotent, Omniscient and Omnipresent Lord for his unlimited love, blessing and protection all the way in my life and during the PhD years. This PhD would not have come to an end without the support, supervision, and encouragement of different people and organizations.

My heartiest gratitude and indebtedness goes to my promoter Prof. Dimitri Solomatine for his scholastic guidance, critical comments, inestimable help, patience and timely response for all academic issues. Dimitri, without your all rounded help and guidance, I could have never finished this PhD, many thanks!!!

I would like to extend my deepest gratitude and appreciation to my supervisors Dr. Schalk Jan van Andel, Dr. Shreedhar Maskey, Prof. Ann van Griensven, Dr. Semu Ayalew Moges, Dr. Tsegaye Tadesse and Dr. Yunquin Xuan for their consistent guidance, critical comments, and suggestions. I was lucky to have such a group of advice that are willing to dedicate their time and share their vast experience and knowledge. Dr. Schalk Jan, I would not forget your commitment, critical comments, patience, respect, and hospitality. You were showing me the same behavior and respect all the way, many thanks!!! Dr. Shreedhar, apart from your dedication, scientific criticism, and encouragement, you were the reason to start and pursue this PhD program at the first glance. Your guidance to secure the scholarship and critical comments on the first concept note was unforgettable and substantial, thank you!!! My sincere gratitude also goes to Prof. Ann van Griensven for her overall contribution to this research, especially on the SWAT hydrological modeling of the basin: thank you!!! Dr. Semu, I have no words to express your all-rounded contribution in this research. I was enjoying a lot sitting together with you and sharing your knowledge on hydrology and discussing other social issues. Moreover, you shared me your office during my time in Ethiopia, many thanks!!! Dr. Tsegaye, you were not only my supervisor but also my intimate friend that I can talk freely what I would like to talk. You made my stay at the University of Nebraska, USA so comfortable and also you helped me to involve in one of the NASA drought projects that you were the principal investigator. Your experience on drought study was an asset for this research and your comments were so critical, many thanks!!! Dr. Yunqing, your contribution during the development stage of the research proposal was great and considerable. Your knowledge of solving problems through writing programming scripts was substantial in this research.

I would like to forward my sincere gratitude to the Dutch government and Netherland Fellowship Program (NFP) for financing all the expenses of this research. I will take also this opportunity to forward my appreciation to Jolanda Boots, Anique Karsten, and other staffs of IHE Delft, for their kindly help and cooperation on addressing and managing all the financial and other issues. My appreciation also goes to Ambo University, Institute of Technology, for granting half of my salary during the study period of the research. I am thankful for National Meteorological Agency (NMA), Ministry of Water, Irrigation, and Electricity, Ministry of Agriculture and Central Statistical Agency (CSA) of Ethiopia for all the meteorological, hydrological and agricultural data you provided for free of charge. My special thanks also go to Dr. Mark Svoboda (director of National Drought Mitigation Center, NDMC) and other staffs for their hospitality and significant contributions in this study. I am grateful to Eastern Nile Technical Regional Office (ENTRO) for arranging office and hot drinks during the write-up period of the dissertation. I really appreciate the hospitality of all the ENTRO staff members: I am really thankful.

I forward many thanks to my parents, relatives, and friends for your encouragement, support, and care. Special credit to my mom W/ro Almaz Kassaye, you are my inspiration and you had a big role for the successful completion of this research, I love you mom! Many thanks to my stepfather Shewarega Badeg, mother and father in law, my brothers Samson, Yonas and Surafel; my sisters Elsabet, Mimi, Yodit, and Zufiye.

Last but not least, words cannot express my grateful and appreciation to my wife Yetnayet Molla and my daughters Eldana Yared and Saron Yared for your unlimited love, care and support. You paid immeasurable sacrifices alone during my absence for the research work. Eldana, you were born at the same day with the PhD program and I know you did not get sufficient love and care that you would have gotten from your dad. I love you both!!!

Yared Ashenafi Bayissa

September, 2018, Ambo, Ethiopia

Dedication

This dissertation is dedicated to those who were a victim of natural disaster, in particular victims of the recurrent drought in Ethiopia.

Summary

Drought is a silent and pervasive disaster that impacts a large area and propagates slowly. Unlike for other natural disasters such as floods, tornados etc., impacts of droughts do not manifest immediately. This makes it more difficult to monitor drought and mitigate adverse effects by early warning. Several drought indices exist to monitor drought. Individually, however, they are unable to provide an integral concise information to characterize and indicate the occurrence of meteorological, agricultural and hydrological droughts. A combined drought index (CDI) using several meteorological, agricultural and hydrological drought indices can indicate the occurrence of all drought types, and can provide information that facilitates the drought management decision-making process. Moreover, development of a CDI can be an impact-based, e.g. by optimizing for monitoring drought-related crop yield reduction. The economic growth in many developing countries relies on the agricultural products, hence developing crop yield monitoring and prediction methods is vital to enhance the economic growth.

In Ethiopia, drought is a frequently recurring phenomenon. In the past few centuries, more than 30 major drought episodes have occurred, of which 13 were severe and covered the entire country and affected several nations. Some studies show that the frequency of drought occurrence in Ethiopia has been increasing over the past decades. Since 1970, severe drought has hit Ethiopia on average every 10 years. Agriculture, which contributes more than half of the gross domestic product (GDP), is a very drought-sensitive sector in Ethiopia because of its dependency on annual rainfall. Rain-fed agricultural is the predominant practice in Ethiopia that often depends on the amount and distribution of annual rainfall. The shortfall of the annual rainfall is often the primary source for drought to occur and exacerbates the reduction in crop yield. In order to mitigate the adverse impacts of drought in Ethiopia, developing a robust drought monitoring system is crucial. Yet, this still lacks in Ethiopia and in the Upper Blue Nile (UBN) basin in particular. The UBN Basin is less-explored in terms of drought studies and there is no basin-specific drought monitoring system, even though the basin contributes 60% of the total share of water to the main Nile River. Therefore, the main objective of this research is to develop an impact-based combined drought index (CDI) and prediction model of crop yield anomalies for the UBN Basin. The impact-based CDI is defined as a drought index that optimally combines the information embedded in other drought indices for monitoring a certain impact of drought (e.g. crop yield).

There are three recurrent challenges in the field of drought monitoring that need to be addressed to achieve the main objective for the case study of the UBN Basin. First, several meteorological stations in the basin are having a relatively short record length (e.g. less than 35 years). Hence assessing the effect of the record length on meteorological drought assessment is important to decide if these stations can be used for the spatio-temporal analysis of drought in the basin. The second challenge is that only few experiments have been published yet that try to develop CDIs with optimized indices weights. Most existing CDI methods use expert-based or subjective ways of assigning weights or apply a sequential ordering of the indices. There is a need for further development and testing new CDIs. The third challenge concerns drought monitoring in ungauged and data-scarce catchments. The potential of a CDI using mainly Earth Observation data as input needs to be assessed. To address these challenges for the case study of the UBN, the following specific objectives were defined:

- Investigate the effect of data record length on drought assessment in the UBN Basin, to validate the use of meteorological stations with short record length in the drought analysis.
- Investigate the spatial and temporal variation of meteorological droughts in the UBN Basin.
- Evaluate and compare the performance of six drought indices (i.e. Standardized Precipitation Index (SPI), Standardized Precipitation Evaporation Index (SPEI), Evapotranspiration Deficit Index (ETDI), Soil Moisture Deficit Index (SMDI), Aggregate Drought Index (ADI), and Standardized Runoff-discharge Index (SRI)) with respect to identifying historic drought events in the UBN Basin.
- Develop an impact-based CDI with weights optimized to monitor crop yield anomalies.
- Develop a prediction model of crop yield anomalies, based on the impact-based CDI and individual drought indices.
- Assess the potential of an impact-based CDI using Earth Observation data as the main input.

Methodology of this research employed various methods of data analysis, statistics, optimisation and modelling, as described in the following steps:

1. For analysing the impact of record length on drought assessment, the SPI was determined (identifying meteorological droughts) for several weather stations available in the UBN Basin. The record length in the majority of the stations is relatively short (1975-2009). There are only 14 weather stations that have a longer record length (1953

– 2009). With these stations (with long record length), two data withholding procedures were applied. The first data withholding experiment was that one additional year of data was taken out starting from 1953 and then SPI values were calculated. The data withdrawing was repeated up to the year 1974 where most of the other stations started recording. Then, the SPI values for a particular drought year between 1975 and 2009 were checked to assess whether or not the values indicate the same drought category. For cross-validation of the results of the first experiment, in the second procedure, one year of data was withdrawn one by one starting from the middle of the record length (from 1970 to 1988).

2. Spatial and temporal analysis of meteorological droughts in the UBN Basin was done using SPI.
3. Comparisons of a range of individual drought indices, i.e. SPI, SPEI, ETDI, SMDI, ADI, and SRI, were carried out using correlation analysis. Their performance was evaluated with respect to identifying onset, severity, and duration of the historic drought events. The information on historic droughts was obtained from the Emergency Events Database (EM-DAT).
4. Developing CDIs was done through assigning weights to the selected drought indices using two objective approaches: Principal Component Analysis (PCA) and an impact-based random search optimisation. PCA combines the indices through calculating the correlation coefficient matrix between each index followed by computing the eigenvalues that could be used as the weight in developing the CDI. The impact-based random search for the optimal weights employed more than 60,000 iterations to identify the combination of weights with maximum correlation with crop yield anomaly. Crop yield anomaly data for the UBN Basin were obtained from the Central Statistical Agency (CSA) of Ethiopia for the period from 1996 to 2009. The UBN Basin is clustered into 16 administrative zones and the annual crop yield data for each zone were used. Crop yield is a combined result of weather, policies, and agricultural practices. To account only for the effects of the weather variations on crop yield, detrending of the crop yield data was carried out. Four common crops in the basin (i.e. teff, maize, barley, and sorghum) were considered in this study. The CDIs developed using these two techniques were compared.
5. Crop-yield anomaly prediction models were developed. The models were developed using multiple linear regression equations linking the drought indices and yield anomalies for the teff, maize, barley, and sorghum crops. In these models, crop yield

anomaly was used as a predictand variable (variable being predicted), whereas the drought indices including the impact-based CDI and the selected drought indices were used as predictor variables. The CDI-based prediction model of crop yield anomalies was compared with the model based on the six individual drought indices.

6. Using the same methods as in steps 3 and 4, an impact-based CDI and crop-yield anomaly models were developed using drought indices based on Earth Observation data. Indices included precipitation Z-score, Evaporative Drought Index (EDI) and Vegetation Condition Index (VCI). The Z-scores were calculated using grid-based rainfall data from the Climate Hazards Group Infrared Precipitation with Stations (CHIRPS). The EDI calculation used the MODIS ET data as a main input. The VCI was derived using Normalized Difference Vegetation Index (NDVI). The CDI was developed using only the impact-based random search for the optimal weight approach.

In the following paragraphs the results of each of these research steps are discussed.

The analyses of the effect of the record length showed that the record length from 1953 to 1974 has limited effect on the indicated drought categories in the period 1975-2009 (period recorded by most stations). Therefore, all the stations (short and long records) were used for the drought analyses of this thesis.

The spatio-temporal analyses of the SPI values showed that throughout the UBN Basin seasonal or annual meteorological drought episodes occurred in the years 1978/79, 1984/85, 1994/95 and 2003/04. Persistence from seasonal to annual drought, and from one year to the next, has been found. The drought-years identified by the SPI analysis for the UBN Basin, are also known for their devastating impact in other parts of Ethiopia.

The performance analysis of SPI, SPEI, ETDI, SMDI, ADI, and SRI, in identifying drought onset, severity, and duration of the most severe historic drought years in 1978/79, 1984/85, 1994/95 and 2003/04, revealed the following:

- SPEI showed too much fluctuation between drought and normal conditions at shorter time scales (SPEI-3 and SPEI-6).
- As compared to the other indices, the SRI was observed to be less fluctuating between dry to wet conditions or vice versa.
- The comparison in terms of identifying the onset of these four events showed that the SPI and SPEI most often indicated the early onsets of droughts, whereas ETDI, SMDI,

ADI, and SRI showed late onsets of the droughts with respect to the onset reported by EMDAT.

- The majority of the drought indices indicated the severity and duration of the historic drought years (e.g. 2003-2004, 1983-1984).
- None of the six drought indices could individually identify the onset of the four selected historic drought events.

This confirmed the relevance of the fourth specific objective of this research to develop an impact-based CDI with optimised weights for individual drought indices.

The developed impact-based CDI correlated well with the crop yield anomalies data of the four crops considered in this study: Teff, Barley, Maize and Sorghum. The CDI using PCA indicated years with negative crop yield anomalies equally well. The maximum correlation coefficient was obtained for the Barley crop (0.7) with the impact-based CDI approach.

The results of the newly developed prediction models for the four crops yield anomalies were encouraging. The maximum value of the R^2 was obtained for barley crop (R^2 = 0.77) and the minimum value was for Maize (R^2 = 0.24). Overall, the patterns of the predicted and the observed yield anomalies are similar, except for variation in the magnitude of the anomaly for some of the years. This variation in the magnitude may be attributable to several factors - mainly to the crop yield data that is aggregated to zonal average, and the data accuracy of the crop yield. Further research would be necessary to develop a more robust crop yield prediction model based on more site-specific information.

Lastly, following the same impact-based approach, a CDI was developed using Earth Observation data as the main input (EO-CDI). The data window considered in this case is from 2001 to 2009, and historic drought events within this time window were assessed. The results show that the three drought indices (Z-score, EDI, and VCI) characterize and identify the historic drought years and the drought-prone parts of the basin. A two-month lag time between the peak rainfall and VCI was observed for the majority (72%) of meteorological stations. Relatively large weights were assigned for EDI (0.5) and Z-score (0.4) in the combined drought index. The EO-CDI correlated well for all the crops with the maximum correlation coefficient of 0.8 obtained with Sorghum.

Overall, for the first time, an extensive evaluation of existing drought indices was undertaken for the Upper Blue Nile basin, through characterizing and assessing the historic drought events. This confirmed that also the UBN Basin faced droughts in the past and needs thorough drought

research and drought monitoring. The developed impact-based CDIs and multiple linear regression models have shown to be effective in indicating historic drought events in the Upper Blue Nile. The impact-based CDI could potentially be used in the future development of drought monitoring in the UBN Basin and support decision making in order to mitigate adverse drought impacts.

The same approach of developing an impact-based CDI optimised for a (sub-)catchment or area, can be applied to other regions of Ethiopia. The approach employed to test the influence of record length on the SPI drought category proved its success in validating the use of a large number of additional meteorological stations with a shorter record length for spatial drought analysis in the UBN Basin. Hence, this approach can be applied to other regions facing challenges of insufficient record length.

The results of the Earth Observation-based CDI showed that Earth Observation information can be used as an alternative data source in drought monitoring for the ungauged and data scarce regions like UBN Basin. Moreover, developing a grid-based CDI using gridded data sets is important to analyse the spatial extent and details of drought, and will be addressed in our future studies. The evaluation of the existing drought indices in this study was carried out using drought characteristics data (onset date and severity) obtained from a global data source. It is recommended to check for availability of measured and local-scale data when adapting the same evaluation procedure for other study areas.

List of symbols

Symbol	Description	Dimension
χ^2	Chi-squared	
α	Shape parameter	
β	Scale parameter	
$\Gamma(\alpha)$	Gamma functions	
G(x)	Cumulative probability excluding probability of zero precipitation	
H(x)	Cumulative Probability including probability of zero precipitation	
q	Probability of zero precipitation where gamma distribution becomes undefined	
R^2	Coefficients of determination	
Q_{obs}	Observed flow	$[m^3/sec]$
Q_{sim}	Simulated flow	$[m^3/sec]$
WS	Monthly water stress ratio	
Z	(n x p) matrix	
n	Number of observations	
X	(n x p) matrix of the observation data	
E	(p x p) matrix of eigenvectors of the correlation matrix	
σ_k	Sample standard deviation	
r	Relative change in the parameter value	
v	Absolute change in the parameter	
S	Drought severity	
M	Mean drought intensity	
D	Drought duration	
R	Correlation matrix	
R_a	Extra-terrestrial solar incident radiation	$[Wm^{-2}]$
μ	Mean	

List of acronyms

ADI	Aggregate Drought Index
AET	Actual evapotranspiration
a.s.l	Above sea level
CDI	Combined drought index
CHIRPS	Climate Hazards Group Infrared Precipitation with Stations
CSA	Central Statistical Agency
ECMWF	Center for Medium Range Weather Forecasting
EDI	Evaporative Drought Index
ENTRO	Easter Nile Technical and Regional Office
EO-CDI	Earth observation based combined drought index
ET	Evapotranspiration
ETDI	Evapotranspiration Deficit Index
fAPAR	Fraction of Absorbed Photo synthetically Active Radiation
LAI/FPAR	Leaf Area Index/Fraction of Photo synthetically
MWSj	Long-term median of water stress of month j
maxMWSj	Long-term maximum water stress of month j
minWSj	Long-term minimum water stress of month j
LST	Land Surface Temperature
MODIS	Moderate Resolution Imaging Spectroradiometer
NDVI	Normalized Differences Vegetation Index
$NDVI_{min}$	Absolute multi-year minimum
$NDVI_{max}$	Multi-year maximum NDVI
NMA	National Meteorological Agency
NSE	Nash-Sutcliffe efficiency
BIAS	Bias
PCA	Principal Component Analysis
PDF	Probability Density Function
PDSI	Palmer Drought Severity Index
PET	Potential evapotranspiration
RF_i	Decadal rainfall at a particular event
EDDI	Evaporative Demand Drought Index
ESI	Evaporative Stress Index
SEBAL	Surface Energy Balance Algorithm for Land
SEBS	Surface Energy Balance System
SMDI	Soil Moisture Deficit Index
SPEI	Standardized Precipitation Evaporation Index
SPI	Standardized Precipitation Index
SRI	Standardized Runoff-discharge Index
St. Dev	Standard deviation
SWAT	Soil water assessment tool
T_{max}	Daily maximum air temperature
T_{mean}	Daily mean air temperature
T_{min}	Minimum air temperature
UBN	Upper Blue Nile
VCI	Vegetation Condition Index
ω_{EDI}	Weights of the Evaporative Drought Index
ω_{ETDI}	Weights of Evapotranspiration Deficit Index

ω_{SPI}	Weights of Standardized Precipitation Index
ω_{SPEI}	Weights of Standardized Precipitation Evaporation Index
ω_{SRI}	Weights of standardized runoff-discharge index
ω_{VCI}	Weights of Vegetation Condition Index
ω_{Zscr}	Weights of the Z-score

Table of contents

1. Introduction

1.1 Background

Drought is one of the world's costliest natural hazards characterized by a significant decrease of water availability during a prolonged period of time over a large area. It causes, for example, an average of 6-8 billion USD damage costs every year and affects society, economy and human lives in the United States (Sheffield and Wood, 2012; Keyantash and Dracup, 2004; Wilhite and Buchanan-Smith, 2005; Wilhite et al. 2007). In Ethiopia, drought is a frequently recurring phenomenon often accompanied by very serious and diversified impacts on human lives and environment (Tagel et al. 2011). Drought in the year 1984/85 caused a million people to lose their lives, destroyed crops and livestock, and forced millions of people into displacement and destitution (Tagel et al. 2011). More specific figures from recent drought episodes in Ethiopia illustrate the magnitude of drought associated impacts. For example, the drought of 2003 led to the worst famine since the mid-1980s, which affected 13.5 million people (Wagaw et al. 2005) and caused large devastation in terms of lives and economical losses. About 20 million people were estimated suffering from food insecurity in East Africa in 2009 (Sheffield and Wood, 2012). The year 2009 is also recorded as one of the severe drought years in Ethiopia; 6 million people were affected and needed food aid from the international emergency services (Sheffield and Wood, 2012). Another severe drought that covered major parts of the country occurred recently, in 2015. The estimate showed that more than 4.5 million people needed food aid and emergency services (http://www.theguardian.com/global-development/2015/aug/25/un-ethiopia-need-food-aid-after-poor-rains). The historic drought events in Ethiopia were highly linked with the occurrence of El Niño weather phenomenon and the 2015 drought was a recent example.

Thus, drought management has become an important issue in the drought-prone parts of Ethiopia in order to reduce the adverse impacts of drought hazards and potential disasters through drought prevention and mitigation measures as well as preparedness. The resulting drought impacts were devastating in areas where agriculture is the main driver of the economic income of the society and rain-fed agriculture is the main dominant practice. The usual steps taken by the government and donors to cope with drought impact and resulting disaster is to follow impact assessment, response, recovery and reconstruction activities to recuperate the region to the pre-disaster state. These actions usually start with assessing the past drought

conditions using drought indices. Drought vulnerability and drought-associated risks can be reduced by developing a drought event management plan and by developing a robust drought monitoring and early warning system. With its dependence on agriculture, for Ethiopia development of crop-yield prediction models could further support drought impact mitigation. The likelihood of the increase of drought frequency and severity in Ethiopia as a result of the changing environment and population growth reinforces the need for the development of drought monitoring and forecasting (Ramakrishna and Assefa, 2002, Edossa et al. 2009, Araya et al. 2010, Tagel et al. 2011).

Drought assessment often employs the measure of the shortfall of the hydro-meteorological parameters such as rainfall, streamflow, soil moisture etc. from the long-term average value. Drought indices are currently used to measure this shortfall and help to derive a numeric value which is more meaningful than the raw data in the decision making process. However, defining an appropriate drought index is a challenging task. One of the main challenges in developing such an index for Ethiopia and other developing countries is a lack of hydro-meteorological input data. Although measured data for some of the variables are freely available for use, the lack of good spatial representation posed by the sparse location of gauging stations is one of the main limitations. For some important variables, it is also inherently difficult to obtain measurements, e.g. for actual evapotranspiration and soil moisture. These two variables are used to characterize agricultural drought, and yet field measurements are often difficult because of the inherent high spatial and temporal variability. However, hydrological models and Earth observation are currently used to simulate and quantify these variables (Narasimhan and Srinivasan, 2005). Therefore, hydrological modelling and Earth observation are used as an alternative source of information and input data in developing the suitable drought index in this study.

The majority of the existing drought indices are region-specific. Their suitability and performance have to be evaluated and tested before using them for a drought study in another area. Moreover, the drought indices have their own merits and weaknesses, and they are specific to drought type. Most often, drought monitoring that uses several drought indices has the better capability of properly characterizing the drought condition than using a single index. Combining multiple existing drought indices into a comprehensive combined drought index for monitoring is more advantageous than developing or using a new single drought index (Niemeyer, 2008). Therefore, extensive evaluation of the existing drought indices and developing the combined drought index (CDI) through potential use of the existing drought

indices is vital for researching the ways to mitigate future drought impacts, e.g. on crop yield reduction.

1.2 Drought monitoring

Drought monitoring includes the wide application of the drought indices that measure the deficit of hydrologic cycle components as compared to the long-term mean (Trambauer et al. 2014, Barua et al. 2011; Hayes et al. 2004). The long-term mean is considered as a reference to measure the deviation of a particular event. Accordingly, meteorological drought is defined based on the degree of dryness or deviation from normal or average amount of rainfall for a prolonged period (Wilhite, 2000; Hayes et al. 2011). Examples of meteorological drought indices are Standardized Precipitation Index (SPI) (McKee et al. 1993), Percent Normal Drought Index (PNDI) (Willeke, 1994), Standardized Precipitation and Evaporation Index (SPEI) (Vicente-Serrano et al. 2010), the Precipitation Decile Index (PDI) (Gibbs, 1967), and the Weighted Anomaly Standardized Precipitation (WASP) (Lyon, 2005).

The deficit in meteorological parameters, mainly rainfall, can be considered as a precursor for the deficit of other hydrological water cycle components (river flow, ground water flow, reservoir storage etc.) known as hydrological drought. Some examples of the hydrological drought indices are the Surface Water Supply Index (SWSI) (Shafer, 1982), Streamflow Drought Index (SDI) (Nalbantis, 2008), Standardized Runoff-Discharge Index (SRI) (Shukla and Wood, 2008) etc. The deficit of the readily available water for plant use to satisfy its water demand is often defined as agricultural drought. Examples of agricultural drought indices are Palmer Drought Severity Index (PDSI) (Alley, 1984), Soil Moisture Deficit Index (SMDI) (Narasimhan and Srinivasan, 2005), Evapotranspiration Deficit Index (ETDI) (Narasimhan and Srinivasan, 2005), the Crop Moisture Index (CMI) (Palmer, 1968), Reclamation Drought Index (RDI) (Weghorst, 1996), etc.

Drought monitoring is often carried out by using indices based on water balance calculation and statistical analysis of the time series of input data. The water balance based drought indices require several climatic and physical variables to quantify the water deficit at the plant root zone. Examples of such indices are the PDSI, SMDI, ETDI, CMI, SWSI and RDI. The main limitations of the water balance based indices are that they require several input variables and that their calculation is not trivial. The statistical analysis based drought indices usually use one parameter, such as rainfall, and seldom two parameters, such as rainfall and temperature to characterize drought. In this category, the most commonly used indices are the SPI, PNDI,

SPEI, PDI, and WASP. The limitations of the statistical methods are a lack of full compliance with the fundamental requirements of the drought definition, since they consider only one or two parameters. They have difficulty in showing the persistence of drought and they require long-term continuous input data.

The calculation procedure of both the water balance and statistical techniques is point-based, corresponding to the locations of the meteorological stations. Hence, the spatial interpolation from the point-based information sometimes lacks appropriate representation, particularly in areas were meteorological stations are sparsely located. The Inverse Distance Weight (IDW), Kriging and other interpolation techniques are commonly used to produce the spatial interpolation of the stations based data (Shepard, 1968; Bayraktar, 2005). Hence developing the combined drought index that makes use of hydro-climatic, model estimates of soil moisture and evapotranspiration and the Earth observation derived information is vital to monitor drought in a more efficient way (Sepulcre et al. 2012). However, reliability of these techniques is still dependent on the availability of a large number of stations, which is perhaps the main challenge in developing countries. Earth Observations data and hydrological models have been recently used to take the advantage of better spatial representation particularly in data scarce regions like the UBN Basin.

A number of researchers have suggested that instead of developing a new single drought indicator, it is worthwhile to combine the existing drought indices into a comprehensive and integrative drought index (Niemeyer, 2008; Balint et al. 2013; Vyas et al. 2015; Sepulcre et al. 2012). Balint et al. (2013) developed a combined drought index for Kenya in the Horn of Africa. Three drought indices, i.e. precipitation deficit index (PDI), temperature deficit index (TDI) and vegetation deficit index (VDI) were combined to develop the combined drought index (CDI). The combination was done through assigning weights for each index subjectively. The paper, however, does not show any objective explanation as to how the weights are assigned to each index. (In this study, the largest weight (50%) was assigned for rainfall based drought index, in this case PDI, and the remaining 50% of the weight was assigned equally for the other two indices, TDI and VDI.)

Vyas et al. (2015) developed an Earth Observation based combined drought index. Earth observation (EO) based rainfall and Normalized Differences Vegetation Index (NDVI) data were considered to calculate the Standardized Precipitation Index (SPI) and NDVI anomaly respectively. The combined drought index was developed based on the relative weight assigned

in a qualitative way. An attempt was made to assign the weight between 0.1 to 0.9, by optimizing validation with ground truth rainfall based SPI, yield data and other Earth Observation based parameters such as land surface temperature, carbon productivity, and evapotranspiration. The procedure followed to assign the weight appears to have a higher objectivity compared to the Balint et al. (2013) approach. However, this procedure is not adaptable for more than two drought indices.

Sepulcre et al. (2012) proposed a combined drought indicator that combines SPI, the anomalies of soil moisture and the anomalies of the fraction of Absorbed Photo synthetically Active Radiation (fAPAR). The combined drought index gave a synthetic and synoptic overview of the drought situation using three classification schemes such as "watch" when a relevant precipitation shortage is observed, "warning" when this precipitation shortage translated into a soil moisture deficit and "alert" when these two conditions are accompanied by unfavourable vegetation vigour (Sepulcre et al. 2012). The combining approach followed in the Sepulcre et al. study depicts a sequential way of drought monitoring.

An objective approach of developing a CDI was carried out in USA and Australia using the principal component analysis (Keyantash and Dracup, 2004; Barua et al. 2009). The PCA based aggregate drought index (ADI) was developed to monitor drought in three diverse climatic regions in California, USA (Keyantash and Dracup, 2004; Keyantash and Dracup, 2002). The result supported the potential use of PCA based ADI to monitor drought. Barua et al. 2009 compared the PCA based ADI with two other drought indices in the Yarra River Catchment in Australia (Barua et al. 2009; Barua and Perera, 2011). It was purported that the ADI, which aggregates several hydrologic variables, outperformed other indices on detecting the historical drought events. These studies showed the potential of the PCA approach to aggregate hydrologic variables that are related to meteorological, agricultural and hydrological drought.

1.3 Problem statement

The Upper Blue Nile (UBN) is an important basin in the Nile region in terms of generating and supplying the annual discharge that satisfies the water demands of the downstream riparian countries (Conway, 2000; Conway, 1997). The basin may generally not be perceived as being drought-prone because of the large amount of rainfall it receives annually and its location in the highlands of Ethiopia where evaporation losses are minimal. Although not well documented, the northeastern part and some pocket areas towards the central part of the basin have been reported to be historically associated with drought (Conway, 2000).

The emerging climate change and occurrences of drought are threatening natural processes in the basin that possibly affect the sustainability of the water resources. There are other factors than drought that aggravate the scarcity of the water resources in the basin. The large and rising population results in greater competition for the scarcity of the available fresh water resources.

Thus far, few drought studies have been conducted using the historic time series of hydro-meteorological variables at a local level (e.g. zones or basins) in Ethiopia (Ramakrishna and Assefa, 2002, Edossa et al. 2009, Araya et al. 2010, Tagel et al. 2011). There is a lack of studies that aim to evaluate the existing drought indices in the UBN Basin. Moreover, we could not find reported studies aiming at developing a CDI for the UBN Basin or, related to the most important drought impact for the basin: on modelling reductions in crop yield.

1.4 Research objectives

The main objective of this research is to develop an impact-based combined drought index (CDI) and prediction model of crop-yield anomalies for the Upper Blue Nile basin. An impact-based CDI is defined as a drought index that optimally combines the information embedded in other drought indices for monitoring a certain impact of drought.

The following specific objectives were defined:

- Investigate the effect of data record length on drought assessment to validate the use of meteorological stations having a relatively short record length in the drought analysis.
- Investigate the spatial and temporal variation of meteorological droughts in the UBN Basin.
- Evaluate and compare the performance of six drought indices, i.e. Standardized Precipitation Index (SPI), Standardized Precipitation Evaporation Index (SPEI), Evapotranspiration Deficit Index (ETDI), Soil Moisture Deficit Index (SMDI), Aggregate Drought Index (ADI), and Standardized Runoff-discharge Index (SRI) with respect to identifying historic drought events in the UBN Basin.
- Develop an impact-based Combined Drought Index (CDI) with weights optimized to monitor crop yield anomalies.
- Develop a prediction model of crop yield anomalies, based on the impact-based CDI and individual drought indices.
- Assess the potential of an impact-based CDI using Earth Observation data as the main input.

1.5 Main steps in research methodology

Methodology of this research employed various methods of hydroinformatics - data analysis, statistics, optimisation and modelling, and included the following steps:

1. The SPI for several meteorological stations was determined in the UNB Basin, and it was analysed whether record length has an impact on drought assessment. The record length in the majority of the stations is relatively short (1975-2009). There are only 14 weather stations that have a longer record length (1953 – 2009). For these latter stations, two data withholding procedures were applied. The first data withholding experiment was that one year of data was taken out starting from 1953, and then SPI values were calculated. The data withdrawing was repeated up to the year 1974 when most of the other stations started recording. Then, the SPI values for a particular drought year between 1975 and 2009 were checked whether or not the values indicate the same drought category. For cross-validation of the results of the first experiment, in the second procedure, the one year of data was withdrawn one by one starting from the middle of the record length (from 1970 to 1988).
2. Spatial and temporal analysis of meteorological droughts in the UBN Basin was done using SPI. Since drought is a regional phenomenon, the point-based SPI time series values of each meteorological station have been interpolated using the inverse distance weighted (IDW) method to assess the spatial extent of drought in the basin. In order to identify the area most frequently struck by drought, the frequency of occurrences of drought was compared by taking the ratio of the number of drought years to the total number of years used in the analysis.
3. Comparison and performance analyses of a range of individual selected drought indices, i.e. SPI, SPEI, ETDI, SMDI, ADI, and SRI, were carried out using correlation analysis. For the SPI, SPEI, and SRI indices for five different aggregation periods were derived, namely 1-, 3-, 6-, 9-, and 12-months. Thus, we have a total of 18 indices; five each from the SPI, SPEI, and SRI and one each from the ETDI, SMDI, and ADI. Next, Pearson correlation coefficients were derived for paired time series values of drought indices. Each drought index is paired with every other drought index, resulting in an 18 by 18 correlation coefficient matrix. The percentage of drought months was calculated by taking the ratio of the total number of months that show drought condition (including mild, moderate, severe, and extreme drought) with the total events in the study period. The comparison of the drought indices based

on drought characteristics, such as percentage of drought months, maximum intensity, and drought duration, was analysed for the selected stations that are representing the study area. The performance of the drought indices was evaluated with respect to identifying onset, severity, and duration of the historic drought events. The information on historic droughts considered in this study was obtained from EM-DAT (http://www.emdat.be/database).

4. CDIs were developed through assigning weights by following an objective approach for the selected drought indices, using principle component analysis (PCA) and impact-based random search optimisation: PCA combines the indices through calculating the correlation coefficient matrix between each index followed by computing the eigenvalues that could be used as the weight in developing CDI. Random search for the optimal weights employed more than 60,000 iterations to identify the combination of finding weights with maximum correlation with crop yield anomaly (i.e. for teff, maize, barley, and sorghum). The CDIs developed using these two techniques were compared.
5. Crop-yield anomaly prediction models were developed based on the impact-based CDI, and compared with a crop-yield prediction models based on the six individual drought indices. Crop yield anomaly data for the UBN Basin was obtained from the Central Statistical Agency (CSA) of Ethiopia for the period from 1996 to 2009. The crop yield prediction model was developed using multiple linear regression equations between the drought indices and each cereal crop (i.e. teff, maize, barley, and sorghum). In the linear regression model, the crop yield anomaly was used as a predictand variable (variable being predicted) whereas the drought indices including both the CDI and the selected drought indices were used as a predictor variable.
6. Impact-based optimal CDI and crop-yield anomaly prediction models were developed using drought indices based on Earth Observation data. Indices include precipitation Z-score, EDI and VCI. The Z-scores were calculated using grid-based CHIRPS rainfall data. The EDI calculation used the MODIS ET data as a main input. The VCI was derived using NDVI. The CDI was developed using the impact-based approach, with random search for establishing the optimal weights. The same approach was adopted as described above in developing the crop-yield anomaly prediction model.

The research steps and methods followed are summarised in Figure 1.1.

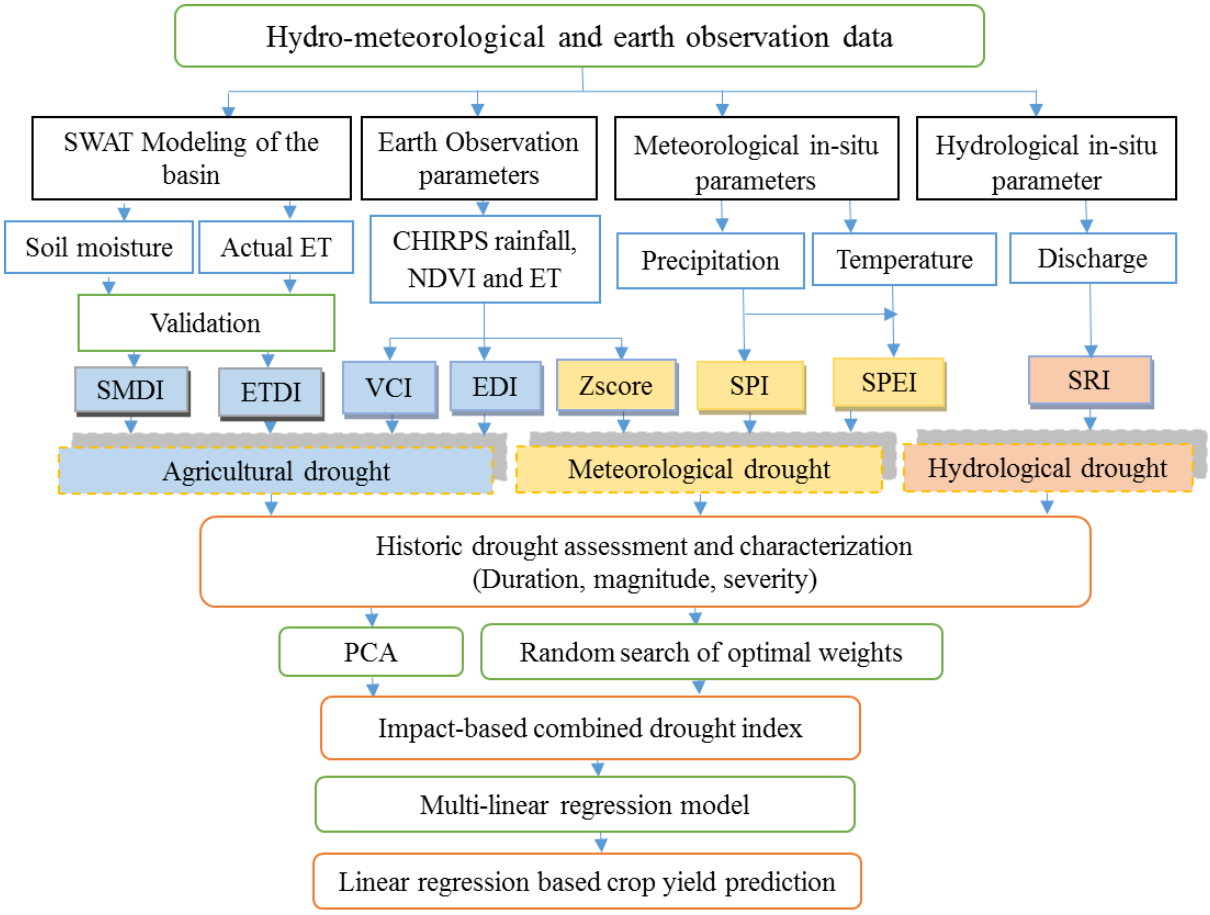

Figure 1.1: Flow chart of the research steps.

1.6 Research significance and innovation

1.6.1 Research significance

This research contributes to drought analysis and future drought monitoring in the UBN Basin. Contributions to the field of drought monitoring are outlined below:

- Assessing the effect of the rainfall record length on the drought category is one of the significant outcomes of this research. This assessment contributes towards understanding the constraints and possibilities of using meteorological records of limited duration, which is the case in the study area and other developing countries.
- Drought assessment using multiple drought indices is seen as a useful contribution in terms of characterizing and identifying the occurrence of the meteorological, agricultural and hydrological droughts.
- The regression model that relates the combined drought index and the crop yield anomaly is a useful technique towards developing drought preparedness and early warning system.

1.6.2 Innovation

The main innovate components of this study are outlined below:

- Development of the impact-based CDI method.
- The crop yield prediction regression model linking combined drought index and the crop yield anomaly. This model could potentially be used for the early indication of the crop yield reduction as a result of drought in the basin. To the best of our knowledge, no such models have been developed for the study area before.
- Assessing the effects of the data length on the SPI drought index. Results of this analysis are helpful for the basin and the method can also be used in any other basin having the data length problem.

1.7 Description of the study area

The UBN Basin is located in the northwestern region of the country between 7º 40' N and 12º 51' N latitudes, and 34º 25' E and 39º 49' E longitudes (Figure 1.1). The basin contributes the large share of water to the main Nile (60% of the Nile total flow) and covers a total area of 176,000 km^2 upstream of the Ethiopia-Sudan border (Conway, 2000; Conway, 1997). It originates from Lake Tana and travels 6853 km before it empties in to the Mediterranean Sea. The topography of the basin signifies two distinct features: the highlands with rugged mountainous areas in the central and eastern part of the basin, and the lowlands in the western part of the basin. The altitude in the basin ranges from 492 m in the lowlands, up to 4261 m in the highlands. Whilst the highlands are the main source of water, the lowlands have expanses of flat lands through which the accumulated flow travels from the highlands to the lower riparian countries. The estimates of mean annual temperature in UBN Basin vary based on the data period considered by the researchers. According to Kim et al. (2008), the mean annual temperature (data years 1961-1990) is estimated to be 18.3 ºC with seasonal variation of less than 2 ºC. Tekleab et al. (2013) reported that the mean annual temperature (period 1995 - 2004) ranges from 13ºC in southeastern parts to 26°C in the southwestern part near the Ethiopian-Sudanese border. The annual rainfall ranges from 787 mm to 2200 mm, with the highlands having the highest rainfall ranging from 1500 to 2200 mm and the lowlands receiving less than 1500 mm (Conway, 2000; Kebede et al. 2006; Yilma and Awulachew, 2009). Following the seasonality of the rainfall, the flow in the UBN River is also seasonal. High flow generates from all the tributary rivers during the main rain season (June to September) and low flow during the dry season (October to May).

The land cover in the basin is dominated by dry land crop, pastures, savannah, grassland, woodland, water bodies and sparsely vegetated plants (Gebremicael et al. 2013). Volcanic rock and Precambrian basement rock are most widely available geological formations in the basin, and small areas are covered by sedimentary rock (Conway, 2000). The dominant soil types are Leptosols and Alisols (21%), Nitosols (16%), Vertisols (15%), and Cambisols (9%) (Betrie et al. 2011).

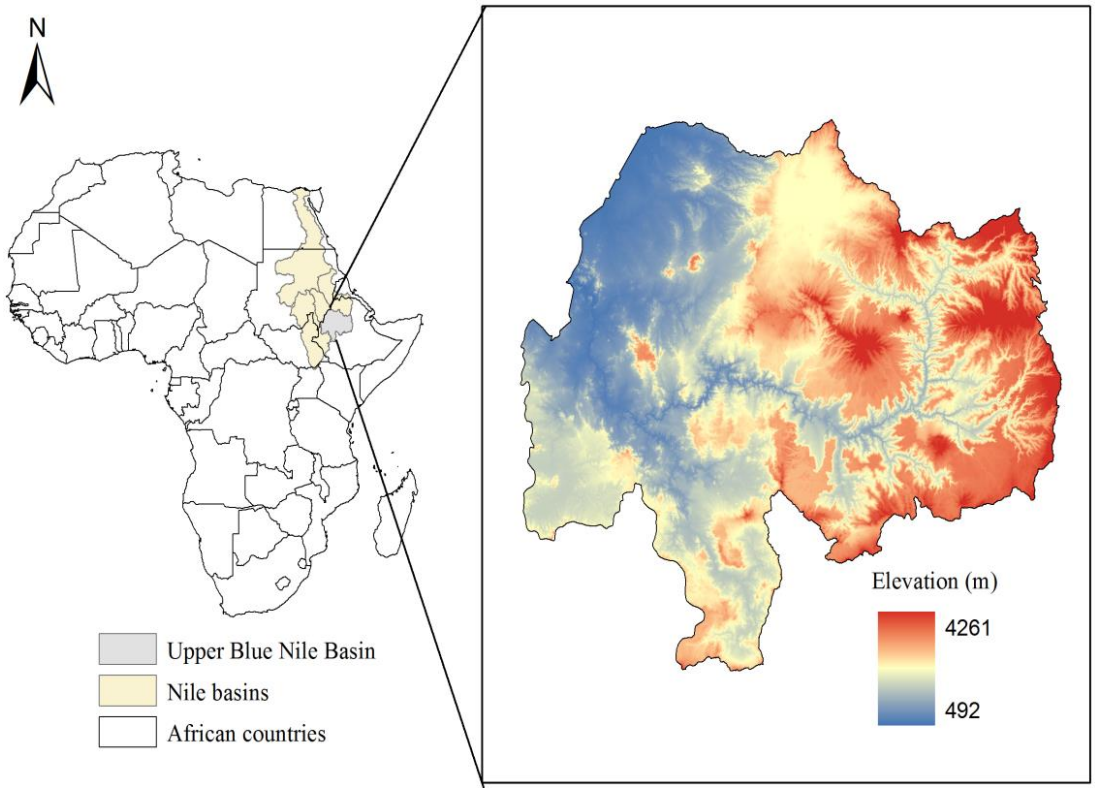

Figure 1.2: Location and elevation map of the Upper Blue Nile basin.

1.8 Dissertation structure

Chapter 2 presents the spatio-temporal assessments of the meteorological drought under the influence of varying record length. The effect of the data length on the drought category of the SPI drought index is discussed in detail in this chapter. Statistical procedures followed to identify the best probability density function (PDF), and to test the homogeneity, and consistency of the rainfall data of each meteorological station are presented in this chapter.

Chapter 3 is devoted to the inter-comparison of the performance of six drought indices to assess and characterise historic drought events in the basin. The SWAT hydrological modeling of the basin that aimed to simulate the soil moisture and evapotranspiration data, is discussed in this chapter.

Chapter 4 discusses the procedure followed to develop the combined drought index and the prediction models to monitor drought-related crop yield reduction in the basin. The principal component analysis (PCA) and impact-based random search of the optimal weights for the drought indices that are used to develop the combined drought index are discussed in detail in this chapter.

Chapter 5 presents the potential use of the Earth observation data for developing the combined drought index from three EO-based drought indices, i.e. Z-score, Evaporative Drought Index (EDI) and the Vegetation Condition Index (VCI), and for developing the linear regression model with the crop yield anomalies. The impact-based optimisation approach presented in Chapter 4, was used to develop the combined drought index.

Chapter 6 summarises the findings of this dissertation. It presents the conclusions of the research and highlights the recommendations for future research work on the topic.

2. Spatio-temporal assessment of meteorological drought under the influence of varying record length[1]

2.1 Introduction

This chapter illustrates the spatial and temporal characteristics of historic meteorological drought events, and the effects of the data length on the SPI drought category in the Upper Blue Nile (UBN) basin. The study first investigates whether climate records with shorter-length affect the assessment of drought events in terms of drought categories (e.g. moderate, severe, extreme drought), before making use of all available observations to assess the spatial and temporal distributions of drought over the UBN Basin. To have long-term monthly rainfall data has been a prerequisite for carrying out drought analysis and modelling for many studies. While the presumption is widely followed, there has been a lack of studies on the effect of data length, which in fact hampers researchers from using records with shorter length, or leaves them in uncertainty if their conclusions are valid.

The Standardized Precipitation Index (SPI) was used to study the effect of the length of records and to characterize drought in the UBN Basin. The SPI is a probability index that uses monthly rainfall data as input. It has been demonstrated to perform well in comparing droughts across different regions (Guttman, 1998). The SPI also gives better spatial standardization than other drought indices, such as Palmer Drought Severity Index (PDSI) in analysing extreme drought events (Sönmez et al. 2005). The SPI has been widely applied and tested in many watersheds. However, very few studies have been conducted in different parts of Ethiopia to analyse drought using the SPI. Edossa et al. (2009) reported the temporal and spatial analysis of meteorological and hydrological droughts for the Awash basin of Ethiopia, applying the SPI for the assessment of meteorological drought using monthly rainfall data from 1963 to 2003. The study showed the potential benefits of the SPI for drought assessment and examined the lag time between the hydrological and meteorological droughts. Tagel et al. (2011) evaluated the spatial and temporal variability of drought using the SPI and the Vegetation Condition

[1] *Based on*: Bayissa, Y.A., Moges, S.A., Xuan, Y., Van Andel, S.J., Maskey, S., Solomatine, D.P., Griensven, A.V., and Tadesse, T., 2015. *Spatio-temporal assessment of meteorological drought under the influence of varying record length: the case of Upper Blue Nile Basin, Ethiopia*. Hydrological Sciences Journal, v. 60, No. 11, p.1927-1942.

Index (VCI) for the Tigray Zone located in the high lands of Ethiopia. The Tigray Zone is proximal to the UBN Basin and located in the Northern part of Ethiopia. The study demonstrated that the large part of the study area is prone to drought. Further, the results showed a time lag between the period of the peak of Vegetation Condition Index (VCI) and precipitation values (Tagel et al. 2011). Cancelliere et al. (2007) used stochastic techniques for seasonal forecasting of the SPI and showed the importance of the SPI for drought assessment and forecasting. Bonaccorso et al. (2003) analysed drought for the island of Sicily using the SPI and showed that the entire island is characterized by drought variability with a multi-year fluctuation and a tendency towards drier periods from the 19-70s onward. Generally, many studies have been conducted using the SPI in different parts of the world for drought assessment and forecasting (Guttman, 1998, Yamoah et al. 2000, Cancelliere et al. 2007, Livada and Assimakopoulos, 2007, Patel et al. 2007, Wu et al. 2007, Khan et al. 2008, Li et al. 2008). However, testing the effect of data length and incorporating the findings on the spatio-temporal assessment of drought using the SPI in Ethiopia has not yet been carried out. The overall objective of this study is to analyse and assess the spatio-temporal variation of drought in the UBN Basin, Ethiopia, using the SPI. Moreover, this study analyses the effect of the length of rainfall time series data used on drought assessment with the aim to validate the use of a large number of stations with relatively shorter record length to investigate drought characteristics of the UBN Basin.

2.2 Stations selection and data analysis

The monthly rainfall recorded by local meteorological stations was the basis upon which the SPI and drought categories were calculated. The rainfall records of 45 stations were collected on monthly time steps from the National Meteorological Service Agency of Ethiopia. Most of these stations are located inside and nearby the UBN Basin (Figure 2.1). However, few of the other stations used in this study are located in different watersheds that have distinct agro-climatic zones. These supplementary stations were used to study the effect of data length on the drought category. The years covered by the records of each station range from 1953 to 2009. While some stations cover the whole period, others start from the 1970s. Regardless of the data length, the quality of the rainfall record needs to be assured prior to applying the data in any drought study. The double mass curve technique was applied to check the consistency and homogeneity of each station. The annual rainfall data for each of the 45 stations was first cumulated in chronological order. The pattern of the mean of the cumulative rainfall is then used to test individual station records. The cumulative rainfall of each station was plotted

against the mean of the cumulative rainfall. A break in the slope of the plot is used as a criterion to identify a change in the precipitation regime.

This criterion was used in this study to select the meteorological stations considered for the spatio-temporal assessments of drought. The double mass curve produced for the Debremarkos station (Figure 2.2) demonstrates the consistency of the rainfall record. The plot shows the consistent record of rainfall data in this station and a break in slope was not observed throughout the record length. A similar procedure is applied for the other stations and similar results were obtained. The results of the data quality assessment led to the choice of 37 rainfall stations data for further use. There was a maximum of four years of missing data in some of the selected stations. No techniques were applied to fill the gaps. Instead, the missing data was omitted during the SPI calculation.

In this study, two distinctive groups of meteorological stations supplied the monthly rainfall data. The first group includes 14 meteorological stations with relatively long records (i.e. over 50 years), located in different parts of the country and different rainfall regions. This group of stations was used to test the effect of data length on drought category. The second group comprises a total of 29 stations located inside and in a close proximity to the UBN Basin. Out of the 29 stations, six stations had longer data length and also were used in the first group. The other 23 stations had a shorter record length (i.e. 35 years, from 1975 to 2009). The second group of the stations was used to study the spatial and temporal assessment of drought in the UBN Basin.

In the first group, most of the meteorological stations have monthly rainfall data and the data recording began in the early 1950's, with two exceptions (Mekelle and Debreziet) where recording started in1960. The Debremarkos and Gondar stations are located inside the basin whereas the rest of the other stations are located outside the UBN Basin boundary (Figure 2.1).

The analysis of the spatial and temporal assessment of droughts was made with the second group of 29 stations with monthly rainfall data from 1975 to 2009. As shown in Figure 2.1, most of these stations are located within the UBN Basin except five stations that are located just outside of the basin. Although there are many meteorological data recording stations in the basin, getting a long-term record length was one of the main challenges that prompted for the necessity of this study.

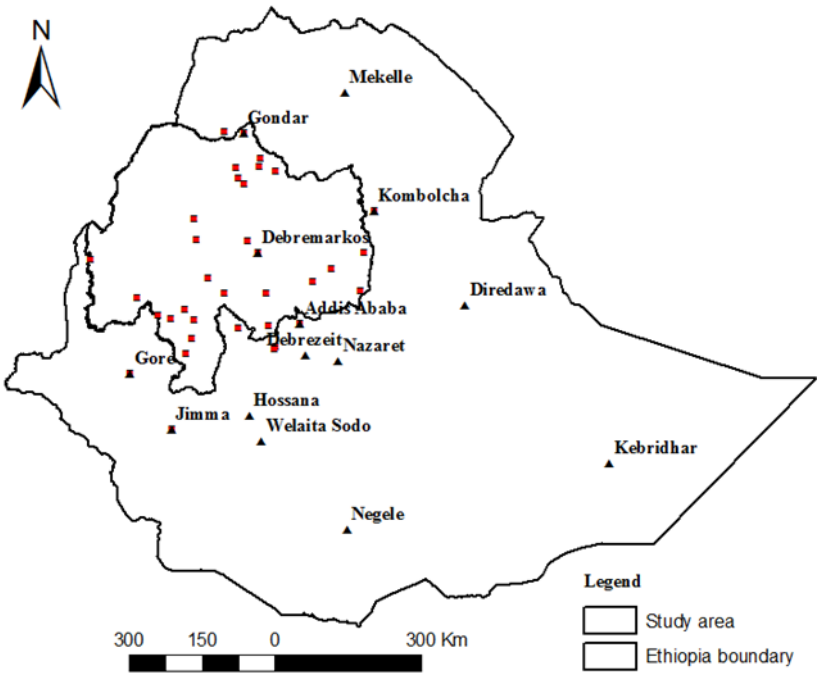

Figure 2.1: The location map of the rainfall stations. Note: the stations represented by triangular shape and labeled with their name were used to study the effect of the data length. Stations represented by rectangular shape were used to study the spatial variability of droughts.

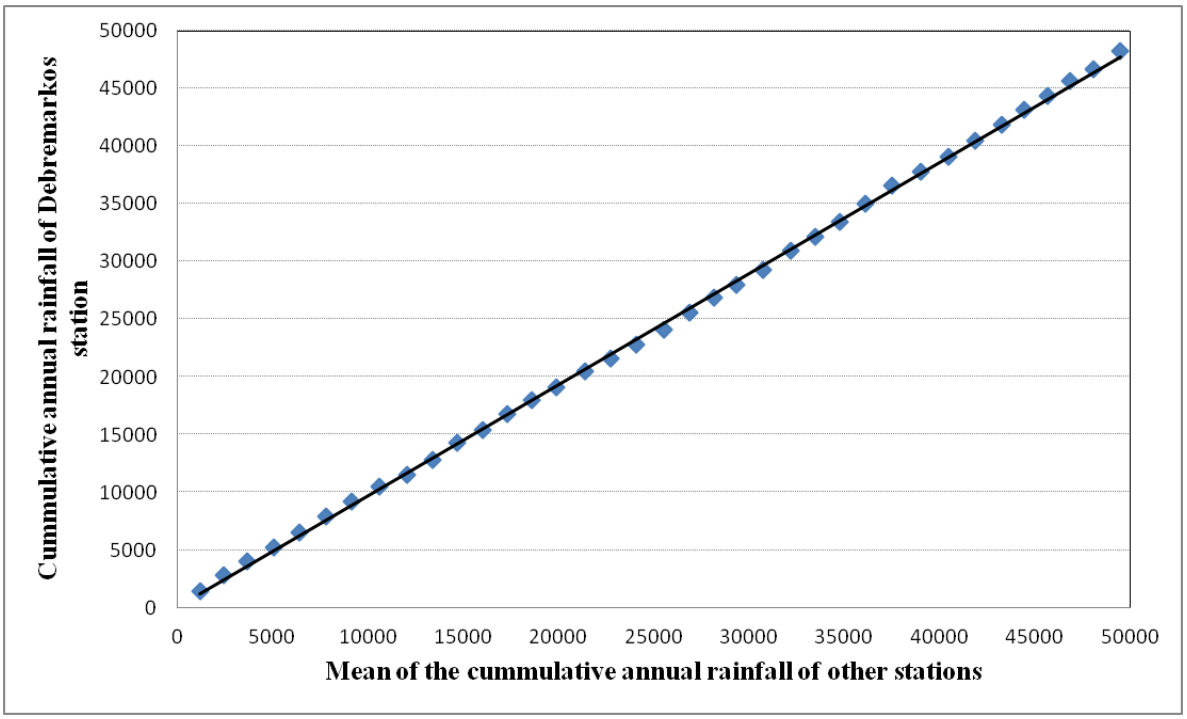

Figure 2.2: The double mass curve produced for the Debremarkos station and used to demonstrate the consistency of the rainfall record.

2.3 Selection of the Probability Distribution Function (PDF) for the Standardized Precipitation Index (SPI)

The effect of the record length on the drought category and the spatial and temporal assessment of droughts were performed using the SPI. This index utilizes the current and historic rainfall data to compute its value, which is proportional to the deviation from the long-term average rainfall. The computation employs fitting the probability density function to the frequency distribution of precipitation summed over the period of interest, in this case from 1970 to 2009 (Khan et al. 2008, Moreira et al. 2008, Tagel et al. 2011). Distributions were built separately for each month and for each location. Each probability density function was then transformed into the standardized normal distribution. Thus, the SPI is said to be normalized in location and time. The conversion of cumulative probability to the standard normal random variable employs fitting the curves for all stations at all-time scales and for each year. This process can be cumbersome and the SPI value is more easily computed using an approximation method proposed by Abramowitz and Stegun, (1965) as shown in equations 2.7 and 2.8. Once standardized, the values of the anomaly of the SPI are categorized based on the McKee et al. (1993) classification as shown in Table 2.1.

Table 2.1: SPI values that show the different categories of drought severity.

SPI Values	Drought category
−2.00 and less	Extreme drought
−1.50 to -1.99	Severe drought
−1.00 to -1.49	Moderate drought
0 to -0.99	Near-normal or mild drought
Above 0	No drought

The SPI calculation involves the selection of a probability distribution function (PDF) that fits best with the "belg", the "kiremt", and annual rainfall seasons of each meteorological station. Belg is a short rainfall season (February to April) whereas kiremt is the main rainfall season (June – August) in the basin. The commonly used statistical probability distributions such as Normal, Gamma, Log-Pearson and Weibull were tested for each station in the study area. We present the detailed calculation procedure of the Gamma distribution below and the details about the other models can be found in the following literature sources (Abtew et al. 2009; Hanson and Vogel, 2008; Sharma and Singh, 2010). Each PDF was then fitted to the belg, kiremt and annual rainfall and the goodness of fit of each PDF was evaluated using the

Kolmogorov-Smirnov test, Anderson Darling test and Chi-squared test ($\chi 2$) (Sharma and Singh, 2010). We used the EasyFit software to fit the probability distribution functions to the rainfall data for each of the stations. Overall, the gamma distribution fitted the rainfall record well in the majority of the stations and hence the gamma distribution has been selected in this study to assess the drought. The details about the gamma distribution can be found in Appendix A.

2.4 Methodology of experiments

The SPI values were computed for two time-scales i.e. three months (SPI-3) and 12 months or annual (SPI-12). The SPI-3 was used to assess drought during belg and kiremt seasons, which represent the two rainy seasons in Ethiopia and SPI-12 was used to assess the annual drought. In assessing the effect of data length on drought category, two data withholding procedures were applied.

The procedure followed in the first data withholding procedure (procedure 1) was that one year of data was taken out starting from 1953 and then SPI values were calculated accordingly. The data withdrawing started from 1953 and was repeated up to the year 1974 where most of the other stations started recording. Then, the SPI values for a particular drought year between 1975 and 2009 were checked whether or not the values indicate the same drought category. As cross-validation of the results of the first experiment, in the second procedure (procedure 2), the one year of data was withdrawn one by one starting from the middle of the record length (from 1970 to 1988).

Since drought is a regional phenomenon, the point-based SPI time series values of each meteorological station have been interpolated using the inverse distance weighted (IDW) method to assess the spatial extent of drought in the basin. The inverse distance weighted method gives better representation for interpolation of rainfall distribution over heterogeneous topographic terrain (Tagel et al. 2011). In order to identify the areas most frequently struck by drought, the frequency of occurrences of drought was computed by taking the ratio of the number of drought years to the total number of years used in the analysis. The frequency of occurrence of drought was also spatially interpolated using inverse distance weighting.

2.5 Results and discussion

2.5.1 Effect of record length on drought analysis

Overall, we found that for all stations the SPI values are within the same drought categories irrespective of the length of records (Figures 2.3 to 2.6). The results for Debremarkos (Figure 2.3b), Hossana (Figure 2.4h) and Welaita Sodo (Figure 2.6n) give consistent SPI values (no clear trends or abrupt changes). The SPI drought categories computed from record length starting from 1953 and record length starting from 1974, therefore, remain the same. The results for Addis Ababa (Figure 2.3a), Gondar (Figure 2.3c), and Jimma (Figure 2.3d) demonstrate that most of the data series (SPI values) remain in the same drought category. Three exceptional SPI values were found falling out of the range of the severe drought category at Gondar (Figure 2.3c) and Jimma (Figure 2.3d) for data lengths of 45 and 46 years. Compared with the total number of drought events considered, the impacts of these exceptions are thought to be negligible. An increasing trend within the drought category was observed at Gore (Figure 2.4g) for procedure 1 (discussed in section 2.4), but not to the extent that the drought category changed.

In the cross-validation procedure, the second data withdrawing procedure (procedure 2) discussed in section 2.4, for meteorological stations located in the UBN Basin as well as in other parts of Ethiopia, results showed little sensitivity of the SPI index to the data length. Only at the Kebridhar station (Figure 2.5j), increasing trends of SPI values were observed, however all the values observed fall in the same drought category.

These analyses show that the record length from 1953 to 1974 has a limited effect on changing the drought category and hence the record length from 1975 to 2009 can be used for drought analysis in the UBN.

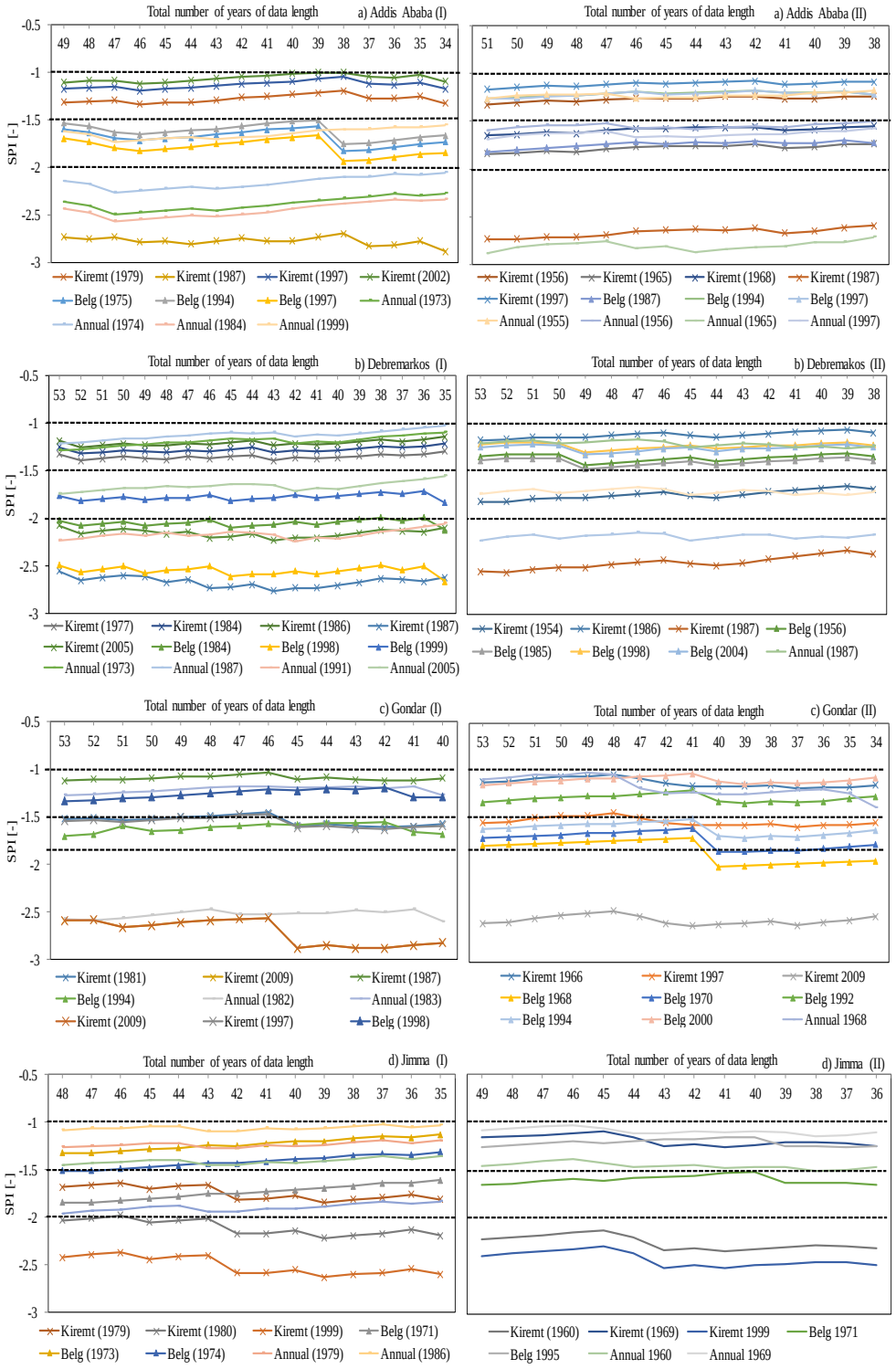

Figure 2.3: Moderate (SPI: -1 to -1.5), severe (SPI: -1.5 to -2) and extreme (SPI: > -2) drought for the Addis Ababa, Debremarkos, Gondar and Jimma stations. Note: the number in the parenthesis in the legend section indicates the drought year. The Roman number I and II in the parenthesis next to the name of each rainfall stations indicate the graphs obtained for data withdrawing in procedure 1 and procedure 2 as described in section 2.4.

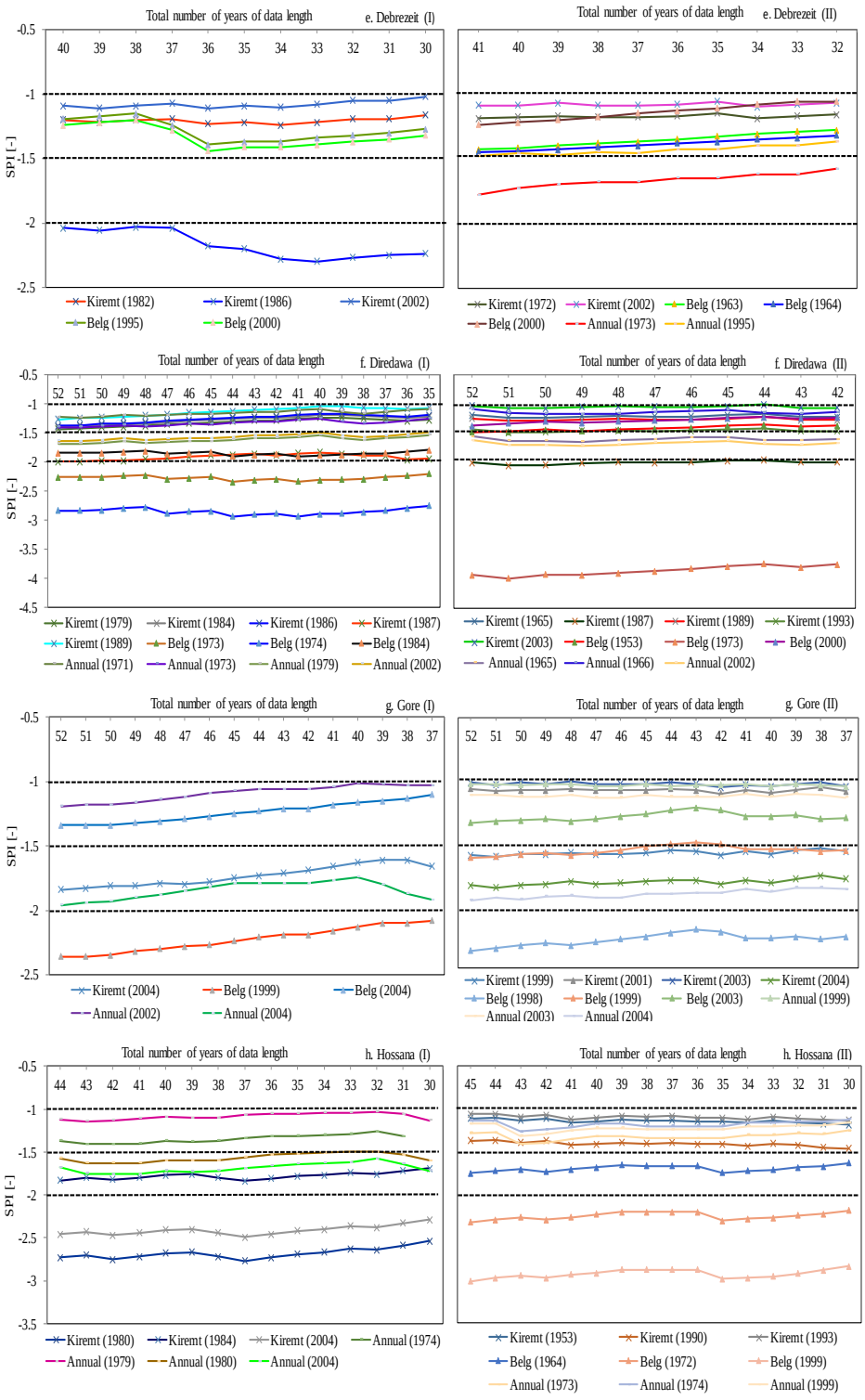

Figure 2.4: Moderate (SPI: -1 to -1.5), severe (SPI: -1.5 to -2) and extreme (SPI: > -2) drought for the Debrezeit, Diredawa, Gore and Hossana stations. Note: the number in the parenthesis in the legend section indicates the drought year. The Roman numbers I and II in the parenthesis next to the name of each rainfall stations indicate the graphs obtained from the data withdrawing from the beginning and from the middle respectively.

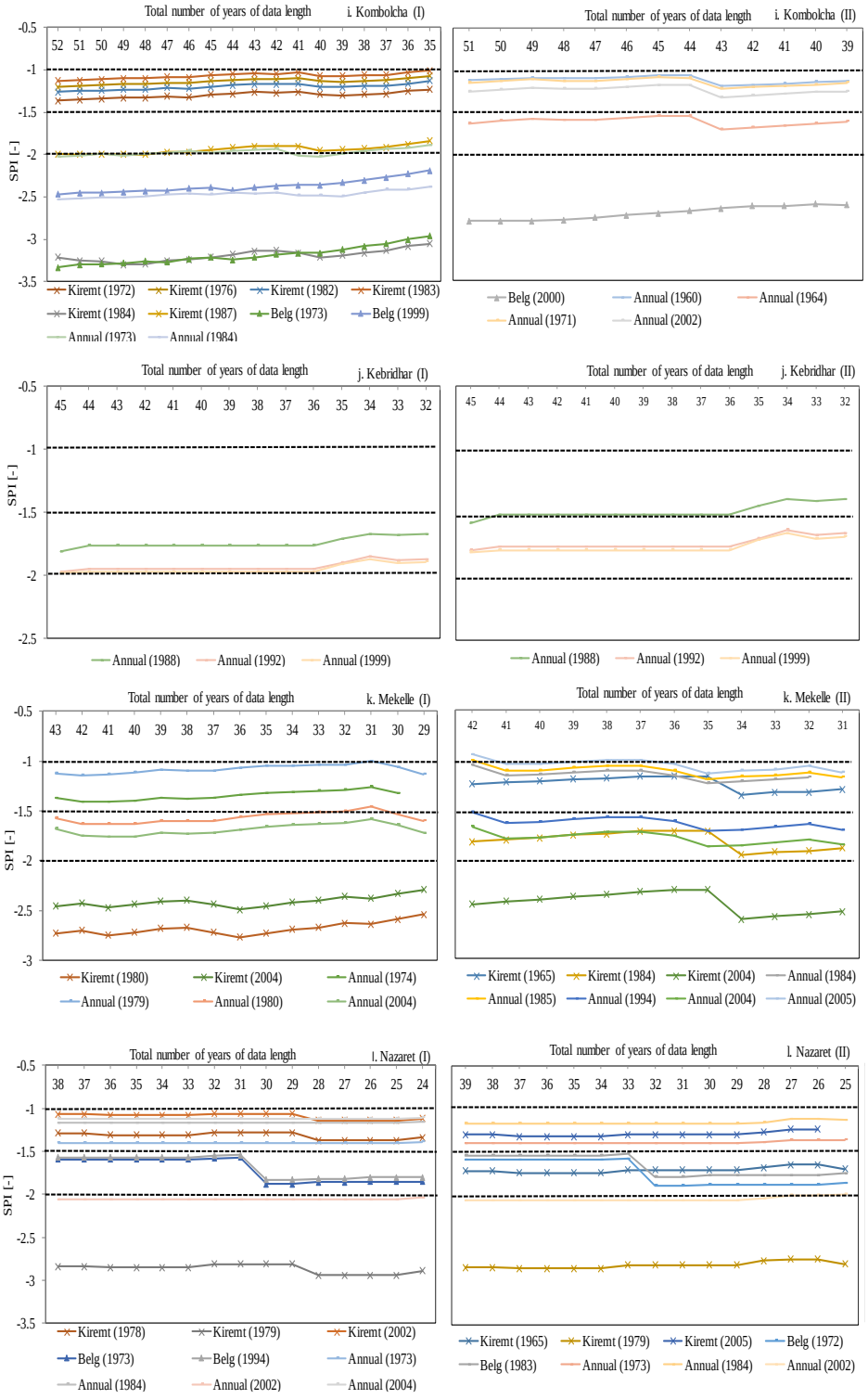

Figure 2.5: Moderate (SPI: -1 to -1.5), severe (SPI: -1.5 to -2) and extreme (SPI: > -2) drought for the Kombolcha, Kebridhar, Mekelle and Nazaret stations. Note: the number in the parenthesis in the legend section indicates the drought year. The Roman numbers I and II in the parenthesis next to the name of each rainfall stations indicate the graphs obtained from the data withdrawing from the beginning and from the middle respectively.

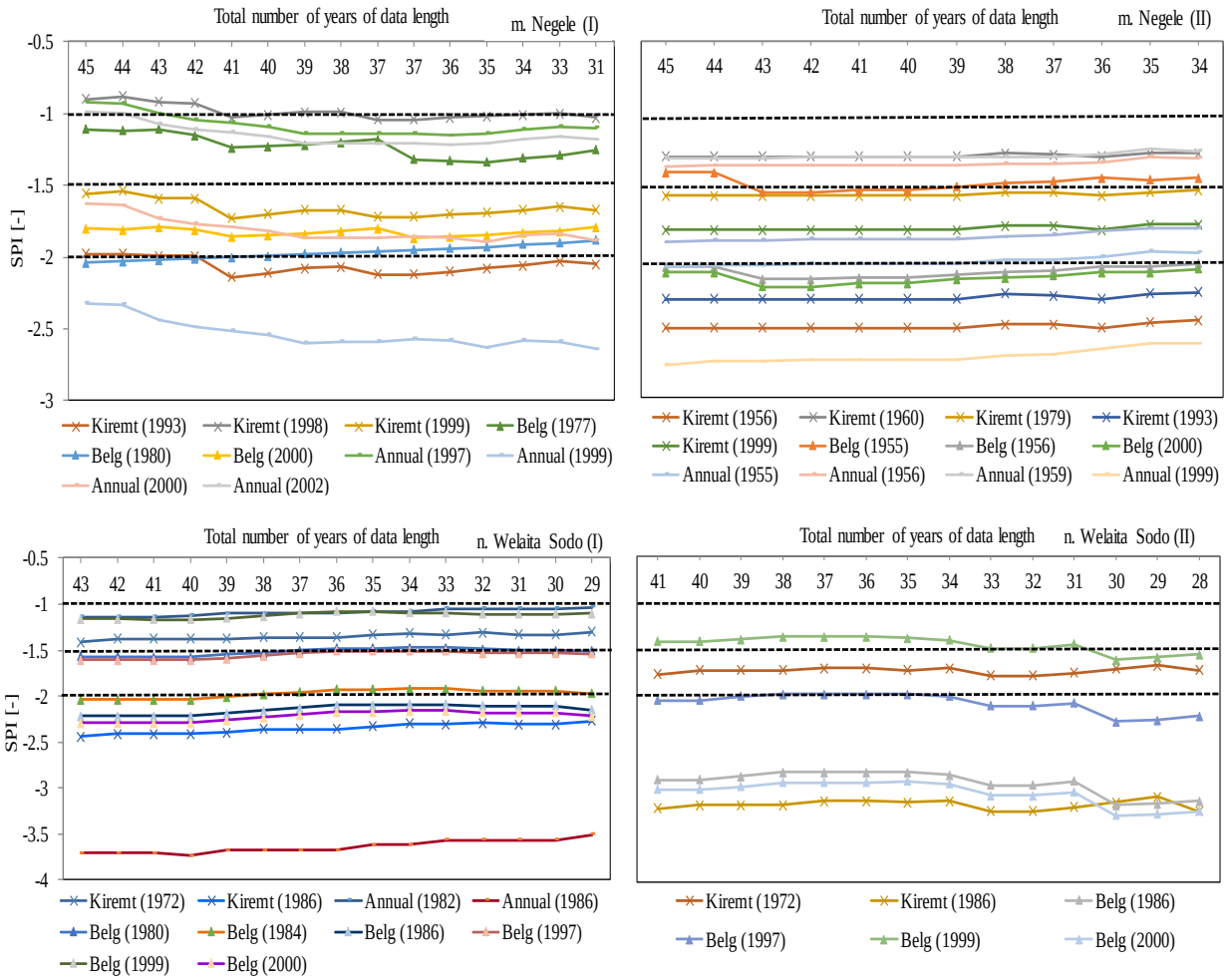

Figure 2.6: Moderate (SPI: -1 to -1.5), severe (SPI: -1.5 to -2) and extreme (SPI: > -2) drought for the Negele and Welaita Sodo stations. Note: the number in the parenthesis in the legend section indicates the drought year. The Roman numbers I and II in the parenthesis next to the name of each rainfall stations indicate the graphs obtained from the data withdrawing from the beginning and from the middle respectively.

2.5.2 Temporal assessment, and trend analysis of drought

Based upon the findings from the first analysis on the influence of data length, the use of more stations with shorter record length in the study area was justified. Thus, the second group that includes all the 29 meteorological stations was used to study drought characteristics using the SPI.

Belg season

As shown from the time series of the SPI for the belg season (short rainy season from February to April) in Debremarkos (Figure 2.7a) and Gondar (Figure 2.7b) stations, moderate drought episodes were indicated for the years 1965, 1978 and 1985 in Debremarkos station; 1977 and 1998 in Gondar station. A severe drought occurred in the years 1954, 1971 and 1999 in Debremarkos station; 1970, 1974, 1984 and 1994 in Gondar station. Extreme drought episodes

were also indicated in the years 1984 and 1998 in Debremarkos station; 1968 and 1983 in Gondar station. The drought episodes in the belg season show multi-year persistence at most stations, although severity often changed from year to year. The moderate, severe and extreme droughts were followed or preceded by mild drought episodes. Although the mild drought episodes represented below the long-term mean, its impact is much less and closer to the normal condition. For this reason, the mild drought episodes were not presented in the temporal assessment of drought in the UBN Basin.

The occurrences of moderate, severe, or extreme drought episodes in the belg season, in some year manifested at the annual time scale as well. However, the impact of the belg drought on the annual drought was not one to one, which means that severe drought in the belg season might be mild on the annual time scale and vice versa. Moderate drought was the dominant drought category in most of the meteorological stations for the belg season. Severe drought was the next predominant drought category in most of the stations and it appeared even more frequent than moderate drought during the belg season for some stations.

Kiremt season

Referring to Figures 2.7a and 2.7b, moderate drought episodes in kiremt season (main rain season from July to September) were observed in the years 1963, 1977, 1978, 1984 and 1986 at the Debremarkos station; 1966, 1971, 1983 and 1987 at the Gondar station. A severe drought occurred in the year 1954 and 1992 at the Debremarkos station and 1981, 1982 and 1997 at the Gondar station. Extreme drought occurred in the year 1987 and 2005 at the Debremarkos station; 2009 at the Gondar station. The minimum SPI value was detected in the year 2009 (-2.59) at Gondar station. Similar to the belg season, the kiremt season droughts also appeared to be persistent with varying severity at most stations. For instance, a persistent 5-year drought occurred at the Gondar station during the kiremt season from 1981 to 1985, with the severity decreasing from -1.58 to -0.32. The occurrence of kiremt drought is found to be a precursor of the drought occurring at the annual time scale in the majority of the stations. However, the severity varies, which means moderate, severe, or extreme droughts in the kiremt season might be in most cases mild drought at the annual time scale and vice versa. Moderate droughts are the most dominant category in the kiremt season.

The analysis of the two rainy seasons, belg and kiremt, shows that droughts can occur in either one or both seasons.

Annual droughts

The drought years in the annual time scale have been identified in Figures 2.7a and 2.7b. Moderate annual droughts have been observed in 1973, 1982, 1987 and 1995 at the Debremarkos station; 1968, 1983, 1990 and 1992 at the Gondar station. Severe drought was observed in 1965, 1978, 1986 and 2005 at the Debremarkos station; 1970 at the Gondar station. Extreme drought occurred in 1991 at the Debremarkos station; 1982 and 1991 at the Gondar station. Moderate droughts are the most dominant drought category at the annual time-scale.

Overall the temporal SPI analysis shows that most of the 29 stations measured severe, moderate and mild drought episodes in the years 1978/79, 1984/85, 1994/95 and 2003/04. Indeed, these years were among the worst drought years in the history of Ethiopia (Edossa et al. 2009, Tagel et al. 2011). Several studies confirm that severe droughts have occurred in these years and caused substantial damage in terms of life and economical losses and covered the entire country (Wagaw et al. 2005, Tagel et al. 2011).

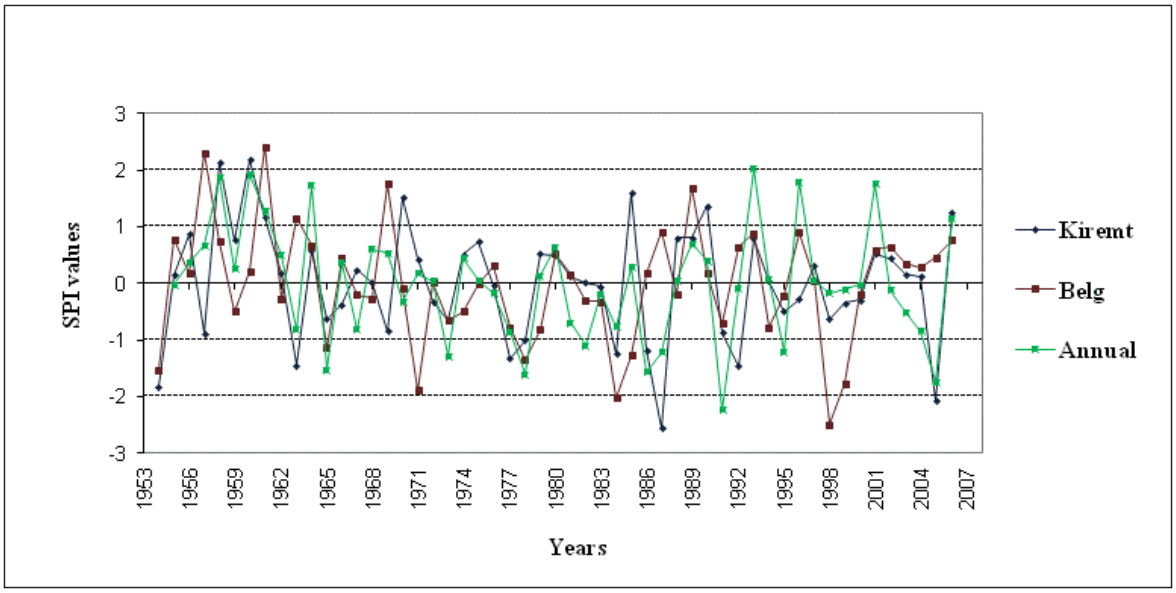

Figure 2.7a: Standardized precipitation index time series values of the Debremarkos station.

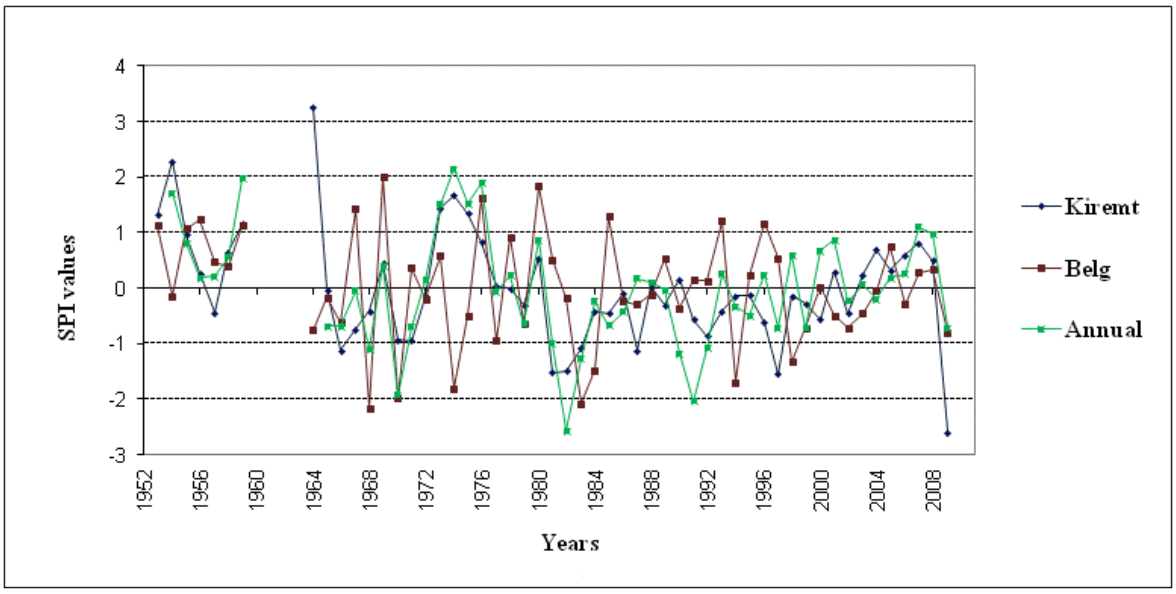

Figure 2.7b: Standardized precipitation index time series values of the Gondar station.

Trend analysis of drought occurrence

A statistical test was conducted to check whether a trend exists or not in the SPI time series of the stations using the Mann-Kendall (Yue et al. 2002, Hamed, 2008) method. The result shows that a negative slope (trend) was observed in both stations for the three SPI time-scales, however, the trend was statistically insignificant at the 95% confidence level. This shows that there is no statistical evidence of any positive or negative trend of meteorological drought severity and frequency for the study area. Although the trends at all time-scales were statistically insignificant, a relatively strong trend of increasing frequency was observed during the kiremt season with the average value of the regression coefficient (R) greater than 23%. It is, therefore, recommended to regularly re-check if this increasing trend becomes significant at a later stage. It is important to note that kiremt is the main rainy season in Ethiopia from which agricultural production is highly dependent.

2.5.3 Areal extent of drought

The spatial coverage of drought over the UBN Basin was obtained using the Thiessen Polygon method. The resulting areal extent was expressed as the percentage of the basin in drought conditions. The drought area percentages were calculated for all SPI time-scales, however, only the result for kiremt and annual time-scales are presented in Figures 2.8a and 2.8b for further discussion.

The areal extent of annual droughts (Figure 2.8a) shows that more than 40% of the area was struck or impacted by mild droughts in 1982, 1987, 1997, 2002, and 2003. The years of 1982

and 2003 could be marked as critical as 63% and 56% of the entire study area was struck by mild drought. In 1984, 1985, 1986 and 1995, the 12-month SPI values indicated 15% of the total area under moderate or more severe droughts. The year 1995 was considered as a critical year as the areas of moderate and severe drought reached up to 26% and 28% respectively. This analysis of the spatial extent of droughts in the UBN Basin shows, with over 25% of the area having been hit by moderate, severe, or extreme droughts, this indicates that considerable parts of the basin are drought-prone.

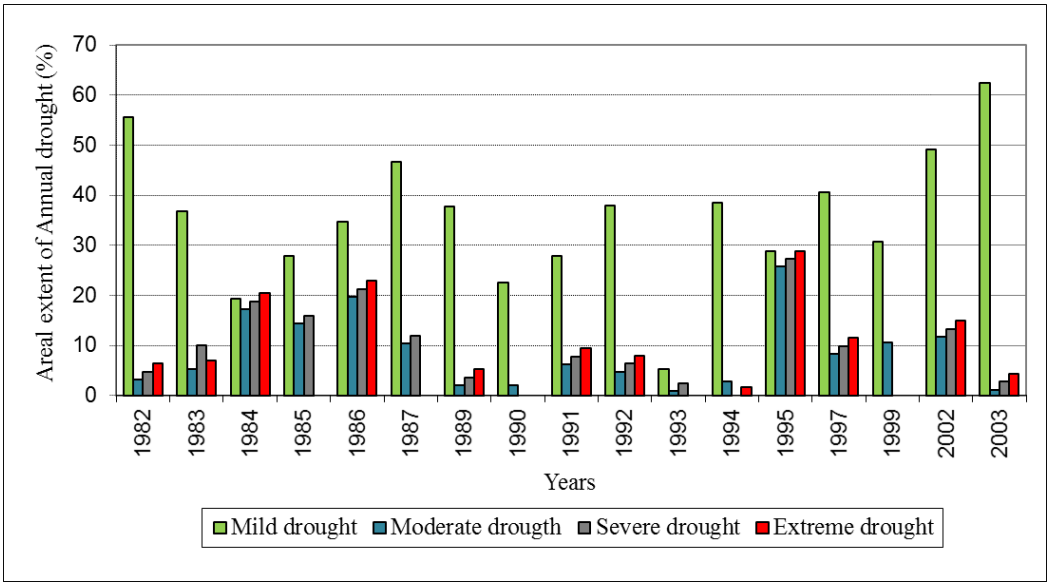

Figure 2.8a: Areal extents of annual drought severity graph based upon the 12-month SPI for September.

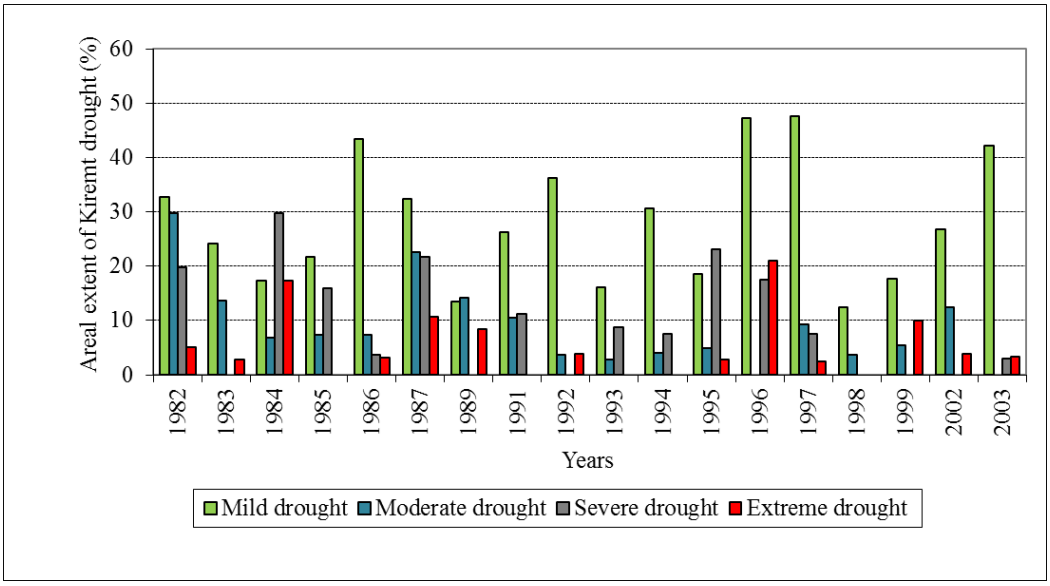

Figure 2.8b: Areal extents of Kiremt drought severity graph based upon the 3-month SPI for September.

2.5.4 Spatio-temporal analysis to assess the spatial variability of drought frequency

Drought frequency in the UBN Basin of Ethiopia was investigated using the SPI for kiremt, belg, and annual time-scales for each meteorological station. The frequency of occurrence of each drought category was computed for each station at each time-scale by taking the ratio of the number of occurrence of the particular drought of a particular category and time-scale to the total number of data years (Edossa et al. 2009). The main objective of this analysis was to identify the areas that are most frequently struck by drought. Figure 2.9a shows that the relative frequency of mild drought in kiremt time-scale was highest in the southwest, central and the north to northeast of the UBN Basin. The annual frequency of mild drought also shows most frequent mild droughts occurred over the southwestern part of the UBN Basin. Relatively large prevalence of moderate drought occurred in central towards south and northeast part of the study area for the kiremt and annual time-scales (Figure 2.9b). The map with the frequency of occurrence of the severe droughts at annual time-scale shows that a large part of the study area was free from severe droughts. The North and North-west parts, however, do show severe droughts during the kiremt time-scale (Figure 2.9c). The frequency of occurrence of extreme droughts (Figure 2.9d) further shows that the central and the northern parts of the study area are struck more frequently by extreme droughts for the kiremt and annual time-scales.

From the analysis above it is clear that the maps of drought frequency show differences for the time-scales and severity considered. A conclusion on which sub-areas of the basin are more prone to droughts is difficult to make. Therefore, the drought frequency was also calculated for the mild, moderate, severe, and extreme drought categories together. The resulting drought frequency maps for annual and kiremt time-scales are shown in Figure 2.10. For the kiremt time-scale (Figure 2.10a) the only clear pattern is that in the eastern parts of the basin drought-frequencies are lower. For the annual time-scale (Figure 2.10b), high drought frequencies (50%) were observed in the south, central and west. It can be concluded that in the UBN Basin the central, south, and western parts are the most drought-prone, while the North and East are less drought-prone. The conclusion needs, however, to be taken with care, because patterns are not very distinct and may be influenced by the limited coverage of rainfall stations in the northwest and northeast parts.

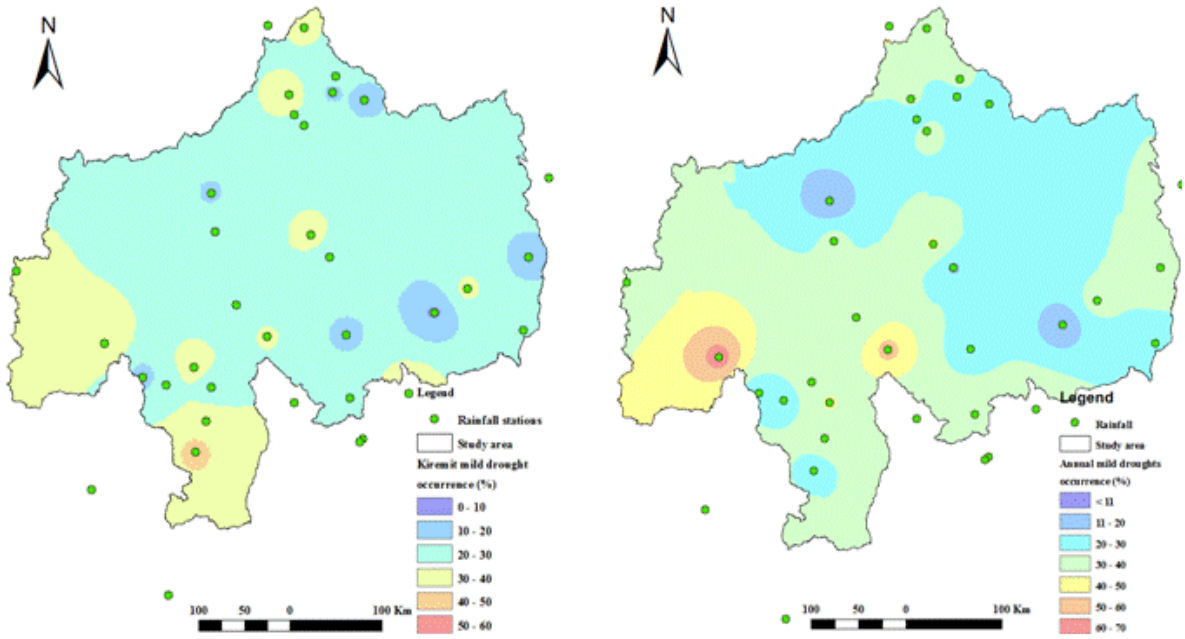

Figure 2.9a: Frequency of occurrence of mild drought.

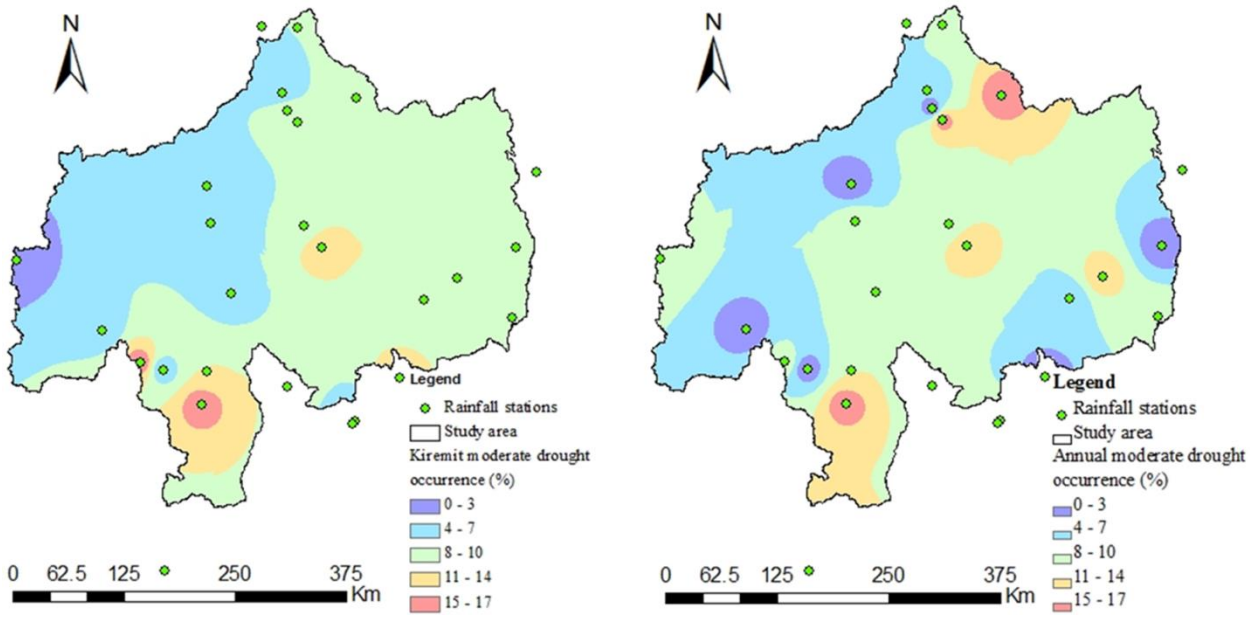

Figure 2.9b: Frequency of occurrence of moderate drought.

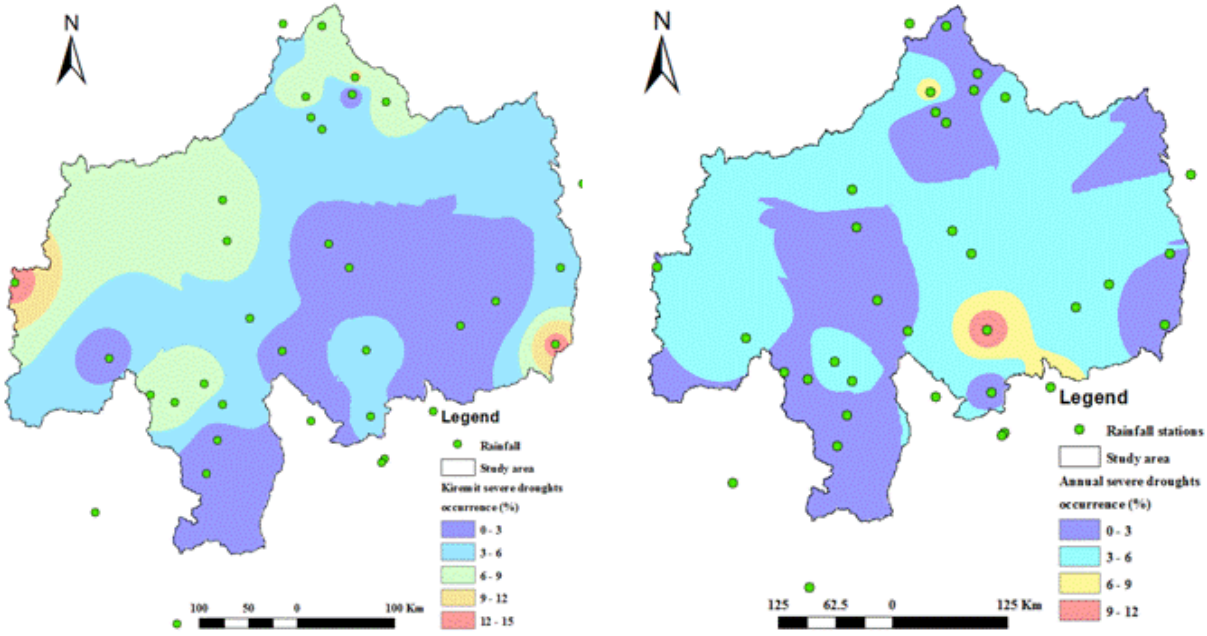

Figure 2.9c: Frequency of occurrence of severe drought.

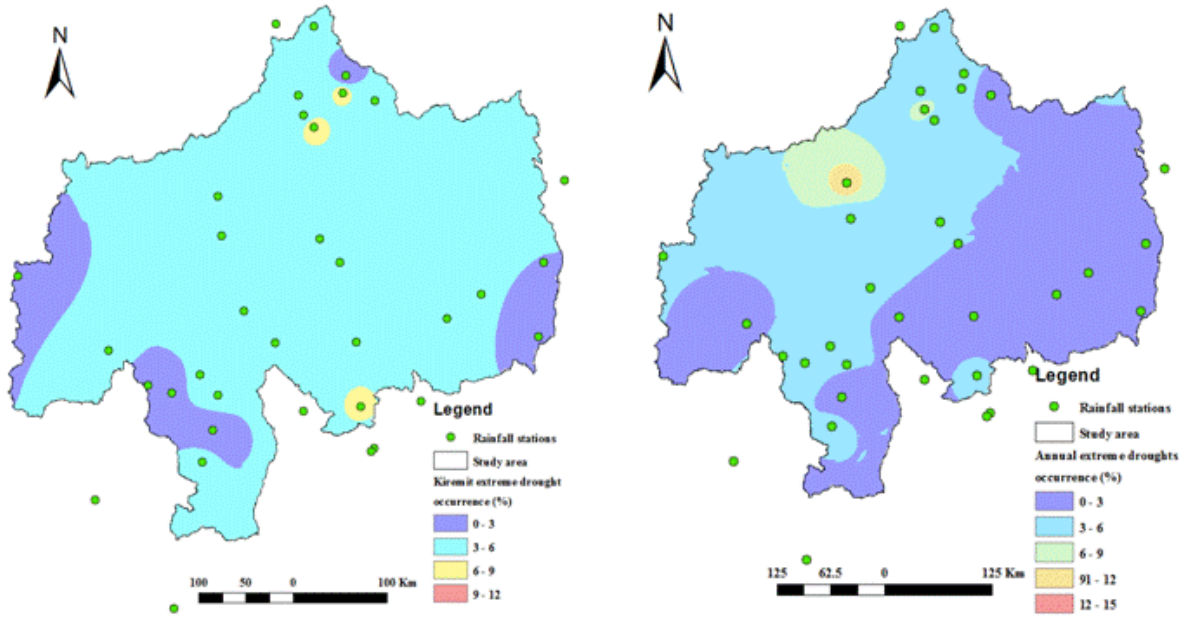

Figure 2.9d: Frequency of occurrence of extreme drought.

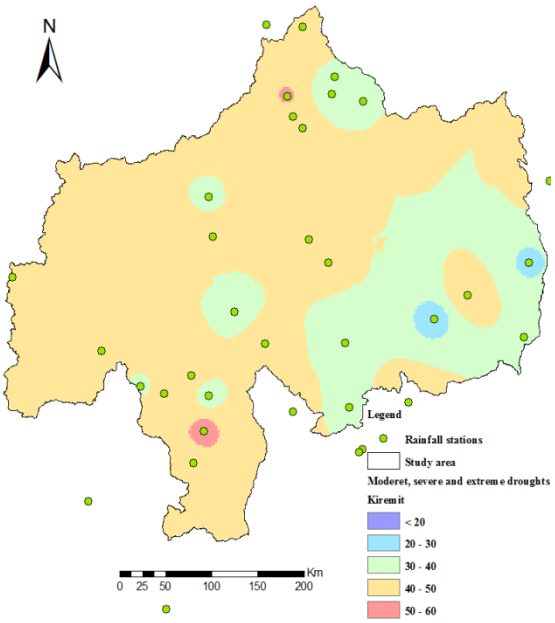

Figure 2.10a. Frequency of occurrence of mild, moderate, severe and extreme droughts in kiremt time scale.

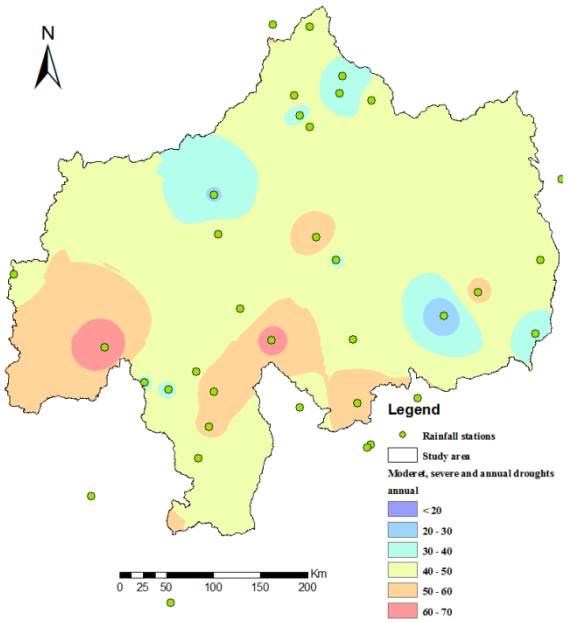

Figure 2.10b. Frequency of occurrence of mild, moderate, severe and extreme droughts in annual time.

2.6 Conclusion

The spatial extent and distribution of drought frequency in the UBN Basin was analysed by interpolating the station SPI values across the study area.

The methodology employed to test the influence of record length on the SPI index proved successful in validating the use of a large number of additional stations with shorter record length for the UBN Basin. The findings of this study may help other researchers and practitioners who face similar challenges of insufficient data length by checking the effect of data length for their drought studies using the SPI.

The trend analysis of the SPI index from 1953 to 2009 showed no conclusive evidence that meteorological drought in the Upper Blue Nile is increasing or declining. SPI droughts occurred throughout the basin. Persistence from seasonal to annual drought, and from one year to the next, has been found. The temporal analysis showed that the historical drought years in the area (1978/79, 1984/85, 1994/95 and 2003/04) were successfully captured using the SPI index. Therefore, the SPI index can be used as an important index to identify the historical drought patterns in the UBN Basin, which could help in predicting drought. Further, a study needs to be conducted to test the procedure employed in this research for other basins and/or the entire country of Ethiopia, emphasizing areas most frequently hit by severe droughts.

3. Comparison of the performance of six drought indices in assessing and characterising historic drought events[2]

3.1 Introduction

This chapter presents the comparison of six drought indices: Standardized Precipitation Index (SPI), Standardized Precipitation and Evaporation index (SPEI), Evapotranspiration Deficit Index (ETDI), Soil Moisture Deficit Index (SMDI), Aggregate Drought Index (ADI), and Standardized Runoff-discharge Index (SRI), and evaluates their performance with respect to identifying historic drought events in the Upper Blue Nile (UBN) basin. The indices were calculated using monthly time series of observed precipitation, average temperature, river discharge, and modelled evapotranspiration and soil moisture from 1970 to 2008. The SPI, SPEI and SRI were calculated for aggregate periods of 3-, 6-, 9-, and 12-months.

Comparative studies of drought indices have been carried out in many other watersheds. For example:

- Zhuo et al. (2016) compared five drought indices for agricultural drought monitoring and impact on wheat yield analysis in North China, and indicated that the Temperature Vegetation Dryness Index (TVDI) outperformed other drought indices and would be a more suitable drought index to monitor wheat yield.
- Morid et al. (2006) compared the performances of seven drought indices in the Tehran Province of Iran and recommended using the EDI and SPI for drought monitoring purposes in the basin. The study further indicated that the EDI was more responsive to the drought and performed better than the SPI.
- Okpara and Tarhule, (2015) evaluated and compared the performance of three drought indices in the Upper Niger sub-watershed. They reported that the SPI ranked first among other meteorological drought indices in the basin.

[2] *Based on*: Bayissa, Y.A., Maskey, S., Tadesse, T., van Andel, S.J., Moges, S,A., van Griensven, A., and Solomatine, D.P, 2018. *Comparison of the performance of six drought indices in characterizing historical drought for the Upper Blue Nile Basin, Ethiopia*. Geosciences, v. 8, No. 3, p.81.

- Barua et al. (2010) evaluated the performance of five drought indices for the Yarra River Catchment in Victoria, Australia, using five subjective decision criteria (robustness, tractability, sophistication, transparency, and extendibility). They found that the Aggregate Drought Index (ADI) was superior and preferable to other indices for the study catchment.
- Similar studies have been conducted in other basins (Naumann et al. 2013; Wang et al. 2013; Vicente-Serrano et al. 2010; Houcine and Bargaoui, 2012; and Heim, 2002).

Also Ethiopia has been subject to drought analyses, especially focusing on the areas in the northern and eastern parts of the country (Tagel et al. 2011; Viste et al. 2013; Edossa et al. 2010). Even though a few attempts have been made in assessing and characterizing droughts in the Upper Blue Nile (UBN) basin (Bayissa et al. 2015; Viste et al. 2013), a comparison of the performance of multiple drought indices for the UBN Basin is still missing.

3.2 Data

3.2.1 Historical drought events

The history of drought in the basin is documented poorly. However, major historical drought events within the study period (1970 – 2008) were identified from previous studies and EM-DAT, the international disaster database (http://www.emdat.be/database) (Bayissa et al. 2015; Viste et al. 2013). According to previous studies, years 1973-1974, 1983-1984, 1994-1995, and 2003-2004 were reported as the major drought years in Ethiopia (Bayissa et al. 2015 (Chapter 2); Viste et al. 2013). EM-DAT (Table 3.1) includes these drought events as well, but reports the 1973 and 1994 events as being part of longer drought periods from 1973 to 1978 and from 1989 to 1994 respectively. This possibly reflects the occurrence of multiple drought events during these years in different parts of the country.

For evaluating the six drought indices (Section 4.2), the EM-DAT drought periods are taken as a reference while keeping in mind their reporting of prolonged droughts. The EM-DAT database is compiled from various sources, including UN agencies, non-governmental organizations, insurance companies, research institutes, and press agencies. The available information for the selected drought events is presented in Table 3.1. The year 1983-1984 stands out as the drought year with the highest percentage (22%) of the population affected. For other drought events, this percentage is 16% or less. The provinces indicated in bold (Table 3.1) are situated (partly) within the UBN Basin. For example, according to the earlier division of provinces (before 1992), Gondar includes the northern part of the basin, whereas Wollo and Shoa include eastern, northeast, and southeast parts of the basin respectively. According to the

current regional classification, Amhara covers the central, northern, northeastern, and northwest parts, and Oromia covers the southern, southeast and southwest parts of the UBN Basin. The eastern and some of the central parts of the basin have not been reported in EM-DAT as being affected by drought. Both the start and end dates of the historic drought events are shown in Table 3.1, but the months of the end dates are not indicated. Hence, the evaluation of the drought indices in identifying drought events focuses on the onset of the drought events.

Table 3.1: The start and end date of the historic drought events and the total number of people affected during the years 1970-2008.

Start date	End date	Location	Total affected population (10^6)	Total number of Population in Ethiopia (10^6)	Ratio (%)
December, 1973	1978	**Wollo**, **North Shoa**, Tigray, Kangra province	3	32.57	9
May, 1983	1984	**Wollo, Gondar**, Gore, Tigray, **Shoa**, Harerge, Sidamo	7.75	35.24	22
June, 1987	1987	Ogaden, Tigray, **Wollo, Shewa**, Gamo Gofa, Sidama, **Gondar**, Bale	7	48.06	15
October, 1989	1994	**Northern Ethiop**ia, Tigray, **Wollo, Gondar**, Harerge	6.5	48.06	14
2003	2004	Tigray, **Oromia, Amhara**, Somali, Afar province	12.6	76.61	16
May, 2008	October, 2009	**Oromia**, Somali, A**mhara**, Afar, Tigray, SNNPR province	6.4	87.56	7

Source: EM-DAT International Disaster Database. Centre for Research on the Epidemiology of Disasters-CRED; http://www.emdat.be/database (last access: 17 July 2016); http://www.worldometers.info/world-population/ethiopia-population/

3.2.2 Actual evapotranspiration (ET) and soil moisture data

A process-based semi-distributed hydrological model (Soil and Water Assessment Tool, SWAT) was developed to simulate the actual evapotranspiration and soil moisture time series data (Arnold et al. 2009; Green and van Griensven, 2008). Previous studies have shown the capability of SWAT to model the hydrological processes in the UBN Basin (e.g. Mengistu and Sorteberg, 2011; Griensven et al. 2012). The SWAT model was calibrated on river discharge data from 1970 to 2008 for five hydrological stations (Figure 3.1). The flow data of Abbay at the Bahirdar station (Figure 3.1) were used as the boundary condition for modelling the part of the catchment downstream of Lake Tana. The monthly calibration results in terms of the coefficient of determination (R^2) and Nash-Sutcliffe efficiency (NSE) between observed and simulated river discharge vary from 0.83 to 0.93 (for R^2) and 0.84 to 0.91 (for NSE). The

Hargreaves method (Hargreaves and Samani, 1982) was used for potential ET in SWAT. Weather data of relative humidity, solar radiation, wind speed, and sunshine hours available from 10 stations were used for developing the SWAT database.

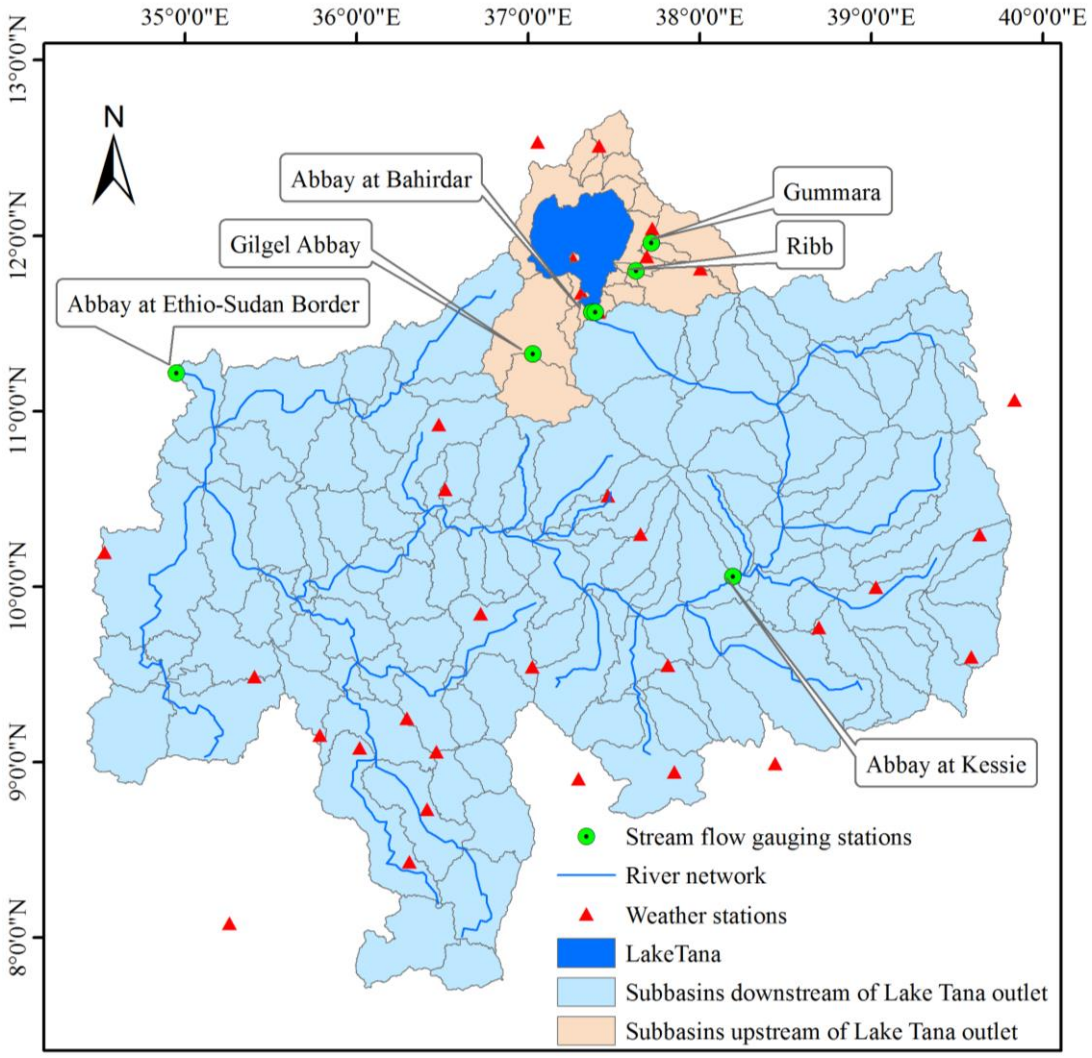

Figure 3.1: Upper Blue Nile basin with river network, gauging stations, weather stations, and the sub-basin discretisation used by the SWAT model, upstream and downstream of the Lake Tana outlet.

Other input data (Digital Elevation Model (DEM), land use, and soil maps) were collected from different sources. The 90m spatial resolution DEM data were obtained from the Shuttle Radar Topography Mission (SRTM) (http://www.cgiar-csi.org/data/srtm-90m-digital-elevation-database-v4-1). Land use classification data at a spatial resolution of 5km by 5km were acquired from the Ministry of Agriculture and Rural Development (MARD, 2004) of Ethiopia. The basin was classified into 32 land use classes. Cultivated land is the dominant land cover in the basin. The soil map and physical and chemical properties at different soil layers were obtained from the Ministry of Water, Irrigation and Electricity of Ethiopia.

Actual evapotranspiration and soil moisture from the model output were used to calculate the Evapotranspiration Deficit Index (ETDI) and Soil Moisture Deficit Index (SMDI), respectively.

3.2.3 Rainfall and temperature data

Precipitation, and maximum and minimum temperature data from 34 stations with records from 1970 to 2008 were used. The data were on a daily time step and the location of each station is shown in Figure 3.1. The weather stations located inside and in the proximity of the catchment boundary were used in this chapter for the hydrological modelling and meteorological drought assessment. The rainfall and temperature data were used to calculate the SPI and SPEI indices.

3.2.4 River discharge data

The river discharge data measured at five selected gauging stations (Gilgel Abbay, Ribb, Gumara, Abbay at Kessie, and Ethiopia-Sudan border) were obtained from the Ministry of Water, Irrigation, and Electricity of Ethiopia (Figure 3.1). The data have a daily time step (except at the Ethiopia-Sudan border, where only monthly data were available). The river discharge data at these selected stations were used to calculate the time series values of SRI.

3.3 Drought indicators

The drought indices collectively characterize meteorological, agricultural, and hydrological drought types. The SPI and SPEI, which are based on precipitation and temperature data, characterize meteorological drought. The ETDI and SMDI, which are based on evapotranspiration and soil moisture respectively, characterize agricultural drought. SRI, which is based on discharge, characterizes the occurrence of hydrological drought. ADI aggregates multiple input data sets that represent meteorological, agricultural and hydrological variables. The definitions and calculation methods applied in this dissertation are described below.

3.3.1 Meteorological drought indicators

Standardized Precipitation Index (SPI): the detailed description of SPI index can be found in section 2.3.

Standardized Precipitation Evaporation Index (SPEI): The SPEI has an advantage over SPI because it incorporates the effect of potential evaporation in addition to rainfall (Abramowitz and Stegun, 1966; Trambauer et al. 2014; Vicente-Serrano et al. 2010). The calculation

procedure of the SPEI is similar to that of the SPI, except that the SPEI accounts for the difference between precipitation and potential evaporation. Like the SPI, the SPEI is calculated at different time scales (e.g. 1-, 2-, and 3-month), and in this study, a log-logistic distribution is applied as it fits observations in the majority of rainfall stations (Bayissa et al. 2015). Negative SPEI values indicate dry conditions due to less precipitation and/or higher potential evaporation (dry conditions) compared to the historical mean.

3.3.2 Agricultural drought indicators

Evapotranspiration Deficit Index (ETDI): The ETDI is based on the anomaly of water stress to its long-term average (Narasimhan and Srinivasan, 2005), in which monthly water stress is defined using potential and actual evapotranspiration (Equation 3.1).

$$WS = \frac{PET - AET}{PET} \tag{3.1}$$

The *WS* ranges from 1 (no evapotranspiration) to 0 (evapotranspiration occurring at the same rate as PET). Next, monthly water stress anomaly (WSA) is calculated as:

$$WSA_{i,j} = \frac{MWS_j - WS_{i,j}}{MWS_j - \min WS_j} \times 100, \quad \text{if } WS_{i,j} \leq MWSj \tag{3.2}$$

$$WSA_{i,j} = \frac{MWS_j - WS_{i,j}}{\max WS_j - MWS_j} \times 100 \quad \text{if } \mathrm{WS_{i,j}} > \mathrm{MWS_j} \tag{3.3}$$

where MWS_j is the long-term median of water stress of month *j*, $maxMWS_j$ is the long-term maximum water stress of month *j*, $minWS_j$ is the long-term minimum water stress of month *j*, and WS is the monthly water stress. The subscripts *i* and *j* are used for years and months respectively.

Finally, ETDI is calculated using Equation 3.4. In the original formula developed by Narasimhan and Srinivasan, (2005), WSA_j was divided by 50 to scale the ETDI between -4 and 4. As suggested by Trambauer et al. (2014), here, the WSA_j values are divided by 100 to scale the ETDI between -2 and 2 to compare with SPI, SPEI, and SRI values.

$$ETDI_j = 0.5ETDI_{j-1} + \frac{WSA_j}{100} \tag{3.4}$$

Soil Moisture Deficit Index (SMDI): The SMDI is calculated in the same way as ETDI, but with the available soil water content in the soil profile (Narasimhan and Srinivasan, 2005). First, the median, maximum, and minimum values for each month were extracted using soil

moisture time series. The median was chosen instead of the mean because it is less affected by the outliers. The SMDI values (deficit or excess) for the 39 years (1970-2008) were calculated using Equations 5-7.

$$SD_{i,j} = \frac{SW_{i,j} - MSW_j}{MSW_j - \min SW_j} \times 100 \text{ if } SWi,j \leq MSWj \quad 3.5$$

$$SD_{i,j} = \frac{SW_{i,j} - MSW_j}{\max SW_j - MSW_j} \times 100 \text{ if } SWi,j > MSWj \quad 3.6$$

where *SDi,j* is the soil water deficit (%) ranging from -100 (very dry condition) to +100 (very wet condition); *SWi,j* is monthly soil water available in the soil profile (mm); and *MSWj*, *maxSWj*, and *minSWj* are long-term median, maximum, and minimum available soil water in the soil profile (mm), respectively.

Thus, the SMDI in any given month is determined by:

$$SMDI_j = 0.5SMDI_{j-1} + \frac{SD_j}{100} \quad 3.7$$

SMDI ranges from -2 to +2, with negative values indicating drought.

3.3.3 Hydrological drought indicator

Standardized Runoff-discharge Index (SRI): The SRI is based on river discharge and its computation procedure is similar to that of SPI. The SRI uses the gamma distribution to fit the river discharge data. The SRI and SPI drought categories are similar. River discharge data at the five selected gauging stations were used to characterize hydrological drought in the UBN Basin.

3.3.4 Aggregate Drought Index (ADI)

The ADI (Keyantash and Dracup, 2004) is a multivariate drought index that aggregates the three types of drought (meteorological, agricultural, and hydrological) through considering rainfall, evapotranspiration, and soil moisture. These three variables are aggregated into a single index (ADI) using Principal Components Analysis (PCA). PCA constructs a symmetric correlation matrix (p x p, where p is the number of variables) between the original input variables. PCA transforms the original p-variables data set to a number of uncorrelated (principal) components z_j ($1 < j \leq p$) (Barua et al. 2010) using Equation 3.8.

$$Z = XE \quad 3.8$$

where Z is the (*n x p*) matrix of PCs (i.e. uncorrelated components), in which n is the number of observations, X is the (*n x p*) matrix of the observation data, and *E* is the (*p x p*) matrix of eigenvectors of the correlation matrix. The ADI was calculated for the first PC (PC1) normalized by the standard deviation. In the case considered, PC1 described more than 65% of the variation in the input data.

$$ADI_{i,k} = Z_{i,1,k} / \sigma_k \quad 3.9$$

where $ADI_{i,k}$ is the ADI value for month *k* in year *i*, $Z_{i,1,k}$ is the first PC for month *k* in year *i*, and σ_k is the sample standard deviation of $Z_{i,1,k}$ for all years *i* and months *k*. The ADI was calculated for each of the station locations and each month. ADI values of -0.96 or lower indicate a drought at a different severity level (*Table 3.2: ADI drought category classification*).

Table 3.2: ADI drought category classification developed based on percentile ranking through constructing cumulative distribution of the time series of ADI.

above 0.92	Wet
-0.95 to 0.92	Near normal
-1.40 to -0.96	Moderate drought
-1.69 to -1.41	Severe drought
-1.70 or less	Extreme drought

3.4 Methods

3.4.1 Correlation between drought indices

First, we derived monthly time series of drought indices that are defined in the previous section. The drought indices were calculated at the corresponding locations of each meteorological station. The spatial extent of SWAT based evapotranspiration and soil moisture were in hydrologic response units (HRUs). The total area of the basin was divided into two major parts: upstream and downstream of the Lake outlet. This division has been made to exclude the Lake Tana from the modelling processes of the basin due to the lack of appropriate data to characterize the lake. The upstream and downstream parts are further divided into 14 and 139 sub-basins and 104 and 1027 HRUs respectively. The HRUs were defined based on percentage combinations of land use, soil and slope. In this study, 10% land use, 20% soil and 10% slope threshold combinations were adopted, based on the findings of Setegn et al. (2008). The HRUs values of evapotranspiration, and soil moisture at the locations of each meteorological stations were extracted and used to calculate ETDI and SMDI drought indices. For all indices, data

from 1970 to 2010 are used. For SPI, SPEI, and SRI, indices were derived for five different aggregation periods, namely 1-, 3-, 6-, -9, and 12-months. Thus, we have a total of 18 indices; five each from SPI, SPEI, and SRI and one each from ETDI, SMDI and ADI. Next, Pearson correlation coefficients were derived for paired time series values of drought indices. Each drought index is paired with every other drought indices resulting in 18 by 18 correlation coefficient matrix.

3.4.2 Comparison of drought indices based on drought onset, duration, and severity

The comparison of the drought indices based on the drought characteristics such as percentage of drought months, maximum drought intensity, and drought duration was analyzed for the selected 16 stations that represent the majority of the study area. The percentage of drought months was calculated by taking the percentage of the ratio of the total number of months that show drought condition (including mild, moderate, severe, and extreme drought) with the total events in the study period. The maximum drought intensity represents the smallest value of the drought index within the study period (1970-2010). The average value of the maximum intensity of the different aggregate periods (1-, 3-, 6-, 9-, and 12-month) was considered for the SPI, SPEI, and SRI and compared with the self-defined single time scale indices (i.e. ETDI, SMDI, and ADI). The drought duration is defined as the consecutive months showing drought conditions (below normal conditions). Drought duration is also considered as one of the evaluation criteria to compare the drought indices for the selected stations.

Other drought indices comparison criteria (i.e. drought onset, duration, and severity) have been used by dividing the UBN basin into upper, middle, and lower parts, representing the areas upstream of the river gauging stations Abbay at Bahirdar, Kessie, and Ethiopia-Sudan border respectively. The drought indices were calculated using areal averages of the variables, namely rainfall, temperature, soil moisture, and actual ET based on the simple arithmetic mean technique. The drought severity, duration, and onset values were extracted for the known historic drought year (1973-1978, 1983-1984, 1989-1994, and 2003-2004). The time series values of the drought indices for these selected drought events were analysed to calculate the drought severity. The consecutive negative values of each drought index were considered to quantify the different drought characteristics. For example, mean intensity (M) and maximum intensity (Mmax) of drought are the average and maximum values within the consecutive negative drought index values respectively. Drought duration (D) represents the time span of the consecutive negative index values. Drought severity defined as the product of drought

duration (D) and the mean intensity (M) (Mishra and Singh, 2010; Narasimhan and Srinivasan, 2005; Wilhite, 2000). The severity interpreted as near normal, moderate, severe and extreme drought based on the drought categorical classification of each drought index as described in section 3.3. Based on drought severity and duration, each drought index was compared whether they characterize and indicate the severity and persistence of drought years in the basin. Moreover, the drought onset (starting month) estimated by each index was compared with similar data obtained from EM-DAT (section 2.2.1).

3.5 Results and discussion

3.5.1 Time series of the drought indices

The time series (1970-2010) of the drought indices were produced for all the stations considered in this study. However, the result obtained at the Gondar and Debremarkos stations are shown in Figure 3.2 for further discussion in this section. These two stations are representative of the upstream and downstream parts of the study basin. Figure 3.2 depicts the performance of the drought indicators for indicating the historic drought events. In general, majority of the drought indices indicated the historic drought years (1973-1974, 1983-1984, 1994-1995, 2003-2004, 2008-2009), except for observing frequent jumps between the drought and normal conditions at the lower time scales (1-, and 3-month). The persistence of the historic drought years were indicated at the longer time scales (e.g. 6-, 9-, 12-month). The meteorological drought indices showed severe drought condition in the year 1991-1992 in the majority of the stations. However, the severity of this drought condition was reflected by other drought indices. The agricultural drought indices showed a similar pattern with the meteorological drought indices of smaller time scales (1-, 3-month). Moreover, the agricultural drought indices showed smaller magnitude of the drought severity in some of the stations (e.g. Gondar) as compared to other drought indices. The hydrological drought indices indicated the persistence of the drought condition even at shorter time scales as compared to the other indices. The possible reason is that perhaps the fluctuation of river flows is very gradual as compared to the other input variables such as rainfall, evapotranspiration etc. The majority of the drought indices indicated the severity of the historic drought condition at different severity levels ranging from mild to extreme drought conditions. Thus, each drought index could potentially be used to assess some of the historic drought conditions in the UBN Basin.

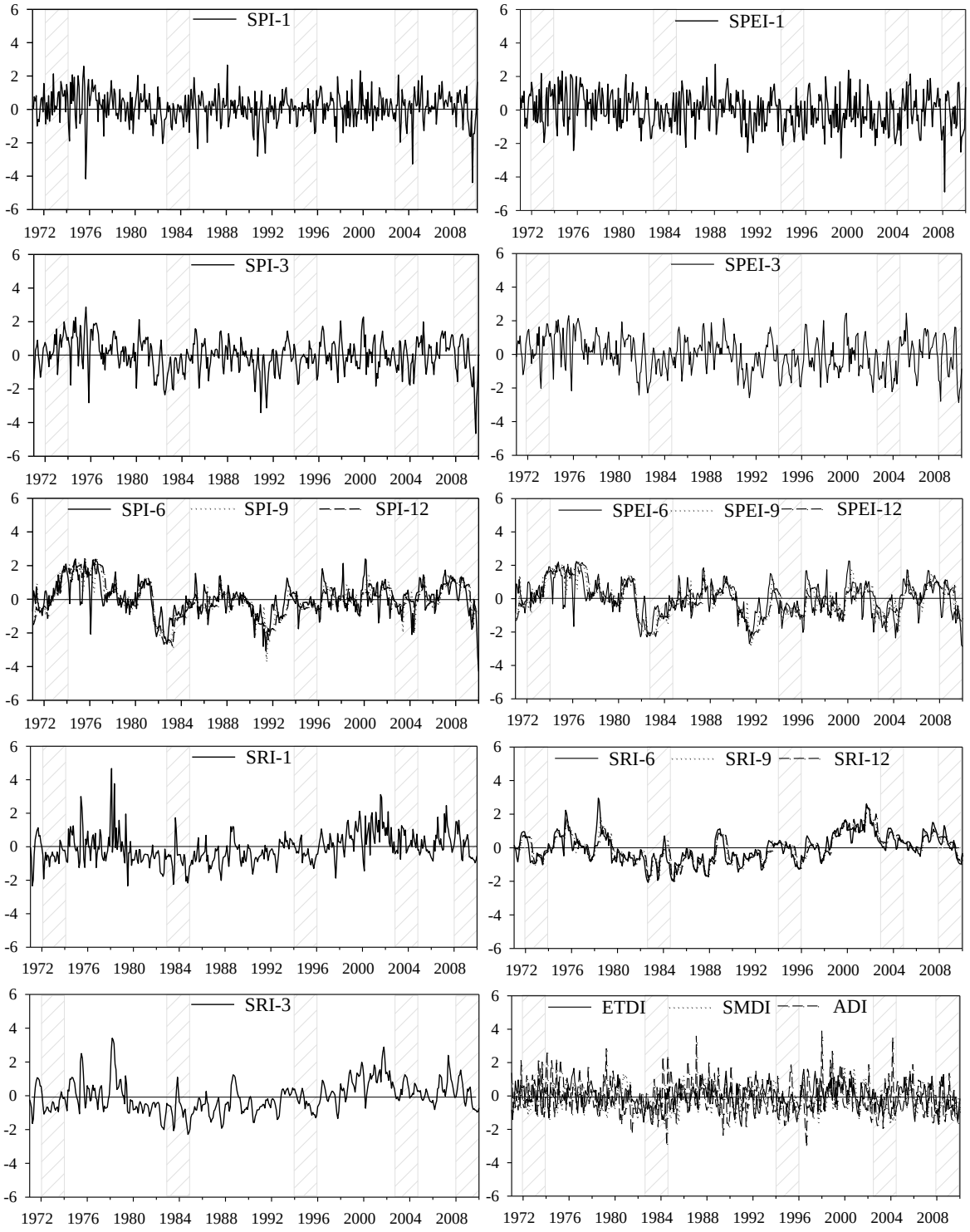

Figure 3.2a: The time series plots of the drought indices for the Gondar station. The plots for SPI, SPEI, and SRI at 6-, 9-, and 12-month time scales are shown in the single panel since it is easier to visualize the trend. A similar approach was considered for ETDI, SMDI, and ADI.

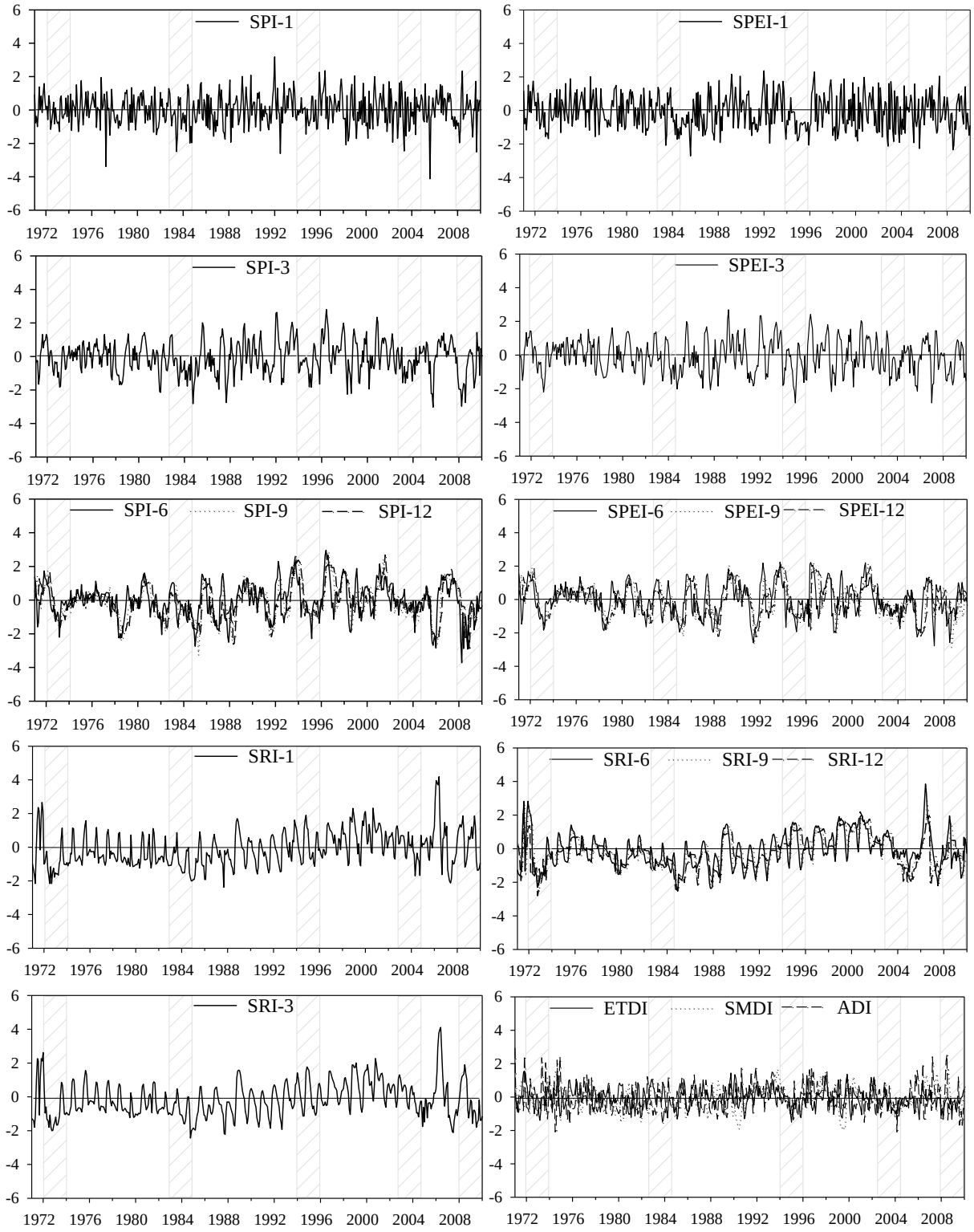

Figure 3.2b: The time series plots of the drought indices for the Debremarkos station. The plots for SPI, SPEI, and SRI at 6-, 9-, and 12-month time scales are shown in the single panel since it is easier to visualize the trend. Similar approach was considered for ETDI, SMDI, and ADI.

3.5.2 Correlation between drought indices

The Pearson's correlation coefficient matrix was developed for the six drought indices for each meteorological station. The results obtained at the Gondar (Table 3.3a) and Debremarkos (Table 3.3b) stations were presented as an example. A correlation matrix of 18 rows by 18 columns was created to investigate the relationship between the drought indices (Table 3.3). SPI-3 showed a relatively high correlation coefficient with a majority of other indices, except SPI among itself at other aggregation periods. For example, SPI-6 correlates better with SPI-9 (0.89) and SPI-12 (0.83) than SPI-3 does with SPI-9 (0.70) and SPI-12 (0.65). However, SPI-3 correlated better with SPI-1 (0.62) than SPI-6 (0.51), SPI-9 (0.48), and SPI-12 (0.41). Table 3.3a and 3.3b show that the correlation coefficients between SPI or SPEI, and SRI consistently increase as the aggregation period for SPI and SPEI increases. For example, SPI-12 and SPEI-12 correlated better with the SRI than the SPI and SPEI at shorter aggregation periods. In general, SRI consistently correlates better with other indices the longer these indices have been aggregated. The highest correlation for SRI was reached when both indices are aggregated over 12 months (correlation of about 0.4). Compared to correlations between other pairs of indices, correlations involving SRI are generally low. SRI is based on river flow, which is a result of the catchment processes, with a certain lag time. This might be one of the possible reasons why the SRI is not correlated well with other, meteorological station-based, drought indices. Table 3.3a, and 3.3b, first five columns, show that there is a strong correlation between drought indices of the same aggregation period. SMDI and ETDI (agricultural drought indices based on monthly data) have a higher correlation with SPI-3 and SPEI-3 (meteorological drought indices based on 3-month aggregated data) than with the other indices or aggregate periods. This indicates that in the UBN Basin the meteorological drought indices at 3-month aggregate period explain best the agricultural drought indices and perhaps the occurrence of an agricultural drought. Similar results were obtained for the other meteorological stations (can be referred from the supplementary document).

Table 3.3a: The Pearson's correlation coefficient matrix computed between the paired values of the drought indices at multiple time scales for the Gondar station. The SRI used in this case is being calculated using flow records at the Bahirdar station.

SPI-1	1.00																	
SPI-3	0.65	1.00																
SPI-6	0.53	0.77	1.00															
SPI-9	0.48	0.73	0.77	1.00														
SPI-12	0.45	0.68	0.72	0.96	1.00													
SPEI-1	0.85	0.55	0.36	0.28	0.26	1.00												
SPEI-3	0.49	0.89	0.61	0.48	0.45	0.63	1.00											
SPEI-6	0.35	0.59	0.93	0.72	0.65	0.42	0.69	1.00										
SPEI-9	0.32	0.53	0.75	0.94	0.83	0.33	0.55	0.79	1.00									
SPEI-12	0.30	0.51	0.69	0.83	0.94	0.31	0.52	0.72	0.89	1.00								
SRI-1	0.20	0.28	0.33	0.40	0.41	0.16	0.23	0.16	0.21	0.25	1.00							
SRI-3	0.22	0.31	0.31	0.44	0.48	0.11	0.26	0.25	0.26	0.30	0.81	1.00						
SRI-6	0.20	0.24	0.37	0.49	0.52	0.07	0.19	0.31	0.31	0.33	0.70	0.88	1.00					
SRI-9	0.24	0.32	0.43	0.51	0.53	0.08	0.16	0.26	0.33	0.34	0.63	0.80	0.93	1.00				
SRI-12	0.21	0.31	0.41	0.52	0.55	0.04	0.15	0.24	0.30	0.36	0.57	0.74	0.87	0.95	1.00			
ETDI	0.53	0.67	0.59	0.43	0.45	0.59	0.49	0.34	0.28	0.28	0.23	0.21	0.22	0.28	0.27	1.00		
SMDI	0.44	0.65	0.45	0.38	0.29	0.43	0.55	0.37	0.32	0.32	0.25	0.28	0.21	0.18	0.17	0.68	1.00	
ADI	0.75	0.59	0.40	0.32	0.30	0.78	0.59	0.39	0.38	0.36	0.33	0.23	0.15	0.12	0.13	0.68	0.63	1.00

Table 3.3b: The Pearson's correlation coefficient matrix computed between the paired values of the drought indices at multiple time scales for the Debremarkos station. The SRI used in this case is being calculated using flow records at the Kessie station.

SPI-1	1.00																	
SPI-3	0.55	1.00																
SPI-6	0.35	0.65	1.00															
SPI-9	0.27	0.48	0.74	1.00														
SPI-12	0.20	0.39	0.61	0.81	1.00													
SPEI-1	0.87	0.54	0.33	0.26	0.20	1.00												
SPEI-3	0.48	0.89	0.59	0.43	0.34	0.59	1.00											
SPEI-6	0.30	0.58	0.91	0.66	0.53	0.36	0.66	1.00										
SPEI-9	0.24	0.44	0.69	0.92	0.73	0.29	0.49	0.74	1.00									
SPEI-12	0.18	0.35	0.56	0.75	0.91	0.22	0.39	0.60	0.81	1.00								
SRI-1	0.10	0.18	0.17	0.14	0.16	0.07	0.15	0.15	0.08	0.07	1.00							
SRI-3	0.10	0.19	0.23	0.17	0.18	0.05	0.14	0.20	0.12	0.08	0.86	1.00						
SRI-6	0.08	0.20	0.28	0.26	0.23	0.05	0.13	0.21	0.20	0.13	0.63	0.83	1.00					
SRI-9	0.06	0.19	0.29	0.32	0.30	0.05	0.14	0.22	0.24	0.21	0.49	0.67	0.87	1.00				
SRI-12	0.05	0.16	0.27	0.32	0.36	0.03	0.12	0.21	0.23	0.24	0.48	0.56	0.71	0.84	1.00			
ETDI	0.27	0.51	0.39	0.25	0.22	0.29	0.49	0.37	0.27	0.26	0.01	0.00	0.03	0.04	0.09	1.00		
SMDI	0.24	0.42	0.35	0.30	0.28	0.23	0.37	0.28	0.23	0.22	0.14	0.13	0.12	0.13	0.08	0.38	1.00	
ADI	0.07	0.10	0.08	0.06	0.03	0.09	0.06	0.05	0.01	0.03	0.16	0.14	0.09	0.02	0.08	0.04	0.00	1.00

The statistical significance of the correlation coefficient values of each station was tested using t-test distribution. The result of the test is shown in Table 3.4 for each drought index. The result shows that for the majority of the drought indices the *p*-values are less than or equal to 0.01 (shown in green in Table 3.4), meaning they are statistically significant at 99% or higher

confident level. Few other correlation values (e.g. SPEI-1 and SPEI-12 with SRI at different aggregation periods, and ADI with all SPEIs) are significant at 90% or higher confidence level (i.e. $p \leq 0.1$) (shown in yellow in Table 3.4). However, the correlation values of ADI with the majority of the other drought indices (e.g. with SPI-6, SRI-9, ETDI, and SMDI) are statistical insignificant at 90% confident level (i.e. $p > 0.10$), and needs further investigation for future studies.

Table 3.4: The summary of the significant test for the selected 16 stations.

	SPI-1&3	SPI-6	SPI-9&12	SPEI-1	SPEI-3,6&9	SPEI-12	SRI-1&3	SRI-6	SRI-9	SRI-12	ETDI	SMDI
SPI-3												
SPI-6												
SPI-9												
SPI-12												
SPEI-1												
SPEI-3												
SPEI-6												
SPEI-9												
SPEI-12												
SRI-1												
SRI-3												
SRI-6												
SRI-9												
SRI-12												
ETDI												
SMDI												
ADI												

p < 0.01 **p < 0.1** **p > 0.1**

3.5.3 Comparison of drought indices based on drought characteristics

The comparison of the drought indices based on drought characteristics such as percentage of drought months, maximum drought intensity, and drought duration was analyzed and used as additional comparison criteria for each index. The results obtained at the selected 16 stations that are representing the majority of the study area were discussed in this section. The percentage of the drought months represents the proportion of the total number of drought months (including mild, moderate, severe and extreme droughts) within the study periods (1970-2010) of each station. The resulting graph is shown in Figure 3.3 and each spider web represents the value of each drought index across the selected stations. In general, the percentages of the drought months of the hydrological (SRI), agricultural (ETDI and SMDI) and ADI depict relatively larger values as compared to the meteorological drought indices (i.e. SPI, and SPEI) in majority of the stations for 1-month, 3-month, 6-month, and 12-month temporal scales. However, meteorological indices showed a smaller improvement (increase) of the percentage of drought months as the time scale increases in majority of the stations. The

comparative analysis of the percentage of the drought months was extended separately for each drought severity categories such as mild, moderate, severe, and extreme drought. Only the result obtained for severe, and extreme drought categories are shown in Figure 3.4. Interestingly, a similar result (as above) was observed only for mild and moderate drought conditions (not shown). However, an opposite result that shows relatively a larger percentage of drought months was observed by meteorological drought indices (Figure 3.4) for severe and extreme drought conditions as compared to other drought indices in a majority of the stations. This perhaps shows meteorological drought indices are influenced by the variability of the amount of rainfall during a drought event. ADI also showed large percentage of the drought months, which may indicate the dominance of rainfall in the ADI index compared to the other two input variables (evapotranspiration and soil moisture).

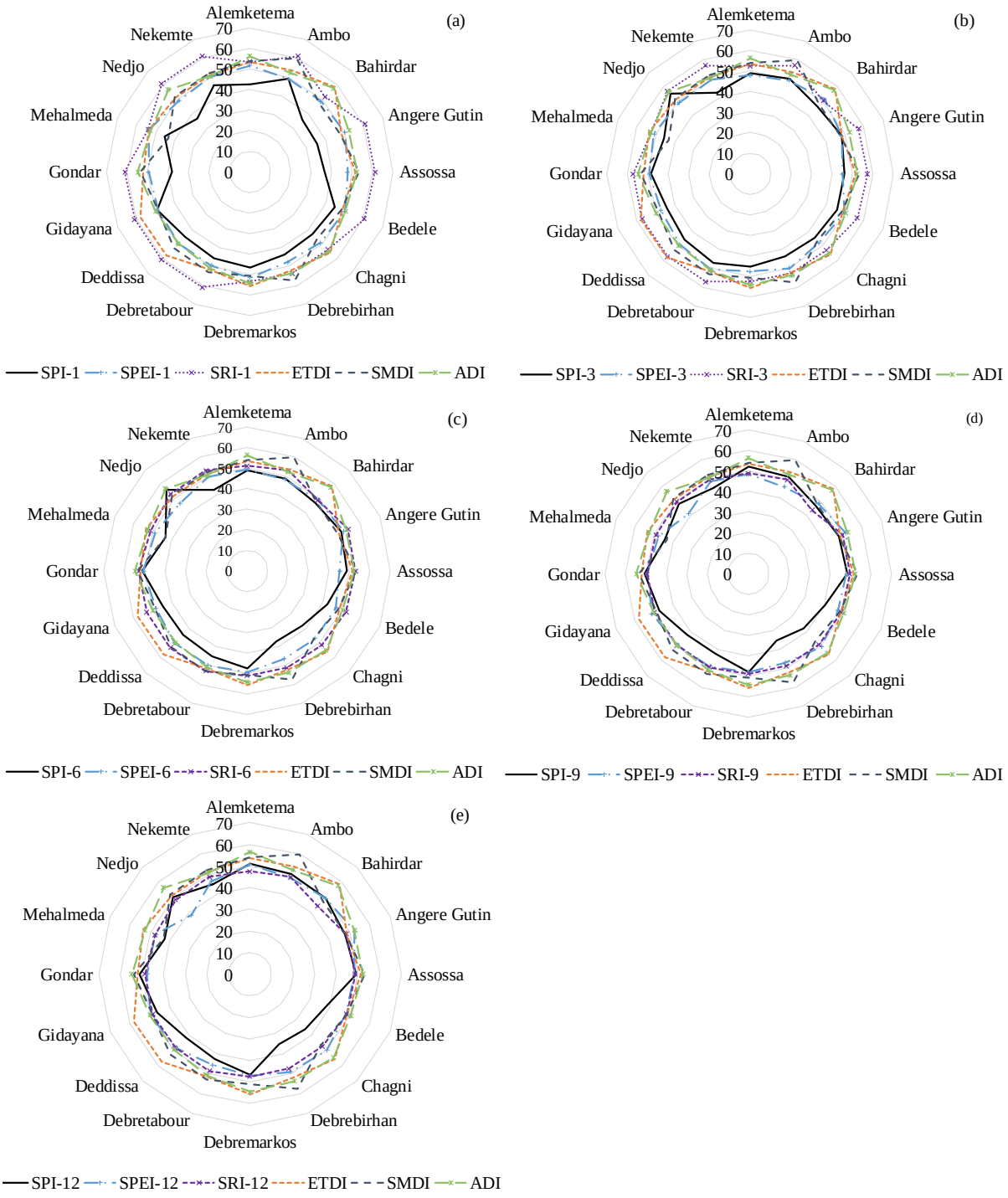

Figure 3.3. Comparison of SPI, SPEI, and SRI with ETDI, SMDI, and ADI at 1-month (a), 3-month (b), 6-month (c), 9-month (d), and 12-month (e) time scales based on percentage of drought months at the locations of the selected meteorological stations. A line is used to connect values of the same variable at distinct locations to increase the visibility of the points in this figure.

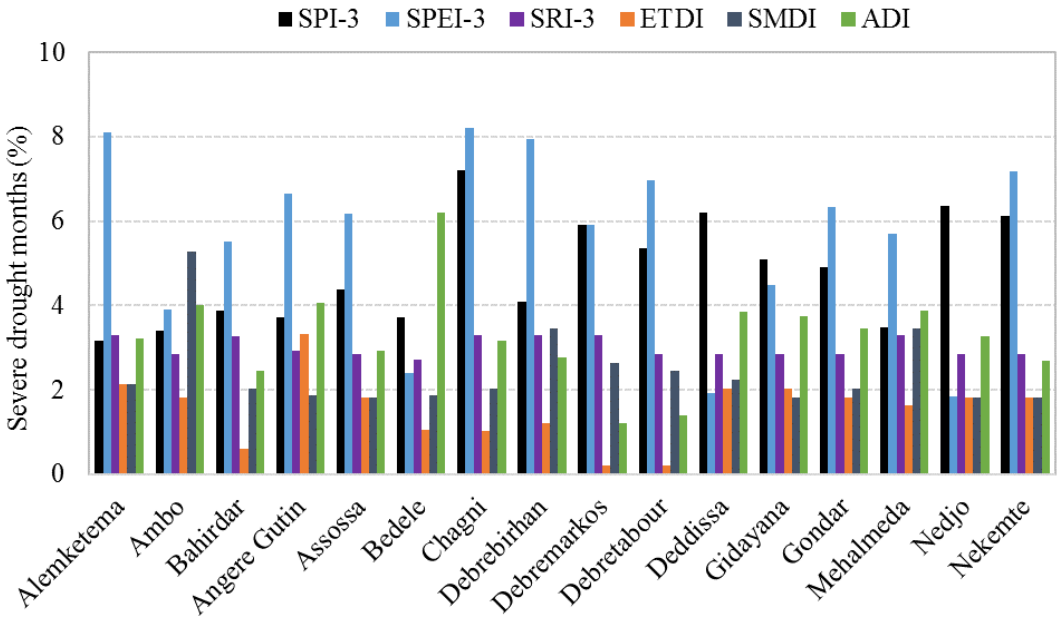

Figure 3.4a. Percentage of severe drought months observed for the drought indices within the study period (1970-2010) for the selected meteorological stations.

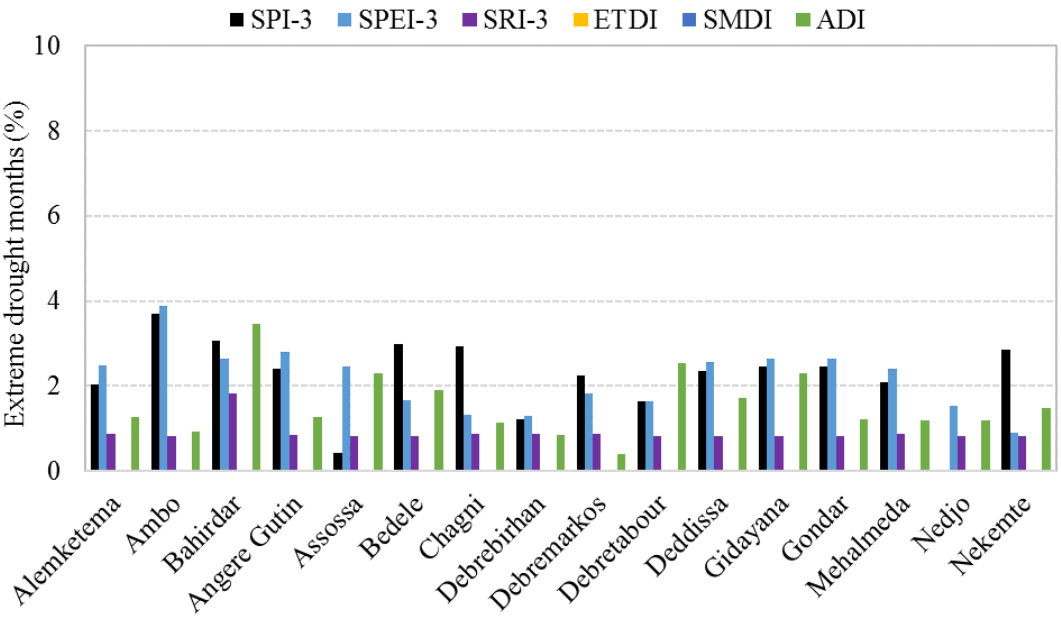

Figure 3.4b. Percentage of extreme drought months observed for the drought indices within the study period (1970-2010) for the selected meteorological stations.

The maximum duration of drought was also considered as another comparison criteria of drought indices for all time scales (Figure 3.5). The number of consecutive drought months that shows drought severity values of -1 and less (representing moderate, severe, and extreme) were counted for the study period. Evaluating drought indices based on the maximum duration of drought helps to evaluate their performance on indicating the persistence of historic drought events. In general, the result shows an increase in the maximum drought duration as the time scale increases for SPI, SPEI, and SRI in the majority of the stations. This shows persistent

drought is indicated at longer time scales (e.g. 12-month) than shorter time scales (e.g. 1-month). ETDI, SMDI and ADI show less persistent drought in majority of the stations and the result corresponds with the persistence indicated by SPI and SPEI at lower time scales (1-, and 3-month). This shows the comparability of the agricultural drought with the meteorological drought indices at lower temporal scales. The comparison of maximum duration of drought of SPI, SPEI, and SRI at the same time scales (e.g. 3-month) shows the performance of SRI on indicated relatively a large drought duration month than the SPI and SPEI. The time series of SRI is derived based on river flow (resulted from the catchment process) so that SRI is less affected by the extreme wet event in between a particular historic drought years. Interestingly, SPEI also showed relatively larger drought duration months as compared to SPI at the same time scale. The possible reason might be the use of additional input variables (e.g. potential evaporation, in the case of SPEI) could help to show the persistence of drought. The maximum duration of drought indicated by ETDI, SMDI, and ADI is relatively less in the majority of the stations. In general, the SPI, SPEI, and SRI at different aggregate periods showed a maximum consecutive drought duration (> 12-months) in a majority of the stations that perhaps reinforces the idea of comparing drought indices at a higher time scale (> 12-months) in future studies.

A similar approach/method that was followed in this study was also tested in other watersheds to compare drought indices (Jain et al. 2015; Naumann et al. 2014). In general, the results of these studies confirmed the capability of the method to identify the drought indices that can better characterize the drought condition in a specific location.

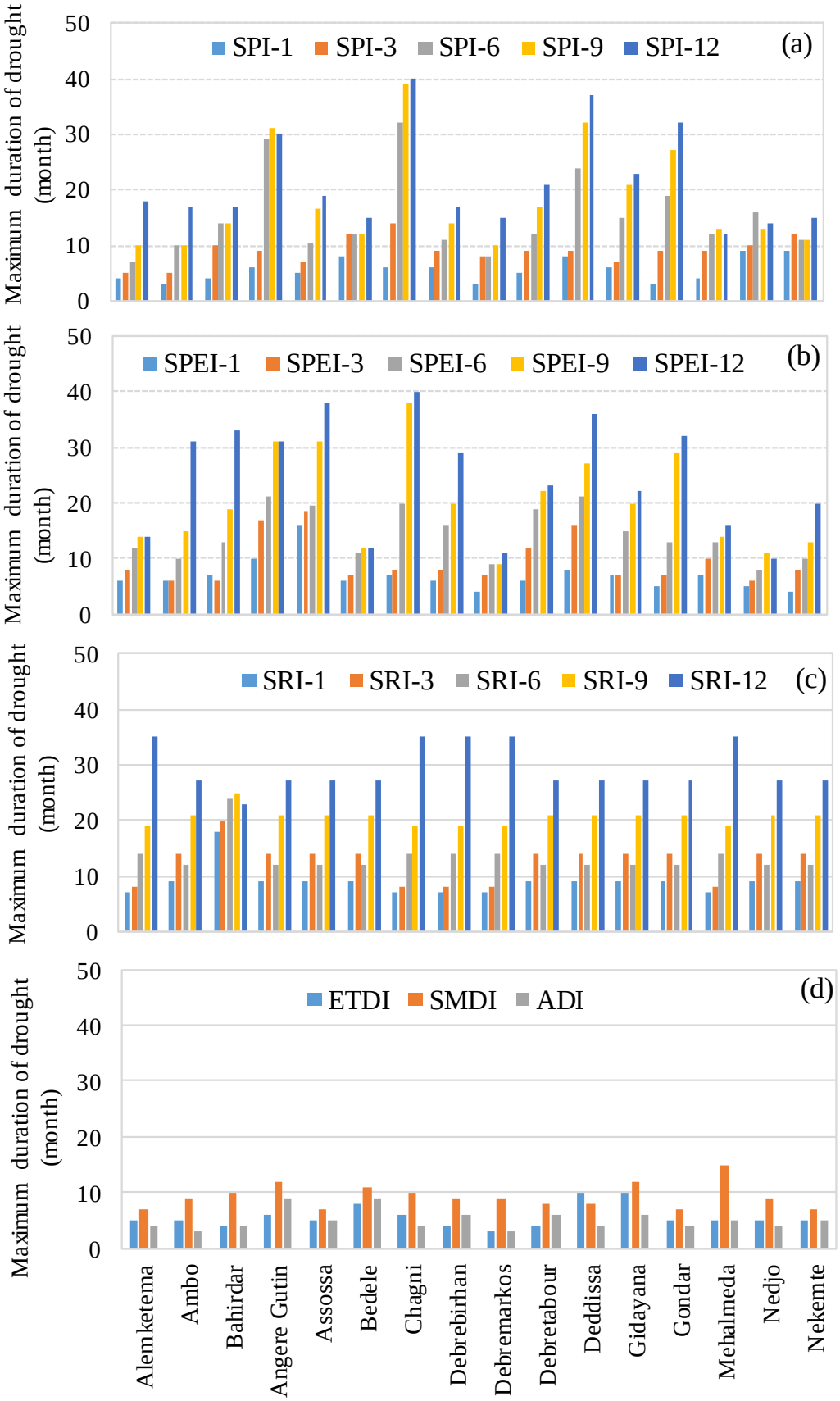

Figure 3.5. The maximum duration of consecutive drought indicated by SPI (a), SPEI (b), SRI (c) and other indices (d) such as ETDI, SMDI and ADI. Five temporal scales (i.e, 1-, 3-, 6-, 9-, and 12-months) were considered for SPI, SPEI, and SRI.

3.5.4 Comparison of drought indices through characterizing the historic drought events

Comparison of the drought indices was carried out at three river gauging stations: Abbay at Bahirdar, Kessie, and Ethiopia-Sudan border (their locations are shown in Figure 3.1). These stations represent the upper, middle, and lower parts of the UBN Basin, respectively. The time series values of the SRI-3 were calculated using the river flow data measured at these three gauging stations, whereas the areal average values were considered for the SPI-3, SPEI-3, ETDI, SMDI, and ADI. The results obtained for the upper part of the basin are presented for further discussion, and the time series of the drought indices for the middle and lower parts of the basin are presented in Appendix B. Table 3.5 shows for the historic drought events, the characteristics resulting from each of the six indices. Based on the severity of the drought, the majority of the drought indices indicated 2003-2004 and 1983-1984 as the most severe drought years in the basin, except the SPEI, which showed 1989-1994 as the most severe drought. The result further reveals that persistent droughts were observed in 2003-2004 and 1983-1984. Based on the mean (*M*) and maximum (*Mmax*) intensities, the SRI indicated the severity of 2003-2004 and 1984-1985 to have been higher than the other drought indices, except the SPEI (*Mmax* =-2.63). The SRI indicated the persistence of the 1983-1984 drought, which extended beyond the start and end year as provided by EM-DAT. The SPI ranks 1973-1974 as the most severe drought year based on mean intensity (*M* = -1.21) and maximum intensity (*Mmax* = -2.57). However, the drought durations of the SPI and SPEI for the same year are relatively small, resulting most likely from the earlier start of the drought in 1972. The onset month of each drought year is used as the other comparison criteria, and the result is shown in Table 3.5. According to EM-DAT, the 1973-1978 drought started in December 1973 and lasted until 1978. The ETDI showed the closest onset (November 1973) for this year. The SMDI showed a slightly earlier onset (July 1973) of the 1973-1978 drought whereas the SPI and SPEI (January 1973) and SRI (March 1973) indicated an early start of this drought. The ADI showed the latest onset (July 1976) of this particular drought event. According to EM-DAT, the 1983-1984 drought started in May 1983, but all indices except the ETDI and ADI showed an early start (January 1983) of this drought event. The ETDI and ADI show a late start (December 1983 and September 1983, respectively) of the 1983-1984 drought. The 1989-1994 drought started in October 1989; the SPI and SPEI showed an August 1989 start, the SRI showed a December 1989, and the ETDI and SMDI indicated drought earlier than all the other indices. The drought start month indicated by ADI is December 1993. While this doesn't correspond

with EM-DAT, it corresponds to the historic drought 1993-1994 reported in other studies (see section 2.2.1). Note that it is likely that the 1993-1994 drought has been included in the EM-DAT database as part of the prolonged drought period from 1989 to 1994. For 2003-2004, there is no reference onset from EM-DAT to compare with the six drought indices. However, all the indices indicated the onset of the drought in January and February 2003, except the SRI, which indicated the onset of drought in July 2003. Overall, the meteorological drought indices (SPI and SPEI) indicate the start date four or more months before the reported start month, whereas agricultural drought indices indicate the start date three or more months after the reported starting date of a historic drought. The aggregate drought index (ADI) most often lagged by some months. It can be noted from this result that no single drought index consistently indicates the exact onset of the drought. Similar results are obtained for the middle, and lower parts of the UBN Basin.

Table 3.5: Characteristics of the historic drought events as identified by the six drought indices for the Upper Blue Nile basin upstream of Bahirdar. Note that if the index indicated the onset to be before January of the reported calendar year of the historic drought, this is presented in the table with "before" and if, according to the index, a drought extended beyond December of the reported calendar year, this is presented with "after". The drought duration in these cases is based on a start in January and an end in December of the reported drought year.

Drought index	**SPI-3**	**SPEI-3**	**SRI-3**	**ETDI**	**SMDI**	**ADI**
1973-1978 drought (Onset in December according to EM-DAT)						
Starting date	before/1973	before/1973	03/1973	11/1973	07/1973	07/1976
Ending date	04/1973	04/1973	06/1974	06/1974	05/1974	04/1977
Mean Intensity, *M*	-1.21	-1.23	-0.75	-0.48	-0.42	-0.94
Maximum intensity, M_{max}	-2.57	-2.33	-1.36	-1.47	-1.19	-2.43
Duration, *D* (months)	4	4	16	8	11	10
Severity, *S*	-4.84	-4.91	-11.94	-3.85	-4.57	-9.38
1983-1984 drought (Onset in May according to EM-DAT)						
Starting date	before/1983	before/1983	before/1983	12/1983	before/1983	09/1983
Ending date	05/1984	07/1983	after/1984	after/1984	after/1984	04/1984
Mean Intensity, *M*	-0.99	-0.86	-1.36	-0.66	-0.53	-0.46
Maximum intensity, M_{max}	-2.45	-1.95	-2.53	-1.53	-1.78	-1.98
Duration, *D* (months)	17	7	24	13	24	8
Severity, *S*	-16.82	-6.02	-32.59	-8.62	-12.79	-3.68
1989-1994 drought (Onset in October according to EM-DAT)						
Starting date	06/1989	07/1989	12/1989	04/1990	02/1990	12/1993
Ending date	08/1990	08/1990	12/1990	02/1991	01/1991	after/1994
Mean Intensity, *M*	-0.69	-0.65	-0.70	-0.85	-0.46	-0.57
Maximum intensity, M_{max}	-2.49	-2.09	-1.38	-1.92	-1.18	-1.57
Duration, *D* (months)	15	14	13	9	11	13
Severity, *S*	-10.30	-9.13	-9.06	-7.62	-5.08	-7.38
2003-2004 drought (Onset not defined according to EM-DAT)						
Starting date	before/2003	02/2004	07/2004	before/2003	before/2003	before/2003
Ending date	10/2004	12/2004	12/2004	after/2004	after/2004	12/2003
Mean Intensity, *M*	-0.59	-0.71	-1.61	-0.51	-0.45	-0.92
Maximum intensity, M_{max}	-1.95	-2.63	-2.13	-1.23	-1.36	-2.27
Duration, *D* (months)	22	11	6	24	24	12
Severity, S	-12.95	-7.79	-9.64	-12.26	-10.85	-11.09

Figure 3.6 compares the time series patterns of the six drought indices for the historic drought years 1973-1978, 1983-1984, 1989-1994, and 2003-2004. In the 1973-1978 drought (Figure 3.6a), the majority of the drought indices showed the occurrence of moderate to severe drought condition in several months between 1973 and 1975 (index value < -1.0 and lower) whereas mild drought and wet conditions were observed from 1976 to 1978 except for the ADI, which showed severe drought for ten months. Relatively persistent drought was indicated by the SRI and ETDI in 1973-1974 whereas other indices show a frequent jump between drought and non-drought conditions. In this study, persistent drought is defined if consecutive months (> 10

months) showed below average values (zero). The majority of drought indices indicated mild to severe drought condition for several months (> 6) in the year 1983/1984 (Figure 3.6b). The SRI showed the severity and persistence of the 1983-1984 drought and indicated drought conditions throughout 1983/1984. The SPI also showed mild to severe drought conditions for several months except for non-drought conditions in mid-1984. The 1989-1994 drought is not well defined except for 1990, 1991, and 1994; the majority of the indices showed the occurrence of moderate to severe drought condition during these years. Like the 1983/1984 drought, the majority of the drought indices showed mild to extreme in 2003-2004, although the SRI, SPEI and ADI showed non-drought conditions for some months. The SRI showed severe to extreme drought conditions whereas the SMDI showed mild to moderate drought conditions for several months in 1983-1984. The SPI-3, SPEI-3, ETDI, and ADI showed out of drought conditions for the period of 4 to 10 months. However, the SPI-3, SMDI, and ETDI indicated the drought conditions in the year 2003-2004, whereas the SRI showed an opposite pattern than other indices. In general, the SPI and SPEI showed similar patterns in most cases while the ADI showed a frequent jump between drought and non-drought conditions. Moreover, ADI showed relatively higher positive and negative values perhaps because of a direct consideration of the eigenvector as weights/coefficients in combining the input variables. Other approaches, such as the percentage of contribution could be considered for future studies. The SRI showed the persistence of the drought and non-drought conditions for several months possibly because of less fluctuation of the river flow with time as compared to the rainfall.

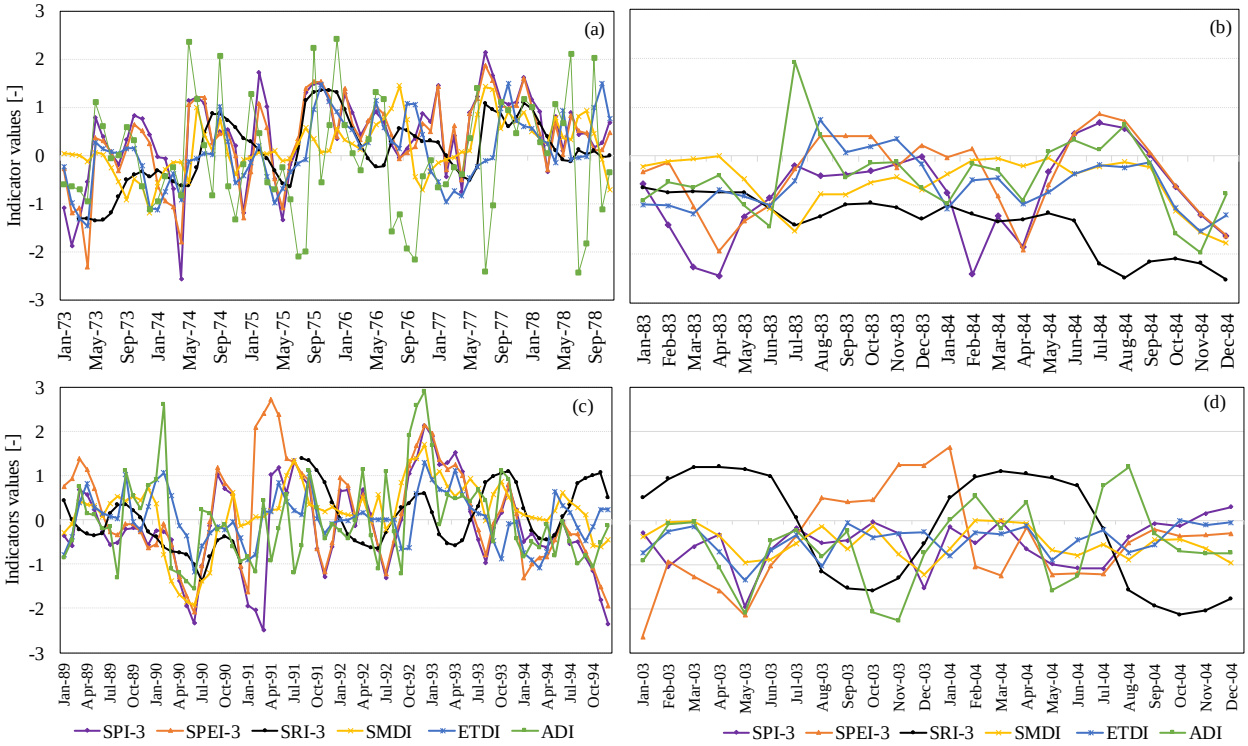

Figure 3.6: The time series plot of the six drought indices for 1973/1978 (a), 1983/1984 (b), 1989/1994 (c), and 2003/2004 (d) historic drought years in the UBN Basin.

3.6 Conclusion

In this study, we compared six drought indices—SPI and SPEI (meteorological indices), ETDI and SMDI (agricultural indices), SRI (hydrological index), and ADI (aggregate index)—to investigate how well characteristics of historic drought events in the Upper Blue Nile basin are identified by these indicators. Observed data were used for the precipitation, temperature, and streamflow inputs. Soil moisture, and actual evapotranspiration data were estimated using the SWAT hydrological model.

In general, meteorological drought indices SPI-3 and SPEI-3 show a higher correlation with the agricultural drought indices SMDI and ETDI compared to the hydrological drought index (SRI) whereas the hydrological drought index (SRI) correlates better with meteorological drought indices at a 12-month aggregate period (SPI-12 and SPEI-12). This indicates that there exists some interconnections between drought indices in the sense that one drought index can explain more than one specific drought category to a certain degree. Moreover, each index has the potential to characterize and explain at least one recorded (historical) drought condition. It seems that a combination of more than one drought index, appropriately selected for the specific region, is usually required for drought monitoring.

When comparing the drought onset dates indicated by the six indices for the historical (recorded) droughts, the meteorological drought indices (SPI and SPEI) showed early onsets compared to the other drought indices, except for the 2003-2004 drought where SPEI showed a late onset. The agricultural (ETDI, SMDI, and ADI) and hydrological (SRI) drought indices showed late onsets, particularly the ADI, which lagged by several months for all events except 2003-2004. When the onset dates indicated by the six drought indices are compared with the EM-DAT, meteorological drought indices (SPI-3, and SPEI-3) showed earlier onsets except for the 2003-2004 drought where the EM-DAT onset was unavailable. Similarly, the agricultural (ETDI and SMDI) and hydrological (SRI-3) drought indices showed earlier onsets of drought for two drought events and a late onset for one drought event. In contrast, ADI showed late onsets for two drought events and an early onset for 1983-1984. The comparison showed that none of the six drought indices could individually identify the onset of the four selected historic events. They could identify all events if all six indices (including different aggregation periods) were combined. Note that the ADI index tested in this study considers only three input variables at a 1-month aggregate period. The years 2003/2004 and 1983/1984 were indicated as the most severe drought years in the basin. Effective drought monitoring and planning is essential to mitigate drought impacts in the basin. For future drought monitoring for the Upper Blue Nile basin, developing a method that makes optimal use of multiple drought indices is recommended.

4. Developing a combined drought index and prediction model to monitor drought-related crop yield reduction[3]

4.1 Introduction

The main objective of this chapter is to develop a combined drought index (CDI) and prediction model of crop yield anomalies in the Upper Blue Nile (UBN) Basin. Developing a combined drought index is important because it would effectively incorporate the available and useful information from individual drought indices (Zargar et al. 2011; Niemeyer, 2008; Sivakumar et al. 2011; Heim, 2002). The individual drought indices have a limitation on providing a comprehensive characterization of drought events and they are region specific and are applied for specific objectives. Several attempts have been made recently to combine several drought indices into a single comprehensive aggregate index including the US Drought Monitor (USDM) (Svoboda et al. 2002) and the Vegetation Drought Response Index (VegDRI) (Brown et al. 2008). These two indices aggregate, or combine, several climatic input variables, mainly the Standardized Precipitation Index (SPI), Palmer Drought Severity Index (PDSI), and NDVI-based indicators: Percent Average Seasonal Greenness (PASG) and Start of the Season Anomaly (SOSA). Karamouz et al. (2009) developed a hybrid drought index (HDI) by combining SPI, PDSI and surface water supply index (SWSI). These researches have shown the usefulness of combining drought indices or several input variables representing several aspects of the environment.

Other researchers have worked on developing CDIs before, but often the combination of individual drought indices is based on subjective or expert-based approaches. Balint et al. (2013), for example, developed such combined drought index for Kenya in the Horn of Africa. A large weight (50%) was assigned for rainfall-based drought index, in this case PDI. The remaining 50% of the weight was assigned equally for the other two indices, TDI and VDI. Sepulcre et al. (2012) proposed a CDI that combines the SPI, anomalies of soil moisture, and anomalies of the fraction of Absorbed Photo synthetically Active Radiation (fAPAR). The

[3] *Based on*: Bayissa, Y.A, Tadesse T., Mark D. Svoboda, Brian D. Wardlow, Calvin Poulsen, John Swigart and S.J. van Andel 2018. *Developing and evaluating a satellite based combined drought index to monitor historic drought: a case study for Ethiopia*. Under review in GIScience & Remote Sensing.

combined drought index gave a synthetic and synoptic overview assuming a general progression of drought, according to three classifications, from "watch" when a relevant precipitation shortage is observed, to "warning" when this precipitation shortage translated into a soil moisture deficit, and finally "alert" when these two conditions are accompanied by unfavorable vegetation vigor. One of the limitations of this study was that it assumed uniform phenology/plant growing period for the whole of Europe. Vyas et al. (2015) developed an Earth Observation-based CDI for which a procedure was followed to assign the weights, which appears to have better objectivity compared to the Balint et al. (2013) approach. However, this procedure is not adaptable for more than two drought indices.

In this study, two CDI methods are implemented that combine individual indices following an objective procedure. The first method uses a Principal Component Analysis (PCA) (Bordi et al. 2006; Keyantash and Dracup, 2004), and the second method uses a random search optimisation to maximize the correlation between the resulting CDI and drought impact: in this case crop-yield anomalies.

Both methods use the same input variables. To the best of our knowledge, this second type of CDI, defined here as Impact-based CDI, has not been presented in literature before except for the work by Balint et al. (2013). Unlike the procedure adopted by Balint et al. (2013), the impact-based CDI developed in this study considers several input variables, and uses an iterative procedure of assigning the optimal weights. The resulting impact-based CDI is used as input to a regression model of crop yield anomalies in the Upper Blue Nile Basin.

Developing the regression model between the drought indices and the crop yield anomalies is the second objective addressed in this study. The regression model postulates the impacts of drought on the crop yield, and involves the potential use of the impact-based drought index on assessing drought impact on agriculture, mainly on crop yield. Developing such a model is important especially in an area where agriculture has the key role in the economy. Four commonly grown cereal crops were considered in developing the regression model for the sixteen administrative zones across the UBN Basin.

4.2 Data

Crop yield data were obtained from the Central Statistical Agency (CSA) of Ethiopia. The data are organized in administrative zones as shown in Figure 4.1. The Upper Blue Nile basin is classified into sixteen administrative zones excluding Lake Tana. The areas of the zones range

from 3453 km^2 (North Wello) to 26206 km^2 (Metekel). For each administrative zone, the CSA uses standard statistical data collection and analysis to generate the estimate of the crop yield (CSA, 2014). The crop yield data that corresponds to each administrative zone are calculated by taking the ratio of the crop production (Quintal) to the total cultivable land (hectare) of each crop.

In this study, four cereal crops most commonly cultivated in the study area are considered. These cereal crops are Teff, Barley, Sorghum, and Maize. These four cereals are the major food crops and principal stable crops in terms of area planted and volume of production (CSA, 2014; Tadesse et al. 2015). The annual crop yield data that have been collected for each administrative zone represents the main rainy season (Meher season) in the basin. The crop yield in this season accounts for 90-95% of the annual crop production in the basin (FEWSNET, 2003) and thus kiremt growing season is the focus in this chapter. The main crop growing season (Meher or kiremt) is from June to October (Diro et al. 2008; Gissila et al. 2004) and fifteen years of historic records of the yield data (1996-2008) were considered. However, the data for 2001, 2002 and 2005 were missing and not considered in this study.

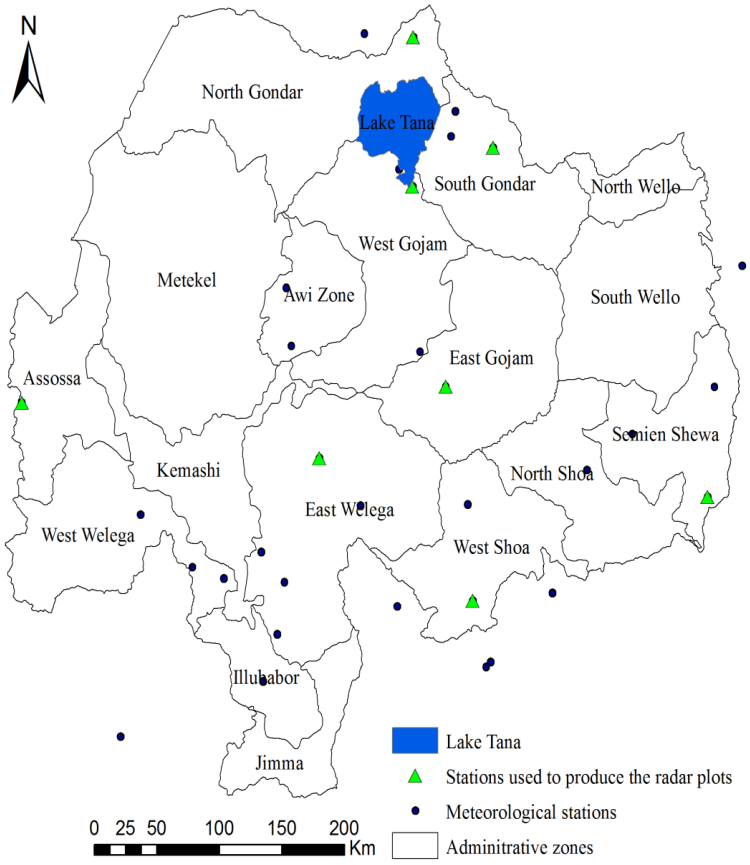

Figure 4.1: The distribution of administrative zones and meteorological stations used for the CDI development. The name labels in the figure refer to the administrative zones.

4.3 Methods

Figure 4.2 shows the summary of the methodology followed in this chapter, aimed at developing the combined drought index and the crop yield prediction model. The principal component analysis (PCA) and the random search of the optimal weights were used. The combined drought index was developed based on several other drought indices (SPI, SPEI, SMDI, ETDI, and SRI) as inputs. The details of the methodology followed in this chapter is described in detail in the next subsections.

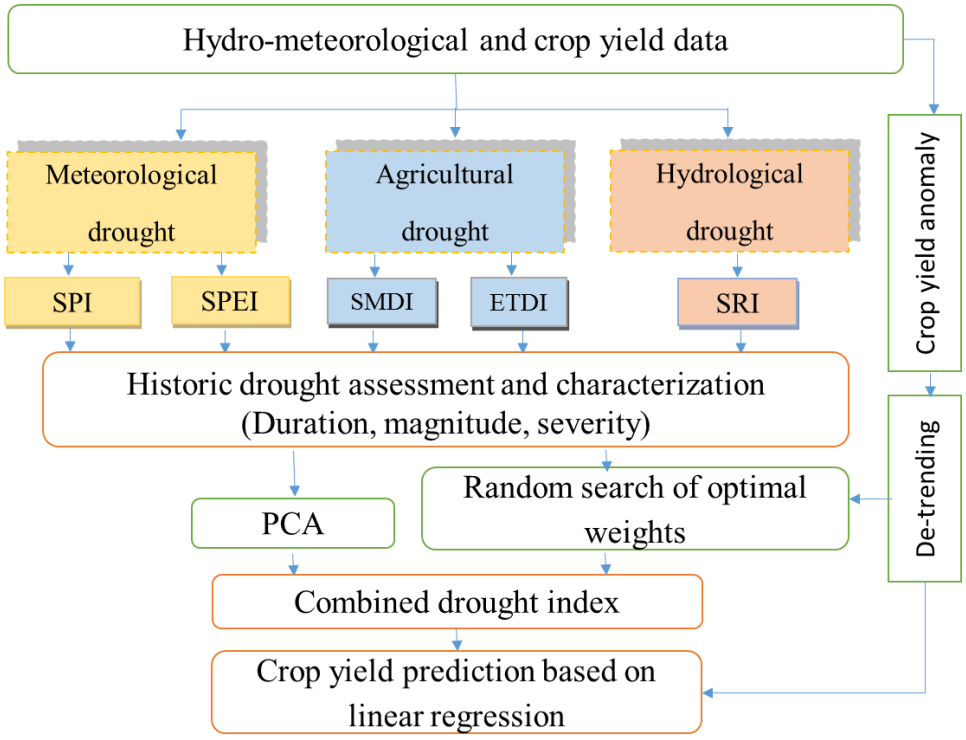

Figure 4.2: Summary flow chart showing the steps followed in this chapter.

4.3.1 Detrending the crop yield data

According to FAO, (1999), factors affecting agricultural yields can be categorized into three major groups: (i) technology and management trends such as mechanization, crop varieties, advance in the water application technology, (ii) intermittent factors such as change in policy that affect management decisions, and (iii) climate variability in space and time (Figure 4.3).

The majority of the drought indices considered in this study are developed using the climate data as the main input. The effects of climate on the drought assessment is significant, hence, the effects of climate on the crop yield production is more significant than the other factors in evaluation of the drought indices. However, it is often difficult to separate the effects of climate from other factors. Detrending is often used to remove the trend resulting from factors other

than climate by subtracting the estimated trend value from the actual yield data values for each given year (FAO, 1999, Tadesse et al. 2015). It is also assumed that removing a trend from the data enables researchers to focus the analysis on the yearly variations in the crop yield data (Tadesse et al. 2015). Hence, the crop yield data were first detrended before further use to correlate with the combined drought index.

Detrending of the crops yield time series data for the sixteen administrative zones in the study area was carried out to eliminate the upward trend assumed to be resulting from factors other than climate (in this, we followed Tadesse et al. 2015; Lu et al. 2017). A linear regression equation (top right corner of Fig 4.4) that considers the entire crop yield data series was used to detrend the annual crop yield data. For detrending, we used the detrend function in Matlab (MathWorks, 2009).

Detrending was carried out for all administrative zones in the study area and for the four cereal crops. An example of detrending the Teff crop yield data for North Gonder Zone is shown in Figure 4.4.

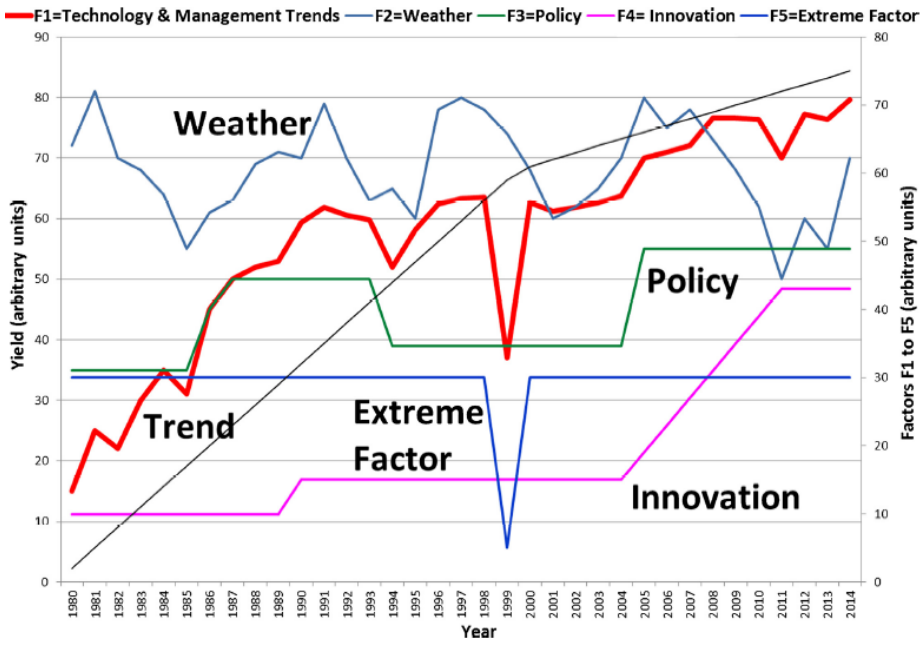

Figure 4.3: Factors affecting agricultural yields: technology and management trends (heavy red line), innovation, policy, extreme factors, and weather (adapted from FAO, 1999).

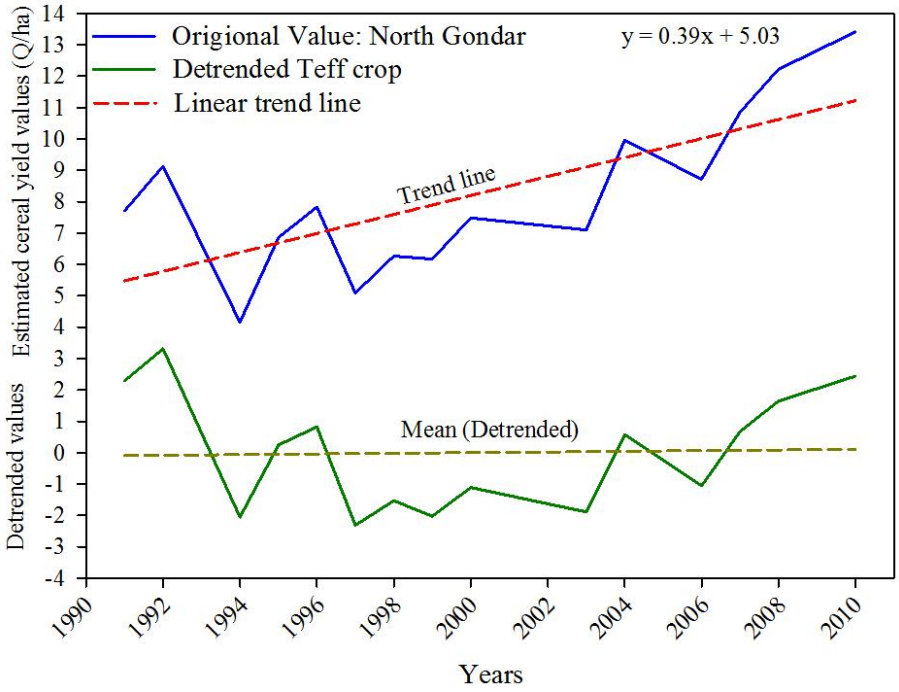

Figure 4.4: An example of the detrended North Gondar zone historic data (the crop yield average). The positive values (above the trend line) show more productive years and the negative values show lower production as compared to the expected mean.

4.3.2 Correlation analysis of crop yield with drought index

The correlation coefficient matrix between the drought indices and detrended crop yield anomalies was developed to get insight in the agreement between these two parameters at the corresponding locations of each meteorological station. The time series of drought indices (SPI, SPEI, ETDI, SMDI, and SRI at 3-month aggregate period) and crop yield anomalies (Sorghum, Barley, Maize, and Teff crops) during the crop-growing season were considered for the period of 1996 to 2008. For the crop yield data, we used an aggregated value for each administrative zone and hence the stations within each administrative zone were used to generate the correlation coefficient matrix.

4.3.3 Qualitative analysis of crop yield and drought index values

The qualitative approach was adapted to visually compare the existence of consistency between drought indices values and the detrended crop yield anomalies. Radar and bar-chart plots were produced for the drought indices and the crop yield anomalies respectively.

4.3.4 Principal Component Analysis (PCA) based CDI

The principal component analysis (PCA) is one of the techniques used in this study to develop the combined drought index. In the literature (Barua, 2010; Keyantash and Dracup, 2004), the PCA analysis is most often based on the input data to generate the correlation coefficients matrix. It is later used to develop the directional vector that is used to combine the input parameters. In this study, the time series values of the drought indices that include the SPI, SPEI, ETDI, SMDI, and SRI were used to develop the combined drought index. The PCA combines the indices values through calculating the correlation coefficient matrix between each index followed by computing the Eigenvalues and the Eigenvector. The eigenvector, called the direction vector, is used to convert the indices values into a single index (the combined drought index).

For example, ($n \times m$) is an observational data matrix ($\boldsymbol{H}$), where n is the number of observations and m is the number of variables. Each variable h_j in the j^{th} column of $\boldsymbol{H}$ has a vector of n ($n \times 1$) observational data, with j = 1, ..., m. Twelve matrices of $\boldsymbol{H}$ were used separately for PCA, one for each month. After an iterative process of PCA, the matrix $\boldsymbol{H}$ is replaced by the ($n \times m$) matrix of $\boldsymbol{Q}$, containing the transformed variables q_j ($q_j = \phi_j(h_j)$).

Each month's transformed variable matrix is standardised in such a way that the mean is subtracted from each value and the result is divided by the standard deviation. A square ($p \times p$, where p is the number of variables), symmetric, correlation matrix $\boldsymbol{R}$ is used to describe the relationship between the original data. The correlation was computed among data representing the same month. There is a separate $\boldsymbol{R}$ for each month to describe the correlations between variables. The eigenvalues and then the eigenvector were derived through PCA that was used to establish the relationship between the PCs and original data.

$$\boldsymbol{Z} = \boldsymbol{XE} \tag{4.1}$$

where $\boldsymbol{Z}$ is the $n \times p$ matrix of the principal components
$\boldsymbol{X}$ is the $n \times p$ matrix of standardized observational data
$\boldsymbol{E}$ is the $p \times p$ matrix of eigenvectors

The CDI is the first principal component (PC1), normalized by its standard deviation (this is done to avoid a higher jump in the time series values of CDI posed by the month that possesses a higher degree of variability).

$$CDI_{i,k} = \frac{Z_{i,1,k}}{\sigma} \quad 4.2$$

where $CDI_{i,k}$ is the CDI value for month *k* year *i*, $Z_{i,1,k}$ is the first principal component during year *i*, for month *k*, and σ is the sample standard deviation of $Z_{i,1,k}$ over all year *i*.

The first PC explains a large fraction of the variance, and all PCs are orthogonal to each other.

Threshold determination of CDI: The CDI thresholds were based on the SPI drought category (Table 4.1). The SPI dryness thresholds are the Gaussian variants of -2, -1.5, -1 and 1 standard deviations, which correspond to 2.3th, 6.7th, 16.0th and 84th percentiles in CDI cumulative distributions.

Table 4.1: CDI drought category classification based on the corresponding percentile ranking.

Standardized values	Corresponding percentiles	Drought category
above 0.92	100	Wet
-0.95 to 0.92	84	Near normal
-1.40 to -0.96	16	Moderate drought
-1.69 to -1.41	6.7	Severe drought
-1.70 or less	2.3	Extreme drought

4.3.5 Impact-based CDI

The method followed in this section is aimed to develop the impact-based CDI. The same input variables are considered as in the PCA based approach described in section 4.3.4. However, a different technique is implemented here to quantify the relative weights of each input variable. This weight shows the contributions of each variable in developing CDI. The optimal weight of each input variable is quantified through a random search procedure. This procedure uses a random combination of weights (ranging from 0.1 to 0.9) and does more than 60,000 iterations to identify the combination of weights that gives the maximum correlation coefficient with the crop yield anomaly. The combination of weights that gave the highest correlation coefficient between the CDI and the crop yield anomaly was finally selected as the best set of weights for the CDI. We find that such an optimization approach avoids the inherent challenge of subjectivity observed in other CDI research (Svoboda et al. 2002; Balint et al. 2013). The presented algorithm was implemented in MATLAB.

Equation 4.3 shows the general equation used to compute the time series values of CDI. Five drought indices (SPI, SPEI, SMDI, ETDI and SRI) were combined and their relative

contribution depends on the magnitude of weight. The higher weight assigned for the particular input variable shows its higher influence on the CDI.

$$CDI_{i,m} = w_{SPI} \times SPI_{i,m-n} + w_{SPEI} \times SPEI_{i,m-n} + w_{SMDI} \times SMDI_{i,m-n} + w_{ETDI} \times ETDI_{i,m-n} + w_{SRI} \times SRI_{i,m-n} \quad 4.3$$

where w_{SPI}, w_{SPEI}, w_{SMDI}, w_{ETDI}, and w_{SRI} are the weights of each index

4.3.6 Prediction model of crop-yield anomalies

The combined drought index and the five drought indices values were the basis to develop the prediction model with the crop yield anomaly based on linear regression approach. First, the multiple linear regression model between the CDI values and the crop yield anomaly was developed. Secondly, the prediction model between the five drought indices and the crop yield anomalies was also developed. The performance of the two models was compared.

4.4 Results and discussion

4.4.1 Correlation analysis of the individual drought indices with crop-yield anomalies

Correlation analysis was done for each meteorological station location representing the administrative zones. Table 4.2 shows the correlation coefficient matrix between the drought indices and the detrended crop yield at the station of Debremarkos (East Gojjam). In general, the result reveals that there is a good correlation between drought indices and crop yield. All crops show a high correlation coefficient with the SPEI index (> 0.4). Unlike Teff and Maize, all indices except the SRI performed better for Barley and Sorghum crops. The barley crop appears to be highly correlated with the ETDI and SMDI indices. Likewise, the SPEI and SPI indices performed relatively well in the majority of the meteorological stations for all crops. It can be also observed that the SMDI and ETDI correlated very well with the Sorghum and Barley crops in the majority of the meteorological stations with a correlation coefficient ranging between 0.6 and 0.8. The Teff crop has a weak correlation with drought indices, compared to the other crops (Table 4.2). The possible explanation for the weak correlation of Teff could be its drought tolerant characteristics (as compared to the other crops considered in this study). The tolerance of the Teff crop to drought is reported by Ketema, (1987). In the majority of the stations, the Barley crop correlated better than the others. From this result, it can be argued that the type of Barley cultivated in the study area might be drought sensitive.

Table 4.2: Correlation coefficients matrix for the drought indices and crop yield anomalies (1996-2008).

	Sorghum	Barley	Maize	Teff
SPI-3	0.57	0.57	-0.06	0.12
SPEI-3	0.51	0.60	0.40	0.50
ETDI	0.53	0.68	0.07	-0.07
SMDI	0.46	0.66	0.29	-0.05
SRI-3	0.47	-0.27	0.24	-0.04

4.4.2 Comparison of drought indices with crop yield anomalies

In order to visually compare whether there is consistency between all the drought indices and detrended crop yield on indicating the historic drought events, the radar and bar chart plots were produced for the selected eight stations (their location is shown in Figure 4.1). The radar and bar plots produced for the Debremarkos and Gondar stations were presented for further discussion (Figures 4.5 and 4.6) and similar plots for the other stations were also annexed (Appendix C). The drought indices and the detrended crop yield values were normalized between -1 and 1 to compare to each other.

The visual inspections of the radar and the bar plots showed that one or more than one of the drought indices characterized the relationship between drought and crop yield reduction during the drought years. The wet and dry years were clearly indicated by most of the drought indices and the crop yield anomaly in the majority of the stations. For example, the years 2006, 2007 and 2008 were marked as the wet years in the basin and hence a narrow spider ring (shows positive values of drought indices), and positive crop yield anomaly were observed. Similarly, the year 2003 was recorded as one of the drought years in the basin. This year was characterized by the wider spider rings and negative crop yield anomaly (Figures 4.5, 4.6 and 4.7). Generally, process based drought indices such as the SMDI and ETDI identified the drought characteristics that are responsible for yield reduction in the majority of the stations in comparison to the SPI and SRI. The SPEI and SPI indices partly reveal and partly conceal the existence of reduction of crop yield due to concurring drought in some stations in some particular year. For instance, in the West Gojjam zone (Bahirdar station) in the year 2000, the observed data indicates there was a reduction of crop yield. While the SPEI indicates the strong existence of drought that may reduce yield, the process based SMDI and ETDI concealed this information. This indicates that the aggregate use of all indices is helpful to extract maximum information pertaining to yield reduction and effective monitoring of drought.

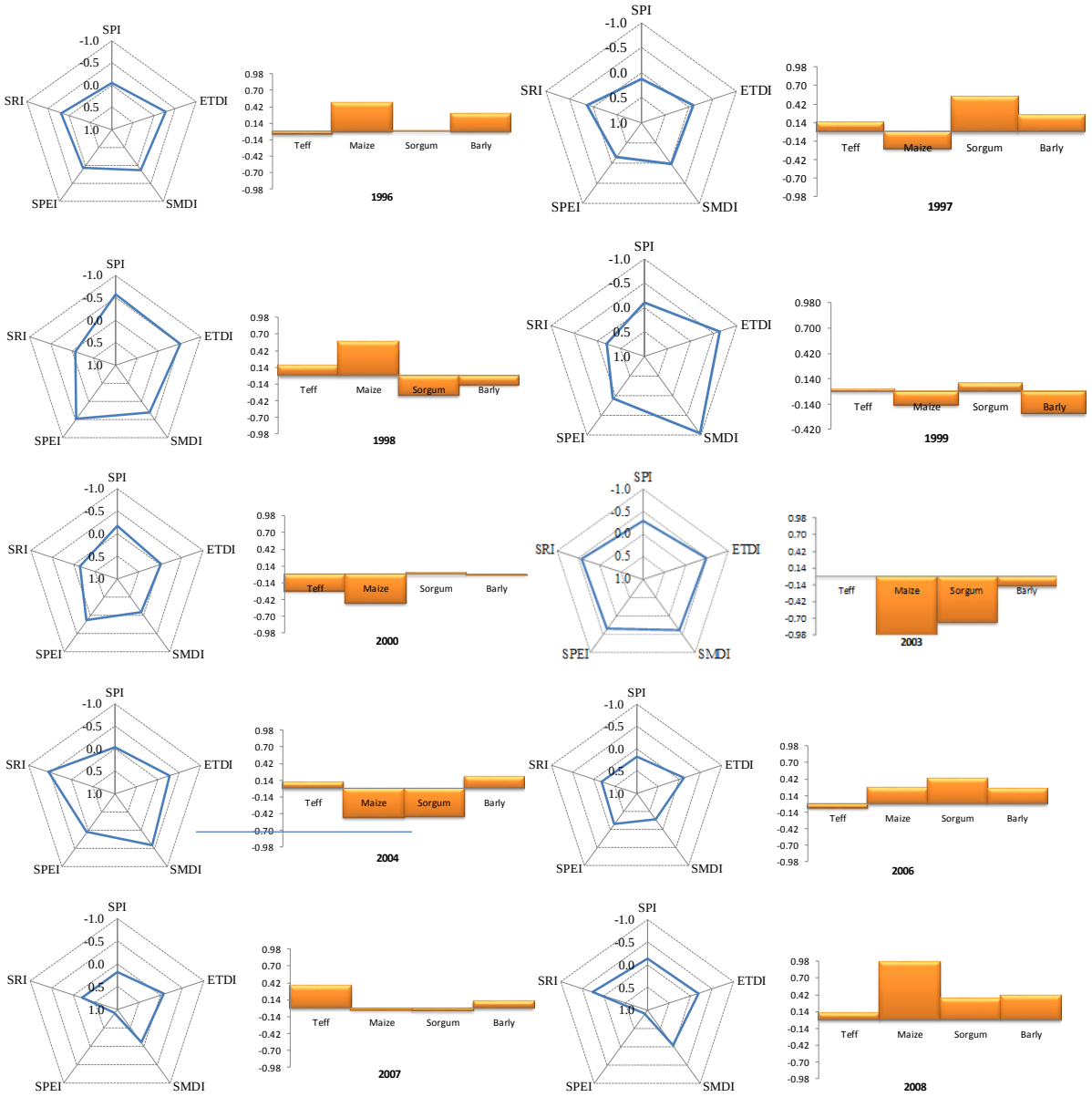

Figure 4.5: The radar and bar plots show the minimum drought indices values within the crop growing period (June to October) and the anomaly of the crop yield of four crops (bar graph) at the Debremarkos station.

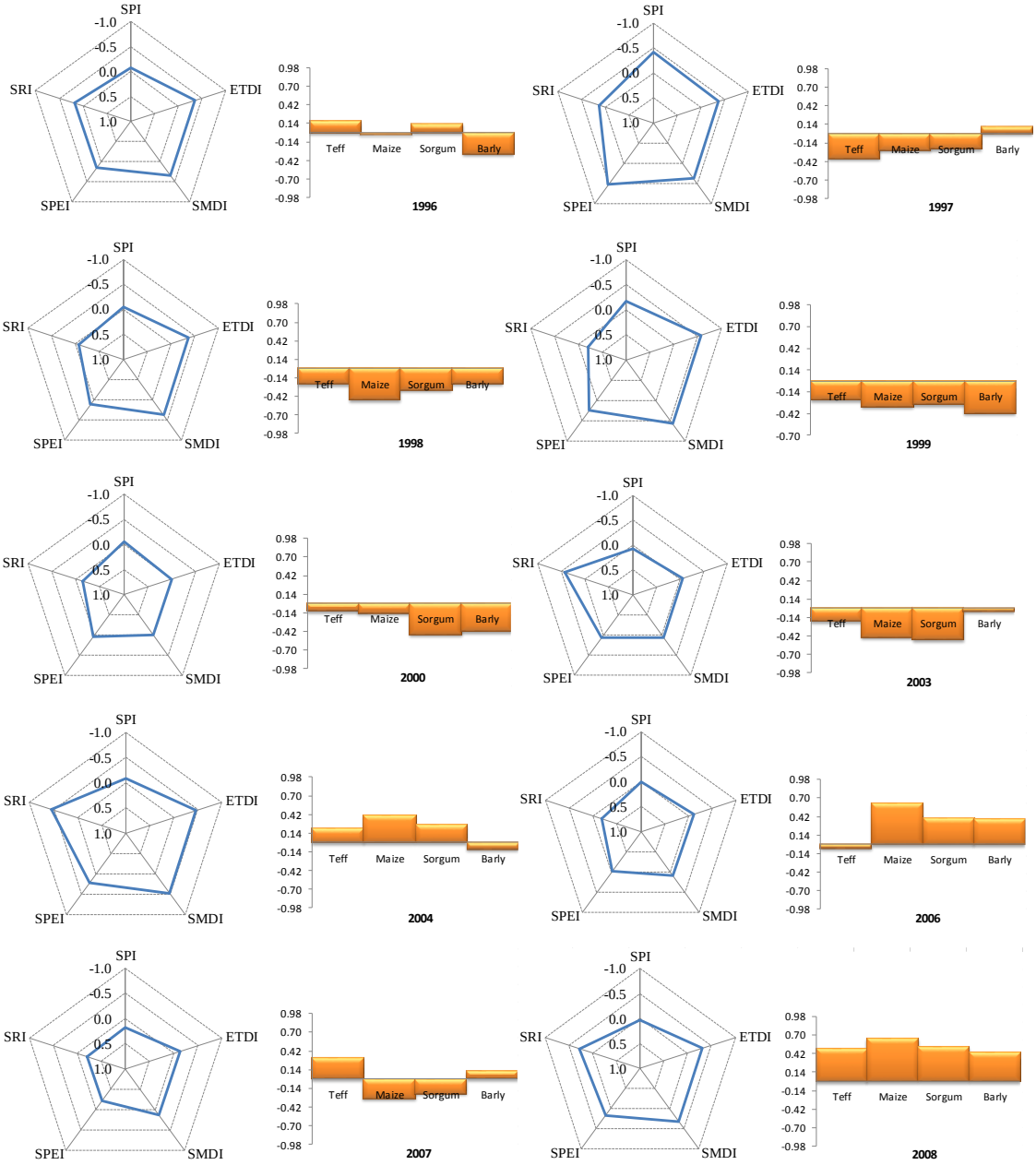

Figure 4.6: The radar and bar plots show the minimum drought indices values within the crop growing period (June to October) and the anomaly of the crop yield of four crops (bar graph) at the Gondar station.

4.4.3 Combined drought index developed using Principal Component Analysis (PCA)

Principal Component Analysis (PCA) is used as one of the techniques to develop the combined drought index in this study. All the drought indices values were first normalized to the scale between -1 and 1 in order to maintain consistency in the range of drought category. The PCA analysis was carried out using the entire time series of drought indices to develop the time series values of the combined drought index (1970-2008). Then the combined drought index

values within the cropping period (June to October) are selected to analyse the correlation with the crop yield data.

In general, the albeit values of the weights assigned for each input variable are very close to each other. However, the maximum weight was assigned to the SPI (0.50) and the minimum was assigned for SRI (0.41). The weights assigned for the other indices are shown in equation 4.4. The correlation coefficient matrix between the drought indices and crop yield anomalies is shown in Table 4.3. Very close correlation coefficients were obtained for the SPI (0.75), ETDI (0.86) and SPEI (0.82) and the minimum coefficient for SRI (0.39) with CDI-1. The combined drought index CDI-1 correlated much better with Sorghum (0.68) and Barley (0.65) as compared to the other crops (Teff and Maize).

$$CDI\text{-}1 = 0.501 \times SPI + 0.44 \times ETDI + 0.462 \times SMDI + 0.425 \times SPEI + 0.403 \times SRI \quad 4.4$$

Table 4.3: The correlation coefficient matrix of the combined drought index with the other indices and the crop anomaly for the second experiment for Debremarkos station.

	Teff	Maize	Sorghum	Barley	CDI-1
SPI	0.12	-0.06	0.57	0.57	0.75
SPEI	0.50	0.40	0.51	0.60	0.82
ETDI	-0.07	0.07	0.53	0.68	0.86
SMDI	-0.05	0.29	0.46	0.66	0.79
SRI	-0.04	0.24	0.47	-0.27	0.39
CDI-1	0.20	0.31	0.68	0.65	1.00

Figure 4.7 shows the scatter plots between the anomalies of the Barely crop yield with individual drought indices and the PCA-based CDI-1. The measure of agreement between the drought index and the crop yield anomalies can be assessed as the number of scatter points falling in the top-right (both positive) and bottom-left quadrants (both negative). Hence, a relatively strong agreement was observed between Barley and the SPEI and SPI, with 80% and 70% of the scatter points (i.e. 8 and 7 out of 10) falling in both the positive and negative quadrants. There is a poor agreement of Barley with SRI, with only 30% of the scatter points falling in the both positive and both negative quadrants. Relative to individual drought indices, CDI-1 showed an improvement in terms of showing similar trend with the Barley crop yield anomaly except an opposite trend for some of the scatter points (20%). Similar scatter plots were produced for other crops (Sorghum, Maize and Teff) and can be referred to in Appendix D and Figure 4.8.

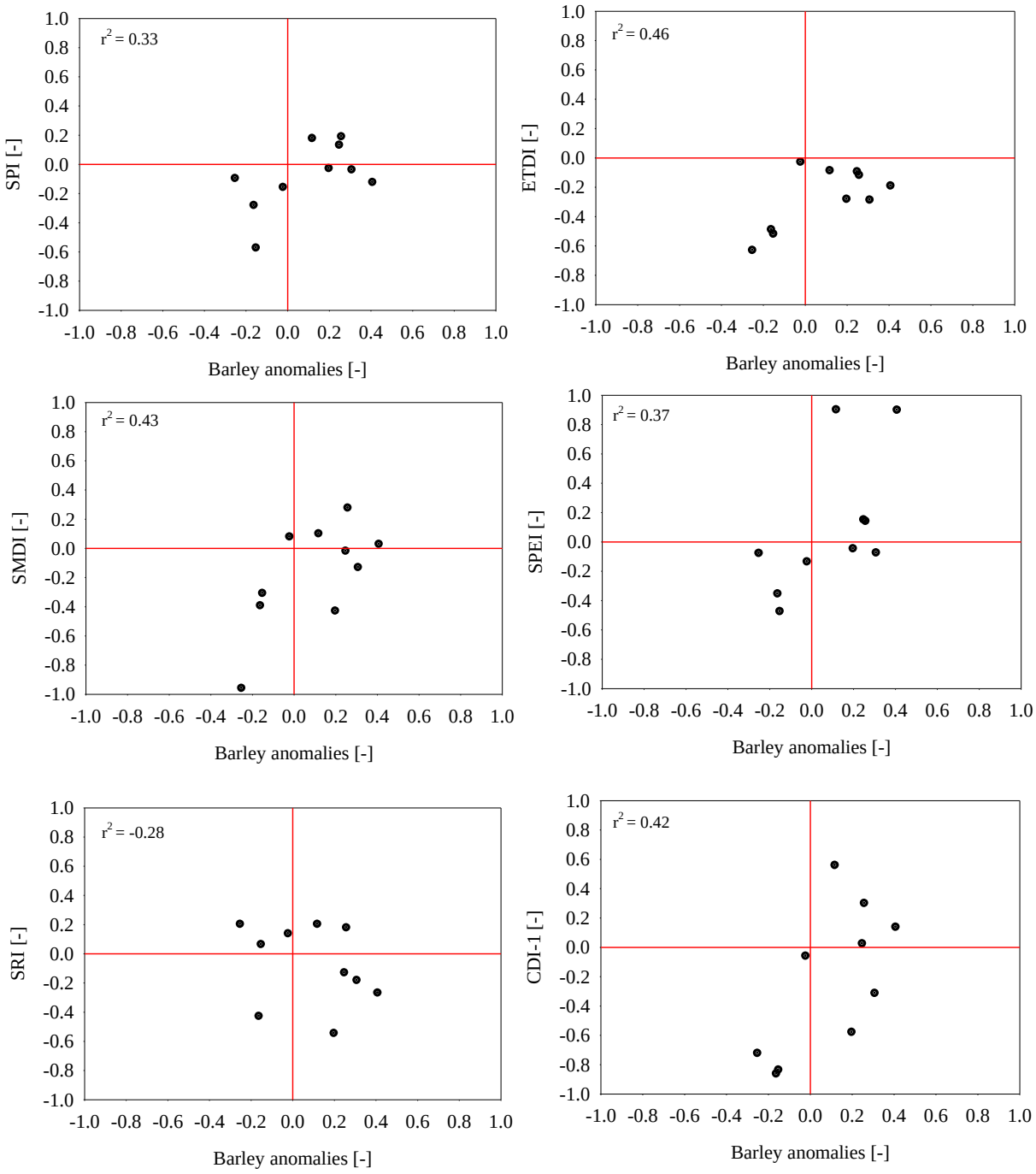

Figure 4.7: Scatter plots of individual drought indices and CDI-1 versus the Barely crop yield anomalies for the Debremarkos station. CDI-1 was computed using the Principal Component Analysis (PCA).

4.4.4 Combined drought index developed using an impact-based optimal CDI relative weights

In this section, the combined drought index was developed by optimizing the relative weights for each index to maximize correlation between the CDI and crop yield anomalies. Table 4.4 shows the resulting weight of each index for the four crops: Teff, Sorghum, Maize, and Barley. The result showed that the maximum correlation coefficient was obtained with Barley (0.88).

The maximum weight was assigned for ETDI and minimum for SMDI and SRI. The coefficients assigned for Sorghum and Barley were the same. Maximum weight was assigned for SRI for Maize crop and ETDI for Teff crop.

Table 4.4: The weights assigned for the drought indices and the corresponding correlation coefficient with the crop yield anomalies for the Debremarkos station.

Crops	Correlation Coefficients (R)	Weights/Coefficients of each drought index				
		SPI	SPEI	ETDI	SMDI	SRI
Sorghum	0.74	0.2	0.2	0.4	0.1	0.1
Barley	0.88	0.2	0.2	0.4	0.1	0.1
Maize	0.70	0.1	0.3	0.1	0.1	0.4
Teff	0.66	0.1	0.3	0.4	0.1	0.1

Hence, the values of the combined drought index were obtained using the equations 4.5 and 4.7. The same equation, because of the same optimal weights found, for Sorghum and Barley (Equation 4.5) and separate equations for Maize (Equation 4.6) and Teff (Equation 4.7) were considered. The resulting time series values of the combined drought index were shown in Tables 4.5a, b and c respectively. The correlation coefficient matrix of the combined drought index with other indices and crops is also shown in Table 4.6. The combined drought index correlates best with Barley with a coefficient of 0.7.

$$CDI\text{-}2 = 0.2\times SPI + 0.2\times SPEI + 0.4\times ETDI + 0.1\times SMDI + 0.1\times SRI \quad (4.5)$$

Equation of the combined drought index validated with Maize crop,

$$CDI\text{-}3 = 0.1\times SPI + 0.3\times SPEI + 0.1\times ETDI + 0.1\times SMDI + 0.4\times SRI \quad (4.6)$$

Equation of the combined drought index validated with Teff crop,

$$CDI\text{-}4 = 0.1\times SPI + 0.3\times SPEI + 0.4\times ETDI + 0.1\times SMDI + 0.1\times SRI \quad (4.7)$$

Table 4.5a: The time series values of the combined drought index developed using the weights corresponding with the best correlation with the Sorghum and Barley crops for the Debremarkos station.

	SPI	**SPEI**	**ETDI**	**SMDI**	**SRI**	**Sorghum**	**Barley**	**CDI-2**
Weights / years	**0.2**	**0.2**	**0.4**	**0.1**	**0.1**			
1996	-0.04	-0.08	-0.29	-0.13	-0.18	0.01	0.31	**-0.17**
1997	0.13	0.15	-0.10	-0.02	-0.13	0.54	0.25	**0.00**
1998	-0.58	-0.48	-0.52	-0.31	0.06	-0.33	-0.15	**-0.44**
1999	-0.10	-0.08	-0.63	-0.96	0.20	0.09	-0.25	**-0.36**
2000	-0.16	-0.14	-0.03	0.08	0.14	0.03	-0.02	**-0.05**
2003	-0.28	-0.36	-0.49	-0.39	-0.43	-0.77	-0.16	**-0.41**
2004	-0.03	-0.05	-0.28	-0.43	-0.55	-0.47	0.20	**-0.23**
2006	0.19	0.14	-0.12	0.27	0.18	0.43	0.26	**0.06**
2007	0.18	0.90	-0.09	0.10	0.20	-0.04	0.12	**0.21**
2008	-0.13	0.90	-0.19	0.03	-0.27	0.36	0.41	**0.05**

Table 4.5b: The time series values of the combined drought index developed using the weights obtained from best correlation with the Maize crop for the Debremarkos station.

	SPI	**SPEI**	**ETDI**	**SMDI**	**SRI**	**Maize**	**CDI-3**
Weights / years	**0.1**	**0.3**	**0.1**	**0.1**	**0.4**		
1996	-0.04	-0.08	-0.29	-0.13	-0.18	0.50	**-0.14**
1997	0.13	0.15	-0.10	-0.02	-0.13	-0.26	**-0.01**
1998	-0.58	-0.48	-0.52	-0.31	0.06	0.57	**-0.26**
1999	-0.10	-0.08	-0.63	-0.96	0.20	-0.15	**-0.11**
2000	-0.16	-0.14	-0.03	0.08	0.14	-0.48	**0.00**
2003	-0.28	-0.36	-0.49	-0.39	-0.43	-0.99	**-0.40**
2004	-0.03	-0.05	-0.28	-0.43	-0.55	-0.49	**-0.31**
2006	0.19	0.14	-0.12	0.27	0.18	0.27	**0.15**
2007	0.18	0.90	-0.09	0.10	0.20	-0.03	**0.37**
2008	-0.13	0.90	-0.19	0.03	-0.27	0.97	**0.13**

Table 4.5c: The time series values of the combined drought index developed using the weights obtained for the Teff crop for the Debremarkos station.

	SPI	**SPEI**	**ETDI**	**SMDI**	**SRI**	**Teff**	**CDI-4**
Weights / years	**0.1**	**0.3**	**0.4**	**0.1**	**0.1**		
1996	-0.04	-0.08	-0.29	-0.13	-0.18	-0.05	**-0.17**
1997	0.13	0.15	-0.10	-0.02	-0.13	0.15	**0.00**
1998	-0.58	-0.48	-0.52	-0.31	0.06	0.17	**-0.43**
1999	-0.10	-0.08	-0.63	-0.96	0.20	0.03	**-0.36**
2000	-0.16	-0.14	-0.03	0.08	0.14	-0.27	**-0.05**
2003	-0.28	-0.36	-0.49	-0.39	-0.43	0.00	**-0.41**
2004	-0.03	-0.05	-0.28	-0.43	-0.55	0.11	**-0.23**
2006	0.19	0.14	-0.12	0.27	0.18	-0.07	**0.06**
2007	0.18	0.90	-0.09	0.10	0.20	0.37	**0.28**
2008	-0.13	0.90	-0.19	0.03	-0.27	0.13	**0.15**

Table 4.6: The correlation coefficient matrix of the combined drought index and other indices and the four cereal crops for the Debremarkos station. The numbers in the parenthesis show the number of CDI's (e.g. 2 indicates for CDI-2).

	Sorghum	Barley	Maize	Teff
SPI	0.57	0.95	-0.06	0.12
SPEI	0.51	0.60	0.40	0.50
ETDI	0.46	0.68	0.07	-0.07
SMDI	0.46	-0.27	0.29	-0.05
SRI	0.47	0.24	0.24	-0.04
CDI	0.66 (2)	0.70 (2)	0.40 (3)	0.26 (4)

Figure 4.8 shows the comparative plots of the PCA-based CDI (CDI-1) and impact-based optimized CDI's (CDI-2, CDI-3, and CDI-4) for Barley, Sorghum, Maize, and Teff. In general, CDI-2 showed a good match with Barley crop anomalies, except for two points that were falling in the lower-right quadrant that shows opposite signal between the CDI and crop yield anomaly. There is no significant outliers observed in CDI-2 in the lower left corner. The same proportion of scatter points, for CDI-1 and CDI-2 falls in the bottom-right quadrant that shows an opposite signal between CDI's and Barley crop anomalies.

The comparative plot between CDI-1 and CDI-2 (impact-based) for the Sorghum crop anomalies shows proportionality between the values. The plots for Maize and Teff show higher coefficient determination (R^2) values for the impact-based CDIs (CDI-3 and CDI-4) as compared to the PCA-based CDI-1. The PCA-based CDI-1 in general shows a larger spread than the impact-based CDIs. This can be explained from the weights (Eigenvalues) adding to greater than one (Equation 4.4). The impact-based CDI was used for further analysis in the next section (Section 4.4.5) on linear regression modelling of crop yield anomalies.

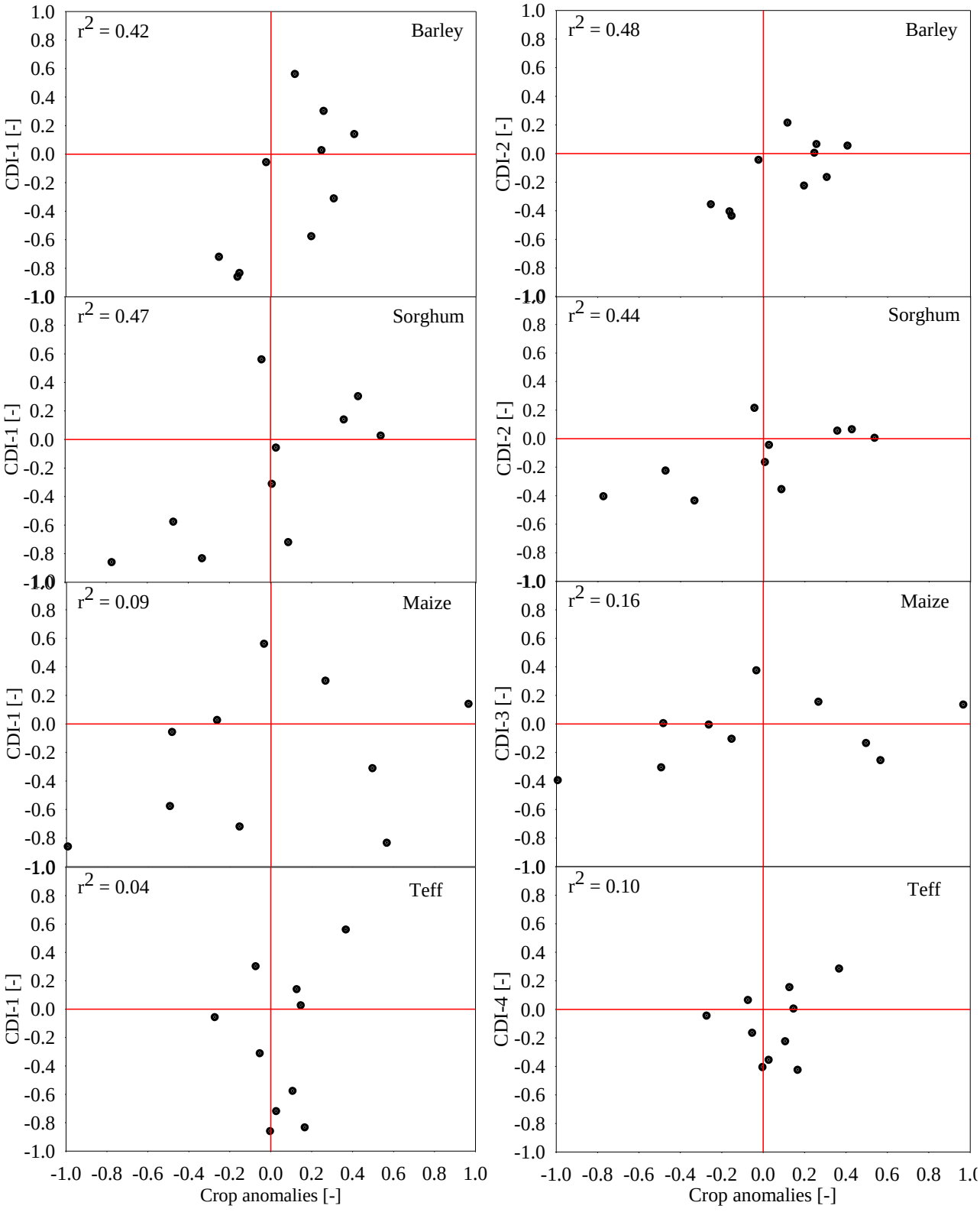

Figure 4.8: Comparative plots of the PCA based CDI (CDI-1) and impact-based CDI (CDI-2, CDI-3, and CDI-4) for the Barley, Sorghum, Maize, and Teff crop yield anomalies for the Debremarkos station.

4.4.5 Prediction models of crop yield anomalies

This section presents the result obtained employing the crop yield prediction model based on the linear regression approach. Two sets of crop prediction equations were developed to link the drought indices (predictors), and the four crops yield anomalies (predictands). These equations help to predict the crop yield anomalies for the given prior values of the drought indices. The first set of equations was formulated to link the detrended crop yield anomaly and the five drought indices (i.e. SPI, SPEI, ETDI, SMDI, and ADI), whereas the second set of equations was derived to link the detrended crop yield anomalies with the combined drought index (impact-based CDI). These equations were derived for all the administrative zones in the basin, however, the results obtained at the selected eight representative administrative zones are presented in this thesis.

The results obtained at the Debremarkos station are presented below for further discussion in this section, and the results for the other seven zones can be found in Appendix E. The first set of prediction equations at the Debremarkos station, for Teff, Maize, Sorghum, and Barley, is presented in equations 4.8 to 4.11, whereas the second set of regression equations is shown in 4.12 to 4.15.

These equations were used to predict each crop yield anomaly, and the resulting scatter plots between the observed and predicted crop yield anomalies is shown in Figure 4.9. Overall, the prediction accuracy of most of the yield anomaly equations is above the coefficient of determination (R^2) of 0.44 for all zones. The maximum value of R^2 was obtained for the Barley crop (R^2 = 0.77) for the first set of equations, based on linear regression with the individual drought indices as input.

$$\textit{Teff yield anomaly} = 0.01\times SPI - 0.52\times ETDI + 0.07\times SMDI + 0.23\times SPEI - 0.05\times SRI - 0.10 \quad (4.8)$$

$$\textit{Maize yield anomaly} = -0.67\times SPI - 2.39\times ETDI + 1.36\times SMDI + 0.78\times SPEI + 0.36\times SRI - 0.52 \quad (4.9)$$

$$\textit{Sorghum yield anomaly} = 0.52\times SPI + 0.29\times ETDI + 0.07\times SMDI + 0.16\times SPEI + 0.56\times SRI + 0.15 \quad (4.10)$$

$$\textit{Barley yield anomaly} = 0.32\times SPI - 0.14\times ETDI + 0.37\times SMDI + 0.13\times SPEI - 0.36\times SRI + 0.11 \quad (4.11)$$

$$\textit{Sorghum yield anomaly} = 1.217\times CDI\text{-}2 + 0.147 \quad (4.12)$$

$$\textit{Barley yield anomaly} = 0.705\times CDI\text{-}2 + 0.191 \quad (4.13)$$

$$\textit{Maize yield anomaly} = 1.229\times CDI\text{-}3 + 0.049 \quad (4.14)$$

$$\textit{Teff yield anomaly} = 0.482\times CDI\text{-}4 + 0.077 \quad (4.15)$$

Figure 4.9 shows the scatter plot of the observed versus the predicted crop yield anomalies. The comparison for Sorghum crop anomalies (Figure 4.8a and a') shows no large differences between Set 1 (based on individual indices) and Set 2 (based on CDI), in terms of the coefficient of determination and in terms of the number of scatter points falling in the top right and lower left quadrants. Sorghum crop predictions based on Set 1 and Set 2 scored R^2 values of 0.54 and 0.44 respectively, indicating that for Sorghum linear regression based on the individual indices works better than based on CDI.

An improvement by using CDI instead of individual indices has been observed in predicting Barley crop yield anomaly, in terms of the number of scatter points falling in the top-right, and bottom-left quadrants. Only 10% of the scatter points are out of these two quadrants for the CDI-based Barley crop prediction, whereas 20% of the scatter points are out the two quadrants for the prediction model based on the five individual drought indices. However, the R^2 values showed significant decline (0.49) for the CDI-based prediction model, as compared to regression based on the five drought indices (0.77).

Significant improvement of Teff crop prediction has been observed on the CDI-based prediction model, in terms of both R^2 and the number of scatter points falling in the two quadrants. 30% of the scatter points fall out of the two quadrants in CDI-based prediction model, whereas 60% in the five drought indices - based prediction model. Moreover, significant improvement in the R^2 value is observed in the CDI-based prediction (0.57), as compared to the linear regression based on five drought indices (0.43) for the Teff crop prediction.

An opposite result can be observed for the Maize crop yield anomaly prediction model. The CDI-based model showed a poor performance ($R^2 = 0.24$), compared to the five drought indices based prediction model ($R^2 = 0.32$). Moreover, about 60% of the scatter points are falling out of the two reference quadrants for CDI based prediction model, versus 40% in the case of five drought indices based prediction model.

Overall, it can be said that the regression model developed for each administrative zone to predict crop yield anomalies, is satisfactory and the results highlight the prediction potential of the drought indices (Appendix D). The predicted and observed data are consistently showing the same trend. However, it should be mentioned that the absolute magnitude of the anomaly is not always captured. This variation in magnitude may be attributed to several factors, mainly

to the crop yield data that is aggregated to zonal average, and to the accuracy of the model-based estimation of actual evaporation and soil moisture.

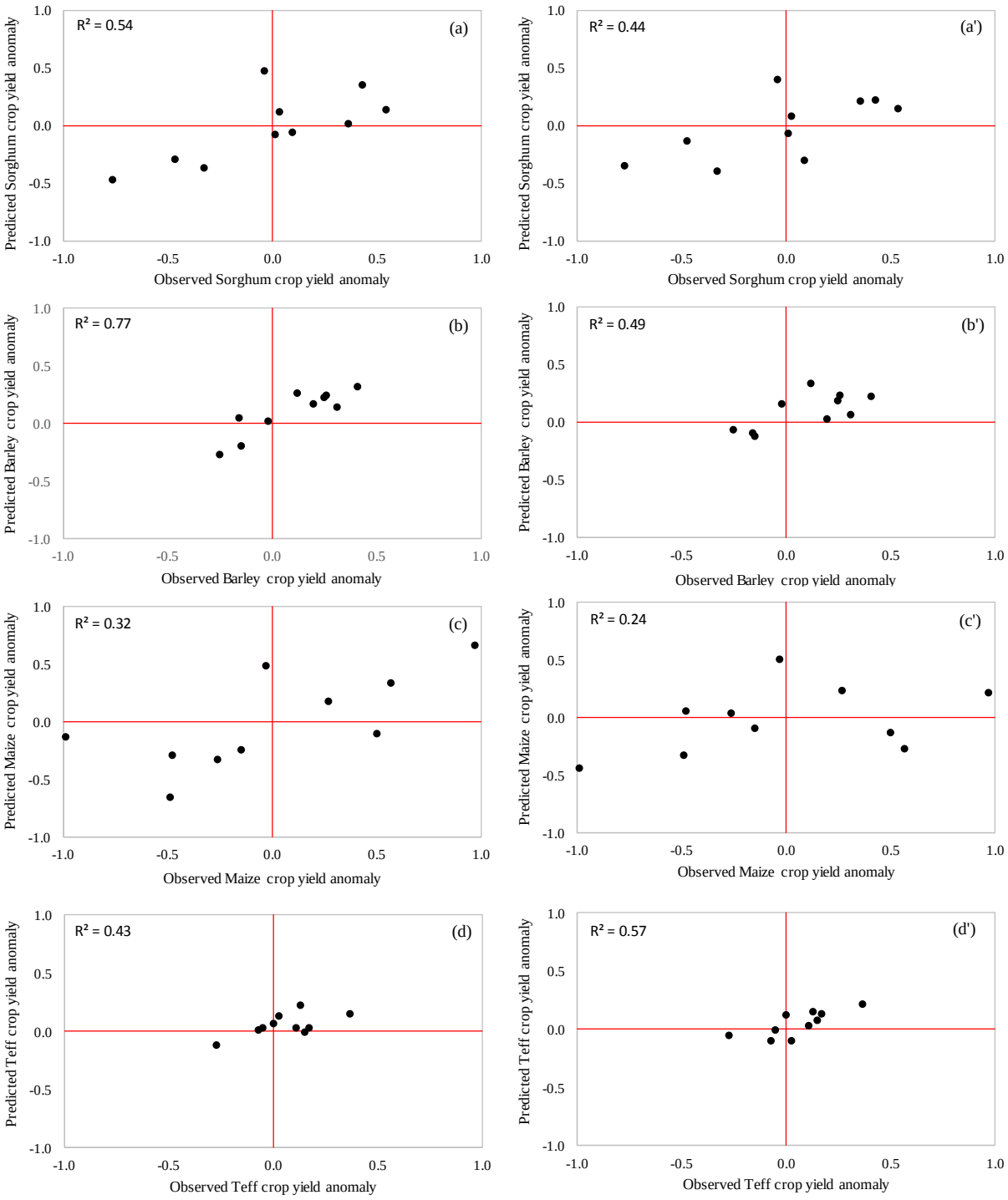

Figure 4.9: Predicted versus observed crop yield anomalies of the Sorghum, Barley, Maize and Teff crops for the Debremarkos station. In the left column of plots, the crop prediction model was based on the five drought indices whereas the right side plots were based on the CDI.

4.5 Conclusions

In this chapter, two approaches were implemented to develop a Combined Drought Index for the Upper Blue Nile Basin. The first approach was based on Principal Component Analysis (PCA), and the second on a random search of the optimal weights. The CDI developed in the second approach was focused on the impact of drought on crop yield. The impact-based CDI, and the individual drought indices it comprises, were used to test to what extent a linear regression model could predict crop yield anomalies in the UBN Basin.

The combined drought index developed using impact-based optimal weights, correlated well with the four crop yield anomalies considered in this study: Teff, Barley, Maize and Sorghum. The combined drought index developed using PCA could indicate years with negative crop yield anomalies equally well. Of the four crops, sorghum correlated best with the combined drought index developed using both techniques. The linear regression model developed using the combined drought index, or directly from the individual drought indices, showed its prediction potential for crop yield anomalies in the Upper Blue Nile basin.

5. Application of Earth observation data for developing a combined drought index and crop yield prediction model[4]

5.1 Introduction

In this chapter, different Earth observation (EO) based input data are utilized to assess and characterize the historic drought events and to develop the impact-based CDI and crp-yield anomaly prediction model for the UBN Basin. The Earth observation based data have relatively high spatial resolution, which is an advantage to use in the data scarce regions in most of the developing countries. Three Earth observation based drought indices, i.e. Z-score, Evaporative Drought Index (EDI) and the Vegetation Condition Index (VCI) were used (Section 5.3). The Z-score values were calculated using the Climate Hazards Group Infrared Precipitation with Stations (CHIRPS) Earth observation precipitation data. CHIRPS blends EO with station-based precipitation data. The EDI (Jiahua et al. 2015) calculation uses the MODIS ET data as the main input in conjunction with the potential ET derived using multiple global data sets. The potential ET were calculated by using the Hargreaves method (Hargreaves and Samani, 1982; Hargreaves and Samani, 1985). The VCI (Kogan and Sullivan, 1993) was used in conjunction with the NDVI to assess the vegetation condition in drought situations affecting agriculture. The time series of the VCI were calculated based on the NDVI values in the study period. The data used are presented in Section 5.2.

Combining these three drought indices helps in providing more detailed information that can facilitate the decision making process and to assess both meteorological and agricultural drought with a single index. Linking the combined drought index with the crop yield anomalies is important for developing a crop prediction model based on EO data. Thus, the main objectives of this chapter are to develop the Earth observation-based combined drought index, using the Z-score, EDI, and VCI, and to derive from the resulting EO-CDI a multiple linear regression model for identifying crop-yield anomalies.

[4] *Based on*: Bayissa, Y.A., Tadesse, T., Demissie, G.B., and Shiferaw, A, 2017. *Evaluation of Satellite-Based Rainfall Estimates and Application to Monitor Meteorological Drought for the Upper Blue Nile Basin, Ethiopia*. Remote Sensing, v. 9, No. 7, p.669.

5.2 Data

5.2.1 Climate Hazards Group Infrared Precipitation with Stations (CHIRPS) rainfall

The CHIRPS satellite rainfall product is used in this study to represent the meteorological components of drought. CHIRPS was developed by the U.S. Geological Survey (USGS) and the Climate Hazards Group at the University of California, Santa Barbara (UCSB). It is a blended product combining precipitation climatology within 5-day periods, quasi-global geostationary thermal infrared (TIR) satellite observations from the Climate Prediction Center and the National Climate Forecast System version 2 (CFSv2) (Saha et al. 2011), and in-situ precipitation observations (Funk et al. 2014). CHIRPS is used in this study because of its quite high accuracy shown for Ethiopia (Bayissa et al. 2017). In addition, CHIRPS has a higher spatial resolution (~5km) and covers a longer period (1982-present) than other products. CHIRPS data was used to calculate the 3-month Z-score (Source: ftp://ftp.chg.ucsb.edu/pub/org/chg/products/CHIRPS-2.0/).

5.2.2 MODIS actual ET (MOD16)

The MODIS actual ET product (MOD16) for the Upper Blue Nile Basin is acquired from the Nile Basin Initiative (http://nileis.nilebasin.org, accessed on April 12, 2014). The data were available at 1-km spatial resolution and at 8-day, monthly and annual temporal time scales. For the estimation of ET, the MOD16 algorithm employs the Penman–Monteith ET method (Monteith, 1965). This method uses the MODIS products, including 14 land cover types, Leaf Area Index/Fraction of Photo synthetically Active Radiation (LAI/FPAR), and white sky-albedo for the estimation of ET (Schaaf et al. 2002). The improved version uses additional Terra MODIS daytime LST, NDVI and Enhanced Vegetation Index (EVI) data to estimate ET over the different land-use in the basin (Sims et al. 2008).

5.2.3 Normalized Difference Vegetation Index (NDVI)

The NDVI data used to derive the Vegetation Condition Index (VCI) were obtained from the SPOT vegetation ten-day composite NDVI images (S10 product) of vgt4africa of the DevCo-Cast project (http://www.vgt4africa.org) for the study period from 2001 to 2009. The spatial resolution of the SPOT NDVI images is 1km by 1km, which covers the Africa continent. The qualities of the images were checked through the application in many disciplines such as crop and agricultural monitoring and drought early warning (Gebrehiwot et al. 2011). A total of 396 NDVI images were processed and used for the derivation of VCI.

5.2.4 Climate data

The daily rainfall and temperature data were acquired from the National Meteorological Agency (NMA) of Ethiopia. The data were collected for thirty-four meteorological stations and the location of the stations is shown in Figure 5.1. Ten out of the thirty-four stations are independent stations (not blended in CHIRPS), and these stations were used to validate the CHIRPS rainfall estimate. The location of these independent stations is shown in Figure 5.1. The rainfall and temperature data were used to calculate the potential ET. The temporal scale of the data is on a daily basis for a period from 2001 to 2009. The other input data used to calculate the potential ET were extra-terrestrial solar incident radiation values. These data were acquired from the ECMWF ERA-interim data portal (ECMWF, 2013).

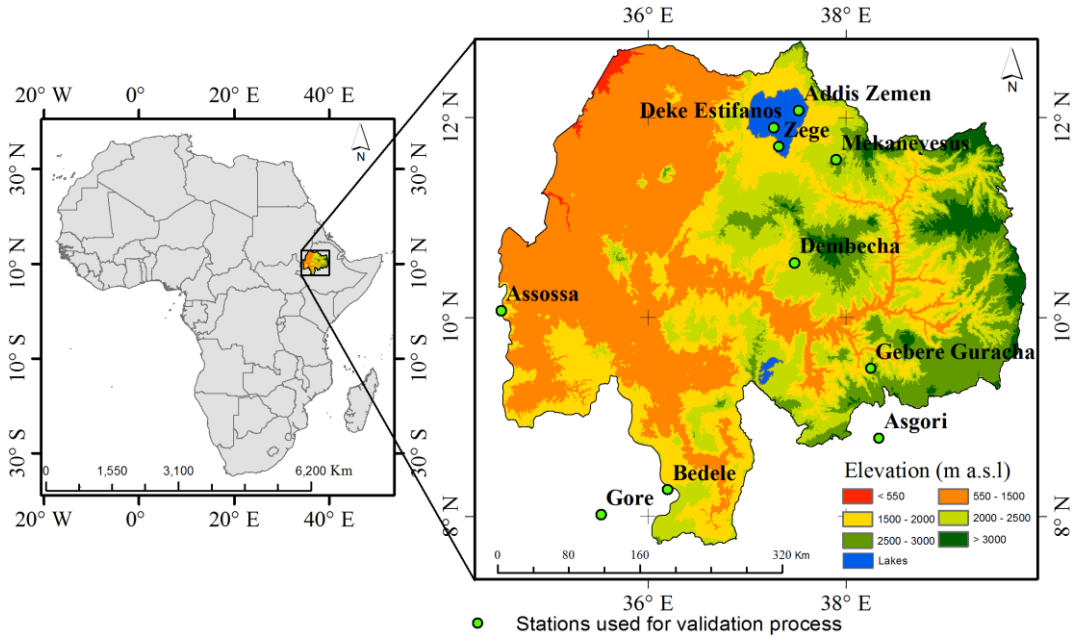

Figure 5.1: Locations of the independent weather stations (green circles) used for validation of the CHIRPS rainfall product.

5.3 Methods

The method described in the subsections below aims to address the main objective of this chapter - which is developing the Earth observation based combined drought index and prediction model.

5.3.1 Validation of the CHIRPS rainfall estimates

The commonly used pairwise comparison statistics techniques such as the Pearson correlation coefficient (r), Mean Error (*ME*), Root Mean Square Error (*RMSE*) and Bias were applied to evaluate CHIRPS satellite rainfall estimates.

The Pearson correlation coefficient (*r*) measures the goodness of fit and linear association between two variables. It measures how well the satellite rainfall product corresponds to the observed rainfall; see Equation 5.1. Its value ranges between 0 to 1 in which one indicates the perfect score.

$$r = \frac{\sum (O - \bar{O})(S - \bar{S})}{\sqrt{\sum (O - \bar{O})^2} \sqrt{\sum (S - \bar{S})^2}} \quad 5.1$$

where *r* is the correlation coefficient, *O* = gauge rainfall measurement, $\bar{O}$ = average gauge rainfall measurement, *S* = satellite rainfall estimate, $\bar{S}$ = average satellite rainfall estimate, and n = number of data pairs.

ME is the mean error (Equation 5.2); a positive value indicates an overestimate of the satellite rainfall whereas a negative value indicates an underestimate as compared to the observed rainfall. *ME* value of zero is a perfect score.

$$ME = \frac{1}{n} \sum (S - O) \quad 5.2$$

where *ME* is the mean error, *O* = gauge rainfall measurement, and *S* = satellite rainfall estimate.

The *RMSE* is used to measure the average magnitude of the estimated errors between the satellite rainfall and the observed rainfall; see Equation 5.3. A lower *RMSE* value means greater central tendencies and small extreme error. A *RMSE* value of zero is the perfect score.

$$RMSE = \sqrt{\frac{1}{n} \sum (S - O)^2} \quad 5.3$$

where *RMSE* is the root mean square error, *O* = gauge rainfall measurement, and *S* = satellite rainfall estimate.

Bias reflects how well the mean of the satellite rainfall corresponds with the mean of the observed rainfall; see Equation 5.4. A Bias value closer to one indicates the cumulative satellite rainfall estimate is closer to the cumulative observed rainfall. A bias value of one is the perfect score.

$$Bias = \frac{\sum S}{\sum O} \quad 5.4$$

where *O* = gauge rainfall measurement, and *S* = satellite rainfall estimate.

5.3.2 Computing rainfall based Z-score

The Z-score is another form of the standardized precipitation index (SPI) that accounts only for the normal probability density functions (PDF). Its calculation procedure was similar with that of SPI (Section 2.3) except the Z-score was calculated using the spatial input data and normal PDF.

$$Z\text{-}score_i = \frac{(RF_i - longterm\ mean\ RF)}{St.Dev} \quad 5.5$$

where RF_i is the dekadal rainfall at a particular event;

long-term mean RF is the long-term average values of each dekade rainfall data;

St.Dev is the standard deviation of the dekadal rainfall data.

The rainfall data for each dekade for the analysis period ranging from 2001 to 2009 went through the data quality checks before being used for further analysis. Erroneous values that might be encountered because of the cloud contamination were screened and filtered out. The long-term mean and standard deviation of the rainfall data of each decade were calculated. Eventually, the deviation of rainfall during the particular event from the corresponding long-term mean value was calculated and normalized by dividing the difference by the standard deviation. The equation below summarized the calculation procedures of the Z-score. The Z-scores were calculated at the 3-month time scale to be comparable with the agricultural indices such as EDI and VCI.

5.3.3 Evaporative Drought Index (EDI)

The evaporative drought index (EDI) was calculated using the actual and potential ET obtained from the Earth Observation. The EDI is calculated using equation 5.6.

$$EDI = 1 - \frac{AET}{PET} \quad 5.6$$

where *AET* is the actual evapotranspiration derived from the MODIS product (MOD16)

PET is the potential evapotranspiration estimated using the Hargreaves's method (Equation 5.7)

During drought conditions, the water stress in the soil is very high, which eventually reduces the amount of actual evapotranspiration. The ratio of *AET* and *PET* is smaller when the *AET* value is much smaller than *PET*. The smaller *AET* is often associated with the water stress in the soil often occurring during drought conditions. The smaller the ratio of *AET* and *PET* leads to the relatively higher positive values of EDI. Thus, the positive large value of EDI shows the

drought condition. For sign convention, the EDI values are multiplied by -1 and hence negative EDI values show drought conditions whereas positive EDI values show wet conditions.

$$PET = 0.0023R_a(T_{mean}+17.8)\sqrt{(T_{max} - T_{min})} \quad 5.7$$

where *PET* is the potential evapotranspiration that represents the ideal evaporation without being constrained by the limiting factors such as water and other climatic and biophysical factors.

R_a is the extra-terrestrial solar incident radiation (Wm^{-2})

T_{max} and T_{min} are daily maximum and minimum air temperature respectively

T_{mean} is the daily mean air temperature, and $T_{mean} = (T_{max} - T_{min})/2$

The *EDI* anomaly index was calculated by measuring the deviation of the *EDI* at a particular year, season, month and dekade from the long-term average values (Equation 5.8).

$$\Delta EDI(i) = EDI(i) - \frac{1}{n}\sum_{i=1}^{n} EDI(i) \quad 5.8$$

where *i* represents the year

n is the sample size

5.3.4 Vegetation Condition Index (VCI)

The NDVI data used to derive the VCI were obtained from the SPOT vegetation ten-day composite NDVI images (S10 product) of vgt4africa of the DevCo-Cast project (http://www.vgt4africa.org) for the study period from 2001 to 2009. The spatial resolution of the SPOT NDVI images is 1km by 1km, and they cover the Africa continent. The quality of the images was checked through the application in many disciplines such as crop and agricultural monitoring and drought early warning (Jacobs et al. 2008; Sathyendranath et al. 2009). In this study, a total of 396 NDVI images were processed and used for the derivation of VCI. The VCI maps were produced for the corresponding NDVI images using Equation 5.9.

$$\text{VCI} = \left(\frac{NDVI - NDVI_{min}}{NDVI_{max} - NDVI_{min}}\right) \times 100 \quad 5.9$$

where *NDVI*, $NDVI_{min}$, and $NDVI_{max}$ are the smoothed 10-day *NDVI*, its absolute multi-year minimum and its multi-year maximum NDVI respectively for each pixel.

The minimum and maximum NDVI values maps were derived from the map list within the study period. The VCI map of the corresponding NDVI image was then produced based on the current, minimum and maximum NDVI values.

As aforementioned, the rainfall pattern in the study area is uni-modal and occurs in the monsoon season (June, July, August, and September). Therefore, the failure of the monsoon rainfall obviously causes drought to occur in the study area since rain-fed agriculture is a common practice. VCI images during the monsoon season of each year were considered separately to produce the average VCI map during the monsoon period of each year. The average VCI maps during the monsoon season were then used for drought assessment for each year.

The time series NDVI values at the location of rain gauge stations were extracted to analyze their correlation with rainfall, and to determine the time lag between rainfall and NDVI. The Pearson correlation was used for the correlation analysis.

5.3.5 Impact-based combined drought index

The impact-based optimized CDI approach, developed in chapter 4 section 4.3.5, was also tested in this chapter to determine the EO-based combined drought index (EO-CDI). The impact-based approach assigns the relative weights (ranging from 0.1 to 0.9) iteratively for the three EO-based drought indices (Z-score, EDI, and VCI). We used the random search of weights to identify the best (optimal) combination of weights. The combination of weights (after 60000 iterations) that resulted in the highest correlation coefficient between the CDI and crop yield anomaly was selected to develop the combined drought index for the Upper Blue Nile basin. The resulting equation (Equation 5.10) that combines the three drought indices is given below.

$$EO\text{-}CDI_n = w_{Z\text{-}score} \times Z\text{-}score_{n-2} + w_{EDI} \times EDI_n + w_{VCI} \times VCI_n \quad 5.10$$

where n is the current month, and $w_{Z\text{-}score}$, w_{EDI} and w_{VCI} are the weights of each index. Z-score has index $n-2$, indicating a 2-month lag time (Section 5.4.4) and the time series of the all the drought indices were standardized (Z-score).

5.3.6 Developing the prediction model of crop yield anomalies

The same linear regression approach that was applied in Chapter 4 is also used in this chapter. The combined drought index and the three drought indices values were the basis to develop the prediction model for identifying the crop yield anomalies based on least square solutions approach. First, the multiple linear regression model between the CDI values and the crop yield anomalies was developed. Secondly, the multiple linear regression model between the five

drought indices and the crop yield anomalies was also developed. The performance of the two models was compared and the prediction model with good performance was selected.

5.4 Results and discussion

5.4.1 Validation results of CHIRPS

Evaluation of CHIRPS was carried out using the ground-based measured rainfall data at 10 selected independent gauging stations in the basin. The correlation analysis, bias, mean error, and root mean square error (RMSE) evaluation criteria were considered both for dekadal and monthly time scales for each station. The result shows that there is a good correlation observed between the rainfall from CHIRPS and observed rainfall in the majority of the stations. The correlation coefficient (r) values ranged between 0.881 (Gerbeguracha) to 0.69 (Assossa) on dekadal, and 0.95 (Gerbeguracha) to 0.82 (Bedele) at monthly time scales (Figure 5.2a). The bias values ranging between 0.71 to 1.2 were obtained for both dekadal and monthly time scales. The majority of the stations showed a bias values close to 1 (Figure 5.2b). This shows that there is a good agreement between CHIRPS and the measured rainfall evaluated in terms of bias values. The mean error and RMSE at dekadal time scale is lower than at the monthly time scale. The scatter plots were also produced by considering the time series data of the selected stations for dekadal and monthly time scales – see Figure 5.3. The scatter plots were produced by aggregating the rainfall data of all the stations. The result of the coefficient of determination (R^2) shows the good agreement of CHIRPS with the rainfall data from the gauging stations. R^2 values of 0.7 and 0.86 were obtained for dekadal and monthly time scales respectively. The overall results indicated that CHIRPS monthly rainfall products could potentially be used for assessing meteorological drought assessment in data scarce regions of the basin.

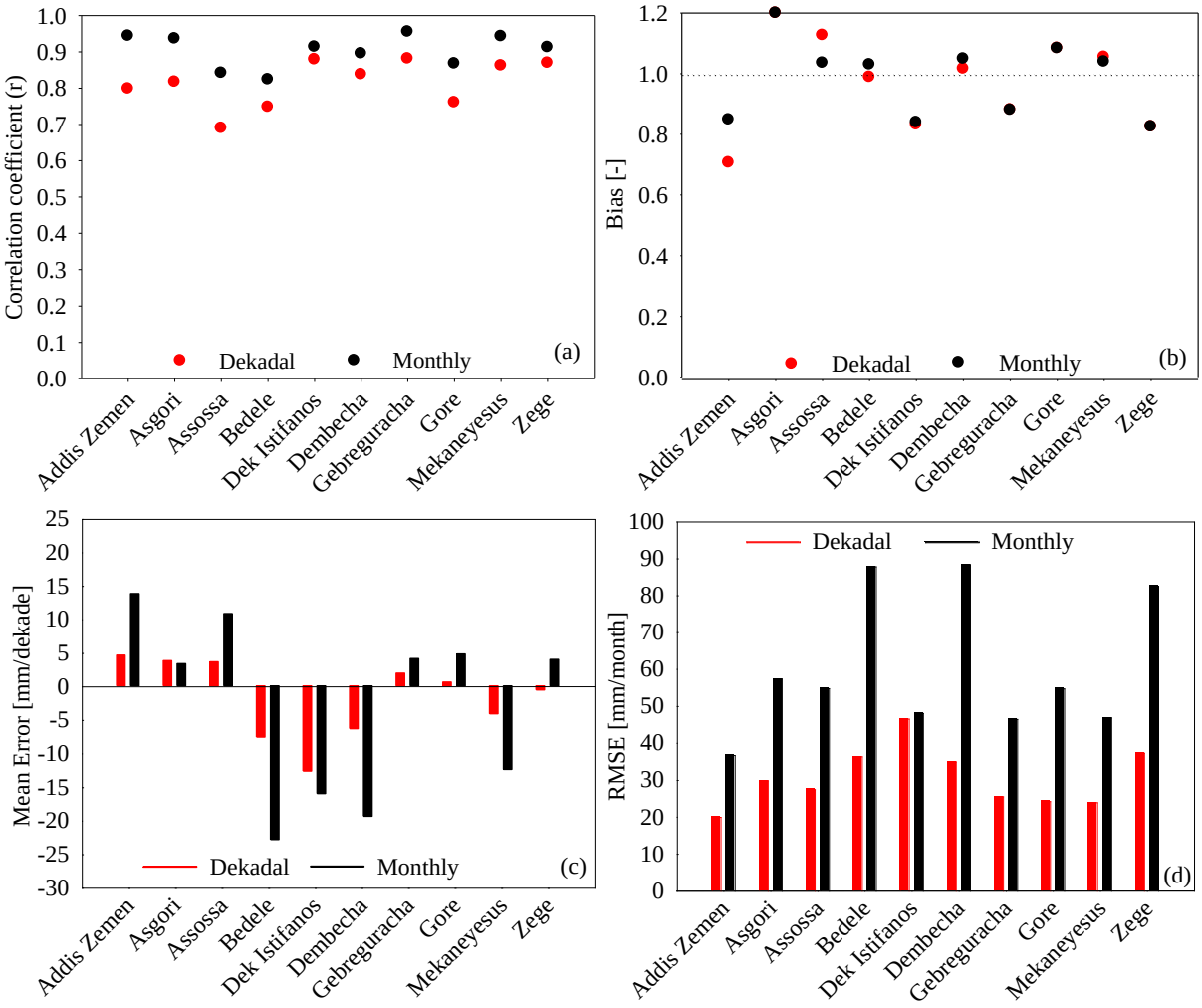

Figure 5.2: The statistical indicators—correlation coefficient (a), Bias (b), mean error (c) and root mean square error (d)—for each station at dekadal and monthly time scales.

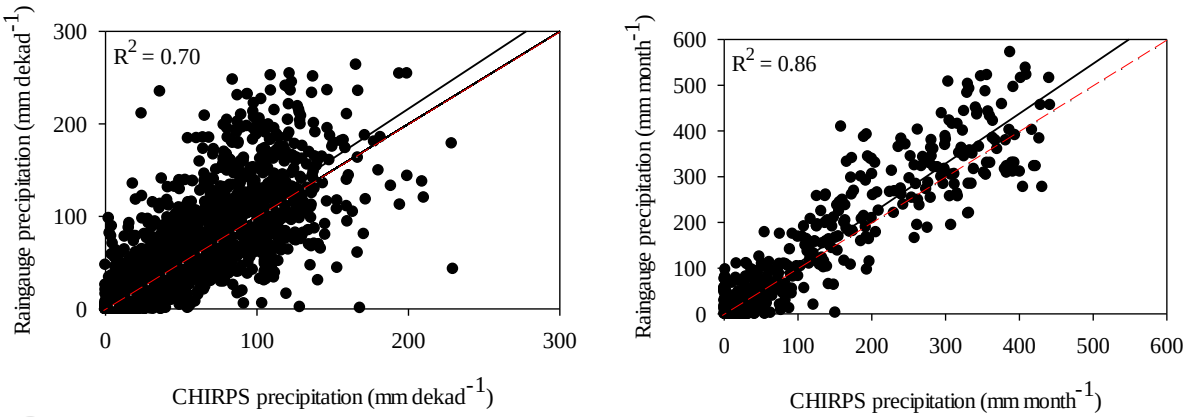

Figure 5.3: Scatter plots comparing the gauge data and CHIRPS rainfall estimates at a dekadal and monthly time scales.

5.4.2 Rainfall deficit index (Z-score) based drought assessment

The results of the visual illustration of the 3-months Z-score (Figure 5.4) revealed the two temporal dry periods associated with the historic droughts (2001-2005 and 2009), and the

consecutive wet period (2006-2008). The years 2002, 2003, 2004 and 2009 can be characterized as the severe drought years that covered the majority of the basin. The central, north and eastern parts of the basin were affected by severe droughts in those years, with the average drought intensity ranging from -1.72 to -0.85. The maximum Z-score intensities were observed in the year 2009 (-2.55) in the northern, part of the central, and eastern part of the basin. Whereas in the central and southern, and southwest part of the basin the maximum intensity of the drought was observed in the year 2001 and 2002 (-2.40). The southwest part was affected by the droughts that occurred in the year 2001. The years 2006, 2007 and 2008 were the wet years, except for the eastern part, which was affected by severe drought in the year 2008.

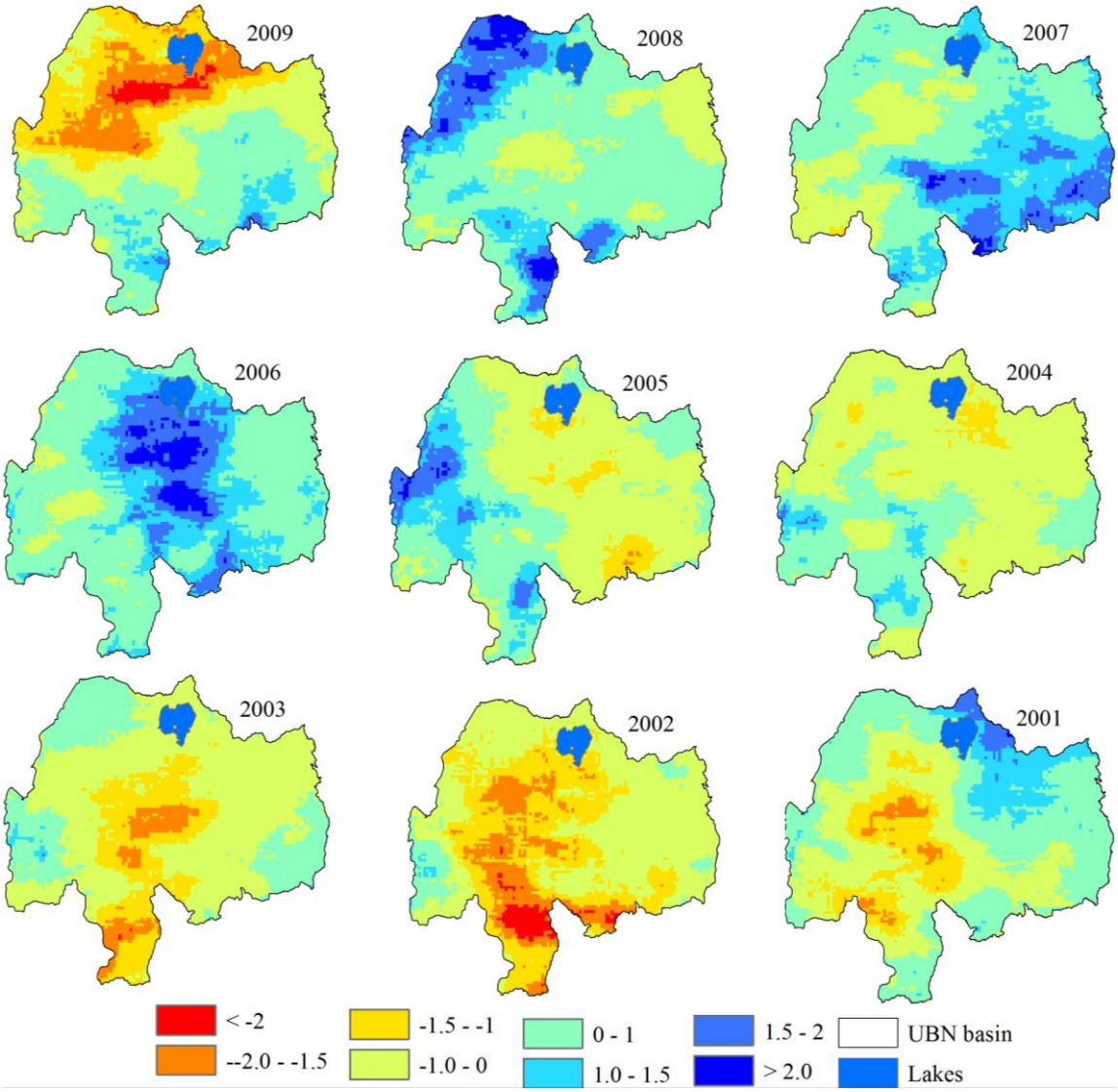

Figure 5.4: The average spatial extents of meteorological drought, as indicated by the 3-month Z-score (red and yellow) for the years 2001-2009. The green and blue colors show no drought condition.

The time series plots of the drought intensities at the corresponding locations of the meteorological stations were extracted as shown in Figure 5.5. The figures were produced for those meteorological stations having high correlation coefficients with each other. The cluster of the stations revealed the similarity of rainfall patterns at each station. The drought years of 2002 and 2009 were clearly indicated at most of the stations, independent of the geographic locations. In the year 2009, those stations located in the far southern part showed no drought condition (Figure 5.5e). This indicates that the drought in these years were severe and covered the majority of the basin. The wet years such as 2006, 2007 and 2008, were also clearly shown in the time series plot for the majority of the stations. The longer drought duration of 19 months was observed in some of the stations between the years 2001 to 2003. The drought duration of the year 2009 was 12 months and it was indicated at the majority of the stations. The maximum drought intensity of -2.55 was also observed in the drought year of 2009, in those stations located in the central and northern parts of the basin (Figures 5.4a and b).

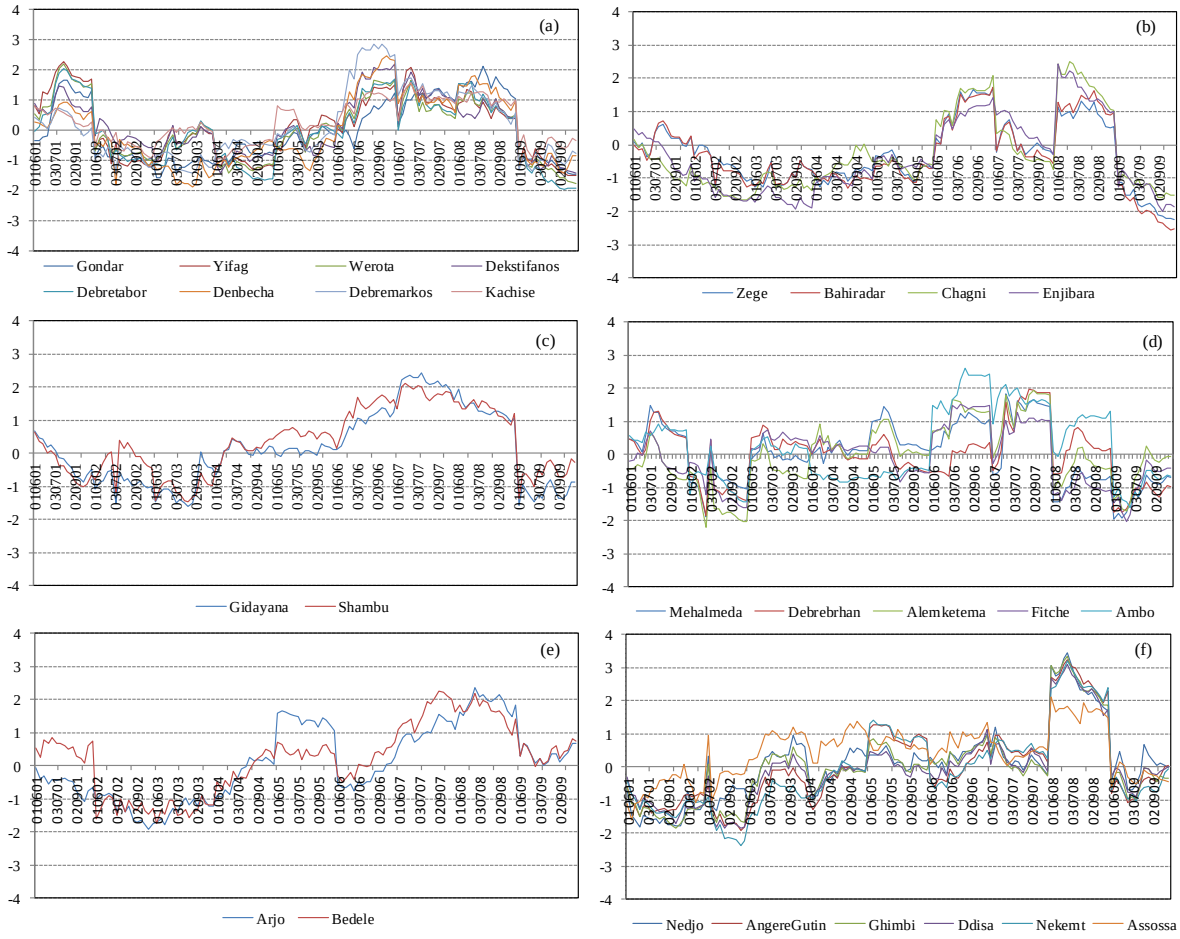

Figure 5.5: The time series (2001-2009) plot of the Z-score at the corresponding locations of the meteorological stations for Kiremt (June-September). Each plot shows the temporal pattern of the Z-score for stations showing a similar pattern. The label of the x-axis shows dekadal (DD), month (MM), and year (YY).

5.4.3 Evaporation Deficit Index (EDI) based drought assessment

The annual spatial distributions of the EDI anomaly for the UBN Basin are shown in Figure 5.6. The figures reveal that the EDI has the capability of indicating the drought and wet conditions in the basin. In the years 2001 and 2002, the central and Eastern parts of the basin were affected by drought with the drought severity ranging between -0.51 to -1.68. In 2009, the majority of the area was affected by the drought. The northwestern, central and northeast parts of the basin were stricken by the onset of drought and shortage of water. Water stress was also observed in the years 2007 and 2008 in the North-West, Western and Southern parts of the basin.

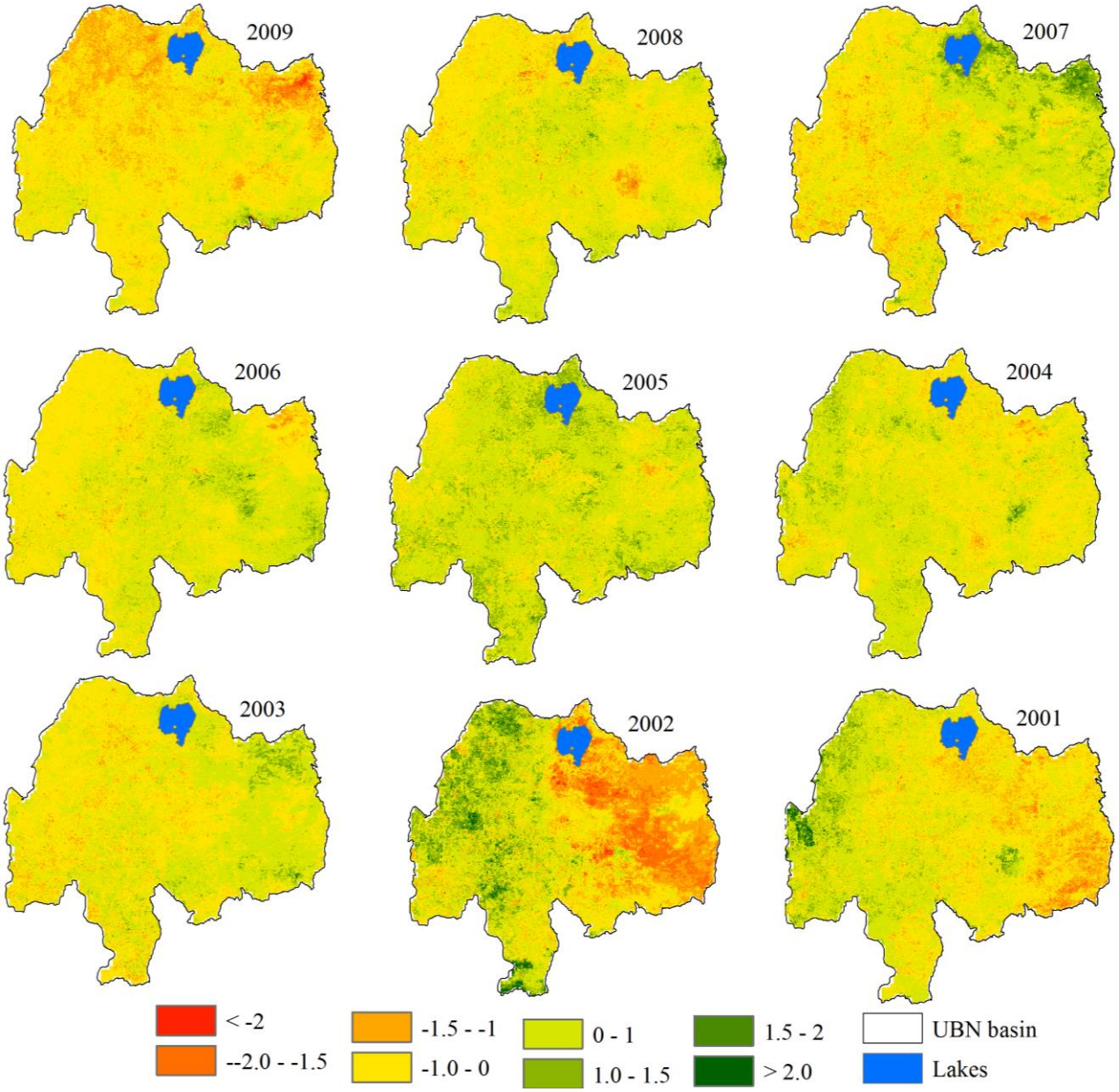

Figure 5.6: The spatial extents of the EDI anomaly in the Upper Blue Nile basin for the year 2001 to 2009.

The time series plots of the EDI anomaly for the selected stations (Debremarkos, Gondar, and Dedissa) are shown in Figure 5.7. The stations are chosen to represent the Northern (Gondar), Central (Debremarkos) and Southern (Dedissa) parts of the study area. The result shows that some of the historic drought years are indicated by the EDI anomaly. The year 2009 is indicated as drought year in all the three stations.

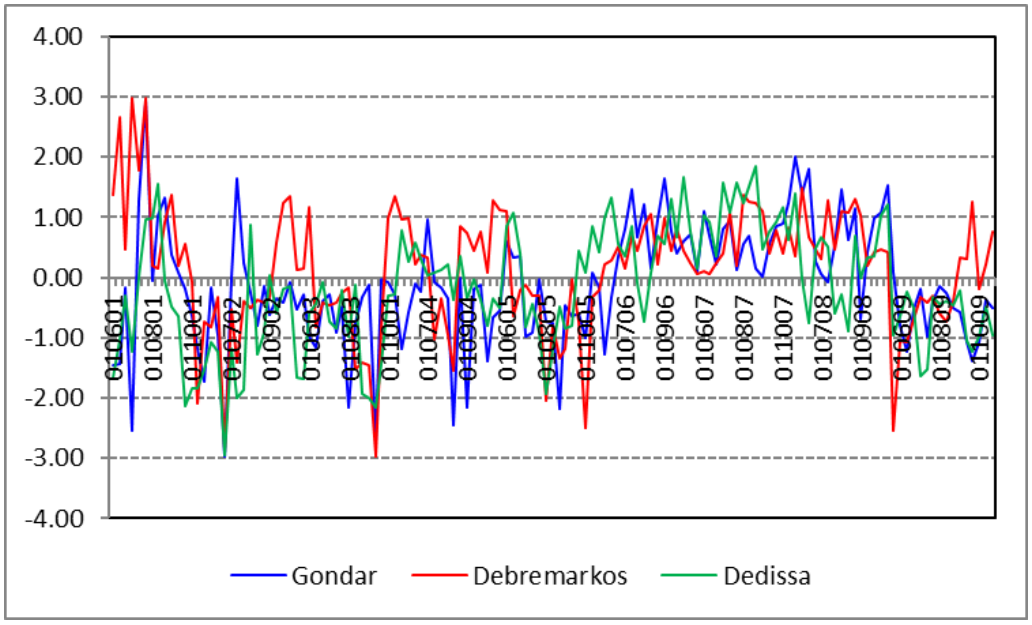

Figure 5.7: The time series (2001-2009) plot of the EDI anomaly for Kiremt season (June-September) at the Gondar, Denremarkos and Dedissa stations representing different parts of the study area. The format of the x-axis shows dekadal (DD), month (MM), and year (YY) format.

5.4.4 Vegetation Condition Index (VCI) based drought assessment

The patterns of the average rainfall during the monsoon season (left) and VCI (right) are shown in Figure 5.8. The monsoon rainfall is associated with the main rainy season, in which rain-fed agriculture is the dominant practice and its failure most often causes water stress in the study area. Failure of the monsoon rainfall is a precursor for drought to occur. The figure shows a decreasing trend of monsoon rainfall from the southwest towards northeast part. The historic drought events, according to VCI, reveal that the northeast part is drought prone and most frequently struck by drought. The long-term average monsoon (2001-2009) VCI maps were processed to analyse the vegetation signals to the rainfall pattern. The pronounced vegetation signals were observed in the southwest part that corresponds to the high amount of monsoon rainfall. The VCI values for the Northeast part are smaller, which gives clear indication of poor vegetation condition that corresponds with the occurrence of drought.

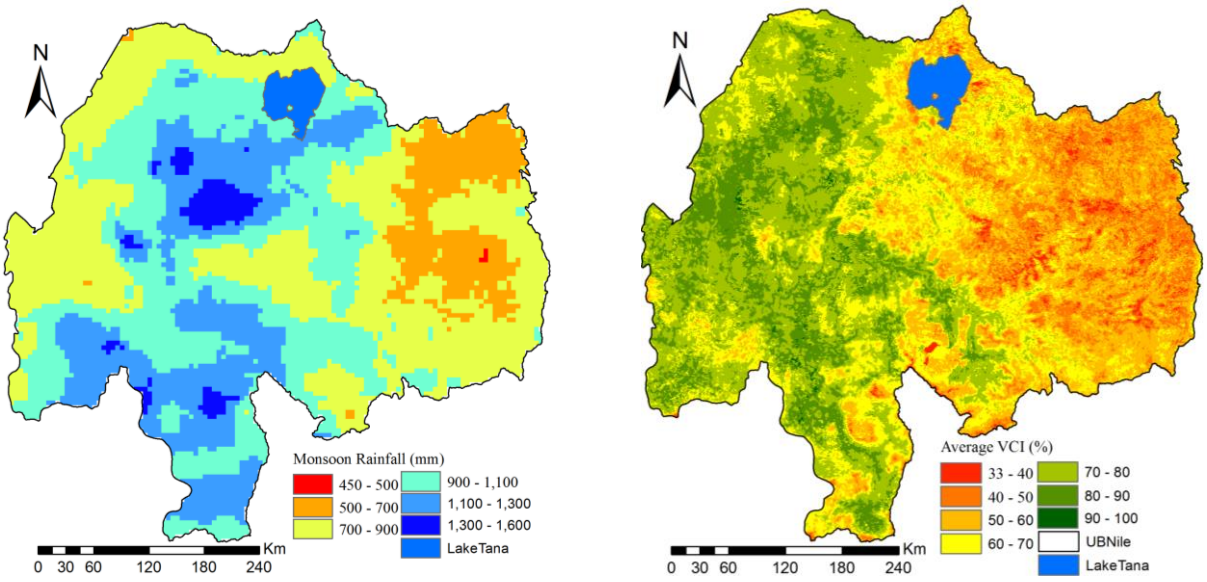

(a) (b)

Figure 5.8: Long-term monsoon rainfall (a) and VCI (b) patterns in the Upper Blue Nile basin.

The spatial and temporal analysis of droughts were investigated using multiple years of processed images. The vegetation condition index (VCI) was calculated from the corresponding NDVI to identify and characterize the drought prone area. According to Kogan, (1993), the VCI values less than 35% indicate extreme drought condition, up to 50% fair to normal vegetation condition, and close to 100% good and brightness vegetation condition. The VCI maps from the year 2001 to 2009 were used to assess the spatial and temporal extents of drought in the study area. Moreover, the VCI maps could help to identify the development of drought within the analysis periods.

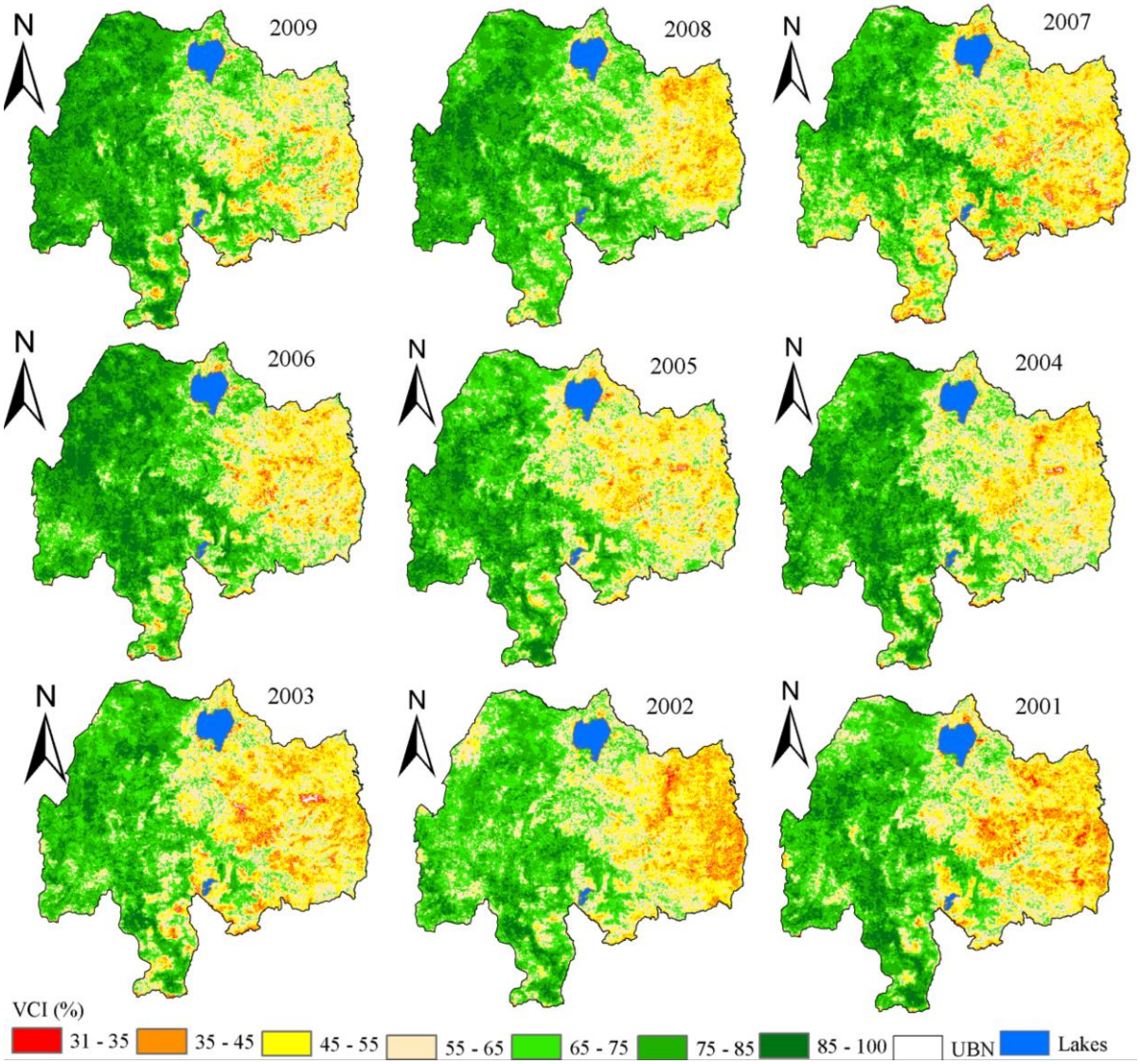

Figure 5.9: The spatial pattern of the Vegetation condition index (VCI) for monsoon season of the years from 2001 to 2009 in the Upper Blue Nile basin.

In general, VCI values less than 35% were observed in the Northeast, eastern and towards the center, with different levels of severity (Figure 5.9). The VCI value less than 35% is a good indication of the presence of water stress, poor vegetation condition, and drought zone. The maps indicate that in the monsoon years 2001, 2002, 2003, 2007, and 2009, more than 15 percent of the area suffered fair to extremely poor vegetation condition (VCI values less than 50 percent). The year 2003 was clearly identified as a drought year, because of a large area (22.5%) with fair to extreme vegetation condition damage. This shows that VCI is also a good indicator to capture the historic drought events.

The comparative result showed that the three drought indices, Z-score, EDI, and VCI, identified the historic drought events well. The three indices indicated different drought frequency, severity and duration for the historic events.

Lag time analysis of the results obtained from the drought indices

The time series VCI values at the location of the rain gauge stations were extracted from each VCI image. Accordingly, correlation analysis between the average rainfall and average VCI within the analysis period (2001-2009) was carried out to identify the lag time between the peak rainfall and the lagged peak VCI values of each station. Figure 5.10 shows the graphs of sample stations produced using average monthly rainfall and VCI from the year 2001 to 2009. The figure shows that the average VCI value reaches to its maximum value during the month September in most of the stations. There is also similar temporal pattern between average rainfall and VCI with a certain lag time. Similarly, Table 5.1 shows the correlation coefficients between rainfall and VCI for each station at different lag time. From the result, it was observed that there is two months lag time between the rainfall and the vegetation response (NDVI/VCI) in most of the stations. Very few stations showed one and three-month lag time as indicated by bold and italic font in Table 5.1. The peaks in actual evapotranspiration were also observed after two months of the peaks of rainfall in the majority of the stations (Figure 5.10). The lag times found here, were used in the development of the Earth observation based CDI (Section 5.4.5).

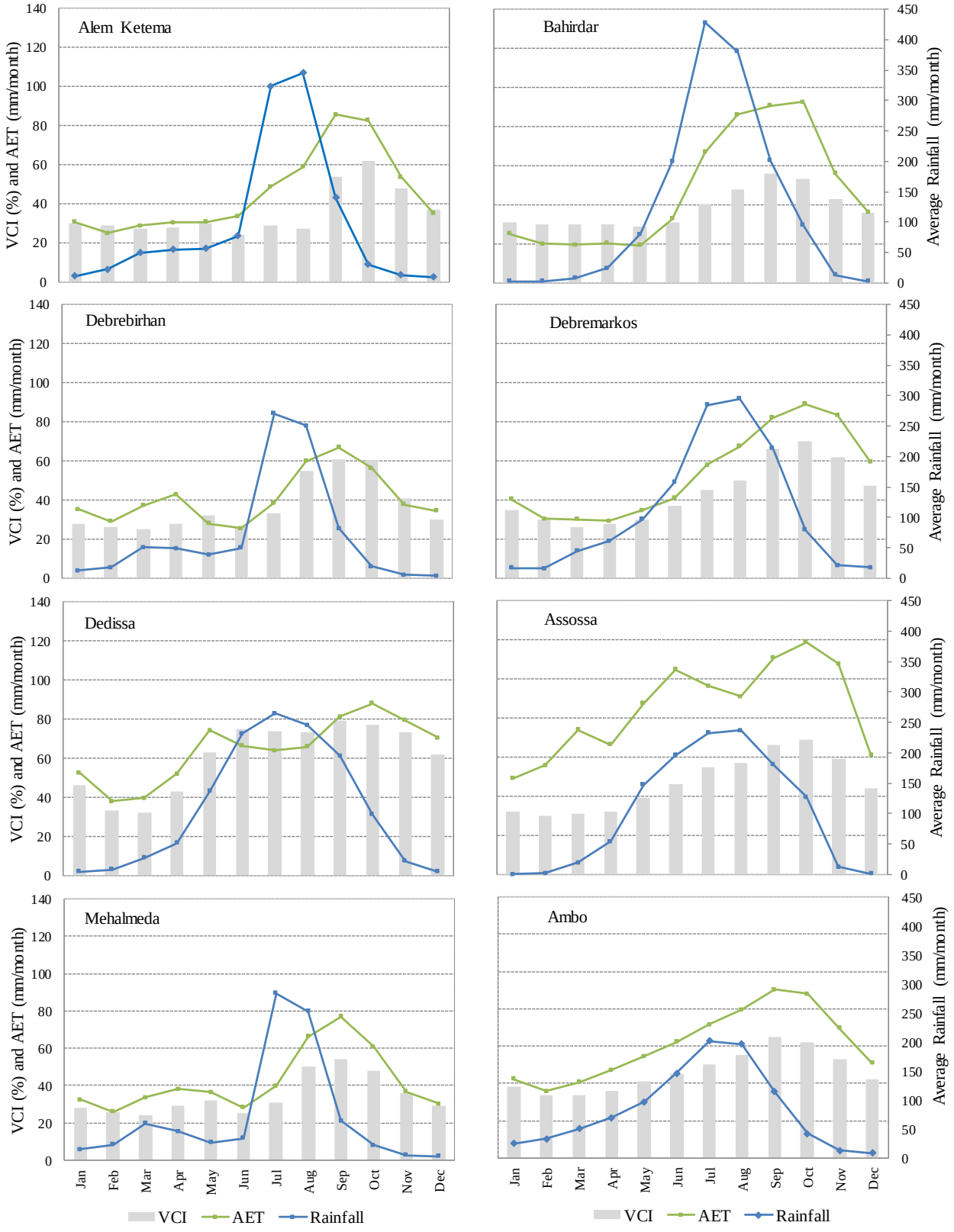

Figure 5.10: Monthly average VCI, AET and Rainfall graphs for the selected stations that show the time lag between peak rainfall and VCI and AET.

Table 5.1: Correlation coefficient between rainfall, VCI, and AET, at different lag times.

Station Name	Correlation coefficient at different lag time							
	Current month		One month lag		Two months lag		Three months lag	
	VCI	AET	VCI	AET	VCI	AET	VCI	AET
Alem Ketema	-0.23	0.31	0.34	0.76	***0.92***	***0.94***	0.76	0.48
Ambo	0.34	0.46	0.76	0.82	***0.98***	***0.98***	0.76	0.66
Angere Gutin	0.54	0.49	0.85	0.74	***0.95***	***0.84***	0.75	0.65
Arjo	0.38	-0.08	0.58	0.16	***0.63***	0.32	0.51	***0.37***
Assossa	0.57	0.64	0.88	0.82	***0.96***	0.65	***0.79***	0.41
Bahirdar	0.44	0.61	0.85	0.90	***0.97***	***0.89***	0.65	0.54
Bedele	0.21	0.43	0.48	0.58	0.62	***0.61***	***0.66***	0.42
Chagni	0.70	0.72	0.95	0.90	***0.91***	***0.81***	0.62	0.53
Debre Markos	0.28	0.31	0.71	0.70	***0.97***	***0.95***	0.85	0.86
DebreBirhan	0.27	0.36	0.79	***0.85***	***0.84***	0.71	0.41	0.15
Deddisa	0.68	0.36	0.80	0.57	***0.76***	***0.73***	0.52	0.78
DekEstifanos	0.40	0.69	0.86	***0.95***	***0.97***	0.86	0.64	0.43
Denbecha	0.28	0.34	0.70	0.66	***0.97***	***0.90***	0.89	0.87
Enjibara	0.78	0.73	***0.91***	***0.57***	0.79	0.25	0.37	-0.23
Fitche	0.33	0.71	***0.86***	***0.93***	0.84	0.61	0.28	-0.06
Ghimbi	0.41	-0.51	0.63	-0.78	***0.72***	***-0.62***	0.67	-0.22
GidAyana	0.48	0.18	0.70	0.44	***0.77***	0.61	0.72	***0.67***
Gondar	0.02	0.14	0.52	0.51	***0.92***	***0.78***	0.88	0.64
Mehal Meda	0.28	0.36	***0.83***	***0.88***	0.76	0.76	0.22	0.05
Nedjo	0.33	-0.39	0.68	-0.54	***0.84***	-0.52	0.81	-0.14
Nekemte	0.11	-0.28	0.33	-0.02	0.56	0.33	***0.74***	***0.62***
Shambu	-0.13	-0.20	0.35	0.24	0.77	0.65	***0.89***	***0.78***
Woreta	0.45	0.61	***0.93***	***0.88***	0.59	0.51	0.15	0.04
Yifag	0.51	0.69	0.88	***0.96***	***0.88***	0.78	0.50	0.24
Zege	0.32	0.43	0.75	0.83	***0.94***	***0.91***	0.78	0.66

5.4.5 Developing the Earth Observation based Combined Drought Index (EO-CDI)

The Earth observation based combined drought index (EO-CDI) is developed using a random search of the optimal weights for each of the three Earth observation based drought indices (Z-score, EDI and VCI) considered in this study. The results obtained at the Debremarkos station are used for further discussion. The same coefficients of the drought indices (Z-score=0.4, EDI=0.5and VCI=0.1) were obtained for the four crops. However, two months of lag time between rainfall and vegetation condition was observed in Debremarkos and the majority of the other stations and hence the equation for the combined drought index (EO-CDI) is shown in Equation 5.11. The seasonal time series plot of the combined drought index and the other indices reveled the same pattern (Figure 5.11). The combined drought index also shows its capability to indicate the historic drought years 2002, 2003, 2005, and 2009. The visual inspection of the time series plot further revealed that the wet years (2006, 2007, and 2008) were also indicated by the combined drought index and this could show the potential of the Earth observation based combined index for drought assessment in the Upper Blue Nile Bain.

$$EO\text{-}CDI_n = 0.4 \times Z\text{-}score_{n-2} + 0.5 \times EDI_n + 0.1 \times VCI_n \quad (5.11)$$

where n is the current month

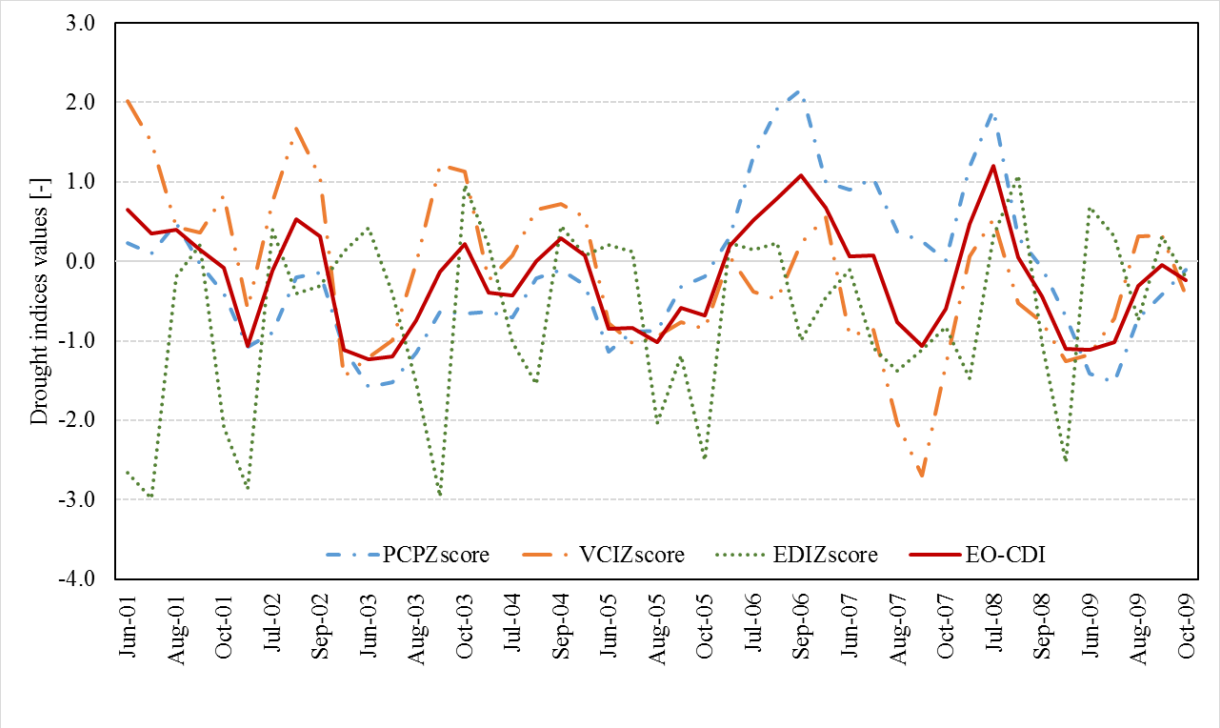

Figure 5.11: Seasonal time series plots of drought indices at the Debremarkos station. The values of the time series of the drought indices including the VCI were standardized (Z-score).

The relationship between the EO-CDI and the crop yield anomalies for all the selected stations were analyzed. The result obtained at the Debremarkos station (Figure 5.12) is shown in this section for further discussion. The relationship between EO-CDI and crop yield anomalies was assessed using the coefficient of determination (R^2) and the number of points (each representing a year between 2001 and 2009) falling in the appropriate quadrant (lower-left and top-right quadrants, indicating that both EO-CDI and crop-yield anomaly were negative or positive). The resulting plots show that there is an agreement between EO-CDI and crop yield anomalies with R^2 between 0.29 (Teff) and 0.41 (Sorghum). The comparison based on the number of scatter points falling in the top-right and bottom-left quadrants, shows the best result for Maize, with 78% (7 out of 9) of the points in the correct quadrant. The number of the scatter points falling in the top-right and bottom-left quadrant for the other three crops is 6 out of 9 (67%). None of the points, regardless of the crop, falls in the upper-left quadrant, indicating that there is no negative crop-yield year missed by the EO-CDI. Similar results were observed in the other selected stations. This is a better result than presented in Section 4.4.4 for the station-

based CDI. This shows the potential application and use of the EO-data in developing a drought monitoring and early warning framework for the UBN Basin.

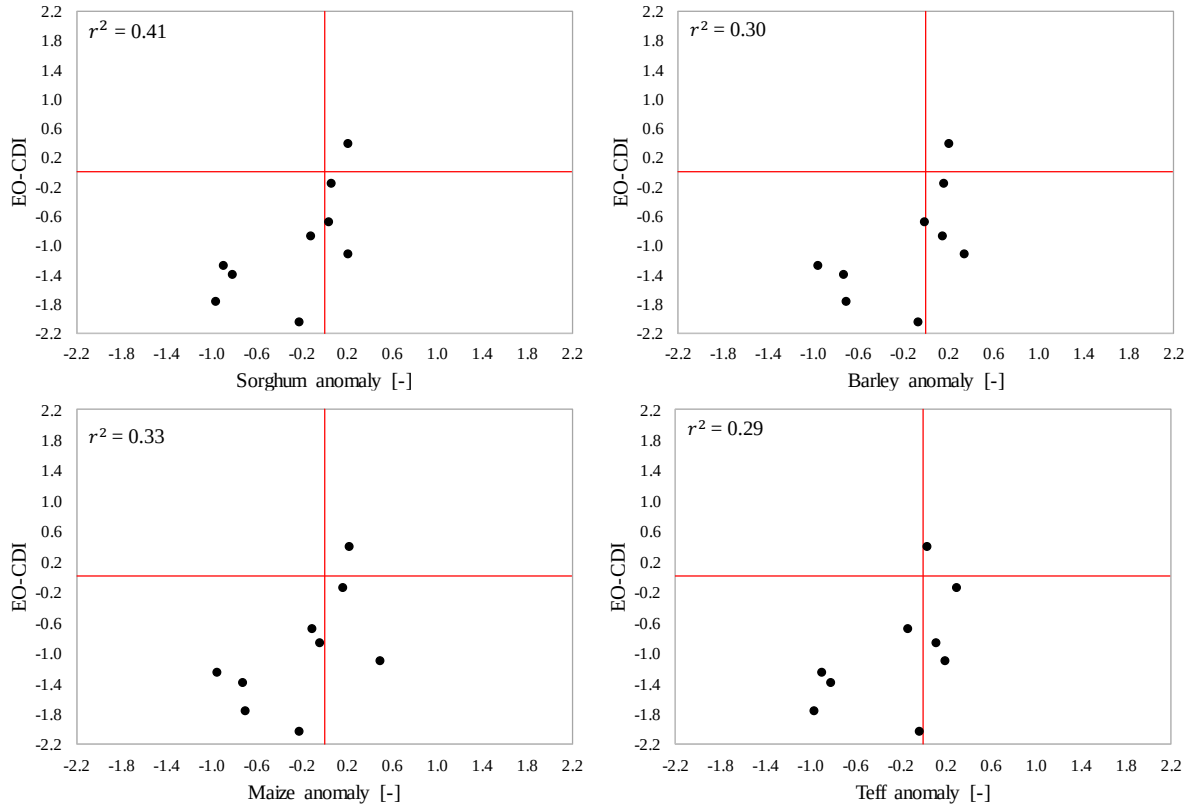

Figure 5.12: The scatter plots of the Earth observation based CDI with Barley, Sorghum, Maize and Teff crops yield anomalies at the Debremarkos station.

5.5 Prediction models of crop yield anomalies

Linear regression equations between the Earth observation based drought index and the four crop yield anomalies at the selected eight zones and the corresponding representative stations were developed. The result obtained at the Debremarkos station is used for further discussion. The resulting regression equations of this station for Teff, Maize, Sorghum and Barley crop yield anomalies are shown in equations 5.12 to 5.15. These equations were used to predict each crop yield anomaly, and the resulting graph between the observed and predicted values of each crop yield anomaly between 2001 and 2009, is shown in Figure 5.13. The prediction accuracy of most of the yield anomaly equations is above 0.5 when explained in terms of coefficient of correlation. The maximum value of the correlation coefficient was obtained for the Sorghum crop (0.64). The mean absolute error (*MAE*) value for the Sorghum crop is 0.64 (smallest among all crops). Lower prediction accuracy is observed for Barley (*MAE* is 0.84) and Teff (0.84). Overall, the model prediction of each crop yield anomaly is not very high but, for such a small sample size, can be qualified as satisfactory. Similar results were also observed in the

other selected stations. The variation in the magnitude between the observed and predicted crop yield anomaly might be attributed to several factors, including the quality and limited length of the crop yield data that is aggregated to Zonal average. From the EO data, the remote sensing model accuracy for actual evaporation and soil moisture may be an important factor.

$$\textit{Teff yield anomaly} = 0.321 \times \textit{EO-CDI} + 0.06 \quad (5.12)$$

$$\textit{Maize yield anomaly} = 0.359 \times \textit{EO-CDI} + 0.144 \quad (5.13)$$

$$\textit{Sorghum yield anomaly} = 0.56 \times \textit{EO-CDI} + 0.20 \quad (5.14)$$

$$\textit{Barley yield anomaly} = 0.365 \times \textit{EO-CDI} + 0.185 \quad (5.15)$$

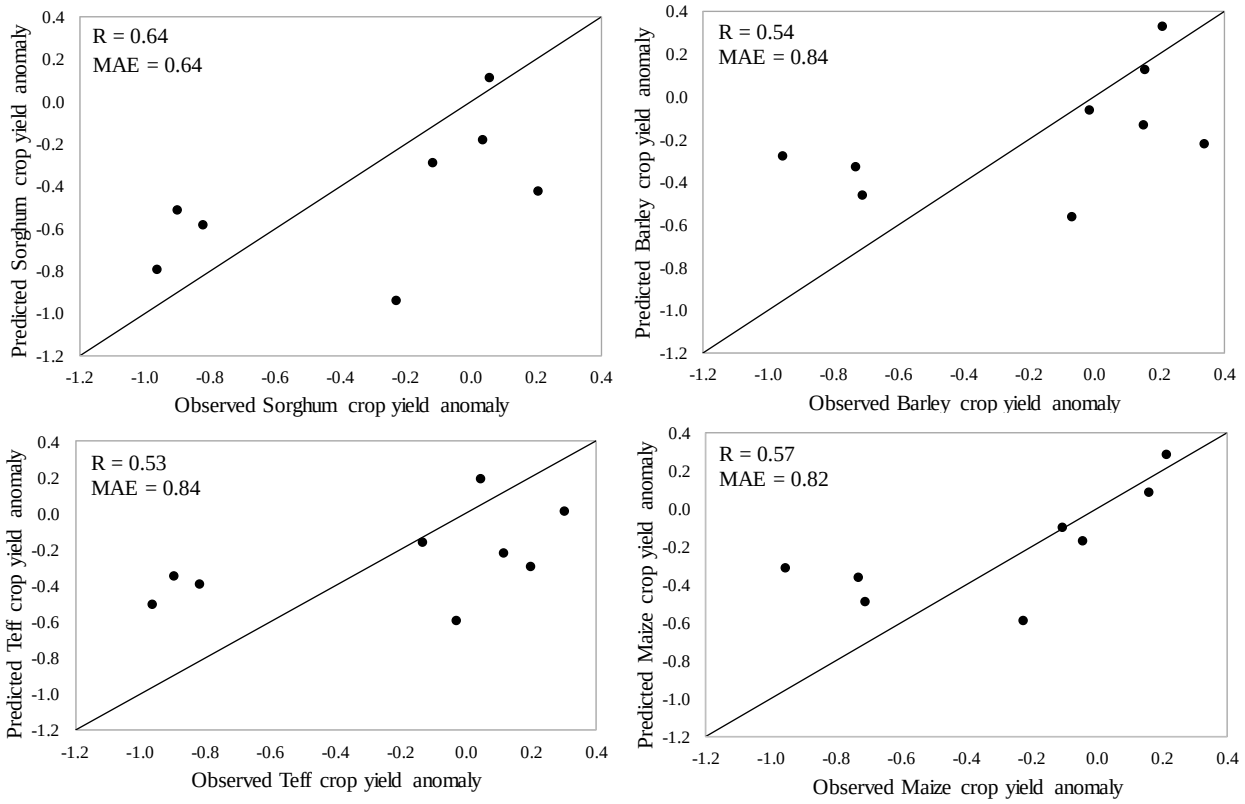

Figure 5.13: Predicted vs observed Teff, Maize, Sorghum and Barley crops yield anomaly at the Debremarkos station respectively.

5.6 Conclusions

In this chapter, the potential of the Earth observation data to assess the historic drought events in the UBN Basin, and to develop the combined drought index (EO-CDI) and crop yield anomaly prediction models, was assessed. The impact-based CDI optimisation approach presented in Chapter 4 was used to develop the EO-CDI. Three drought indices, Z-score, EDI, and VCI, were used to develop the combined drought index and derived crop yield anomaly prediction model.

The drought indices indicated the historic drought events reasonably well. The spatial and temporal patterns and characteristics of the historic drought events were indicated well with the Z-score and VCI drought indices. The combined index (EO-CDI) indicated negative or positive crop yield anomalies correctly for a majority of the years. The maximum correlation coefficient was obtained for Sorghum.

The years 2009 and 2003/04 were identified as some of the severe drought years in the basin. The East and Northeast and Southeast parts are indicated as the drought affected parts of the basin. The EO-CDI developed in this chapter showed an improvement in terms of the coefficient of determination (R^2) and its ability to indicate positive or negative crop-yield anomalies. The combined drought index integrates the information embedded in the other indices and can be used as a potential index to develop drought monitoring systems in the UBN Basin.

6. Summary, conclusions and recommendations

6.1 Summary

The objective of this study was to develop an impact-based combined drought index (CDI) and prediction model of crop-yield anomalies for the Upper Blue Nile basin. The impact-based CDI is defined in this thesis as a drought index that optimally combines the information embedded in other drought indices for monitoring a certain impact of drought (e.g. crop yield).

First, the influence of record length on the drought category was studied by comparing the Standardized Precipitation Index (SPI) results from 14 stations with long record length, when taking out incrementally 1-year records from 1953 to 1974. These analyses showed that the record length from 1953 to 1974 has limited effect on changing the drought category, and hence stations with a shorter record length from 1975 to 2009 could also be used for the drought analyses in this is basin.

A comparison of a range of individual drought indices, i.e. SPI, Standardized Precipitation Evaporation Index (SPEI), Evapotranspiration Deficit Index (ETDI), Soil Moisture Deficit Index (SMDI), Aggregate Drought Index (ADI), and Standardized Runoff-discharge Index (SRI) was carried out using correlation analysis. Their performances were evaluated with respect to identifying onset, severity, and duration of historic drought events in the UBN Basin. An analysis of the impact of data record length on drought assessment was done first, to select the meteorological stations to be included in the analyses. The information on historic drought events was obtained from the Emergency Events Database (EM-DAT).

Developing the impact-based CDI was done through assigning weights to the individual drought indices using random search optimisation. The optimisation identified the combination of weights with maximum correlation with crop yield anomaly. Crop-yield anomaly data for the UBN Basin were obtained from the Central Statistical Agency (CSA) of Ethiopia for the period from 1996 to 2009. Four crops common in the basin were considered (i.e. teff, maize, barley, and sorghum). The impact-based CDI was compared with a CDI developed with Principal Component Analysis.

Crop-yield anomaly prediction models were developed using multiple linear regression equations linking the drought indices and yield anomalies. In these models, crop yield anomaly was used as a predictand variable (variable being predicted), whereas the drought indices, including both CDI and the selected drought indices, were used as predictor variables.

Lastly the same approach for developing an impact-based CDI and crop-yield anomaly models was applied using drought indices based on Earth Observation data. EO-based indices included the precipitation Z-score, Evaporative Drought Index (EDI) and Vegetation Condition Index (VCI).

6.2 Conclusions

After analysing and interpreting the results obtained, a number of conclusions can be drawn. They are formulated in relation to the specific objectives initially posed.

Investigate the effect of data record length on drought assessment in the UBN Basin, to validate the use of meteorological stations with short record length in the drought analysis.
This specific objective was addressed in Chapter 2. From the results obtained, it can be concluded that the influence of record length on SPI drought category was minimal, which validates the use of a large number of additional meteorological stations with shorter data record lengths for the further drought analyses of the UBN Basin in this thesis.

Investigate the spatial and temporal variation of meteorological droughts in the UBN Basin.
The spatio-temporal variability of the meteorological droughts, reported in Chapter 2, indicated that the North and Northeast parts of the basin were the areas most hit by severe to extreme meteorological drought during the historic drought years (1978/79, 1984/85, 1994/95 and 2003/04). The trend analysis of the SPI index from 1953 to 2009 showed no conclusive evidence that the frequency of meteorological drought in the Upper Blue Nile is increasing or declining. The temporal analysis showed that the historical drought years in the area were successfully captured using SPI index. Therefore, the SPI index can be used as an important index to identify droughts in the UBN Basin.

Evaluate and compare the performance of six drought indices, i.e. Standardized Precipitation Index (SPI), Standardized Precipitation Evaporation Index (SPEI), Evapotranspiration Deficit Index (ETDI), Soil Moisture Deficit Index (SMDI), Aggregate Drought Index (ADI), and Standardized Runoff-discharge Index (SRI) with respect to identifying historic drought events in the UBN Basin.
This specific objective was addressed in Chapter 3, and the result obtained led to the general conclusion that each index showed its capability to explain at least one drought type to a certain degree. However, the SPI and SPEI at the three-month time scale explained better the

meteorological and agricultural drought and the same indices at the 12-month time scale explained better the hydrological drought conditions in the basin. Moreover, the meteorological drought indices (SPI and SPEI) showed the early indication of the drought onset in most of the cases. The agricultural (ETDI, SMDI, and ADI) and hydrological (SRI) drought indices showed the late onset of the drought; particularly ADI most often lagged with some months. The agricultural indices, ETDI, SMDI and ADI, and the runoff-based hydrological drought index, SRI, have shown the often hidden aspect of elongated droughts before full recovery. The duration of the historic drought events often exceeded 12 months according to at least one of the indices. In particular, the SRI indicated long durations, up to 24 months for 1984/1985. These longer durations are seen to be likely correct, considering the devastating famine that occurred at that time.

Develop an impact-based Combined Drought Index (CDI) with weights optimized to monitor crop yield anomalies.

From the analysis presented in Chapter 4, it can be concluded that the developed impact-based CDI correlated well with the crop yield anomalies data of the four crops considered in this study: Teff, Barley, Maize and Sorghum. The maximum correlation coefficients were obtained for the Barley crop. The CDI using PCA could indicate years with negative crop yield anomalies equally well.

Develop a prediction model of crop yield anomalies based on the impact-based CDI and individual drought indices.

The developed regression models of crop yield anomalies generally showed satisfactory results, indicating the prediction potential of the impact-based CDI and the drought indices (Chapter 4). The best results were obtained for Sorghum. The predicted and observed crop-yield anomaly data were consistently showing the same trend. However, it should be mentioned that the absolute magnitude of anomaly was not always captured, such that the accuracy of the models should be further improved.

Assess the potential of an impact-based CDI using Earth Observation *data as the main input.*

The Earth Observation-based drought indices were able to indicate well the historic drought events that have occurred in the basin (Chapter 5). The spatial and temporal patterns and characteristics of the historic drought events were indicated well with the Z-score and VCI drought indices. The years 2009 and 2003/04 were identified as some of the severe drought

years in the basin, and the East and Northeast and Southeast parts are indicated as the drought affected parts of the basin. The developed Earth Observation-based combined drought index (EO-CDI), showed its potential to characterize the drought conditions in the basin. The EO-CDI indicated negative or positive crop yield anomalies correctly for a majority of the years. The EO-CDI correlated well with the crop yield anomalies of the four crops. The results indicate that the EO-CDI can be considered as a potential index in future drought monitoring systems in the basin.

The main objective of developing an impact-based combined drought index (CDI) and prediction model of crop-yield anomalies for the Upper Blue Nile basin has been achieved. The developed impact-based CDIs and multiple linear regression models have shown to be effective tools in indicating historic drought events in the Upper Blue Nile.

6.3 Recommendations

Based on the findings of this study, the following major recommendations can be made:

1. The spatial distributions of the meteorological and hydrological stations are not dense in the basin. This influences the accuracy of the spatial representation of the data that eventually affects the spatial assessments of drought over the basin. So it is recommended to increase the density of the stations, optimally distributed across the basin, for future drought management.
2. In this study, the SWAT hydrological model was calibrated using measured river flow data at five gauging stations. However, the simulated evapotranspiration and soil moisture data could not be calibrated or validated with in-situ measured ground-truth data. The Earth Observation estimates of the evapotranspiration were not validated with ground-truth measured data. Hence, it is recommended to install flux towers and soil moisture sensors (e.g. SM300, Neutron moisture gauges, and soil resistivity) to measure actual evapotranspiration and soil moisture respectively for the future drought studies. Moreover, it is recommended to use good quality re-analysis hydro-meteorological data, e.g. GLDAS soil moisture, surface energy balance based actual ET (e.g. SEBAL, SEBS) and other ET products (e.g. EDDI, ESI) for future studies.
3. The hydrological model that is used in this study has some degree of uncertainty in the model structure and its conceptualization. In general, the model uncertainty would play its role to relegate the values of the model estimates of the evapotranspiration and soil moisture

and other water balance components. Efforts to minimize the model uncertainties are recommended for the future studies.

4. The method employed to test the influence of record length on drought index results proved to be successful in validating the use of a large number of additional stations with a shorter record length for spatial drought analysis in the UBN Basin. Hence, we recommend other drought researchers and practitioners who face challenges of insufficient record length to apply the same method.
5. The evaluation of the existing drought indices in this study was carried out using drought characteristics data (onset date and severity) obtained from a global data source. It is recommended to check for availability of measured and local-scale data when adapting the same evaluation procedure for other study areas.
6. The drought indices used in this study explained some aspects of the historic drought events such as severity, onset, duration etc. and no single index consistently indicated all the historic severe drought years. This triggered the development of a customized CDI for the UBN Basin, using all the drought indices tested. For other case studies the result of testing multiple drought indices on historic drought events may be different, e.g. only some of the indices may manage to explain historic events. It can be therefore, recommended to carry out a similar extensive evaluation of existing drought indices when preparing for drought monitoring and early warning in a particular study area.
7. The PCA method for developing CDIs can be further explored, e.g. by considering the percentage contribution instead of directly adopting the Eigenvalues as a weighting factor.
8. As it was reported, the crop yield data were used to validate the performance of the combined drought index and the multiple linear regression model. The crop yield data are on the level of Ethiopia's Administrative Zones, which is spatially coarse (3453.4 to 26206.77km^2), and it would be recommended to use at mesoscale (100km^2 and less) in future drought monitoring work. Moreover, crop yield not only depends on droughts but also on other factors, such as the use of fertilizer and pesticides. Hence, considering experimental procedures that account not only for the effect of drought on crop production, will further increase the level of confidence in the CDI developed.
9. The EO-CDI also showed its capability to monitor drought in UBN Basin. The availability of the EO data in real time can potentially be used to develop a real-time drought monitoring system in the future. Moreover, the EO-CDI approach can be used in other locations with sparse data networks.

10. The temporal scale of the drought assessment in this study was on monthly scale. It would be beneficial to test the method developed in this study at a finer temporal resolution (dekadal or biweekly). This would help developing an operational drought monitoring system and the drought outlook.
11. The approach of developing an impact-based combined drought index for monitoring crop yield anomalies could show the way forward in developing a drought monitoring and early warning framework for the Upper Blue Nile basin. Hence, it is recommended to collaborate amongst universities, drought monitoring practitioners, and drought and disaster managers in the basin as well as government officials, to make the outputs of this research applicable in practice.

References

Abramowitz, M., and Stegun, I.A., 1965. *Handbook of mathematical functions: with formulas, graphs, and mathematical tables*. Courier Corporation, v. 55.

Abtew, W., Melesse, A.M., and Dessalegne, T., 2009. *Spatial, inter and intra-annual variability of the Upper Blue Nile Basin rainfall*. Hydrological processes, v. 23, p. 3075-3082.

Alley, W.M., 1984. *The Palmer Drought Severity Index: Limitations and assumptions*. J. Clim Appl Meteor., v. 23, p. 1100–1109.

Arnold, J., and Allen, P., 1996. *Estimating hydrologic budgets for three Illinois watersheds*. Journal of hydrology, v. 176, p. 57-77.

Arnold, J., Kiniry, R., Srinivasan, R., Williams, R., Haney, B., Neitsch, L., 2009. *Soil and water assessment tool input/output file documentation version 2009*. http://swat.tamu.edu/media/19754/swat-io-2009.pdf.

Araya, A., Habtu, S., Haile, M., Sisay, F., and Dejenie, T., 2010. *Determination of local Barley (Hordeum Vulgare) crop coefficient and comparative assessment of water productivity for crops grown under the present pond water in Tigray, Northern Ethiopia*. Momona Ethiopian Journal of Science, v. 3, No.1, pp. 65-79.

Awulachew, S.B., McCartney, M., Steenhuis, T.S., and Ahmed, A.A., 2009. *A review of hydrology, sediment and water resource use in the Blue Nile Basin*. IWMI, v. 131.

Balint, Z., Mutua, F., Muchiri, P., and Omuto, C.T., 2013. *Monitoring drought with the combined drought index in Kenya*. In Developments in Earth Surface Processes, Elsevier, v. 16, p. 341-356.

Barua, S., Ng, A., and Perera, B., 2011. *Comparative evaluation of drought indexes: case study on the Yarra river catchment in Australia*. Journal of Water Resources Planning and Management, v. 137, pp. 215-226.

Barua, S., 2010. *Drought assessment and forecasting using a nonlinear aggregated drought index*. Doctoral dissertation, Victoria University.

Barua, S., Perera, B., and Ng, A., 2009. *A comparative drought assessment of Yarra River Catchment in Victoria, Australia*. 18th World IMACS/MODSIM Congress, Cairns, Australia, p. 13-17.

Bayissa, Y.A., Moges, S.A., Xuan, Y., Van Andel, S.J., Maskey, S., Solomatine, D.P., Griensven, A.V., and Tadesse, T., 2015. *Spatio-temporal assessment of meteorological drought under the influence of varying record length: the case of Upper Blue Nile Basin, Ethiopia*. Hydrological Sciences Journal, v. 60, No. 11, p.1927-1942.

Bayissa, Y., Tadesse, T., Demisse, G., and Shiferaw, A., 2017. *Evaluation of Satellite-Based Rainfall Estimates and Application to Monitor Meteorological Drought for the Upper Blue Nile Basin, Ethiopia*. Remote Sensing, v. 9, No. 7, p.669.

Bayraktar, H., and Sezer, T., 2005. *A Kriging-based approach for locating a sampling site—in the assessment of air quality*. Stochastic Environmental Research and Risk Assessment, v. 19, No. 4, p.301-305.

Betrie, G., Mohamed, Y., Griensven, A.v., and Srinivasan, R., 2011. *Sediment management modelling in the Blue Nile Basin using SWAT model*. Hydrology and Earth System Sciences, v. 15, p. 807-818.

Bonaccorso, B., Bordi, I., Cancelliere, A., Rossi, G., and Sutera, A., 2003. *Spatial variability of drought: an analysis of the SPI in Sicily*. Water resources management, v. 17, p. 273-296.

Bordi, I., Fraedrich, K., Petitta, M., and Sutera, A., 2006. *Large-scale assessment of drought variability based on NCEP/NCAR and ERA-40 re-analyses*. Water Resources Management, v. 20, p. 899-915.

Brown, J.F., Wardlow, B.D., Tadesse, T., Hayes, M.J., and Reed, B.C., 2008. *The Vegetation Drought Response Index (VegDRI): A new integrated approach for monitoring drought stress in vegetation*. GIScience and Remote Sensing, v. 45, No. 1, p. 16–46.

Cancelliere, A., Mauro, G.D., Bonaccorso, B., and Rossi, G., 2007. *Drought forecasting using the standardized precipitation index*. Water resources management, v. 21, p. 801-819.

Conway, D., 1997. *A water balance model of the Upper Blue Nile in Ethiopia*. Hydrological Sciences Journal, v. 42, p. 265-286.

—, 2000. *The climate and hydrology of the Upper Blue Nile River*. The Geographical Journal, v. 166, p. 49-62.

CSA, 2014. *Annual Agricultural Sample Survey, Addis Ababa, Central Statistical Agency of Ethiopia (CSA)*. http://www.csa.gov.et/index.php/2013-02-20-13-43-35/2013-02-20-13-45-32/annual-agricultural-sample-survey (accessed 012.30.).

Das, H.P., 2005. *Agrometeorological impact assessment of natural disasters and extreme events and agricultural strategies adopted in areas with high weather risks*. Natural Disasters and Extreme Events in Agriculture, Springer, p. 93-118.

Diro, G.T., Grimes, D. F., Black, E. L., O'Neill, A., and Pardo-Igúzquiza, E., 2008. *Evaluation of reanalysis rainfall estimates over Ethiopia using monthly rain gauge data*. Int. J. Climatol. v. 29, No. 1, p. 67–78.

ECMWF 2013. *Era Intrerim data portal*: http://apps.ecmwf.int/datasets/data/interim-full-daily/levtype=sfc/ (accessed 03/06/2014).

Edossa, D.C., Babel, M.S., and Gupta, A.D., 2009. *Drought analysis in the Awash River Basin, Ethiopia*. Water resour manage, v. 24, p. 1441-1460.

Edwards, D., and McKee, T., 1997. *Characteristics of 20th century drought in the United States at multiple scale*. Atmospheric Science Paper No, 634, v. May 1-30.

FAO 1999. *Production variability and losses. R. Gommes (Ed.), Special: Agroclimatic Concepts, Sustainable Development Department (SD), Food and Agriculture Organization of the United Nations (FAO).* (accessed 08.28.) www.fao.org/ sd/ eidirect/ agroclim/ riskdef.htm.

FEWSNET, 2003. *Estimating Meher crop production using rainfall in the 'long cycle' region of Ethiopia,* June 21, revised October 6, http://reliefweb.int/sites/reliefweb.int/files/resources/ 9EC256793FA1685C49256DB90003E3DC-fews-eth-06oct2.pdf (accessed 05.54.).

Funk, C., Peterson, P., Landsfeld, M., Pedreros, D., Verdin, J., Rowland, J., Romero, B., Husak, G., Michaelsen, J., Verdin, A., and Pedreros, P., 2014. *A Quasi-Global Precipitation Time Series for Drought Monitoring*. Available online: pubs.usgs.gov/ds/832/ (accessed on 20 February 2017).

Gebrehiwot, T., van der Veen, A., and Maathuis, B., 2011. *Spatial and temporal assessment of drought in the Northern highlands of Ethiopia.* International Journal of Applied EEarth observation and Geoinformation, v. 13, p. 309-321.

Gebremicael, T., Mohamed, Y., Betrie, G., van der Zaag, P., and Teferi, E., 2013. *Trend analysis of runoff and sediment fluxes in the Upper Blue Nile basin: A combined analysis of statistical tests, physically-based models and landuse maps*. Journal of hydrology, v. 482, p. 57-68.

Gibbs, W., and Maher, J., 1967. *Rainfall deciles as drought indicators*. Bureau of Meteorology Bulletin No. 48, Melbourne, Australia.

Gissila, T., Black, E., Grimes, D., and Slingo, J., 2004. *Seasonal forecasting of the Ethiopian summer rains.* Int. J. Climatol. v. 24, p. 1345–1358.

Green, H., and Van Griensven, A., 2008. *Auto calibration in hydrologic modeling: Using SWAT2005 in small-scale watersheds*. Environmental Modelling & Software, v.23, No.4, p. 422 – 434.

Griensven, A.v., Ndomba, P., Yalew, S., and Kilonzo, F., 2012. *Critical review of SWAT applications in the upper Nile basin countries.* Hydrology and Earth System Sciences, v. 16, p. 3371-3381.

Guttman, N.B., 1998. *Comparing the Palmer drought index and the standardized precipitation index. INDEX1*. JAWRA Journal of the American Water Resources Association, v. 34, p. 113-121.

Hamed, K.H., 2008. *Trend detection in hydrologic data: The Mann–Kendall trend test under the scaling hypothesis*. Journal of Hydrology, v. 349, p. 350-363.

Hanson, L.S., and Vogel, R., 2008. *The probability distribution of daily rainfall in the United States*. Conference proceeding paper, World Environmental and Water Resources Congress.

Hargreaves, G.H., and Samani, Z.A., 1982. *Estimating potential evapotranspiration*. Journal of the Irrigation and Drainage Division, v. 108, p. 225-230.

—, 1985. *Reference crop evapotranspiration from ambient air temperature*. American Society of Agricultural Engineers (Microfiche collection), p. 85-2517.

Hayes, M., Svoboda, M., Wall, N., and Widhalm, M., 2011.*The Lincoln Declaration on Drought Indices: Universal meteorological drought index recommended*. Bulletin of the American Meteorological Society, v. 92, No. 4, p. 485-488.

Hayes M., O. Wilhelmi, and C. Knutson., 2004. *Reducing drought risk: bridging theory and practice*. Natural Hazards Review, v. 5, No. 2, p. 106-113.

Heim Jr, R.R., 2002. *A review of twentieth-century drought indices used in the United States*. Bulletin of the American Meteorological Society, v. 83, No. 8, p.1149-1165.

Houcine, A. and Bargaoui, Z., 2012. *Comparison of rainfall based SPI drought indices with SMDI and ETDI indices derived from a soil water budget model*. In EGU General Assembly Conference Abstracts, v. 14, p. 2666.

Jacobs, T., Borstlap, G., Bartholomé, E., and Maathuis, B., 2008. *Devcocast in support of environmental management and sustainable development in Africa. 7th International Conference of African Association of Remote Sensing of the Environment (AARSE) on EEarth observation and Geo-Information for Governance in Africa, Accra, Ghana*.

Jain, V.K., Pandey, R.P., Jain, M.K., and Byun, H.R., 2015. *Comparison of drought indices for appraisal of drought characteristics in the Ken River Basin*. Weather and Climate Extremes, v. 8, p.1-11.

Jiahua, Z., Fengmei, Y., and Xiaolu, S., 2015. *Estimation and Assessment of Drought in North China based on Evapotranspiration Drought Index and Remote Sensing Data*. AASRI International Conference on Industrial Electronics and Applications (IEA 2015), Atlantis Press.

Karamouz, M., Rasouli, K., and Nazif, S., 2009. *Development of a hybrid index for drought prediction: case study*. Journal of Hydrologic Engineering, v. 14, No. 6, p. 617-627.

Kebede, S., Travi, Y., Alemayehu, T., and Marc, V., 2006. *Water balance of Lake Tana and its sensitivity to fluctuations in rainfall, Blue Nile basin, Ethiopia*. Journal of hydrology, v. 316, p. 233-247.

Keyantash, J.A., and Dracup, J.A., 2004. *An aggregate drought index: Assessing drought severity based on fluctuations in the hydrologic cycle and surface water storage*. Water Resources Research, v. 40, No. 9.

Keyantash, J., and Dracup, J.A., 2002. *The quantification of drought: An evaluation of drought indices*. Bulletin of the American Meteorological Society, v. 83, p. 1167-1180.

Kim, U., Kaluarachchi, J.J., and Smakhtin, V.U., 2008. *Generation of monthly precipitation under climate change for the Upper Blue Nile river basin, Ethiopia.* Journal of the American Water Resources Association, v. 44, No. 5, p. 1231-1247.

Khan, S., Gabriel, H., and Rana, T., 2008. *Standardized precipitation index to track drought and assess impact of rainfall on watertables in irrigation areas*. Irrigation and Drainage Systems, v. 22, p. 159-177.

Kogan, F., and Sullivan, J., 1993. *Development of global drought-watch system using NOAA/AVHRR data*. Advances in Space Research, v. 13, p. 219-222.

Li, W., Fu, R., Juárez, R. N., and Fernandes, K., 2008. *Observed change of the standardized precipitation index, its potential cause and implications to future climate change in the Amazon region*. Philosophical Transactions of the Royal Society B: Biological Sciences, v. 363, p. 1767.

Livada, I., and Assimakopoulos, V., 2007. Spatial and temporal analysis of drought in Greece using the Standardized Precipitation Index (SPI). Theoretical and applied climatology, v. 89, p. 143-153.

Lu, J., Carbone, G.J. and Gao, P., 2017. *Detrending crop yield data for spatial visualization of drought impacts in the United States, 1895–2014*. Agricultural and Forest Meteorology, v. 237, p.196-208.

Lyon, B., and Barnston, A., 2005. *ENSO and the Spatial Extent of Interannual Precipitation Extremes in Tropical Land Areas*. Journal of Climate, v. 18, p. 5095-5109.

MARD, 2004. *Land use/cover classification of Ethiopia*. Woody biomass project Ministry of Agriculture and Rural Development, Addis Ababa, Ethiopia.

MathWorks, 2009. *MATLAB Neural Network Toolbox User's Guide*. The MathWorks, Inc., Natick, MA.

McKee, T.B., Doesken, N.J., and Kleist, J., 1993. *The relationship of drought frequency and duration to time scales*. Proceedings of the 8th Conference on Applied Climatology, American Meteorological Society Boston, MA, v. 17, p. 179-183.

—, 1995. *Drought monitoring with multiple time scales.* In Proceedings of the 9th Conference of Applied Climatology, 15-20 January, Dallas TX. American Meteorological Society, Boston, MA. p. 233–236.

Mengistu, D., and Sorteberg, A., 2011. *Validation of SWAT simulated streamflow in the Eastern Nile and sensitivity to climate change*. Hydrology and Earth System Sciences Discussions, v. 8, p. 9005-9062.

Mishra, A.K., and Singh, V.P., 2010. *A review of drought concepts*. Journal of hydrology, v. 391, p. 202-216.

Monteith, J., 1965. *Evaporation and environment*. Symp. Soc. Exp. Biol, v. 19, p. 4.

Moreira, E.E., Coelho, C.A., Paulo, A.A., Pereira, L.S., and Mexia, J.T., 2008. *SPI-based drought category prediction using loglinear models*. Journal of Hydrology, v. 354, p. 116-130.

Morid, S., Smakhtin, V., and Moghaddasi, M., 2006. *Comparison of seven meteorological indices for drought monitoring in Iran*. International journal of climatology, v. 26, p. 971-985.

Nalbantis, I., and Tsakiris, G., 2008. *Assessment of hydrological drought revisited*. Water Resources Management, v. 23, No. 5, p. 881–897.

Narasimhan, B., and Srinivasan, R., 2005. *Development and evaluation of Soil Moisture Deficit Index (SMDI) and Evapotranspiration Deficit Index (ETDI) for agricultural drought monitoring*. Agricultural and Forest Meteorology, v. 133, p. 69-88.

Naumann, G., Dutra, E., Barbosa, P., Pappenberger, F., Wetterhall, F., and Vogt, J.V., 2014. *Comparison of drought indicators derived from multiple data sets over Africa*. Hydrology and Earth System Sciences, v. 18, No. 5, p.1625-1640.

Narasimhan, B., Srinivasan, R., Arnold, J., and Di Luzio, M., 2005. *Estimation of long-term soil moisture using a distributed parameter hydrologic model and verification using remotely sensed data*. Transactions of the ASAE, v. 48, p. 1101-1113.

Niemeyer, S., 2008. *New drought indices.* Water Management. v. 80, p. 267-274.

Palmer, W., 1968. *Keeping track of crop moisture conditions, nationwide: The new Crop Moisture Index*. Weather wise v. 21, p. 156–161.

Okpara, J.N., and Tarhule, A., 2015. *Evaluation of Drought Indices in the Niger Basin, West Africa*. Journal of Geography, v. 3, No. 2, p.1-32.

Patel, N., Chopra, P., and Dadhwal, V., 2007. *Analyzing spatial patterns of meteorological drought using standardized precipitation index*. Meteorological Applications, v. 14, p. 329-336.

Ramakrishna, G., and Assefa, D., 2002. *An emperical analysis of food insecurity in ethiopia, the case of North Wello*. Africa Development, v. 27, p. 127-143.

Saha, S., Moorthi, S., Pan, H., Wu, X., Wang, J., Nadiga, S., Tripp, P., Kistler, R., Woollen, J., and Behringer, D., 2011. *The NCEP climate forecast system reanalysis*. Bull. Am. Meteorol. Soc. v. 1, p. 1–146.

Sathyendranath, S., Ahanhanzo, J., Bernard, S., Byfield, V., Delaney, L., Dowell, M., Field, J., and Groom, S., Hardman-Mountford, N., and Hoepffner, N., 2009. *ChloroGIN: Use of satellite and in situ data in support of ecosystem-based management of marine resources.* Proceedings of Ocean Observations 09, Sustained Ocean Observations and Information for Society Conference, Volume 1.

Schaaf, C.B., Gao, F., Strahler, A.H., Lucht, W., Li, X., Tsang, T., Strugnell, N.C., Zhang, X., Jin, Y., and Muller, J.-P., 2002. *First operational BRDF, albedo nadir reflectance products from MODIS*. Remote Sensing of Environment, v. 83, p. 135-148.

Sepulcre, G., Horion, S.F., Singleton, A., Carrao, H., and Vogt, J., 2012. *Development of a Combined Drought Indicator to detect agricultural drought in Europe*. Natural Hazards and Earth System Sciences, v. 12, p. 3519-3531.

Setegn, S.G., Srinivasan, R., and Dargahi, B., 2008. *Hydrological modelling in the Lake Tana Basin, Ethiopia using SWAT model*. The Open Hydrology Journal, v. 2, p. 49-62.

Shafer, B.A. and Dezman, L., 1982. *Development of a Surface Water Supply Index (SWSI) to assess the severity of drought conditions in snowpack runoff areas*. Proceedings of the Western Snow Conference, Colorado State University, Fort Collins, CO, p. 164–175.

Sharma, M.A., and Singh, J.B., 2010. *Use of probability distribution in rainfall analysis*. New York Science Journal, v. 3, p. 40-49.

Sheffield, J., and Wood, E.F., 2012. *Drought: Past problems and future scenarios,* Routledge.

Shepard, D., 1968. *A two-dimensional interpolation function for irregularly-spaced data*. Proceedings of the 1968 ACM National Conference. p. 517–524.

Shukla, S., and Wood, A.W., 2008. *Use of a standardized runoff index for characterizing hydrologic drought*. Geophysical Research Letters, v. 35, No. 2.

Sims, D.A., Rahman, A.F., Cordova, V.D., El-Masri, B.Z., Baldocchi, D.D., Bolstad, P.V., Flanagan, L.B., Goldstein, A.H., Hollinger, D.Y., and Misson, L., 2008. *A new model of gross primary productivity for North American ecosystems based solely on the enhanced vegetation index and land surface temperature from MODIS*. Remote Sensing of Environment, v. 112, p. 1633-1646.

Sivakumar, M.K., Motha, R. P., Wilhite, D. A., and Wood, D. A., 2011. *Agricultural Drought Indices*. Proceedings of an Expert meeting. p. 219.

Sönmez, F.K., Koemuescue, A.U., Erkan, A., and Turgu, E., 2005. *An analysis of spatial and temporal dimension of drought vulnerability in Turkey using the standardized precipitation index*. Natural Hazards, v. 35, p. 243-264.

Svoboda, M., LeComte, D., Hayes, M., Heim, R., Gleason, K., Angel, J., Rippey, B., Tinker, R., Palecki, M., Stooksbury, D., and Miskus, D., 2002. *The drought monitor*. Bulletin of the American Meteorological Society, v. 83, No. 8, p.1181-1190.

Tadesse, T., Senay, G.B., Berhan, G., Regassa, T., and Beyene, S., 2015. *Evaluating a satellite-based seasonal evapotranspiration product and identifying its relationship with other satellite-derived products and crop yield: A case study for Ethiopia*. International Journal of Applied Earth observation and Geoinformation, v.40, p. 39-54.

Tagel, G., van der Veen, A., and Maathuis, B., 2011. *Spatial and temporal assessment of drought in the Northern highlands of Ethiopia*. International Journal of Applied Earth observation and Geoinformation, v. 13, p. 309-321.

Tekleab, S., Mohamed, Y., and Uhlenbrook, S., 2013. *Hydro-climatic trends in the Abay/Upper Blue Nile basin, Ethiopia*. Physics and Chemistry of the Earth, Parts A/B/C, v. 61, p. 32-42.

Trambauer, P., Maskey, S., Werner, M., Pappenberger, F., Van Beek, L., and Uhlenbrook, S., 2014. *Identification and simulation of space-time variability of past hydrological drought events in the Limpopo river basin, Southern Africa*. Hydrology and Earth System Sciences, v. 18, No. 8, p.2925.

Vicente-Serrano, S.M., Beguería, S., and López-Moreno, J.I., 2010. *A multiscalar drought index sensitive to global warming. the standardized precipitation evapotranspiration index.* Journal of Climate, v. 23, p. 1696-1718.

Viste, E., Korecha, D., and Sorteberg, A., 2013. *Recent drought and precipitation tendencies in Ethiopia*. Theoretical and Applied Climatology, v. 112, No. 3-4, p.535-551.

Vyas, S.S., Bhattacharya, B.K., Nigam, R., Guhathakurta, P., Ghosh, K., Chattopadhyay, N., and Gairola, R., 2015. *A combined deficit index for regional agricultural drought assessment over semi-arid tract of India using geostationary meteorological satellite data*. International Journal of Applied EEarth observation and Geoinformation, v. 39, p. 28-39.

Wagaw, M., Coleman, T.L., Tsegaye, T.D., and Tadesse, W., 2005. *GIS implementation to support poverty reduction policy and drought management in Ethiopia*. In Proceeding of the United Nations Economic Commission for Africa Committee for Development Information (UNECCODI) IV. April 22-30. Addis Ababa, Ethiopia.

Wang, J.S., Li, Y.P., Ren, Y.L., and LIU, Y.P., 2013. *Comparison among several drought indices in the Yellow River valley*. J. Nat. Resour, v. 28, No. 8, p.1337.

Weghorst, K., 1996. *The Reclamation Drought Index: guidelines and practical applications*. In North American Water and Environment Congress & Destructive Water, ASCE, p. 637-642.

Wilhite, D., and Buchanan-Smith, M., 2005. *Drought as hazard: understanding the natural and social context*. Drought and Water Crises–Science, Technology and Management issues, Taylor & Francis, ISBN 0, v. 847, p. 1.

Wilhite, D.A., 2000. *Drought as a natural hazard: concepts and definitions*. Drought, a global assessment, v. 1, p. 3-18.

Wilhite, D.A., Svoboda, M.D., and Hayes, M.J., 2007. *Understanding the complex impacts of drought: a key to enhancing drought mitigation and preparedness*. Water Resources Management, v. 21, p. 763-774.

Willeke, G., Hosking, J., Wallis, J., and Guttman, N., 1994. *The National Drought Atlas*. Institute for Water Resources Report 94–NDS–4, U.S. Army Corps of Engineers.

Wu, H., Svoboda, M.D., Hayes, M.J., Wilhite, D.A., and Wen, F., 2007. *Appropriate application of the standardized precipitation index in arid locations and dry seasons*. International Journal of Climatology, v. 27, p. 65-79.

Wu, Z., Huang, N.E., Long, S.R., and Peng, C.K., 2007. *On the trend, detrending, and variability of nonlinear and nonstationary time series*. Proc. Natl. Acad. Sci. v. 104, No. 38, p. 14889–14894.

Yamoah, C., Walters, D., Shapiro, C., Francis, C., and Hayes, M., 2000. *Standardized precipitation index and nitrogen rate effects on crop yields and risk distribution in maize*. Agriculture, ecosystems & environment, v. 80, p. 113-120.

Yilma, A.D., and Awulachew, S.B., 2009. *Characterization and atlas of the Blue Nile Basin and its sub basins*.

Yue, S., Pilon, P., and Cavadias, G., 2002. *Power of the Mann–Kendall and Spearman's rho tests for detecting monotonic trends in hydrological series*. Journal of Hydrology, v. 259, p. 254-271.

Zargar, A., Sadiq, R., Naser, B. and Khan, F.I., 2011. *A review of drought indices*. Environmental Reviews, v. 19, p.333-349.

Zhuo, W., Huang, J., Zhang, X., Sun, H., Zhu, D., Su, W., Zhang, C., and Liu, Z., 2016, July. *Comparison of five drought indices for agricultural drought monitoring and impacts on winter wheat yields analysis*. In Agro-Geoinformatics , Fifth International Conference, IEEE, p. 1-6.

Appendix A: Gamma distribution based SPI calculation.

The gamma distribution is defined by its frequency or probability density function:

$$g(x) = \frac{1}{\beta^{\alpha}\Gamma(\alpha)} \int_0^x x^{\alpha-1} e^{\frac{-x}{\beta}} \qquad 2.1$$

where $\alpha > 0$ is the shape parameter, $\beta > 0$ is a scale parameter and $x > 0$ is the amount of precipitation. $\Gamma(\alpha)$ defines the gamma functions.

Fitting the distribution to the data requires α and β being estimated using the approximation of Thom for maximum likelihood as stated in Edwards and McKee, (1997) as follows

$$\hat{\alpha} = \frac{1}{4A}\left(1 + \sqrt{1 + \frac{4A}{3}}\right) \qquad 2.2$$

Where, for n observations

$$A = \ell n(\bar{x}) - \frac{\sum \ln(x)}{n} \qquad 2.3$$

$$\hat{\beta} = \frac{\bar{x}}{\hat{\alpha}} \qquad 2.4$$

G(x) = Cumulative probability excluding probability of zero precipitation

$$G(x) = \int_o^x g(x)dx = \frac{1}{\hat{\beta}^{\hat{\alpha}}\,\Gamma(\alpha)} \int_0^x x^{\alpha} e^{\frac{-x}{\hat{\beta}}} dx \qquad 2.5$$

H(x) = Cumulative Probability including probability of zero precipitation

$$H(x) = q + (1-q)\,G(x) \qquad 2.6$$

q= is the probability of zero precipitation where gamma distribution becomes undefined

For X=0 and q = p (x=0) (probability of zero precipitation is simply the number of observations of zero precipitation divided by the total number of observations).

To convert cumulative probability to the standard normal random variable Z:

$$Z = SPI = -\left(t - \frac{c_0 + c_1 t + c_2 t^2}{1 + d_1 t + d_2 t^2 + d_3 t^3}\right) \quad \text{for } 0 < H(x) \le 0.5 \qquad 2.7$$

$$Z = SPI = + \left(t - \frac{c_0 + c_1 t + c_2 t^2}{1 + d_1 t + d_2 t^2 + d_3 t^3} \right) \quad \text{for } 0.5 < H(x) \leq 1 \qquad 2.8$$

where: $$t = \sqrt{\ln\left(\frac{1}{(H(X))^2} \right)} \quad \text{for } 0 < H(x) \leq 0.5 \qquad 2.9$$

$$t = \sqrt{\ln\left(\frac{1}{(1 - H(X))^2} \right)} \quad \text{for } 0.5 < H(x) \leq 1 \qquad 2.10$$

c_0 = 2.515517, c_1 = 0.802853, c_2 = 0.010328, d_1 = 1.432788, d_2 = 0.189269,

d_3 = 0.001308

Appendix B: Time series of drought indices.

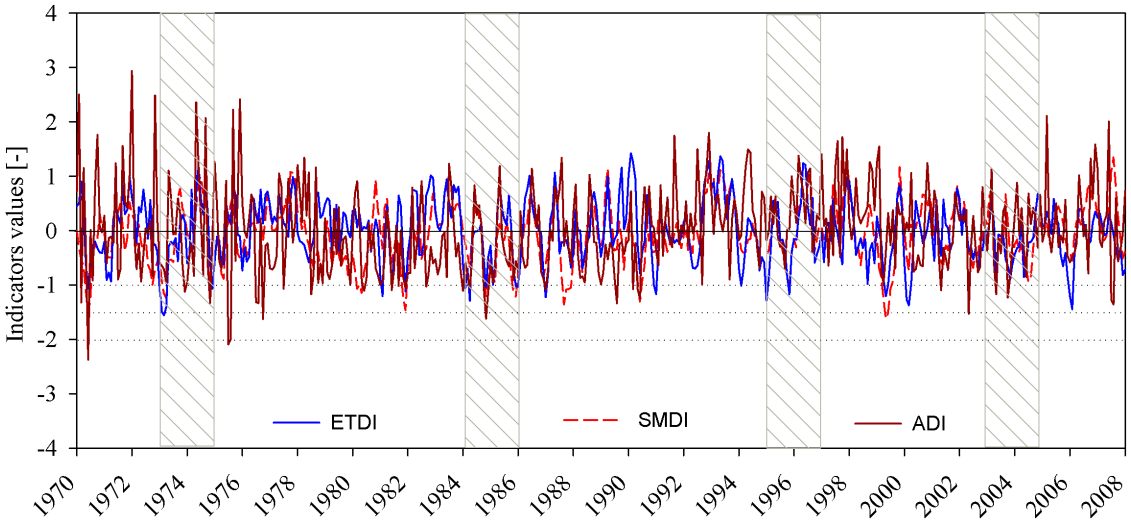

Figure B-1: Time series plot of agricultural drought indices for the area upstream of Abbay at Kessie station and downstream of Lake Tana outlet.

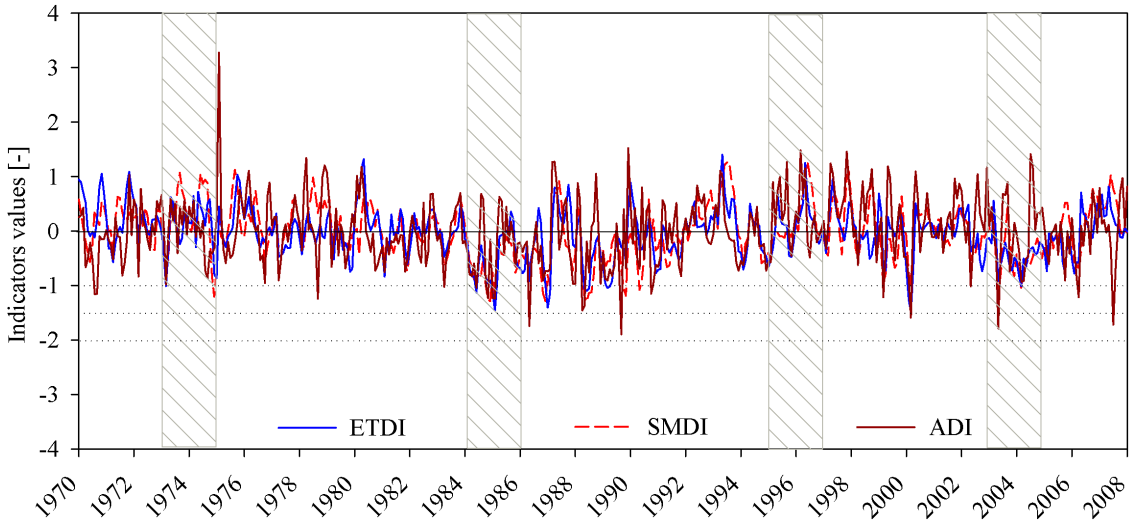

Figure B-2: Time series plot of agricultural drought indices for the area upstream of Abbay at Ethio-Sudana border and downstream of Kessie station.

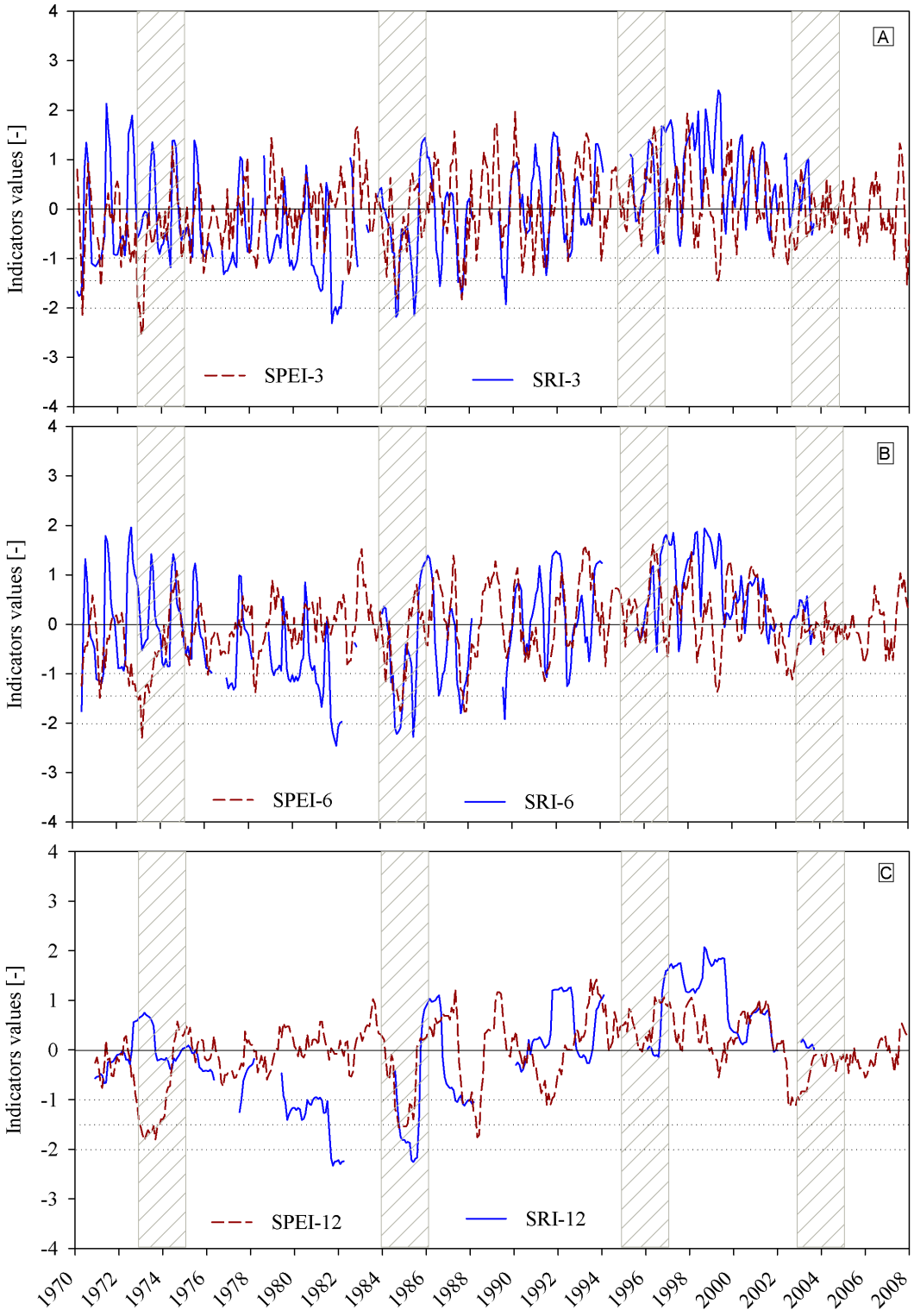

Figure B-3: Time series plots of the meteorological (SPEI) and hydrological (SRI) drought indices at 3 (A), 6 (B) and 12 months (C) time scales for the area upstream of Abbay at Kessie station and downstream of Lake Tana outlet.

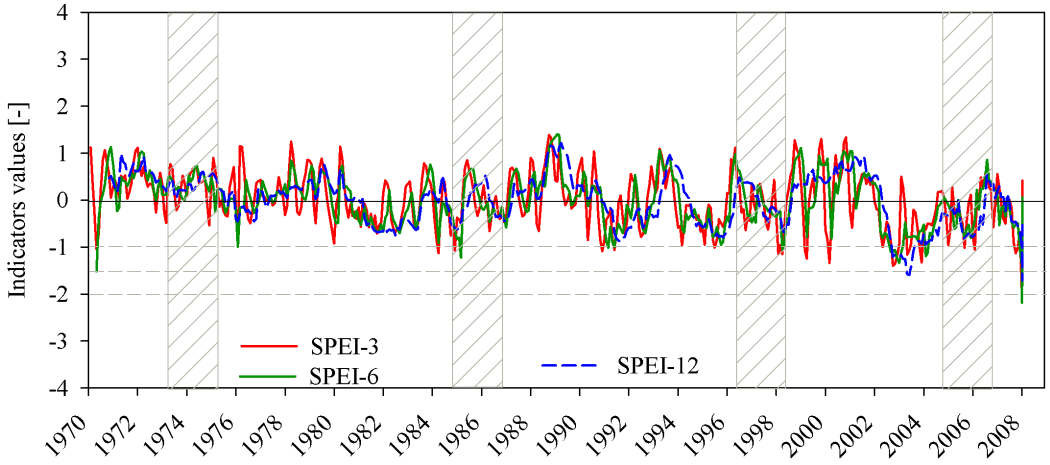

Figure B-4: Time series plots of the meteorological (SPEI) drought index at 3, 6 and 12 months time scales for the area upstream of Abbay at Ethio-Sudan border station and downstream of Kessie station.

Appendix C: Spider web plots of drought indicator results for selected stations.

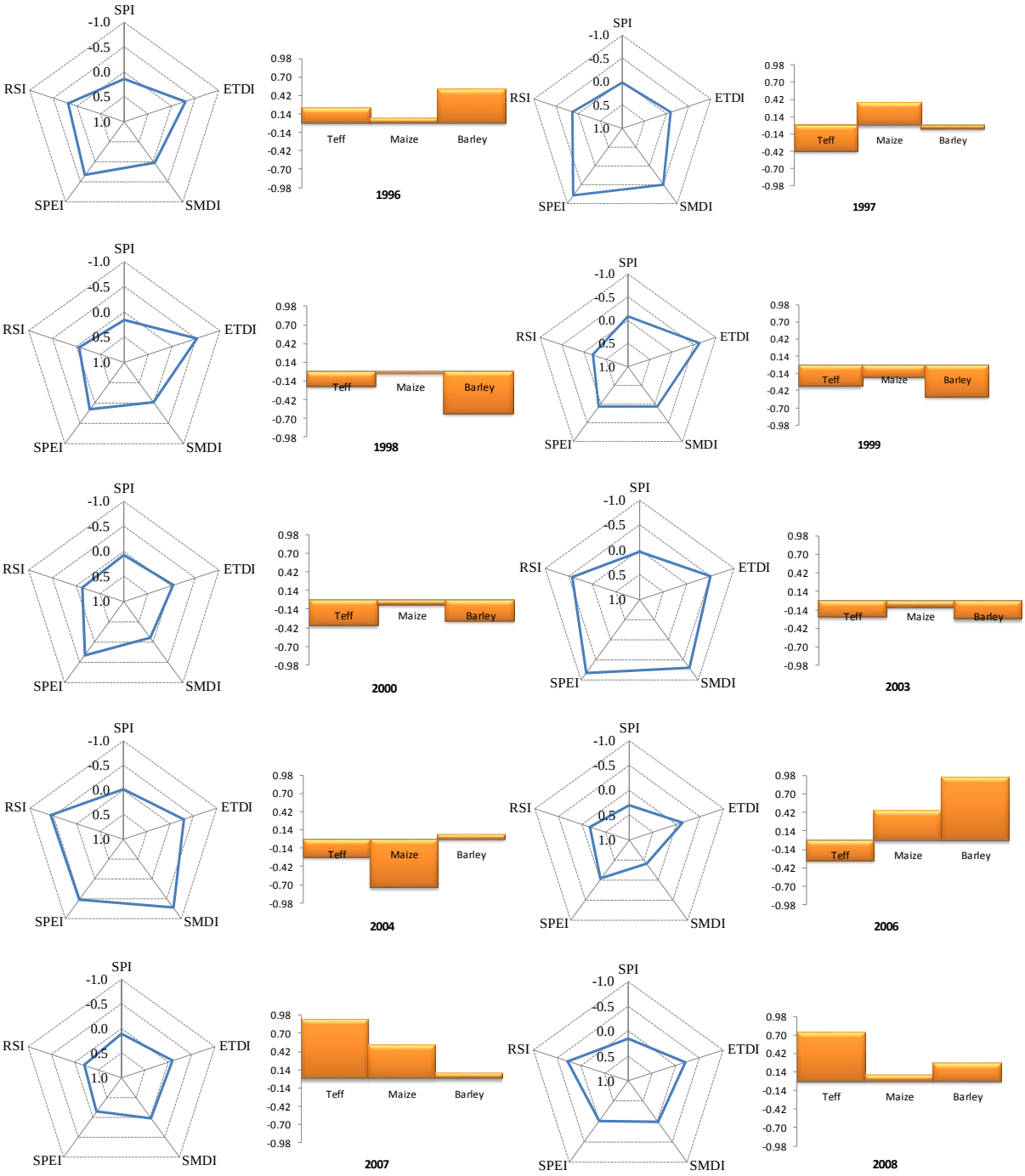

Figure C-1: The radar and bar plots show the minimum drought indices values within the crop growing period (June to October) and the anomaly of the crop yield of four crops (bar graph) at the Bahirdar station.

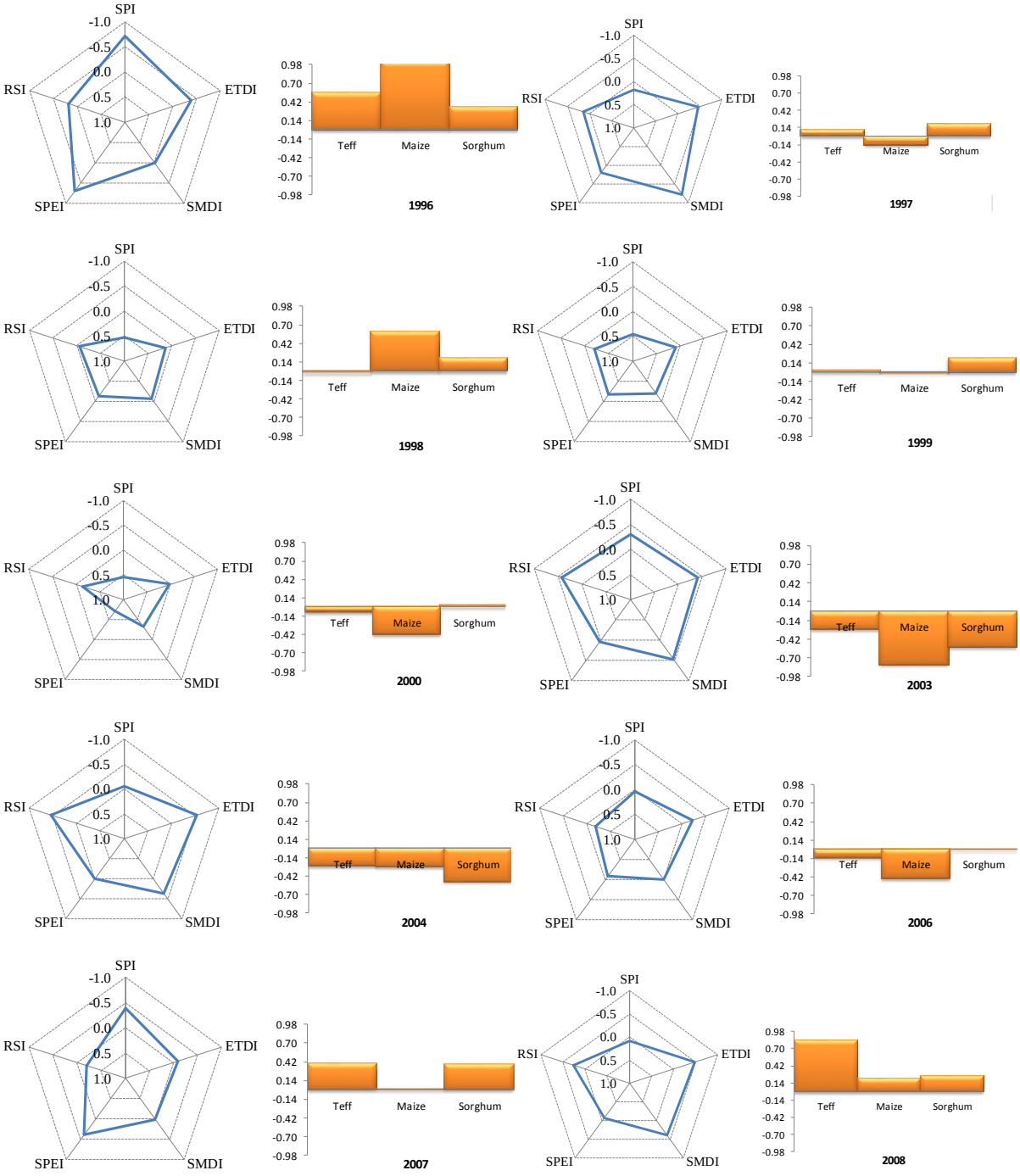

Figure C-2: The radar and bar plots show the minimum drought indices values within the crop growing period (June to October) and the anomaly of the crop yield of four crops (bar graph) at the Assossa station.

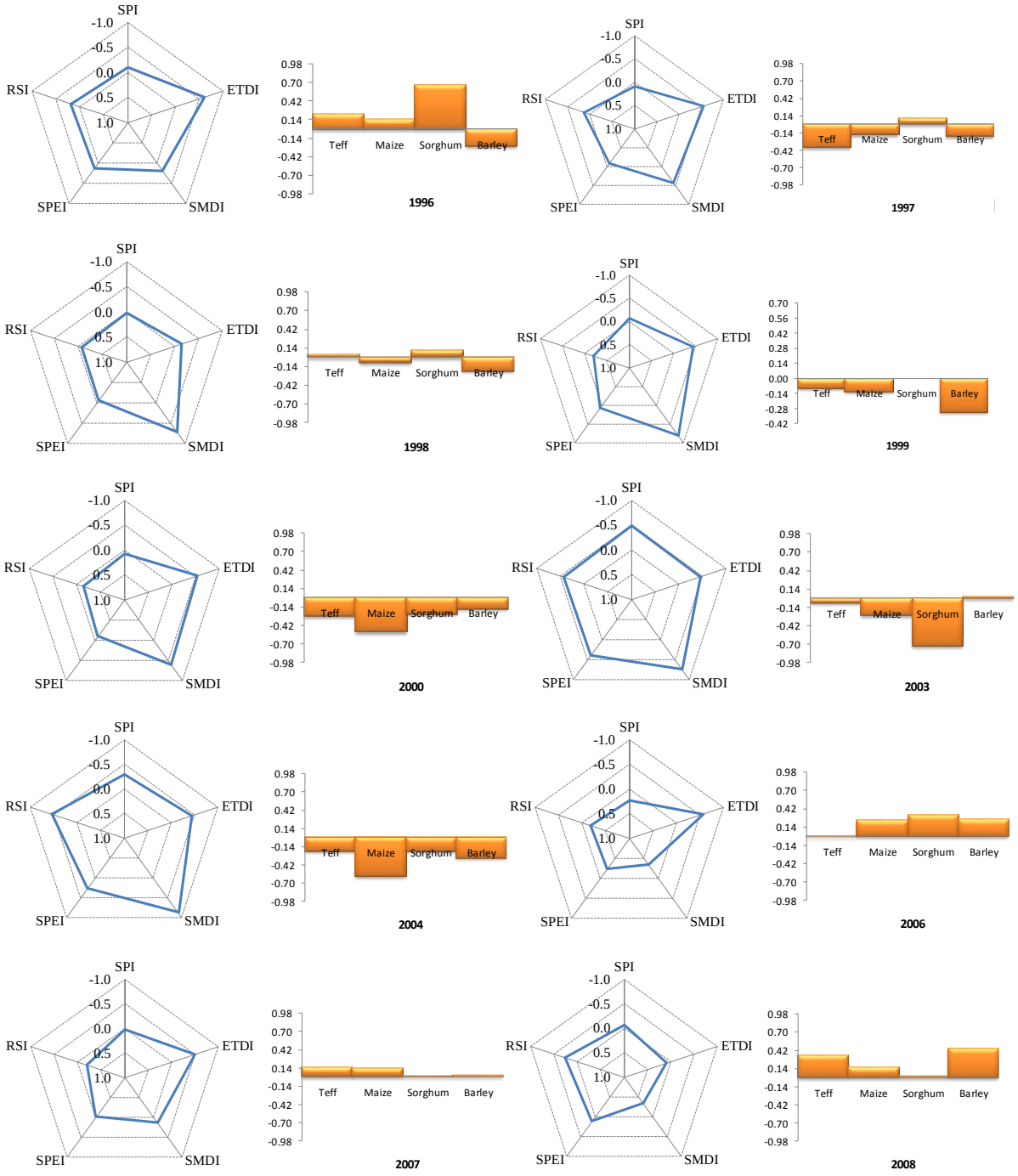

Figure C-3: The radar and bar plots show the minimum drought indices values within the crop growing period (June to October) and the anomaly of the crop yield of four crops (bar graph) at the Debretabor station.

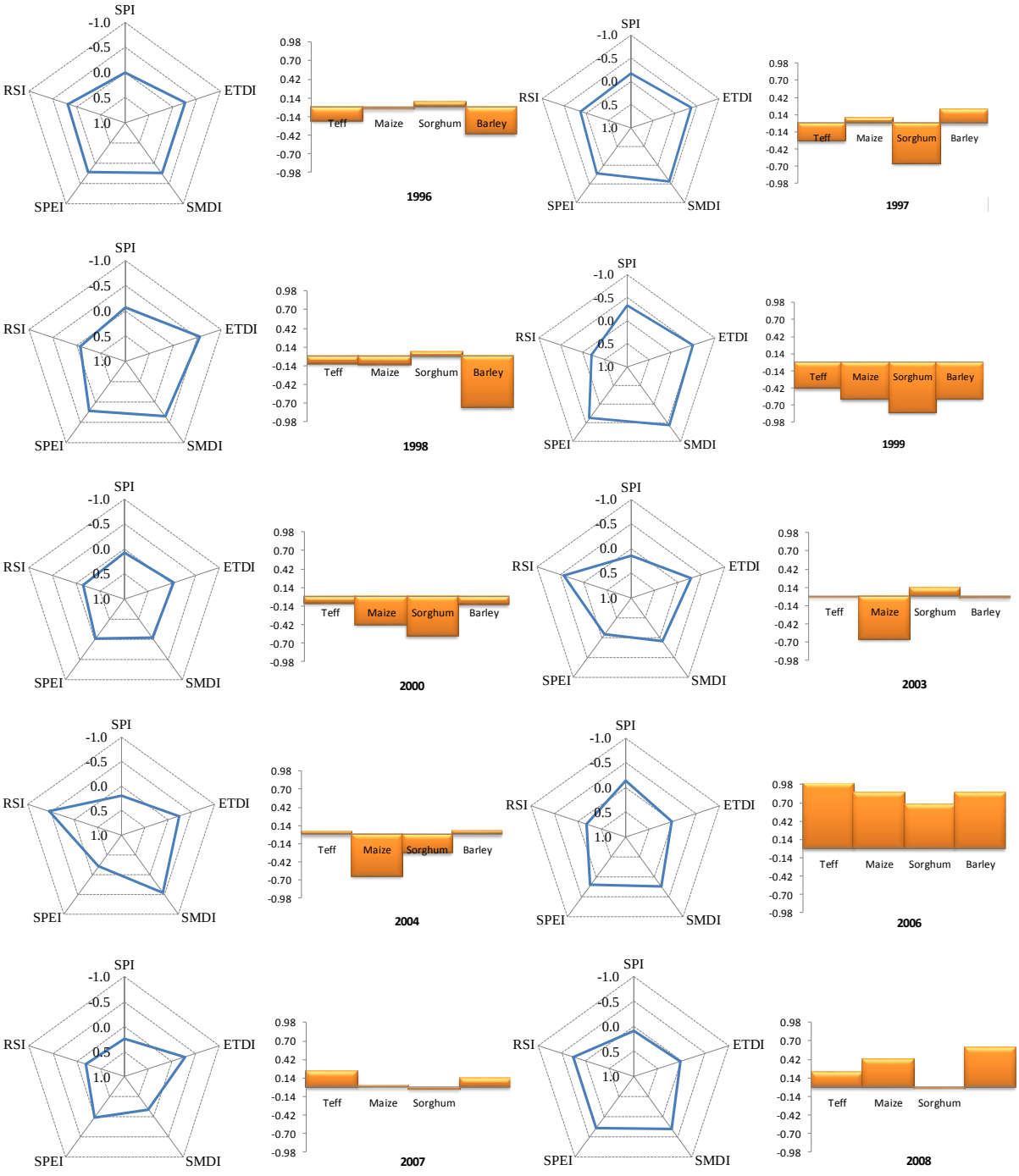

Figure C-4: The radar and bar plots show the minimum drought indices values within the crop growing period (June to October) and the anomaly of the crop yield of four crops (bar graph) at the Debrebirhan station.

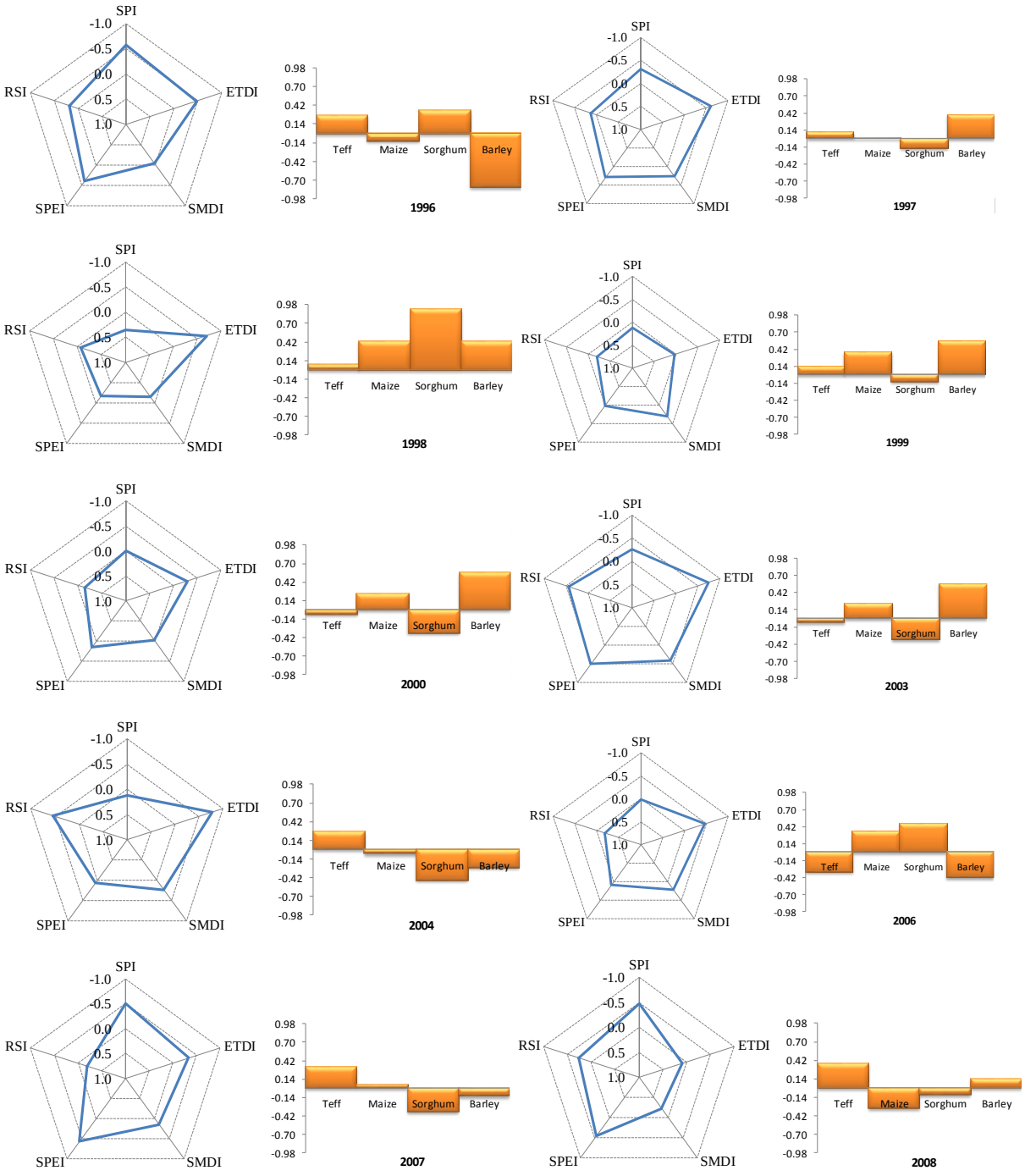

Figure C-5: The radar and bar plots show the minimum drought indices values within the crop growing period (June to October) and the anomaly of the crop yield of four crops (bar graph) at the Gidayana station.

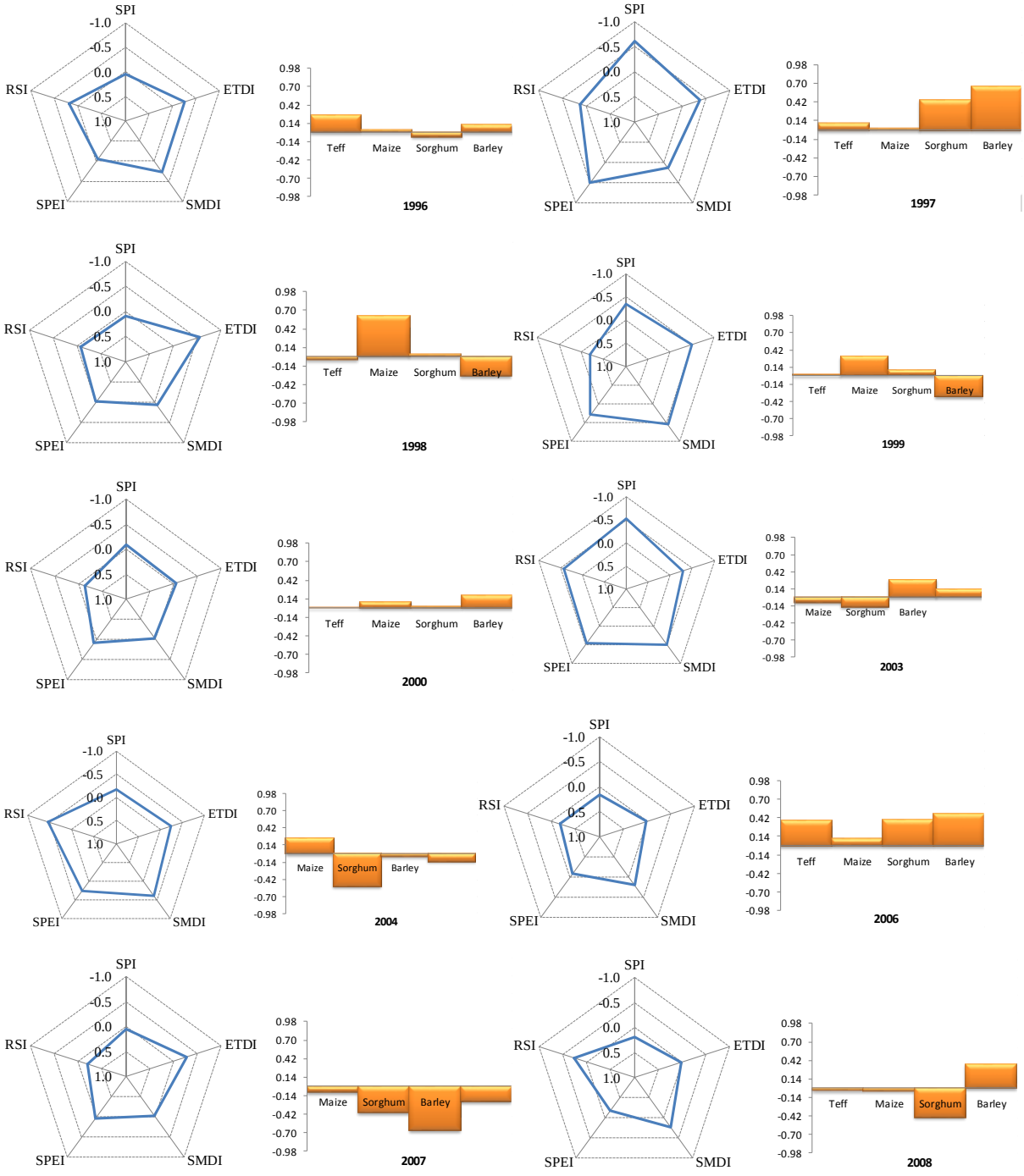

Figure C-6: The radar and bar plots show the minimum drought indices values within the crop growing period (June to October) and the anomaly of the crop yield of four crops (bar graph) at the Ambo station.

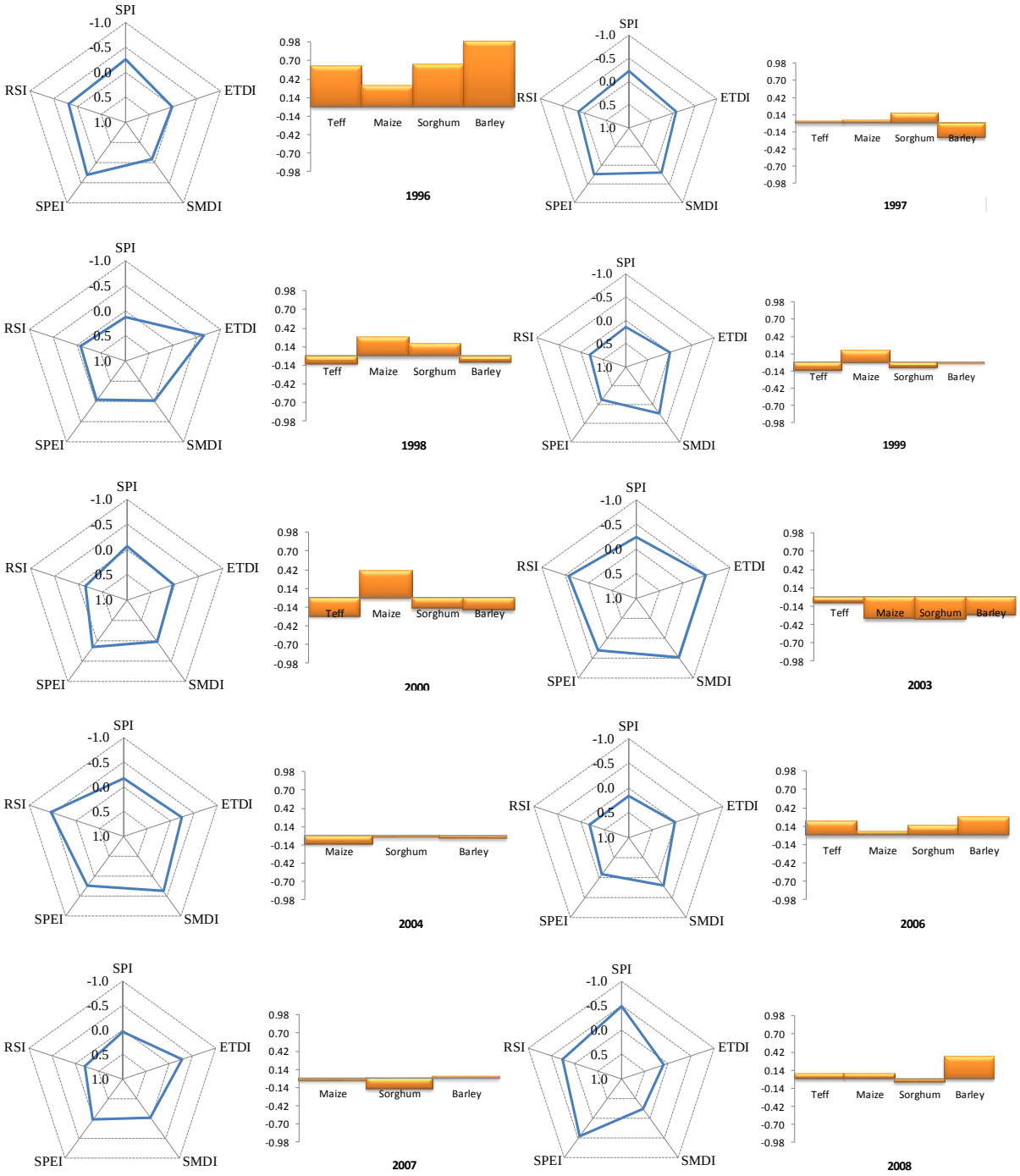

Figure C-7: The radar and bar plots show the minimum drought indices values within the crop growing period (June to October) and the anomaly of the crop yield of four crops (bar graph) at the Bedele station.

Appendix D: Scatter plots of drought indices versus crop yield anomalies.

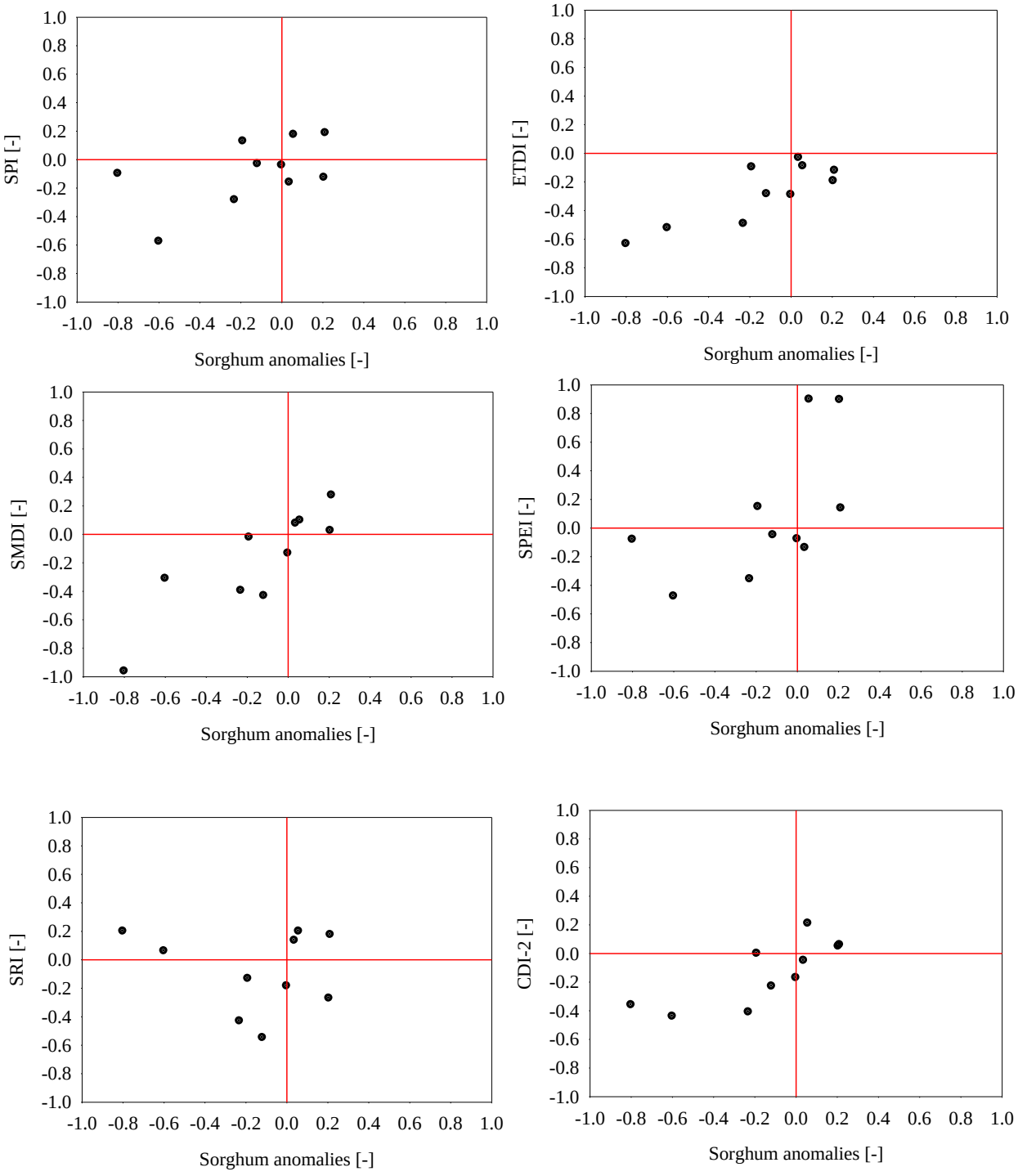

Figure D-1: Scatter plot of individual drought indices versus the Sorghum crop yield anomalies. The CDI-2 was computed using the impact-based approach.

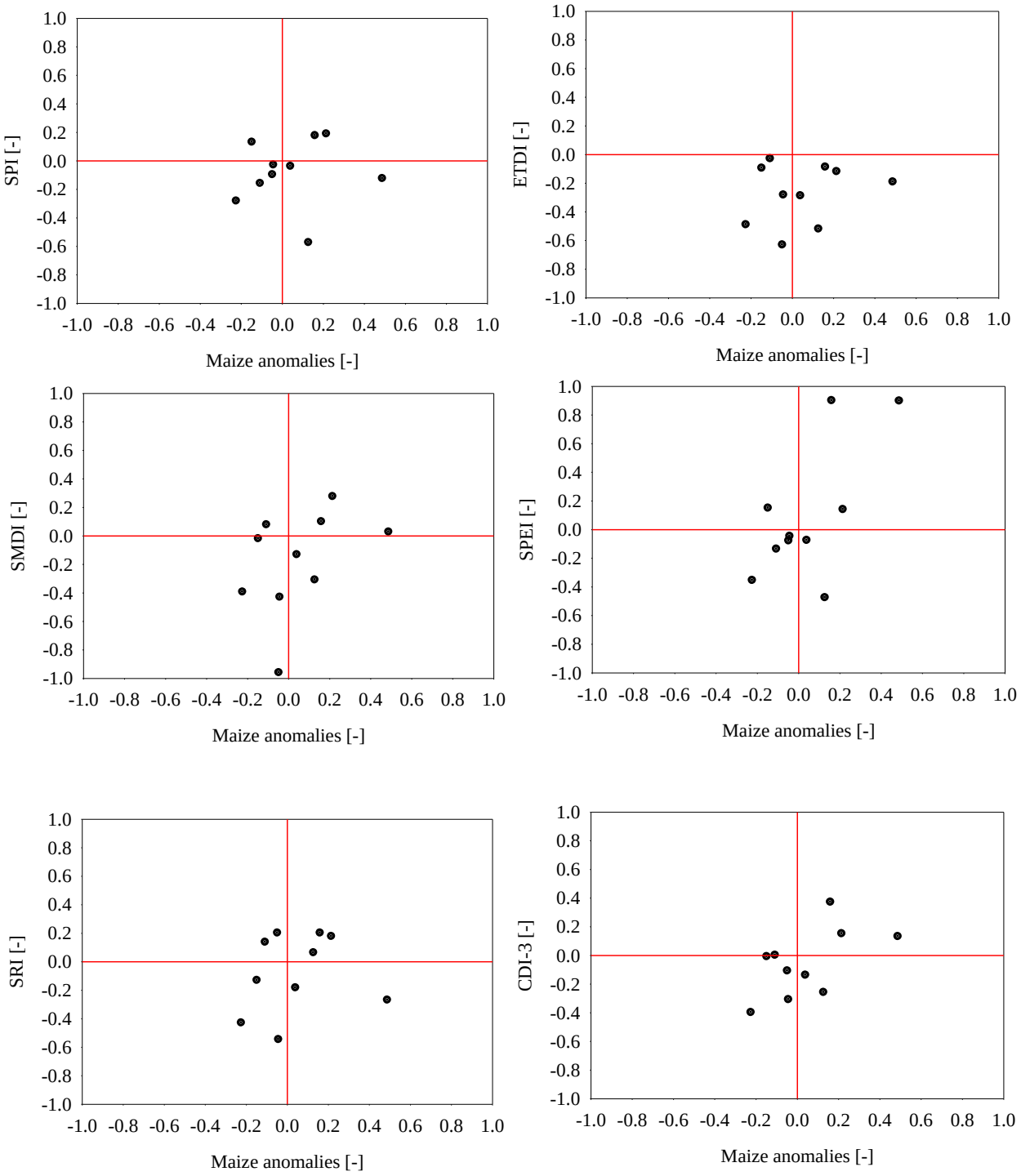

Figure D-2: Scatter plot of individual drought indices versus the Maize crop yield anomalies. CDI-3 compute using the impact-based approach.

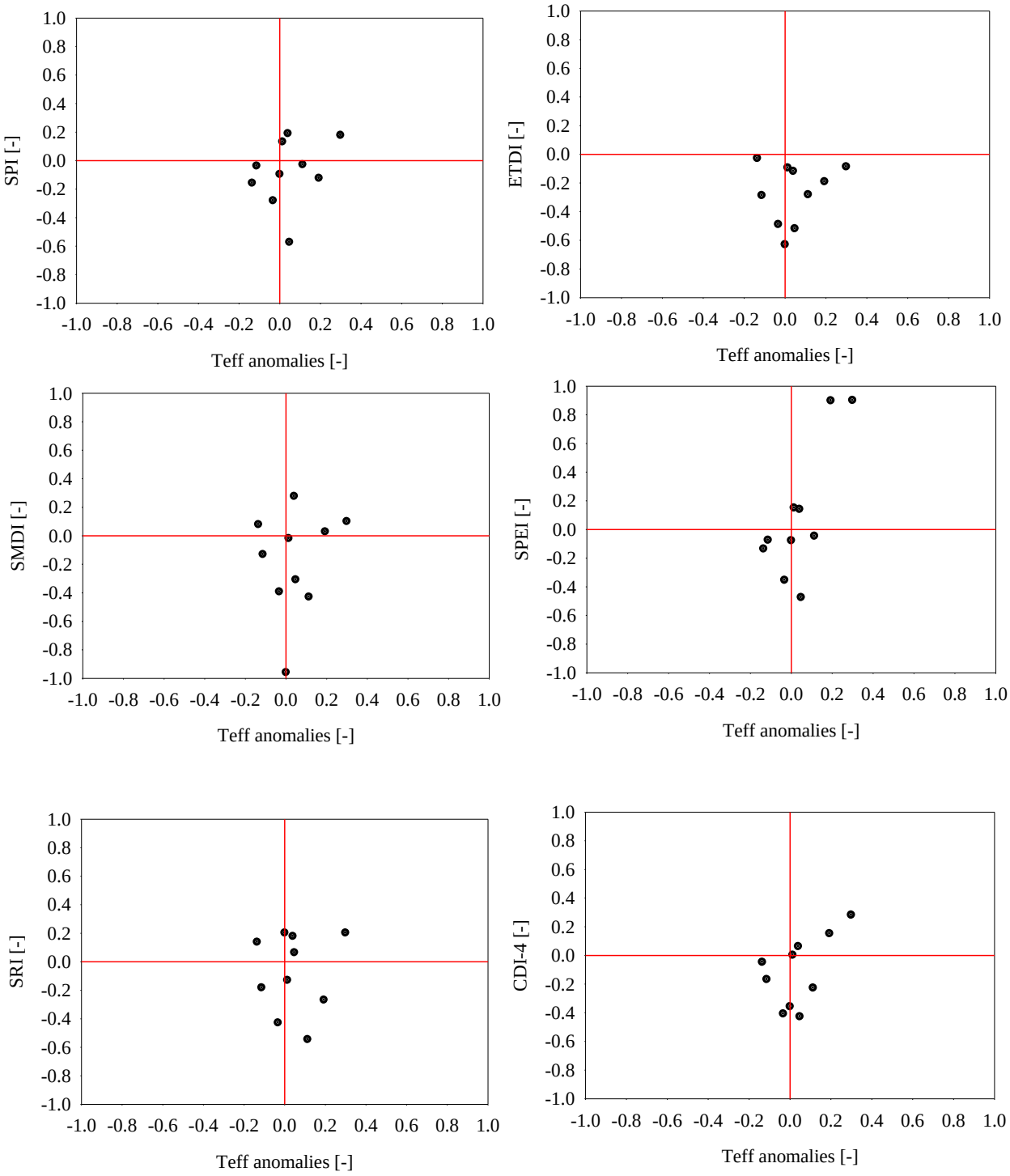

Figure D-3: Scatter plot of individual drought indices versus the Teff crop yield anomalies. CDI-4 was computed using the impact-based approach.

Appendix E: The regression equations developed for the selected eight zones and for the four crops.

Zones Name	Representative Stations	Crops	Regression Equations
East Gojjam	Debremarkos	Teff	*= 0.01*SPI - 0.52*ETDI + 0.07*SMDI + 0.23*SPEI - 0.05*SRI - 0.10*
		Maize	*= -0.67*SPI - 2.39*ETDI + 1.36*SMDI + 0.78*SPEI + 0.36*SRI - 0.52*
		Sorghum	*= 0.52*SPI + 0.29*ETDI + 0.07*SMDI + 0.16*SPEI + 0.56*SRI + 0.15*
		Barley	*= 0.32*SPI - 0.14*ETDI + 0.37*SMDI + 0.13*SPEI - 0.36*SRI + 0.11*
West Gojjam	Bahirdar	Teff	*= 0.27*SPI + 0.285*ETDI - 0.473*SMDI + 0.435*SPEI - 0.083*SRI + 0.479*
		Maize	*= 0.289*SPI + 0.14*ETDI - 0.244*SMDI + 0.0.114*SPEI+0.084*SRI + 0.234*
		Sorghum	*= 0.377*SPI + 0.3144*ETDI - 0.035*SMDI + 0.0.122*SPEI - 0.204*SRI + 0.215*
North Gondar	Gondar	Teff	*= 0.416*SPI -0.104*ETDI + 0.933*SMDI + 0.0013SPEI- 0.0784*SRI + 0.033*
		Maize	*= 0.538*SPI -0.36*ETDI + 0.286*SMDI - 0.18SPEI -0.106*SRI + 0.043*
		Sorghum	*= 0.482*SPI -10.19*ETDI + 10.03*SMDI - 0.159*SPEI -0.083*SRI - 0.0556*
		Barley	*= 0.74*SPI -0.82*ETDI + 0.91*SMDI - 0.491*SPEI -0.013*SRI - 0.007*
Assossa	Assossa	Teff	*= 0.006*SPI - 0.828*ETDI + 0.194*SMDI + 0.107*SPEI + 0.399*SRI - 0.059*
		Maize	*= 0.082*SPI - 0.117*ETDI + 0.153*SMDI - 0.023*SPEI + 0.023*SRI - 0.024*
		Sorghum	*= 0.0025*SPI - 0.27*ETDI + 0.082*SMDI - 0.024*SPEI + 0.191*SRI - 0.0283*
South Gondar	Debretabor	Teff	*= -0.0618*SPI + 0.181*ETDI + 0.201*SMDI - 0.256*SPEI + 0.144*SRI + 0.226*
		Maize	*= -0.375*SPI + 0.123*ETDI + 0.265*SMDI + 0.142*SPEI + 0.143*SRI + 0.307*
		Sorghum	*= -0.33*SPI - 0.00017*ETDI + 0.338*SMDI + 0.693*SPEI - 0.298*SRI + 0.251*
		Barley	*= -0.789*SPI + 0.151*ETDI + 0.242*SMDI + 0.697*SPEI + 0.044*SRI + 0.217*
North Shoa	Debrebirhan	Teff	*= 0.313*SPI + 0.512*ETDI - 0.345*SMDI + 0.048*SPEI + 0.21*SRI + 0.324*
		Maize	*= 0.741*SPI + 0.396*ETDI - 0.522*SMDI - 0.228*SPEI + 0.315*SRI - 0.031*
		Sorghum	*= 0.225*SPI + 0.202*ETDI - 0.063*SMDI - 0.096*SPEI + 0.038*SRI + 0.032*
		Barley	*= 0.198*SPI + 0.684*ETDI - 0.231*SMDI + 0.002*SPEI + 0.082*SRI + 0.358*
East Wellega	Gidayana	Teff	*= 0.266*SPI + 0.209*ETDI + 0.22*SMDI - 0.417*SPEI - 0.078*SRI - 0.069*
		Maize	*= 0.129*SPI + 0.042*ETDI + 0.045*SMDI - 0.132*SPEI + 0.044*SRI + 0.008*
		Sorghum	*= 0.133*SPI - 0.037*ETDI + 0.187*SMDI - 0.158*SPEI + 0.037*SRI - 0.077*
		Barley	*= 0.737*SPI + 0.283*ETDI + 0.155*SMDI - 0.856*SPEI + 0.0041*SRI - 0.088*
West Shoa	Ambo	Maize	*= 0.035*SPI + 0.038*ETDI - 0.06*SMDI + 0.0045*SPEI + 0.045*SRI + 0.005*
		Sorghum	*= 0.329*SPI + 0.317*ETDI + 0.504*SMDI - 0.452*SPEI - 0.20*SRI + 0.059*
		Barley	*= 0.0937*SPI + 0.541*ETDI + 0.023*SMDI - 0.181*SPEI + 0.0012*SRI + 0.199*

Samenvatting

Droogte is een indringende natuurramp die zich langzaam ontwikkelt en een groot gebied treft. In tegenstelling tot andere natuurrampen zoals overstromingen en tornado's, manifesteren de gevolgen van droogte zich niet direct. Dit maakt het moeilijker om droogte te monitoren en negatieve effecten tegen te gaan door er in een vroeg stadium voor te waarschuwen.

Er bestaan verschillende indices voor droogtemonitoring. Op zichzelf kan een dergelijke index geen geïntegreerd beeld geven van zowel meteorologische, agrarische, als hydrologische droogtes. Een gecombineerde index (Combined Drought Index: CDI) waarin deze verschillende aspecten worden gecombineerd kan de verschillende typen droogte wel identificeren, en zo bruikbare informatie verschaffen ter ondersteuning van beslissingen over beheersmaatregelen. Daarnaast kan de ontwikkeling van een CDI zich toespitsen op een specifiek gevolg van droogte, bijvoorbeeld door de CDI te optimaliseren voor het monitoren van aan droogte gerelateerde vermindering van gewasopbrengst. In veel ontwikkelingslanden is de economie in grote mate afhankelijk van de landbouwproductie. Het ontwikkelen van methoden voor het monitoren en voorspellen van gewasopbrengst is zodoende voor deze landen van groot belang voor het bevorderen van economische groei.

In Ethiopië is droogte een regelmatig terugkerend verschijnsel. In de afgelopen eeuwen kwamen meer dan 30 droogtes voor, waarvan er 13 ernstig waren en het hele land (en buurlanden) troffen. Sommige studies laten zien dat de laatste decennia de frequentie waarmee droogte voorkomt in Ethiopië is toegenomen. Sinds 1970 is Ethiopië gemiddeld eens in de 10 jaar getroffen door ernstige droogte. Landbouw, de sector die meer dan 50% van het bruto nationaal product levert, is erg gevoelig voor droogte. De meeste landbouw in Ethiopië vindt plaats zonder beregening en is daarom voor een groot deel afhankelijk van de hoeveelheid en spreiding van jaarlijkse natuurlijke neerslag. Een tekort in jaarlijkse neerslag is vaak de voornaamste oorzaak van het optreden van droogte en heeft een afname van gewasopbrengst tot gevolg. Voor het verminderen van de negatieve gevolgen van droogte in Ethiopië, is de ontwikkeling van een robuust systeem voor droogtemonitoring cruciaal. Een dergelijk systeem ontbreekt nog altijd voor Ethiopië en in het bijzonder voor het stroomgebied van de Upper Blue Nile (UBN). Voor het UBN gebied is nog relatief weinig droogteonderzoek gedaan en er is geen gebiedsspecifiek droogtemonitoringssysteem, terwijl dit deelstroomgebied 60% van de totale hoeveelheid water aan de hoofdrivier van de Nijl bijdraagt. Daarom is de hoofddoelstelling van dit onderzoek een 'impact-based' gecombineerde droogte-index (impact-based CDI) en voorspellingsmodel te ontwikkelen voor afwijkende gewasopbrengsten in het

UBN stroomgebied. Onder een impact-based CDI wordt hier verstaan een index die de informatie in andere indices optimaal combineert voor het monitoren van een bepaald gevolg van droogte (in dit geval gewasopbrengst).

Om de hoofddoelstelling voor de UBN praktijkstudie te bereiken, moeten er drie terugkerende uitdagingen in het vakgebied van droogtemonitoring worden aangepakt. Ten eerste hebben verschillende meteorologische stations in het gebied een relatief korte meetreeks (minder dan 35 jaar). Het is daarom belangrijk het effect van de lengte van meetreeksen op beoordeling van droogtes te onderzoeken, om te kunnen beslissen of ook de stations met kortere meetreeksen gebruikt kunnen worden voor de analyse van temporele en ruimtelijke karakteristieken van droogtes in het gebied. De tweede uitdaging is dat er nog maar weinig studies zijn gepubliceerd over CDI's waarbij de gewichten van de individuele indices worden geoptimaliseerd. De meeste methodes voor CDI gebruiken 'expert-based' of subjectieve gronden voor het toekennen van gewichten, of passen een sequentiële ordening toe van de individuele indices. Er is grond voor het verder ontwikkelen en testen van nieuwe CDI's. De derde uitdaging betreft droogtemonitoring in gebieden met weinig of geen meetgegevens. Het potentieel van een CDI die voornamelijk gebruik maakt van satellietgegevens moet worden bepaald. Om deze uitdagingen aan te pakken voor het UBN gebied waren de volgende deeldoelstellingen opgesteld:

- Onderzoek het effect van observatieperiode op de analyse van droogte in het UBN gebied, om het gebruik van meetstations met een relatief korte observatieperiode in het onderzoek te valideren of af te keuren
- Onderzoek de temporele en ruimtelijke variatie van meteorologische droogtes in het UBN gebied
- Evalueer en vergelijk de prestaties van zes individuele droogte-indices (Standardized Precipitation Index (SPI), Standardized Precipitation Evaporation Index (SPEI), Evapotranspiration Deficit Index (ETDI), Soil Moisture Deficit Index (SMDI), Aggregate Drought Index (ADI), en Standardized Runoff-discharge Index (SRI)) voor het identificeren van historische droogtes in het UBN gebied
- Ontwikkel een impact-based CDI met de gewichten van de individuele indices geoptimaliseerd voor het monitoren van afwijkende gewasopbrengsten
- Ontwikkel een voorspellingsmodel voor afwijkende gewasopbrengsten, op basis van de impact-based CDI en individuele droogte-indices

- Onderzoek het potentieel van een CDI die voornamelijk satellietgegevens als input gebruikt.

De methodologie van dit onderzoek omvatte verschillende data analyse, statistische, optimalisatie en modelleringtechnieken, zoals beschreven in de volgende stappen:

1. Voor het analyseren van het effect van de lengte van observatieperiode op droogteanalyse, is de SPI berekend (voor het identificeren van meteorologische droogtes) voor beschikbare meteorologische stations in het UBN gebied. De observatieperiode van de meeste van deze stations is relatief kort, van 1975 t/m 2009. Slechts 14 stations hebben een langere meetreeks, van 1953 t/m 2009. Met de stations met een lange meetreeks zijn twee experimenten uitgevoerd met het weglaten van gegevens. Bij het eerste experiment werd vanaf 1953 steeds 1 extra jaar aan data weggelaten en opnieuw de SPI berekend, tot aan het jaar 1974 (vanaf dat jaar hebben de meeste stations gegevens beschikbaar). De resulterende SPI waarden voor droogtes in de periode 1975-2009 werden vervolgens met elkaar vergeleken om vast te stellen of dezelfde droogtecatagorieën werden aangegeven of niet. Om de gevoeligheid van de resultaten op de specifieke observatieperiode te analyseren, zijn bij het tweede experiment gegevens achtergehouden uit de periode 1970-1988.

2. Temporele en ruimtelijke analyse van meteorologische droogtes in het UBN gebied is uitgevoerd op basis van SPI

3. Het vergelijken van een verscheidenheid aan individuele droogte indices (SPI, SPEI, ETDI, SMDI, ADI, en SRI) is uitgevoerd op basis van correlatie-analyse. De werking van de verschillende indices is beoordeeld op basis van de effectiviteit in het bepalen van aanvang, ernst en duur van historische droogtes. De informatie over historische droogtes was afkomstig van de Emergency Events Database (EM-DAT).

4. De CDI’s zijn ontwikkeld door het toekennen van gewichten aan individuele indices met twee objectieve methodes: 'Principal Component Analysis (PCA)' en optimalisatie met 'impact-based random search'. Bij PCA worden de indices gecombineerd door de onderlinge correlatie-coëfficiënt matrix te bepalen en vervolgens de eigenwaarden te berekenen als basis voor het gewicht van elke individuele index in de CDI. Voor de random search optimalisatie zijn meer dan 60.000 iteraties toegepast om de combinatie van gewichten van indices te vinden die de maximale correlatie opleveren van de CDI met afwijkende gewasopbrengst (anomalie). Gewasopbrengst gegevens voor het UBN

gebied zijn beschikbaar gesteld door het Central Statistical Agency (CSA) van Ethiopië voor de periode van 1996 t/m 2009. Het UBN gebied is onderverdeeld in 16 administratieve zones. De jaarlijkse gewasopbrengst per zone is gebruikt in het onderzoek. Gewasopbrengst is het resultaat van een combinatie van weer, beleid, en toegepaste landbouwtechnieken. Om alleen het effect van het weer mee te laten wegen, is 'detrending' analyse toegepast op de gewasopbrengstgegevens. In het onderzoek zijn vier veel in het UBN gebied verbouwde gewassen meegenomen: teff, maïs, gerst en sorghum. De resulterende CDI's van de twee verschillende objectieve methodes zijn met elkaar vergeleken.

5. Voorspellingsmodellen voor anomalieën in gewasopbrengst zijn ontwikkeld op basis van meerdere lineaire regressievergelijkingen tussen de droogte-indices en gewasopbrengst anomalieën van teff, maïs, gerst en sorghum. In deze modellen is gewasopbrengst-anomalie gebruikt als de 'predictand' (te voorspellen variabele), en de impact-based CDI en de zes individuele indices zijn gebruikt als 'predictor' (voorspellende) variabelen. De resultaten van het model gebaseerd op de CDI, zijn vergeleken met het model dat de individuele indices als 'predictors' gebruikt.

6. Met dezelfde technieken als beschreven in stap 3 en 4, zijn een impact-based CDI en modellen voor gewasopbrengst anomalieën ontwikkeld die alleen droogte-indices gebruiken die voornamelijk satellietgegevens als input nodig hebben. De gebruikte droogte-indices zijn Precipitation Z-score, Evaporative Drought Index (EDI) en Vegetation Condition Index (VCI). De Z-scores zijn uitgerekend met raster neerslag data van de Climate Hazards Group Infrared Precipitation with Stations (CHIRPS). Voor de EDI-berekening zijn de MODIS ET gegevens als voornaamste input gebruikt. De VCI is berekend op basis van de Normalized Difference Vegetation Index (NDVI). De CDI met deze individuele indices op basis van satellietgegevens is ontwikkeld met alleen de impact-based optimalisatie benadering.

De volgende paragrafen behandelen de resultaten van de bovenstaande onderzoeksstappen.

De analyses van het effect van lengte van observatieperiode lieten zien dat de gegevens van de periode 1953 t/m 1974 weinig invloed hebben op de kwalificatie van droogtes in de periode 1975-2009 (beschikbaar voor de meeste meteorologische stations in het UBN gebied). Daarom zijn voor de droogte-analyses in deze dissertatie beide groepen beschikbare stations gebruikt (met korte en lange observatieperiode).

De temporele en ruimtelijke analyses van SPI-waarden lieten zien dat in het hele UBN gebied meteorologische droogtes van een seizoen of een jaar voorkwamen in de jaren 1978/79, 1984/85, 1994/95 en 2003/04. Ook is persistentie van seizoen tot jaar, en van jaar tot jaar, van sommige droogtes vastgesteld. De jaren met droogte in het UBN gebied zoals geïdentificeerd met de SPI-analyse, zijn bekend als jaren van droogte met desastreuze gevolgen in andere gebieden in Ethiopië.

De analyse van de effectiviteit van SPI, SPEI, ETDI, SMDI, ADI, en SRI in het bepalen van de aanvang, ernst en duur van de meest extreme historische droogtes, van 1978/79, 1984/85, 1994/95 en 2003/04, leidde tot de volgende observaties:

- SPEI liet voor de korte tijdschalen (3 en 6 maanden) te veel fluctuatie zien tussen droogte en normale condities
- SRI liet, in verhouding tot de andere indices, de minste fluctuatie zien tussen droge en natte omstandigheden
- De vergelijking voor wat betreft het bepalen van de aanvang van de vier historische droogtes liet zien dat in vergelijking tot de start als aangegeven door EMDAT, SPI en SPEI meestal de aanvang eerder inschatten, terwijl ETDI, SMDI, ADI, en SRI een latere aanvang aangaven.
- De meerderheid van de indices gaf de ernst en duur van de historische droogtes weer (bijvoorbeedld voor 2003-2004 en 1984-1985)
- Geen van de zes indices identificeerde op zichzelf de aanvang van alle vier de geanalyseerde historische droogtes.

Dit bevestigde het nut van de vierde deeldoelstelling van dit onderzoek: het ontwikkelen van een impact-based CDI met geoptimaliseerde gewichten van de individuele droogte-indices.

De ontwikkelde impact-based CDI liet een goede correlatie zien met de gewasopbrengst anomalieën van de vier gewassen die in deze studie in beschouwing zijn genomen: teff, gerst, maïs en sorghum. De CDI ontwikkeld met PCA identificeerde jaren met negatieve gewasopbrengst-anomalieën even goed als de impact-based CDI. De maximale correlatie (0.7) was verkregen voor gerst met de impact-based CDI. De resultaten met de ontwikkelde voorspellingsmodellen voor de opbrengstanomalieën van de vier gewassen zijn bemoedigend. De voorspellingsnauwkeurigheid (uitgedrukt in 'r-squared' waarden, R^2) voor de meeste gewasopbrengstanomalieën was 0.24 of meer voor alle administratieve zones. De maximale R^2 waarde werd verkregen voor gerst ($R^2 = 0.77$) en de laagste waarde voor maïs ($R^2=0.24$).

Over het algemeen zijn de patronen van voorspelde en waargenomen gewasopbrengst anomalieën vergelijkbaar, behalve wat betreft de verschillen in de grootte van anomalieën in sommige jaren. De verschillen in grootte kunnen aan verscheidene factoren worden toegeschreven, met name aan de aggregatie van de gerapporteerde gewasopbrengst tot gemiddelde voor een administratieve zone, en de nauwkeurigheid van de gewasopbrengstgegevens. Vervolgonderzoek zal nodig zijn om meer robuuste voorspellingsmodellen voor gewasopbrengst-anomalieën te ontwikkelen op basis van meer locatie-specifieke informatie.

Tot slot van dit onderzoek is een CDI ontwikkeld met dezelfde impact-based methode, maar dan met satellietgegevens als voornaamste input (EO-CDI). Dit deel van het onderzoek beslaat de periode van 2001 t/m 2009, en de opgetreden droogtes in deze periode zijn geanalyseerd. De resultaten laten zien dat de drie individuele indices (Z-score, EDI, en VCI) de historische droogtejaren en droogtegevoelige delen van het UBN gebied identificeren en karakteriseren. Voor de meerderheid van meteorologische stations (72%) werd een verschuiving van 2 maanden waargenomen tussen maximale neerslag en VCI. Een relatief groot gewicht werd in de CDI toegekend aan EDI (0.5) en aan Z-score (0.4). De EO-CDI liet een goede correlatie met gewasopbrengst-anomalieën zien voor alle vier de gewassen, met een maximale correlatiecoëfficiënt van 0.8 voor sorghum.

Samenvattend is er voor het eerst een uitgebreide evaluatie van bestaande droogte-indices uitgevoerd voor het deelstroomgebied van de Upper Blue Nile, door historische droogtes te karakteriseren en analyseren. Dit bevestigt dat ook het UBN gebied in het verleden met droogte te kampen heeft gehad en dat daarom uitgebreid droogteonderzoek en droogte monitoring in het gebied nodig is. De ontwikkelde impact-based CDI's en 'multiple linear regression' modellen hebben laten zien effectief te zijn in het identificeren van historische droogtes in het UBN gebied. De impact-based CDI kan mogelijk worden gebruikt bij de toekomstige ontwikkeling van een systeem voor droogtemonitoring in het UBN gebied voor beslissingsondersteuning ter vermindering van de negatieve gevolgen van droogte.

Dezelfde benadering van het ontwikkelen van een impact-based CDI, geoptimaliseerd voor een bepaald (deelstroom) gebied, kan worden toegepast voor andere regio's in Ethiopië. De analyse die is toegepast om het effect van de lengte van meetperiode op SPI droogte-kwalificatie vast te stellen, bleek een succesvolle manier om het gebruik te valideren van een groot aantal meteorologische stations met kortere meetperiode bij ruimtelijke droogteanalyse in het UBN

gebied. Deze benadering kan worden toegepast op andere gebieden waar droogte-onderzoek wordt gelimiteerd door ontoereikende meetperioden.

De resultaten van de EO-CDI laten zien dat satellietgegevens kunnen worden gebruikt als alternatieve informatiebron voor droogtemonitoring in gebieden met weinig of geen meetstations, zoals het UBN gebied. Daarnaast lenen satellietgegevens zich voor het ontwikkelen van een 'grid-based' (raster) CDI, hetgeen belangrijk is voor het analyseren van ruimtelijke details van droogtes. Dit zal onderwerp zijn van onze toekomstige studies. De evaluatie van bestaande droogte-indices is in deze studie uitgevoerd op basis van gegevens van historische droogtes (aanvang en ernst) afkomstig van een bron in mondiale schaal. Bij het toepassen van dezelfde evaluatieprocedure op andere gebieden verdient het aanbeveling om beschikbaarheid na te gaan van gegevens op lokale schaal.

About the author

Yared Ashenafi Bayissa was born in July 27, 1979 in Ambo town in Ethiopia. He studied his Bachelor of Science (Bsc) degree in Irrigation Engineering at Arbaminch Water Technology Institute (AWTI) and graduated in the year 2002. Then he was employed in Bahirdar Construction Technology College with assistance lecturer position and worked until 2007.

His main duties in the college were to give lecture to students enrolled under Irrigation and Drainage, and Water Supply and Sanitation departments. Moreover, he worked as the head of Irrigation and Drainage department and advised students on academic and personal issues. After enriching himself with the academic work experience, he joined Addis Ababa Institute of Technology (AAiT) for his Masters of Science (MSc) degree in the year 2007. He graduated in Civil Engineering field of specialization in Hydraulic Engineering in the year 2009. He completed his MSc study with an outstanding performance and he got an awarding certificate from the institute for the outstanding performance and best graduating research dissertation. He also had a chance to work in the institute on part time bases and offered water related courses and other Civil Engineering courses for undergraduate students under Civil Engineering department. In the year 2009, he was employed in Ambo University, Institute of Technology on full time bases and delivered courses for undergraduate students under Civil Engineering, and Water Resources and Hydraulic Engineering departments.

From the year 2011 to 2018, he pursued his PhD in the sandwich program between IHE Delft/TU-Delft, The Netherlands and Ambo University, Ethiopia. His research topic was developing an impact based combined drought index and multiple linear regression model to monitor drought related crop yield reduction in the Upper Blue Nile Basin, Ethiopia. Furthermore, he attended the course requirement for the graduate school for Socio-economic and Natural Sciences of the Environment (SENSE). Besides working his PhD research, he was supervising MSc students from AAiT and Arbaminch University and also reviewed journal papers. He also got a chance to work as a researcher scientist in National Drought Mitigation Center (NDMC), Nebraska, USA since 2016. He involved and worked on the drought project for the Great Horn of Africa (GHA) (funded by NASA) and the US Drought Monitor (USDM) objective blend research.

Publications, conferences and workshops

Peer reviewed Publications

Bayissa, Y.A., Maskey, S., Tadesse, T., van Andel, S.J., Moges, S,A., van Griensven, A., and Solomatine, D.P, 2018. *Comparison of the performance of six drought indices in characterizing historical drought for the Upper Blue Nile Basin, Ethiopia*. Geosciences, v. 8, No. 3, p.81.

Bayissa, Y.A., Tadesse, T., Demissie, G.B., and Shiferaw, A, 2017. *Evaluation of Satellite-Based Rainfall Estimates and Application to Monitor Meteorological Drought for the Upper Blue Nile Basin, Ethiopia*. Remote Sensing, v. 9, No. 7, p.669.

Bayissa, Y.A., Moges, S.A., Xuan, Y., Van Andel, S.J., Maskey, S., Solomatine, D.P., Griensven, A.V., and Tadesse, T., 2015. *Spatio-temporal assessment of meteorological drought under the influence of varying record length: the case of Upper Blue Nile Basin, Ethiopia*. Hydrological Sciences Journal, v. 60, No. 11, p.1927-1942.

Other peer reviewed publications

Demisse, G.B., Tadesse, T., **Bayissa, Y.B,** Atnafu, S., Argaw, M. and Nedaw, D., 2018. *Vegetation condition prediction for drought monitoring in pastoralist areas: a case study in Ethiopia*. International Journal of Remote Sensing, p.1-17.

Demisse, G.B., Tadesse, T., Atnafu, S., Hill, S., Wardlow, B.D., **Bayissa, Y**. and Shiferaw, A., 2017. *Information Mining from Heterogeneous Data Sources: A Case Study on Drought Predictions*. Information, v. 8, No. 3, p.79.

Tadesse, T., Champagne, C., Wardlow, B.D., Hadwen, T.A., Brown, J.F., Demisse, G.B., **Bayissa, Y.A**. and Davidson, A.M., 2017. *Building the vegetation drought response index for Canada (VegDRI-Canada) to monitor agricultural drought: first results*. GIScience & Remote Sensing, v. 54, No. 2, p.230-257.

Demisse, G.B., Tadesse, T., Wall, N., Haigh, T., **Bayissa, Y.**, and Shiferaw, A., 2018. *Linking Seasonal Drought Product Information to Decision Makers in a Data-sparse Region: A Case Study in the Greater Horn of Africa*. Remote Sensing Applications: Society and Environment.

Bitew, M.M., Gebremichael, M., Ghebremichael, L.T. and **Bayissa, Y.A**., 2012. *Evaluation of high-resolution satellite rainfall products through streamflow simulation in a hydrological modeling of a small mountainous watershed in Ethiopia*. Journal of Hydrometeorology, v. 13, No. 1, p.338-350.

Bayissa, Y.A, and Hasfaw, D., 2014. *Assessment of the use of remotely sensed rainfall products for runoff simulation in the Upper Blue Nile Basin of Ethiopia*. Zede Journal v. 31 p. 1-9.

Journal articles under review

Bayissa, Y.A, Tadesse T., Mark D. Svoboda, Brian D. Wardlow, Calvin Poulsen, John Swigart and S.J. van Andel 2018. Developing and evaluating a satellite based combined drought index to monitor historic drought: a case study for Ethiopia. Under review in GIScience & Remote Sensing.

Bayissa, Y.A, Tadesse, T., and Demisse, G.B., 2018. *Building high-resolution vegetation outlook model to monitor agricultural drought for Upper Blue Nile Basin, Ethiopia*.

All Others

Demisse, G.B., Tadesse, T. and **Bayissa, Y.,** 2017**.** *Data Mining Attribute Selection Approach for Drought Modeling: A Case Study for Greater Horn of Africa*. arXiv preprint arXiv:1708.05072.

Nigusssie, T. and **Bayissa, Y.A.,** 2010. *Effect of land use/land cover management on Koga reservoir sedimentation*. Nile Basin Capacity Building Network.

Conferences and workshops

Oral presentation: 3rd Open Water Symposium and Workshops. September 16-17, 2015, Symposium and Workshops organized by International Water Management Institute (IWMI), Addis Ababa, Ethiopia.

Poster presentation: Water for food global conference, May 5-8, 2013, LINCOLN, NEBRASKA, USA.

Workshop: Climate change information for improved decision making, organized by world Bank, June 3-4, 2013, ADDIS ABABA, ETHIOPIA.

Oral presentation: Water Resources Management. March 26-27, 2012, Workshop Organized by Water and Water Related Research Center of Bahir Dar University, BAHIRDAR, ETHIOPIA.

Second participatory research workshop: NASA IDS*: Seasonal prediction of hydroclimatic extremes in the Great Horn of Africa (GHA), July 28-29, 2015, ADDIS ABABA, ETHIOPIA.

Oral presentation: 3rd Open Water Symposium and Workshops. September 16-17, Organized by International Water Management Institute, Addis Ababa, Ethiopia.

98th Annual meeting: American Meteorological Society. January 7-11, 2018. Austin, Texas.

Netherlands Research School for the
Socio-Economic and Natural Sciences of the Environment

D I P L O M A

For specialised PhD training

The Netherlands Research School for the
Socio-Economic and Natural Sciences of the Environment
(SENSE) declares that

Yared Ashenafi Bayissa

born on 27 July 1979 in Ambo, Ethiopia

has successfully fulfilled all requirements of the
Educational Programme of SENSE.

Delft, 11 September 2018

the Chairman of the SENSE board	the SENSE Director of Education
Prof. dr. Huub Rijnaarts	Dr. Ad van Dommelen

The SENSE Research School has been accredited by the Royal Netherlands Academy of Arts and Sciences (KNAW)

KONINKLIJKE NEDERLANDSE
AKADEMIE VAN WETENSCHAPPEN

The SENSE Research School declares that **Yared Ashenafi Bayissa** has successfully fulfilled all requirements of the Educational PhD Programme of SENSE with a work load of 50.4 EC, including the following activities:

SENSE PhD Courses

- Environmental research in context (2011)
- Geostatistics (2013)
- Research in context activity: '"Co-organizing two workshops in Addis Ababa on 'Seasonal prediction of Hydro-Climatic Extremes in the Great Horn of Africa (2014)' and on 'Participatory research workshop on seasonal prediction of Hydroclimatic Extremes in the Great Horn of Africa' (2015)."'

Selection of other PhD and Advanced MSc Courses

- Modelling theory and uncertainty, IHE Delft (2011)
- Data driven modelling and computational intelligence, IHE Delft (2011)
- Data assimilation and Real time control, IHE Delft (2011)
- MATLAB, IHE Delft (2011)
- Introduction to Optimization, IHE Delft (2011)
- Advanced GIS: Applied to Water Resources Engineering, Addis Ababa University, Ethiopia (2012)

External training at a foreign research institute

- Attended hands on training and involved in drought research, National Drought Mitigation Center, USA (2014)

Management and Didactic Skills Training

- Supervising three MSc students with thesis (2014-2015)

Oral Presentations

- *Effects of data length on spatio-temporal assessment of drought for Upper Blue Nile Basin of Ethiopia.* Workshop on Water Resources and Management, March 26-27, 2012, Bahirdar, Ethiopia
- *Inter-comparison of the performance of different drought indices through assessing the spatial and temporal variability of historic drought events in Upper Blue Nile Basin of Ethiopia.* 3rd Open Water Symposium and Workshops, 16-17 September 2015, Addis Ababa, Ethiopia
- *Comparison of the performance of five drought indices through assessing the historic drought events in Upper Blue Nile Basin of Ethiopia.* Natural Resources Management and Food Security, 22-23 October, 2015, Hawassa, Ethiopia

SENSE Coordinator PhD Education

Dr. Peter Vermeulen